

Electrohydraulic Control Systems

John Watton



Download free books at

John Watton

Electrohydraulic Control Systems

Principles Of Operation, Circuit Analysis & Design



Electrohydraulic Control Systems: Principles Of Operation, Circuit Analysis & Design

1st edition

© 2016 John Watton & bookboon.com

ISBN 978-87-403-1187-7

Peer reviewed by Dr Nigel Johnston, Bath University

Contents

About the author	8
Preface	9
1 An introduction to the operation of electrohydraulic valves	11
1.1 Aim	11
1.2 Electrohydraulic valves, direction and pressure relief types	11
1.3 Electrohydraulic valves, the servodrive concept	18
1.4 Servovalve operation and design	21
2 Servovalve flow characteristics	37
2.1 Aim	37
2.2 Servovalve flow characteristics, critically-lapped spool	37
2.3 Servovalve flow characteristics, under-lapped spool	41
2.4 Valve rating	44
2.5 Servovalve specification by the manufacturer	45
2.6 Maximum power transfer to the load and selection of supply pressure	49

www.sylvania.com

We do not reinvent the wheel we reinvent light.

Fascinating lighting offers an infinite spectrum of possibilities: Innovative technologies and new markets provide both opportunities and challenges. An environment in which your expertise is in high demand. Enjoy the supportive working atmosphere within our global group and benefit from international career paths. Implement sustainable ideas in close cooperation with other specialists and contribute to influencing our future. Come and join us in reinventing light every day.

Light is OSRAM

OSRAM SYLVANIA



3	Connecting a servovalve to an actuator, steady-state behaviour	52
3.1	Aim	52
3.2	Connecting a servovalve to a cylinder, the open-loop steady-state behaviour	52
3.3	Connecting a servovalve to a motor, the open-loop steady-state behaviour	56
3.4	Connecting a servovalve to a motor, the closed-loop steady-state behaviour	60
3.5	Connecting a servovalve to a cylinder, the closed-loop position transient response	62
3.6	Servodrive damping, leakage and friction losses, efficiency	67
3.7	Improving the steady-state performance of an open-loop motor servodrive using a Programmable Servo Controller	74
4	System dynamics and computer simulation	79
4.1	Aim	79
4.2	Fluid compressibility and its effect on flow rate	79
4.3	Force and torque equations for actuators with moving mass or rotary inertia	82
4.4	Undamped natural frequency of an actuator	82
4.5	Actuator equations with losses and dynamics	87
4.6	Linearisation of the system equations	91
4.7	Pipe resistance, compressibility and inertia	94



Discover the truth at www.deloitte.ca/careers

Deloitte.

© Deloitte & Touche LLP and affiliated entities.



Click on the ad to read more

4.8	Servodrive open-loop linearised differential equation with losses and dynamics	98
4.9	Servovalve dynamics	101
4.10	The role of computer simulation	106
5	Laplace transforms, transfer functions, block diagrams, transient and frequency response	114
5.1	Aim	114
5.2	Laplace transforms	114
5.3	Transfer functions and block diagrams	116
5.4	Undamped natural frequency with connecting line effects	120
5.5	Transient response and its specification	129
5.6	Frequency response	137
5.7	The effect of a pure delay	153
6	Closed-loop stability	155
6.1	Aim	155
6.2	Closed-loop stability	155
6.3	The use of frequency response	158

SIMPLY CLEVER

ŠKODA



We will turn your CV into
an opportunity of a lifetime



Do you like cars? Would you like to be a part of a successful brand?
We will appreciate and reward both your enthusiasm and talent.
Send us your CV. You will be surprised where it can take you.

Send us your CV on
www.employerforlife.com



Click on the ad to read more

7	Improving closed-loop behaviour	170
7.1	Aim	170
7.2	Some preliminary comments	170
7.3	The use of servoamplifier dither to improve steady-state error drift for a position control system	170
7.4	The effect of spool under-lap on the steady-state error for a position control system	172
7.5	Steady-state tracking error in response to a velocity demand for a position control system	178
7.6	Optimising the closed-loop transient response	182
7.7	Velocity sensing or Derivative computation	183
7.8	Additional acceleration, or pressure, feedback	185
7.9	Proportional+Integral+Derivative (PID) control	188
7.10	Gain scheduling using a PSC	191
7.11	Digital control algorithms using a PSC	192
7.12	Improving the dynamic performance of an open-loop motor servodrive using a PSC and pressure derivative feedback	195
8	Pressure and force control	199
8.1	Aim	199
8.2	Pressure control of a fixed-volume container	199
8.3	Force control of a servoactuator	210
9	Closing comments and further reading guidance	228

About the author

John Watton BSc PhD DSc FEng FIMechE CEng

The author has taken a broad approach to the study of fluid power control, covering a period of almost forty years. He started his career in industry working on heat exchangers and then obtained BSc and PhD degrees in Mechanical Engineering. He returned to industry as a systems engineer working on the automated electrohydraulic steering control of mobile light-guided vehicles. Following a period at Huddersfield Polytechnic, where he was involved in developing electromechanical control systems, he then moved to Cardiff University. He set up a new fluid power laboratory and developed new courses in fluid power and condition monitoring which he taught together with control theory, fluid mechanics and dynamics. He has published over 170 papers and 4 books on fluid power and has supervised many MSc and PhD students. He was awarded the degree of DSc for his contributions to fluid power and became Professor of Fluid Power.

Industrial work has included the co-design of other novel mobile machines for agricultural and civil engineering applications, and moving into commercial operation. He has originated and managed some major projects in the steel processing industry with some moving to plant on-line implementation. Projects have varied from continuous casting, bar and strip rolling through high speed mills, strip quality/coiling and no-twist mill wire production. Savings due to improved production have run into many millions of pounds. He has also undertaken a variety of consultancy projects for the fluid power industry, varying from component analysis and design to hydraulic control strategies for high-power forging presses. He has also been active as an Expert Witness on fluid power issues varying from system failures to patent litigation.

He was awarded the Institution of Mechanical Engineers Bramah Medal and received an honour from the Japan Fluid Power Society. He is a Chartered Engineer, a Fellow of the Institution of Mechanical Engineers and a Fellow of the Royal Academy of Engineering. He is now retired from Cardiff University, taking the title of Emeritus Professor, but has since undertaken further book writing together with consultancy projects for industry.

Preface

Fluid power is used in a vast range of applications, often with fast response times and for power levels that can be up to several MW and where no other form of actuation is feasible. Fluid power control systems may be placed in environmentally-difficult applications and increasingly with alternative fluids to pure mineral oil. A useful feature is that they almost always have a more competitive power/weight ratio when compared with electrically actuated systems, and have the capability of being able to accurately control several parameters such as pressure, force, speed, position.

This book specifically considers the application of electrohydraulic valves in control systems, an extremely important part of fluid power. The aim is to bring together various key aspects and up to a design level beyond a basic text but without an overload of fundamental derivations. Some background theory is still considered essential but only at a level that allows the reader to get a 'feel' for how it is used in practice. The layout of the book is such that the reader may progress through it from basics of steady-state operation to essential concepts of dynamic design and control. This book is divided into 9 chapters covering:

- how and why electrohydraulic valves work
- the performance of open-loop and closed-loop servoactuators
- the effect of system dynamics
- the derivation and use of block diagrams for design
- computer simulation using Matlab Simulink and Control System Toolbox
- the stability of closed-loop systems
- the use of Programmable Servo Controllers for control and performance improvement

Other important features of this book are the use of real data and performance characteristics together with 27 worked examples of varying complexity. A brief list of references is included to take the reader towards several hundred other references and more advanced techniques continually being researched and developed. The reader will find much more detailed theoretical and experimental information from these references and also from two of the author's earlier, and more substantial, supporting books.

J Watton [2007]. Modelling, Monitoring and Diagnostic Techniques for Fluid Power Systems. Springer. ISBN 978-1-84628-373-4.

J Watton [2009]. Fundamentals of Fluid Power Control. Cambridge University Press. ISBN 978-0-521-76250-2

Portuguese translation:

J Watton [2012]. Fundamentos de Controle em Sistemas Fluidomecânicos. Direitos exclusivos para a língua portuguesa, LTC Rio de Janeiro. ISBN 978-85-216-2025-9

John Watton

Llandaff, Cardiff, 2015

1 An introduction to the operation of electrohydraulic valves

1.1 Aim

This chapter introduces the reader to the basics of operation of electrohydraulic valves by a number of objectives as follows:

- to give examples on how they are used in practice
- to explain how and why electrohydraulic valves work
- to show some different designs of industrial servovalves

1.2 Electrohydraulic valves, direction and pressure relief types

This book is primarily concerned with the design of control systems employing electrohydraulic servovalves and related electrohydraulic proportional valves, both often being simply referred to as *servovalves*.

The combination of a servovalve and a connected linear cylinder for position control, or a motor for speed control, may be referred to as a *servodrive* although it should be noted that servovalves may be used to control other parameters such as pressure and force. Figure 1.1 shows just two examples of many commercial servodrives available. A single-rod cylinder is shown although double-rod cylinders are commonly used, the “inactive end” often being enclosed for both safety and assembly purposes.

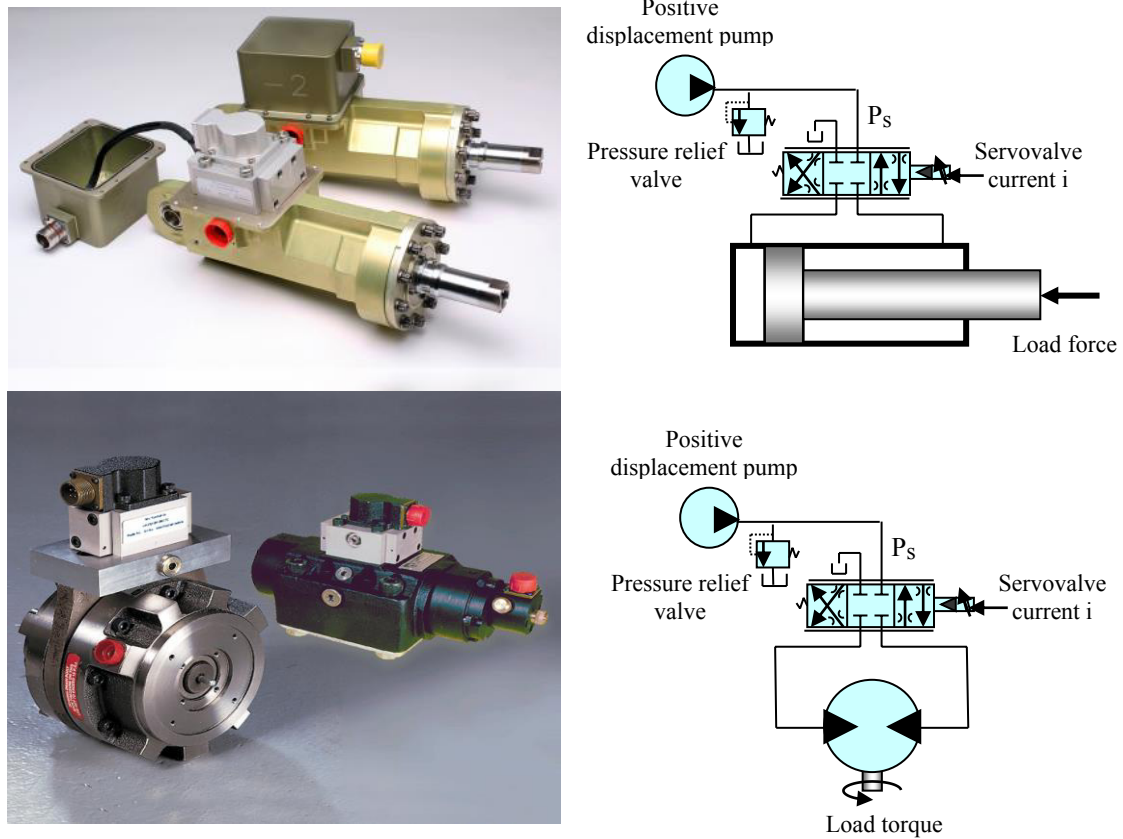


Figure 1.1 Linear and rotary servodrives units [www.star-hydraulics.co.uk]

Also shown is the positive displacement pump flow supply with a pressure relief valve to both set the supply pressure and to protect the system when flow is not demanded by the servodrive.

Applications are vast with load force requirements that can vary from just a few hundred N up to several hundred MN, the latter from the author's practical project experience on steel mills and forging presses. The following list covers typical application areas:

- mineral extraction, mining and rock drilling, materials transportation
- materials primary processing, steel mills, forging presses
- process industries, chemical and materials
- general manufacturing, robotics
- materials testing machines, pressure testing, vehicle testing systems
- bridges, canal/barrage locks
- road and racing vehicles, rail vehicles, marine
- military vehicles
- aerospace
- mobile machines for construction, agriculture and forestry work
- public services, road cleaning, health, maintenance, elevators
- leisure, theme parks, wave generators, animation, opera and musical productions

In practice the design, manufacture and application of electrohydraulic control valves embraces many disciplines such as:

- materials selection, new materials
- fluid mechanics, wear and lubrication, alternative fluids
- thermodynamics
- energy efficiency
- vibration and noise analysis
- component/systems steady state and dynamic design
- sensor and electromagnetic technologies
- signal processing and associated algorithms
- computer control techniques
- control theory and artificial intelligence
- condition monitoring and fault diagnosis

Just a few of these issues are appropriate to this book and further details may be obtained from the references given.

I joined MITAS because
I wanted **real responsibility**

The Graduate Programme
for Engineers and Geoscientists
www.discovermitas.com



Month 16
I was a construction supervisor in the North Sea advising and helping foremen solve problems

Real work
International opportunities
Three work placements



It should be pointed out at this stage that strictly speaking the term 'electrohydraulic' is not restricted to servovalves since it can be applied to directional control valves, proportional pressure relief valves or any fluid power device that uses an electrical input signal to change its fluid power output function. However in the context of control, electrohydraulic valves are used here to indicate that the output flow rate can be varied proportionally to the electrical input signal.

Figure 1.2 shows a basic **directional control valve** which is really an on-off valve for selecting flow rate direction. Applying a voltage, either ac or dc, to either of the solenoids creates an electromagnetic force that throws the spool to the end of its stroke thus opening the appropriate flow ports. Usually with no solenoid actuation the spool returns to its central position. The spool ports can have a variety of configurations depending upon the requirement, and this type of valve is the backbone of many industrial applications requiring sequencing-type operations.

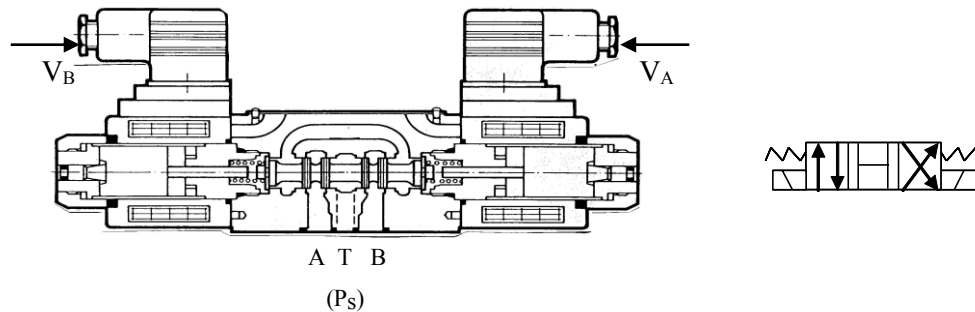


Figure 1.2 A directional control valve with solenoid actuation

A **pressure relief valve (PRV) with off-loading** is another form of electrohydraulic component and a two stage PRV is shown as figure 1.3. A pilot pressure can also be applied to the valve to cause it to open at a minimum pressure and this is useful for sequencing operations. The pressure is normally hydromechanically set but in this example the PRV has an added stage that can off-load the system pressure by opening the top port via a spool valve with solenoid control. The use of a remote electrical signal can be invaluable as an energy saving operation if the full system pressure is not needed during a manufacturing cycle.

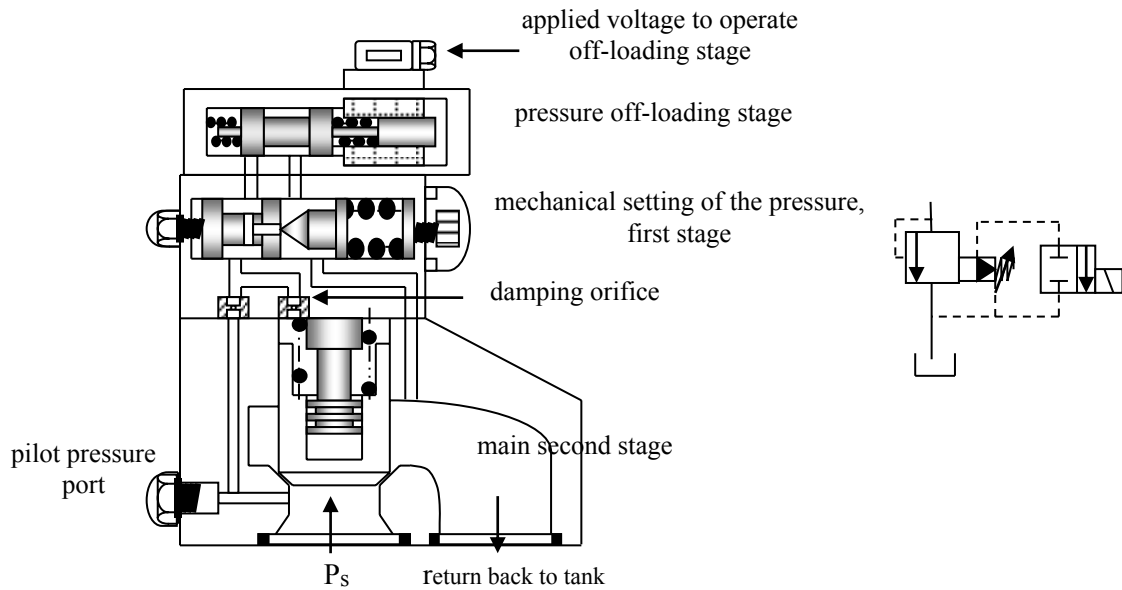


Figure 1.3 A two stage pressure relief valve with off-loading

The first stage stiff spring is used to set the required system pressure. When the set force, equivalent to set pressure, is overcome at the first stage then the poppet attempts to open by a very small amount allowing a smaller pressure to be fed to the top of the second stage spool, which has a much weaker spring, allowing the system flow rate to pass through the valve and return back to tank. This is a much better way of off-loading flow rate rather than using a single stage valve with a stiff spring. Flow rate is off-loaded more quickly compared with a single stage valve and the increase in system pressure with flow rate through the second stage is much less pronounced than with a single stage valve. A two stage valve is less prone to vibration of the moving parts compared with a single stage valve, and helped by the damping orifice at the top of the second stage.

An *electrohydraulic pressure relief valve* is shown in figure 1.4 where in this case the system pressure may be set directly via a variable input voltage to the “proportional solenoid”, that is the solenoid is designed to produce a force that is ostensibly proportional to its applied current.

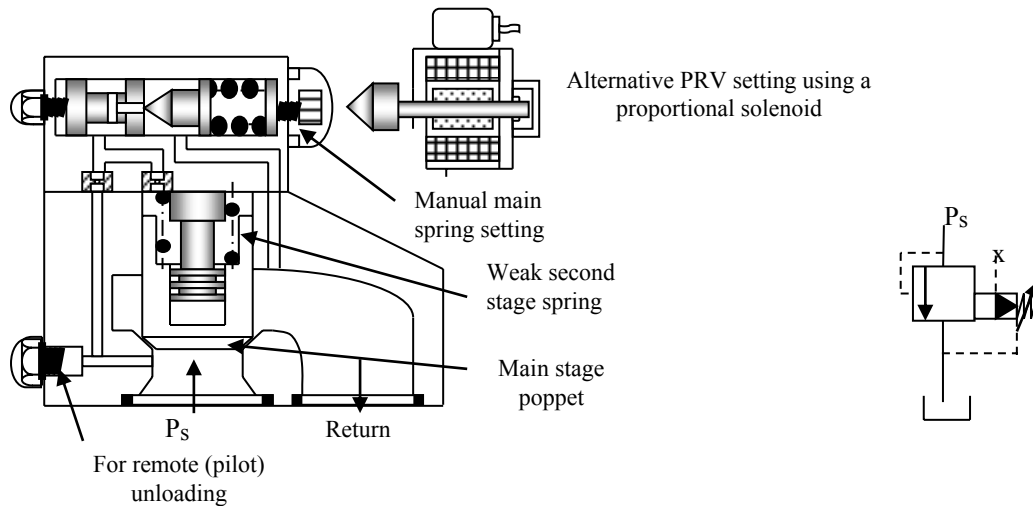


Figure 1.4 A two stage pressure relief valve with electrical control

The application of an increasing voltage to the solenoid produces an electromagnetic force that attempts to move its poppet to the left thus increasing the resistance to flow through the conical poppet/restrictor and hence the pressure at the valve first stage. The operation of the second stage spool is then as described for the valve shown as figure 1.3.

ie business school

#1 EUROPEAN BUSINESS SCHOOL
FINANCIAL TIMES 2013

#gobeyond

MASTER IN MANAGEMENT

Because achieving your dreams is your greatest challenge. IE Business School's Master in Management taught in English, Spanish or bilingually, trains young high performance professionals at the beginning of their career through an innovative and stimulating program that will help them reach their full potential.

- Choose your area of specialization.
- Customize your master through the different options offered.
- Global Immersion Weeks in locations such as London, Silicon Valley or Shanghai.

Because you change, we change with you.

www.ie.edu/master-management | mim.admissions@ie.edu | Facebook | Twitter | LinkedIn | YouTube | Instagram



Figure 1.5 shows measurements taken by the author on two commercial PRVs. For the first valve the pressure/voltage relationship is highly non-linear at low pressures, and with a poor hysteresis characteristic. Hysteresis is dominated by the electromagnetic component of the valve such that if the applied voltage direction is changed then the pressure does not immediately respond until a small voltage threshold change has occurred. The second valve shows a much better characteristic with a much reduced hysteresis characteristic.

These characteristics do show the importance of understanding the application performance required and then selecting the correct proportional pressure relief valve. However, a poor hysteresis characteristic may well be acceptable for a particular application.

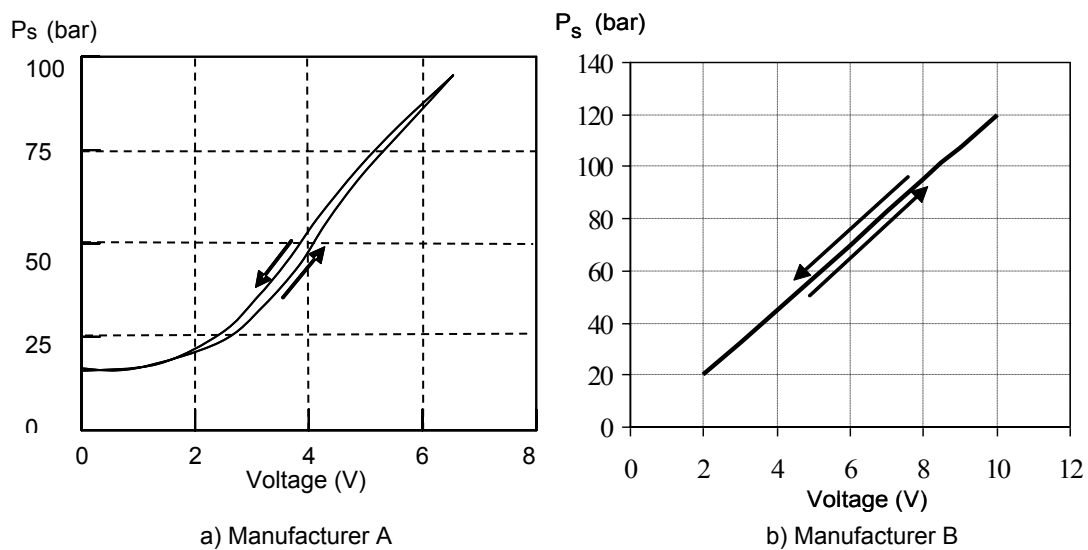


Figure 1.5 Two proportional pressure relief valve characteristics

Fortunately, or perhaps by good design, the non-linear region for the first valve is within a low pressure range that is probably not needed for the important part of the duty cycle, apart perhaps for pressure off-loading. For pressures beyond 25bar the characteristic has an acceptable near-linear relationship although the hysteresis evident is a disadvantage for closed-loop dynamic control of pressure. Solenoids of the type being discussed here usually operate with a high current of typically 1A \rightarrow 2A.

1.3 Electrohydraulic valves, the servodrive concept

Figure 1.6a) shows a linear actuator servodrive in open-loop mode and figure 1.6b) shows how it is configured to form a closed-loop position control system.

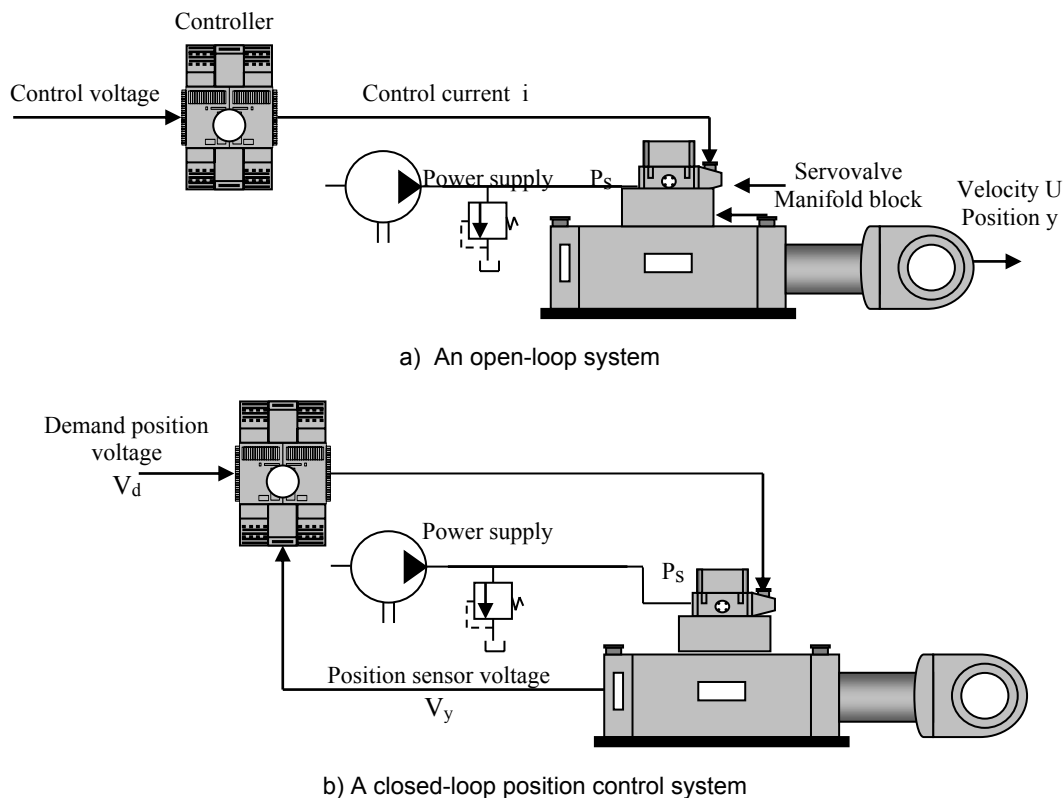


Figure 1.6 A linear servodrive in open-loop and closed-loop modes

Figure 1.6 also shows the power supply consisting of a positive displacement pump with a pressure relief valve to set the supply pressure and protect the system when flow is not demanded by the servodrive. Note that for the servodrives illustrated the servovalve is mounted, via its manifold block, on the actuator to minimise fluid volumes and their associated compressibility effects. This ensures the highest possible hydraulic undamped natural frequency of the system, as will be discussed later. However if fluid volumes are very small, for example at the ends following full stroke in either direction, then very high rates of pressure change within small volumes can cause control stability problems in some applications.

Consider first the *open-loop servodrive* shown as figure 1.6a). The application of an input voltage to the electronic controller causes the actuator to move at a particular velocity as dictated by the servovalve supply pressure and load force characteristic to which the actuator is connected. Doubling the input voltage will double the actuator velocity, more-or-less. Since the application of an input voltage creates actuator motion then this is an integrator characteristic, a very useful and inherent property of a servovalve/actuator for closed-loop position control. The actuator will continue to move unless the servovalve input signal is removed or closed-loop position control is introduced.

For the **closed-loop position servodrive** shown in figure 1.6b), if the demanded position voltage exceeds the actual position voltage, from its position sensor, then the net error voltage to the servovalve causes it to supply flow to the actuator. Hence the actuator moves, reducing the error, and the error voltage, with time until the error between the demanded position voltage and the actual position voltage is zero and the load comes to rest at the demanded position. Setting a low servoamplifier gain will cause the motion to be sluggish whereas a higher servoamplifier gain will cause the motion to be fast and possibly oscillatory.

A good design will cause the desired position to be achieved in an optimum manner but it is crucial to note here that increasing the servoamplifier gain to an increasingly higher value will eventually create an unstable closed-loop behaviour due to system dynamic effects, and which is clearly undesirable.

An **electronic controller** is needed to accept the various electrical signals and then form the signal that is sent to the servovalve. It is a combination of a summing junction/servoamplifier and receives the command signal, and the feedback (subtracted) signal for closed-loop control, and sends the resulting error voltage, converted to a current, to the servovalve coils. The basic amplifier cards used in most applications have several analogue input and output channels and represent high-quality low-cost approaches for closed-loop control.



no.1
nine years
in a row

Sweden
Stockholm

STUDY AT A TOP RANKED INTERNATIONAL BUSINESS SCHOOL

Reach your full potential at the Stockholm School of Economics, in one of the most innovative cities in the world. The School is ranked by the Financial Times as the number one business school in the Nordic and Baltic countries.

Visit us at www.hhs.se

STOCKHOLM SCHOOL
OF ECONOMICS

For research and development, test rigs and more advanced control applications a digital controller may be used with programmable facilities that can significantly improve performance. These programmable controllers are now standard supply by the servovalve manufacturer. Note that some servovalves have integrated electronics within the cap thus simplifying the electrical connection.

Figure 1.7 shows a Programmable Servo Controller, referred to as a PSC, and in this example on a test rig used by the author to identify dynamics and then improve the control of a racing car active suspension.

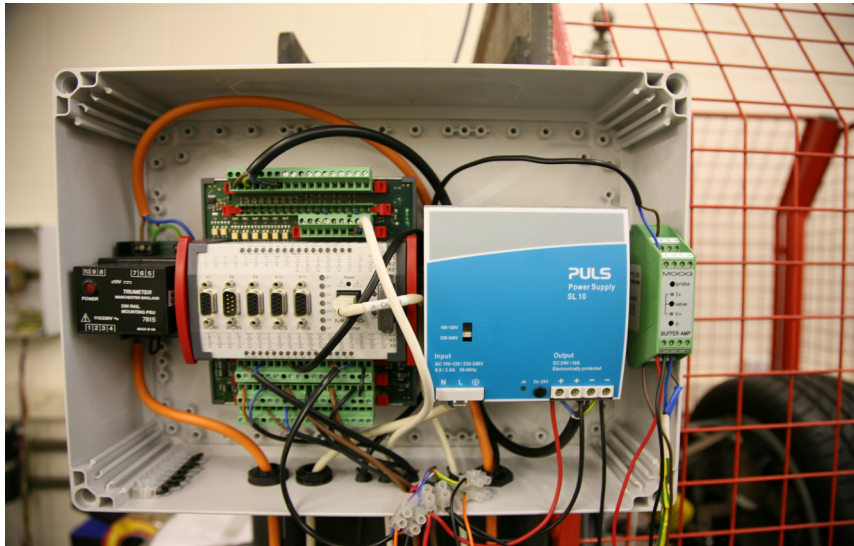


Figure 1.7 A Moog Programmable Servo Controller (PSC)

The controller shown in figure 1.7 is the Moog MSC I and is best suited for applications where one or two actuators need to be controlled via an analogue interface. Typical applications are the closed-loop control of one or two hydraulic axes. The PSC is set up by connecting a PC and using the Moog Axis Control Software (MACS). The controller has many features, but for the purpose of this application some of the 8 analogue input channels and 2 analogue output channels, with 16 bit resolution, were used.

The analogue input/outputs may be operated in either current or voltage mode depending on hardware default settings. The PSC card is programmed by means of a serial set up link which is connected to a PC. Once a program has been downloaded to the card it is not necessary to maintain the set up link with the PC as the PSC contains its own microprocessor and storage facilities. However, it may be necessary to maintain the link in order to make changes to the setup, supervise the performance, or monitor the values of control parameters. The PSC can be set up to perform advanced closed-loop control with up to two nested control loops for each axis of control. All the required summations, filters, limiters and non-linear functions, etc. can be structured using a text based programming language. Commands can either be entered directly from a PC or stored in an ASCII text file and downloaded from the PC to the PSC in blocks.

The Moog MSC II controller is best suited for applications where multiple axes need to be controlled via a fieldbus interface, and also uses the MACS programming software. Typical applications are closed-loop control with or without profile generation of multiple electric or hydraulic axes. Computations cycle times are extremely fast but for control of hydraulic systems it is usual to use a sampling frequency of typically 500→1000Hz since higher frequencies will tend to sample undesirable noise and other hydraulic frequencies. More specification and performance details of these controllers may be found in (www.Moog.com).

Electrohydraulic **control system design** is really about selecting the correct servovalve for the application and integrating it into a system to give an acceptable system steady-state and dynamic behaviour.

1.4 Servovalve operation and design

Consider now some common types of servovalve design. The electrohydraulic servovalve, with a flapper nozzle stage, was invented by William C Moog in the early 1950s, the design being as shown in figure 1.8. The earliest form of internal feedback, to set the spool position, used springs placed at each end of the spool. The symbol T is the tank connection and P_s is the supply pressure connection.

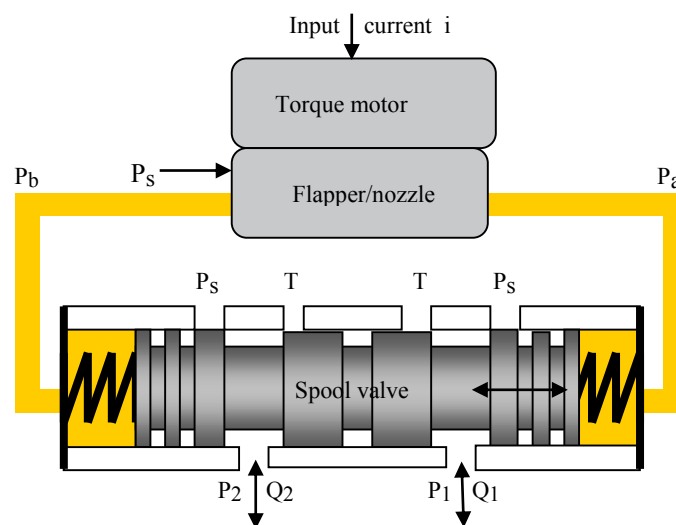


Figure 1.8 An early servovalve design with spool spring feedback

An input current to the coils of the electromagnetic torque motor creates a deflection of the flapper which then creates a pressure differential ($P_a - P_b$). This is applied across the spool which moves it in the appropriate direction and at a constant velocity if no restraining force is present. The pressure differential is created by use of two nozzles and two orifices and the final spool displacement is determined when the applied hydraulic force across the spool is matched by the resisting spring force at that displacement. The flapper remains at its displaced position during operation with a constant input signal. It can be shown that dynamic performance is possibly slightly deteriorated from the case when the flapper is in its null condition. Flapper clearance has to be very small in all servovalve designs to minimise flow loss and hence power loss, so the nozzle with the reduced clearance when operating is susceptible to fluid particle blockage particularly in the presence of poor filtration. The introduction of this new electrohydraulic valve had a major impact in the hydraulic control field.

The electromagnetic first stage, or *torque motor*, is achieved by using a pair of small wire-wound solenoids, combined with an armature/flapper, which are then placed within a pair of permanent magnets as shown in figure 1.9.



#1
in eco-friendly
attitude

**STUDY AT
LINKÖPING UNIVERSITY, SWEDEN**
RANKED AMONG TOP 50 UNIVERSITIES UNDER 50

Interested in Strategy and Management in International Organisations? Kick-start your career with a master's degree from Linköping University, Sweden.

→ **Click here!**

 **Linköping University**

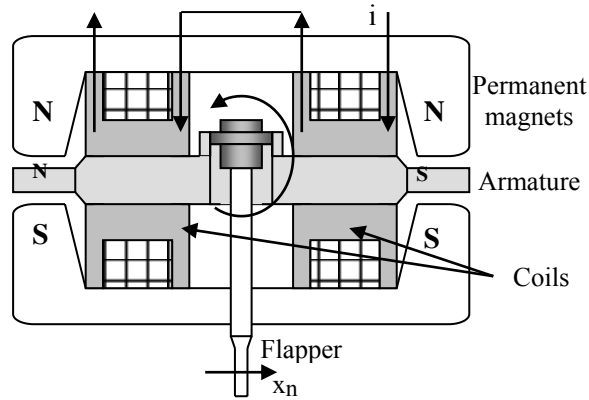


Figure 1.9 The electromagnetic torque motor first stage

Coils may be connected in series, parallel and individually as shown in figure 1.10.

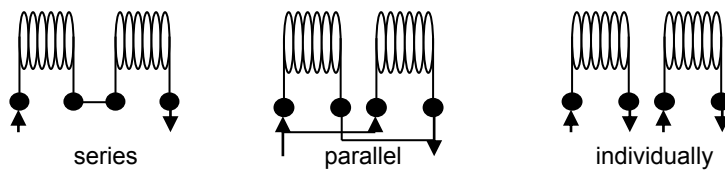


Figure 1.10 Coil pair connections possible

Application of a small current, of the order of mA, then creates an electromagnetic field along the axis of the armature and the generated magnetic poles react with the poles of the permanent magnets. This causes a very small rotation of the armature/flapper and the very small displacement, x_n , at the end of the flapper is used to generate a pressure differential that is applied across the spool to move it.

Consider next how this pressure differential may be generated; two methods discussed here are the flapper/nozzle and the jet pipe. The **flapper/nozzle** stage is the earliest method of generating a pressure differential which is achieved using a pair of very small diameter restrictors, or orifices, either side of the flapper. This resistance bridge is similar to an electrical voltage potential divider and is shown as figure 1.11.

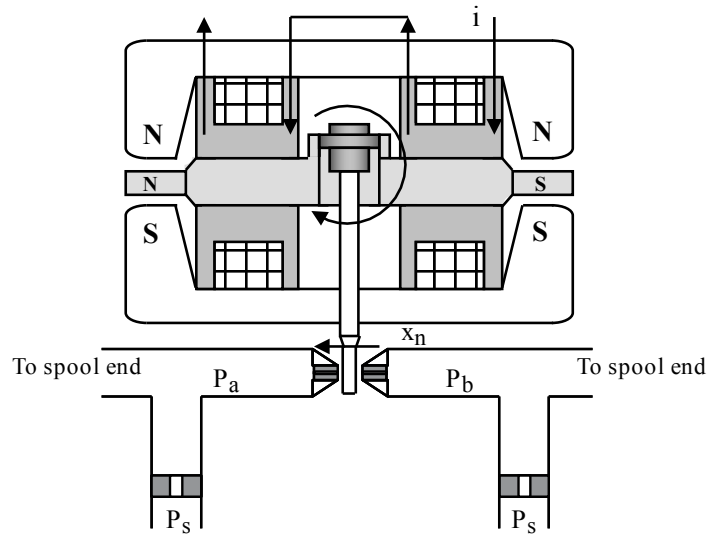


Figure 1.11 The hydraulic first stage flapper/nozzle concept

With the flapper centralised the pressures P_a and P_b are equal and typically around half supply pressure $P_s/2$ although the actual value depends upon the choice of restrictor diameters. A small displacement x_n to the left as shown will increase the nozzle restriction at side 'a' and decrease the nozzle restriction at side 'b'. Consequently pressure P_a will increase and pressure P_b will decrease. The combined effect is that a pressure differential $P_a - P_b$ is generated and is then sensed across the spool. By careful selection of the restrictor diameters and the clearance either side of the flapper a reasonably-linear relationship between pressure differential and torque motor input current can be designed over a good operating range. The normalised characteristic is typically as shown in figure 1.12 and determined using real servovalve data. The maximum pressure differential generated at maximum flapper displacement, for the design parameters selected here, is 80% of the supply pressure.

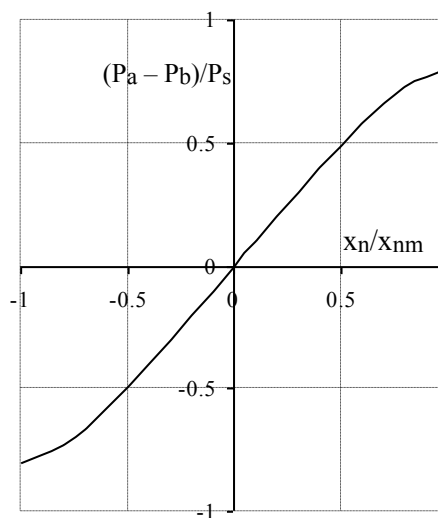


Figure 1.12 A double flapper/nozzle characteristic

Consider next the use of a *jet pipe* rather than a flapper/nozzle to generate the pressure differential as shown in figure 1.13. The jet pipe device is essentially a fluidic device and produces a jet that diverges in width, and height to a smaller extent, due to fluid entrainment as it progresses downstream towards the two receivers, eventually with a Gaussian-type velocity profile in the dominant plane shown.

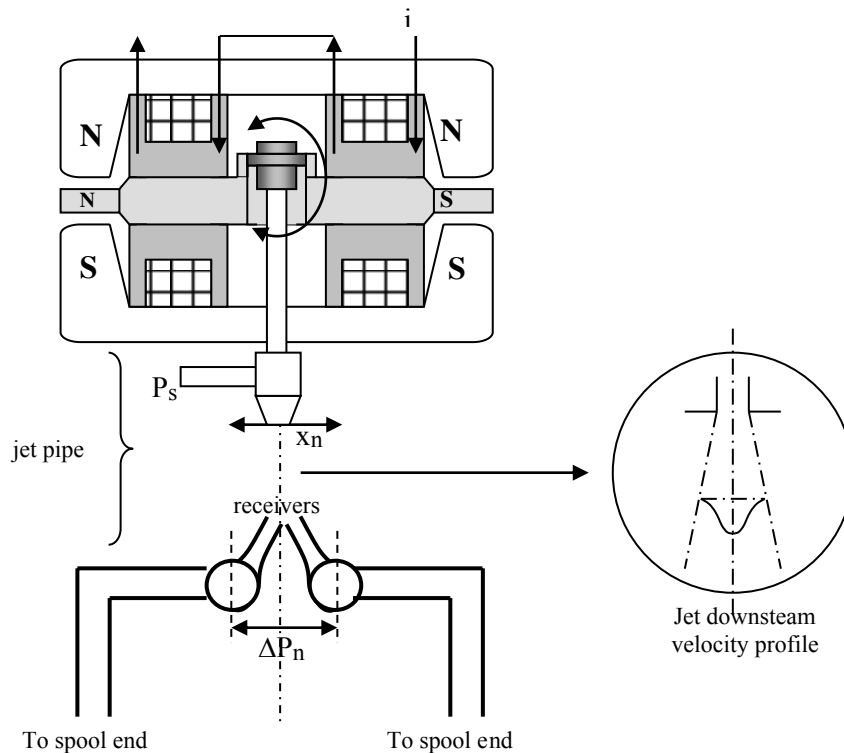


Figure 1.13 The jet pipe concept to generate a pressure differential

Consequently the two receivers, or diffusers, will only collect part of the total flow rate available due to their finite widths. The jet pipe is moved by the torque motor and with the jet pipe at the central, null, condition the pressure recovered in each receiver will be equal with the sum being less than supply pressure due to jet spillage. Analysis of this type of device is difficult due to its complicated practical shape but the pressure differential recovery characteristic will be similar to that shown in figure 1.14, and again calculated using real servovalve data.

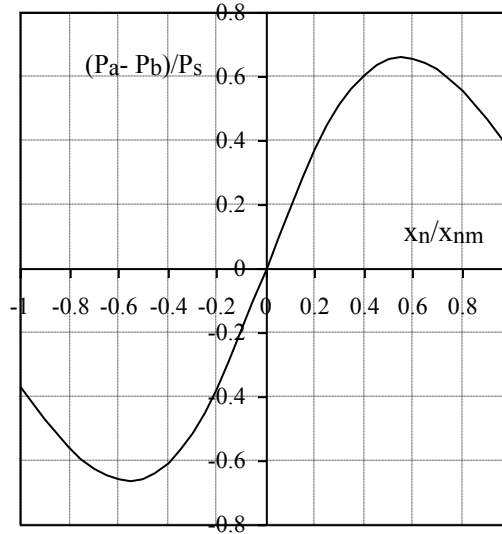


Figure 1.14 Pressure differential for a jet pipe device

This characteristic was derived by the author from a two-dimensional analysis of a typical fluid jet with an established Gaussian velocity profile. The useable near-linear region is much less than for the flapper/nozzle bridge but this type of device is now in commercial use. The maximum pressure recovery may be less than a flapper/nozzle device but a stated advantage of the jet pipe is that it is less susceptible to fluid particle blockage compared with the flapper/nozzle approach.

“I studied English for 16 years but...
...I finally learned to speak it in just six lessons”
Jane, Chinese architect

ENGLISH OUT THERE

Click to hear me talking before and after my unique course download



The *second hydraulic stage is the spool* which is moved by the pressure differential applied across it. Figure 1.15 shows just three common spool designs with circumferential grooves to minimise hydraulic lock. The faces at each port where flow may exist are known as the spool *lands*. Spool lands perfectly matched are known as *critically-lapped lands*. Lands deliberately overcut to minimise flow loss at the null condition are known as *over-lapped lands*, and lands deliberately undercut are known as *under-lapped lands*.

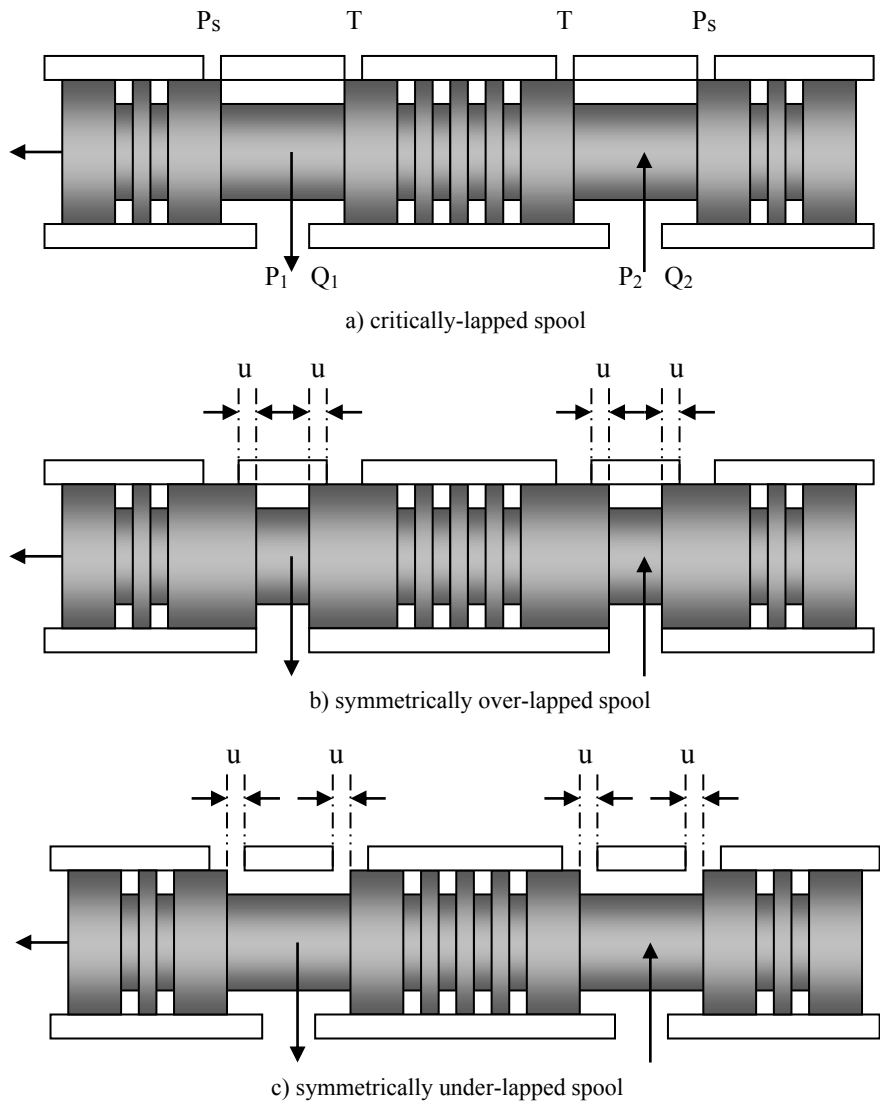


Figure 1.15 Servovalve spool configuration with different land options

In all cases the flow slots machined around the spool sleeve are rectangular and hence the area exposed varies in a linear manner with spool displacement. For perfectly matched, critically-lapped, lands a small displacement of the spool, to the left in figure 1.15, opens supply pressure and allows flow through its port to the load actuator. The return flow from the actuator passes across the return port back to tank. Usually the two tank return ports are internally connected and the two pressure ports are internally connected. In practice a servovalve must be connected to the hydraulic system using a connecting, or manifold, block that is bolted to it. This manifold block will have screwed connection for supply pressure, tank, the two output ports and the valve is termed a 4-way valve.

Historically, the servovalve with spool spring force feedback was then modified to a *servovalve with force feedback*. This still uses the flapper/nozzle concept, but with an added feedback wire that has a ball at its end, the ball fitting into a matched groove around the spool as shown in figure 1.16.

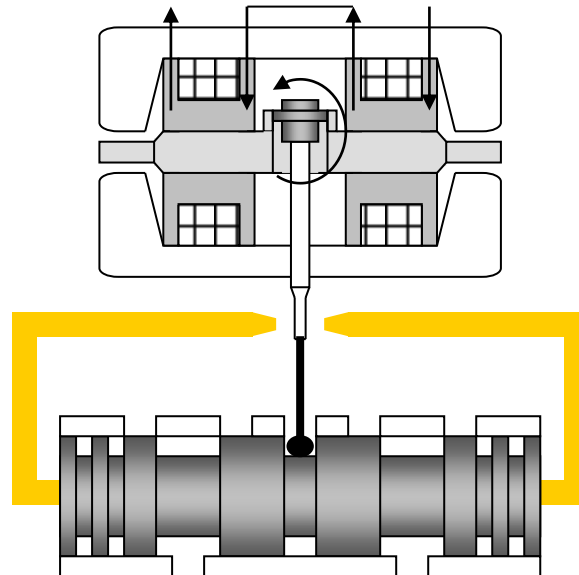


Figure 1.16 Servovalve with force feedback

The ball is typically manufactured from carbide or sapphire, both giving a similar wear characteristic and much better than stainless steel. Furthermore, developments of the ball-in-hole method of retaining the ball, rather than ball-in-slot method shown, has improved reliability and is becoming the preferred approach for a class of servovalves [www.moog.com]. Restrictors used in flapper/nozzle devices can now also be manufactured from sapphire to ensure dimensional accuracy and repeatability together with a significantly improved wear characteristic.

When a current is applied to the servovalve then the flapper is rapidly displaced causing spool displacement. This spool displacement then bends the feedback wire which creates a reacting torque to balance that generated electromagnetically. It can be shown by careful design that when the electromagnetic and mechanical torques are balanced then the flapper returns to its null condition, spool motion stops and the spool displacement becomes proportional to the input current as required. An analysis of the dynamic behaviour of the flapper/nozzle stage is beyond the remit of this book but it does seem that flapper centralisation gives the best dynamic performance. A commercial torque motor design is shown as figure 1.17.

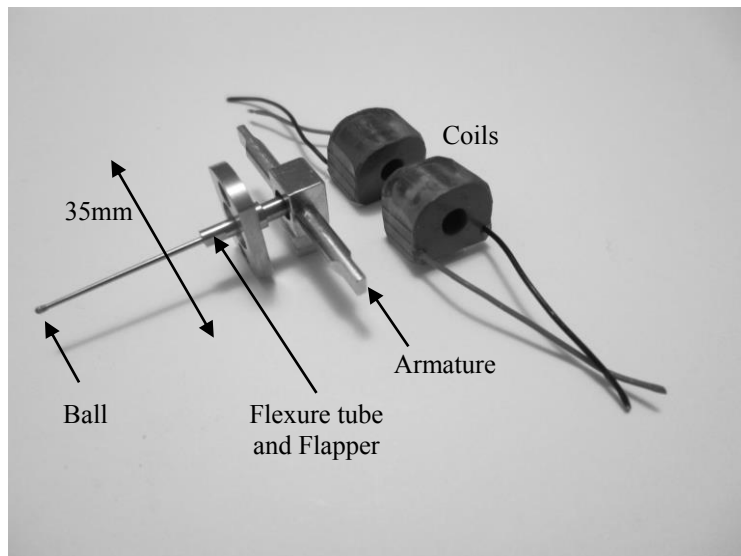


Figure 1.17 A typical torque motor armature/flapper and a pair of coils

The thin-walled flexure tube is actually fixed within the outer tube, having two flat flapper faces, and the unit may be rigidly held while still allowing the desired flexibility of rotation of the flapper and feedback wire. A typical spool and matched bush is shown as figure 1.18 and two of the four-rectangular flow slots for each of the four ports can be seen.

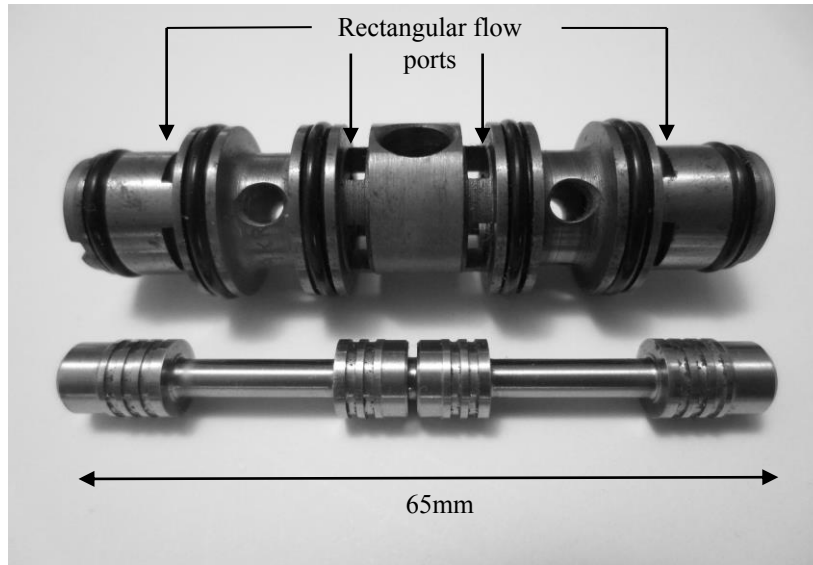


Figure 1.18 A servovalve spool with its matched bush

A photograph of a low flow rate servovalve is shown as figure 1.19 and illustrates how compact the torque motor and flapper/wire assembly has been developed.

Excellent Economics and Business programmes at:



university of
 groningen



**“The perfect start
of a successful,
international career.”**

CLICK HERE
to discover why both socially
and academically the University
of Groningen is one of the best
places for a student to be

www.rug.nl/feb/education



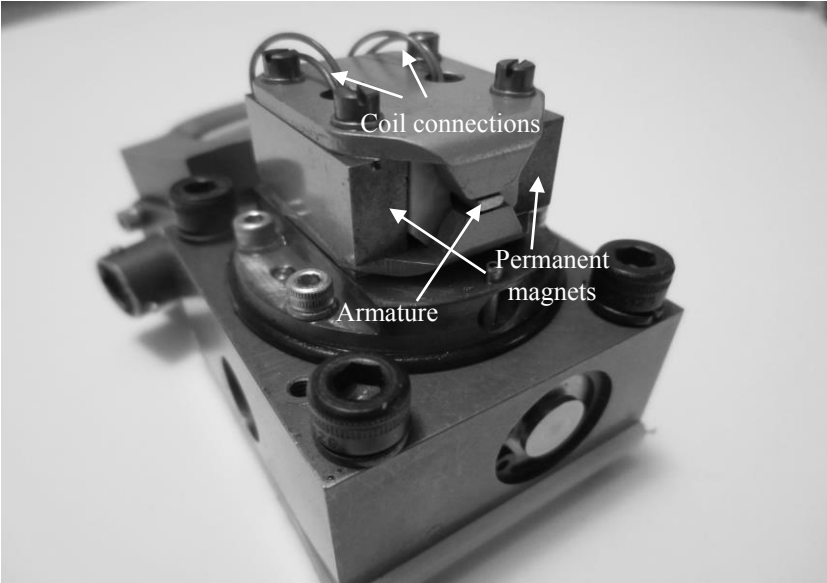


Figure 1.19 A low flow rate servovalve employing force feedback

Figure 1.20 shows an industrial servovalve with force feedback used by the author and bolted to its subplate, or manifold block, allowing conventional hydraulic pipework to be connected to the servovalve. This servovalve forms part of an active suspension test rig, discussed in relation to figure 1.7, and used to position an actuator that represents the road position.

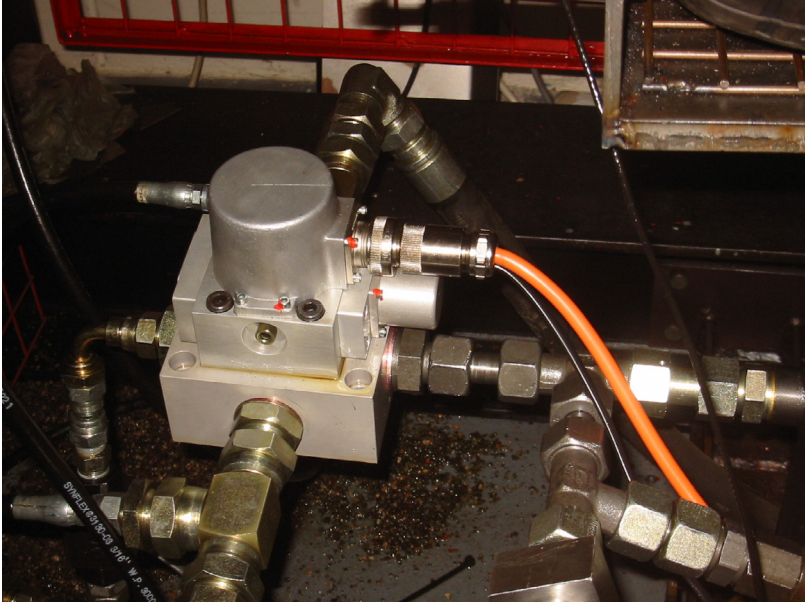


Figure 1.20 Coupling a servovalve to its manifold block

If a **servovalve with a jet pipe is used** then there is no connection between the jet pipe and spool as was the case with the flapper/nozzle/springs or the flapper/nozzle/wire devices previously described. The approach here is to add a spool position sensor and the servovalve is then known as a servovalve with **spool position electrical feedback**. This makes good control sense since the parameter being controlled, spool position, is directly measured. This concept is shown in figure 1.21.

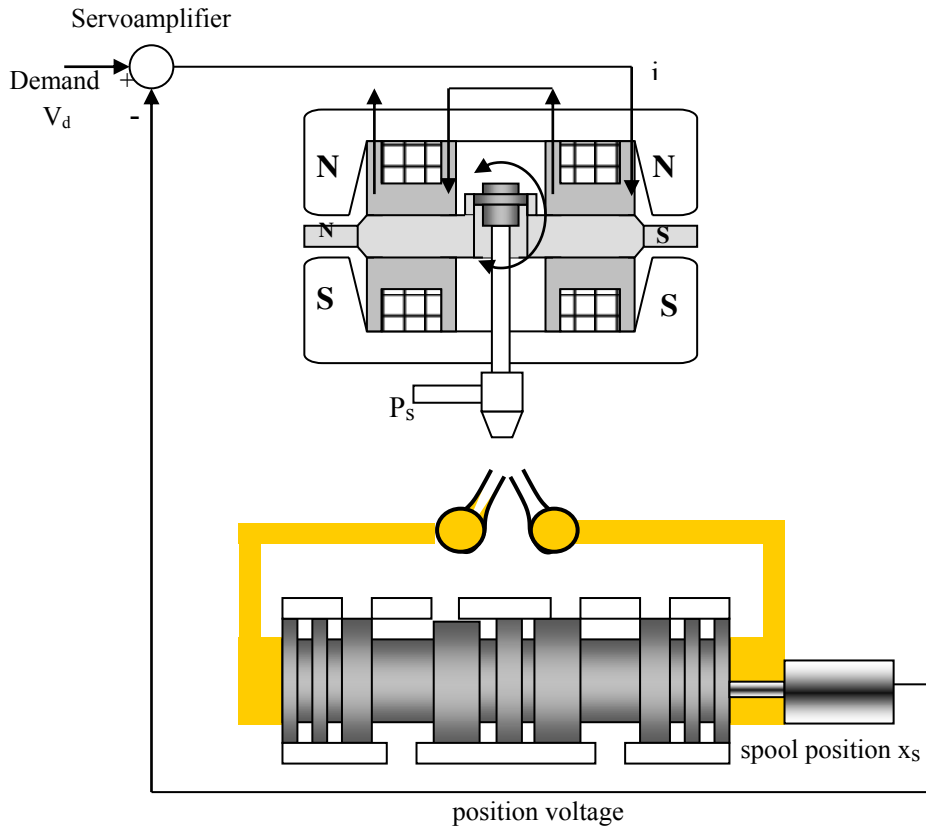
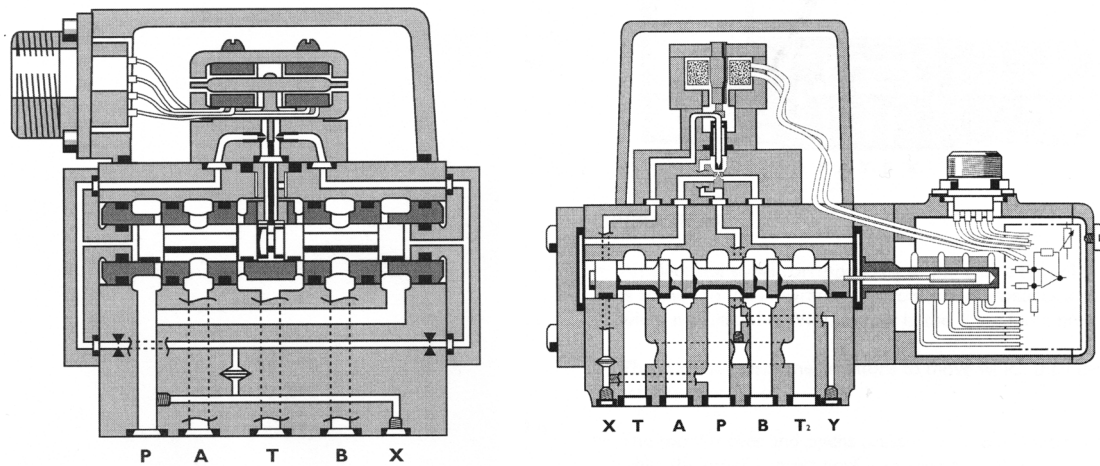


Figure 1.21 The jet pipe concept with spool position electrical feedback

The actual position voltage is compared with its demanded value and the error voltage, when converted to a drive current, is fed to the servovalve torque motor. The nature of this control loop has a zero steady state error when the spool achieves its demanded position. Since the error signal to move the jet pipe is now zero then the jet pipe is centralised in a similar way to a servovalve with force feedback described earlier.

A vast range of servovalves are commercially available and just two servovalves from the range manufactured by Moog are shown as figure 1.22. The first shown is the flapper/nozzle pilot and force feedback type and the second is the jet-pipe pilot and spool position feedback type.




a) flapper/nozzle with force feedback

b) jet pipe with spool position electrical feedback

Figure 1.22 Two types of servovalve designs [www.moog.com]

Another design of servovalve is also available and is called a **direct-drive proportional valve**. In this type of design a **linear force motor**, actually a permanent magnet differential motor with spring return, is used as shown in figure 1.23.



In the past four years we have drilled

89,000 km


That's more than **twice** around the world.

Who are we?
 We are the world's largest oilfield services company¹.
 Working globally—often in remote and challenging locations—we invent, design, engineer, and apply technology to help our customers find and produce oil and gas safely.

Who are we looking for?
 Every year, we need thousands of graduates to begin dynamic careers in the following domains:

- Engineering, Research and Operations
- Geoscience and Petrotechnical
- Commercial and Business

What will you be?



Schlumberger

¹Based on Fortune 500 ranking 2011. Copyright © 2015 Schlumberger. All rights reserved.



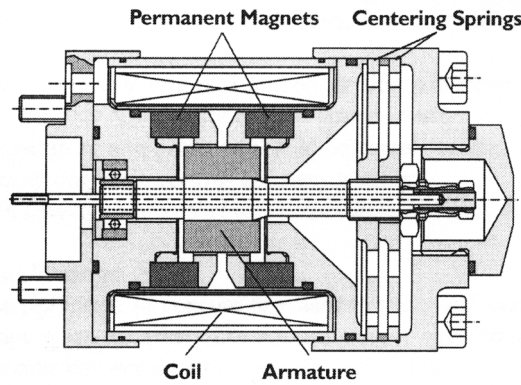


Figure 1.23 A linear force motor [www.moog.com]

The motor is a pair of high energy rare earth magnets and without an input current the magnets and springs hold the armature at equilibrium. When an input current is applied to the coil with one polarity the flux in one of the air gaps surrounding the magnets is increased, cancelling out the flux in the other. This non-equilibrium condition allows the armature to move in the direction of the stronger flux. The armature is moved in the opposite direction by changing the polarity of the input current in the coil [www.moog.com]. More force is generated when compared with a conventional solenoid, for example as used for the directional valve shown in figure 1.2, and at a significantly lower drive current. Figure 1.24 shows how a linear force motor is combined within the hydraulic stage of the valve. The spool is connected to the force motor armature and the displacement of the spool is proportional to the input current applied.

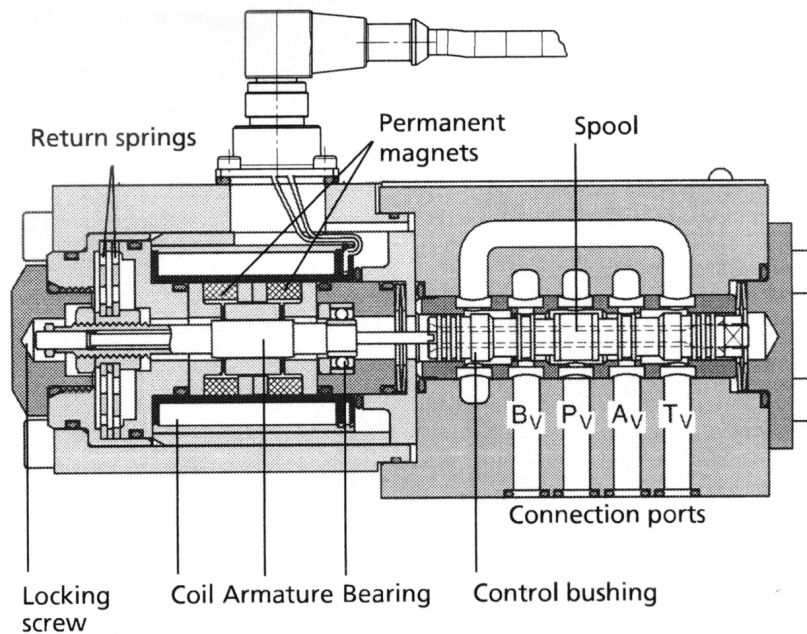
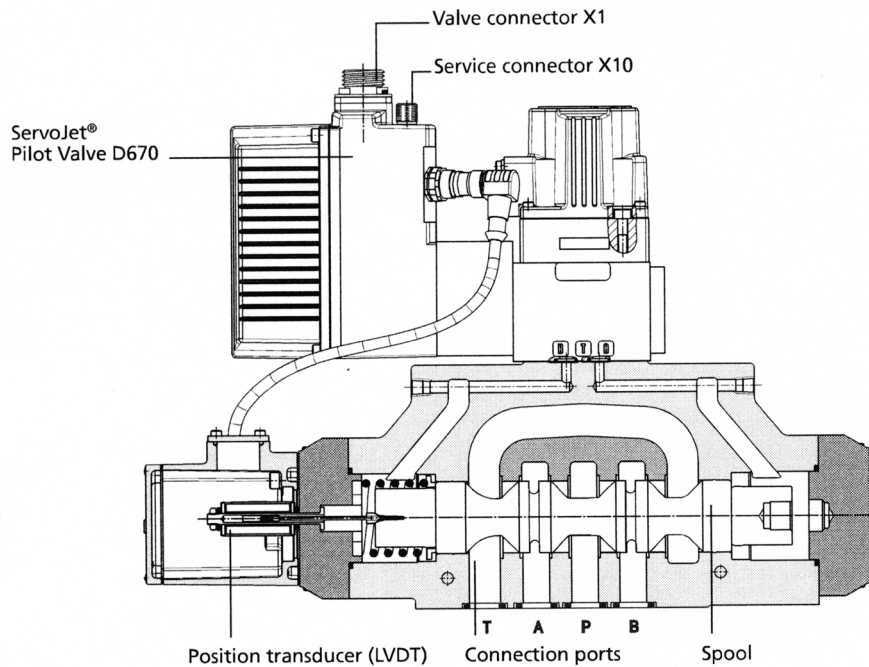
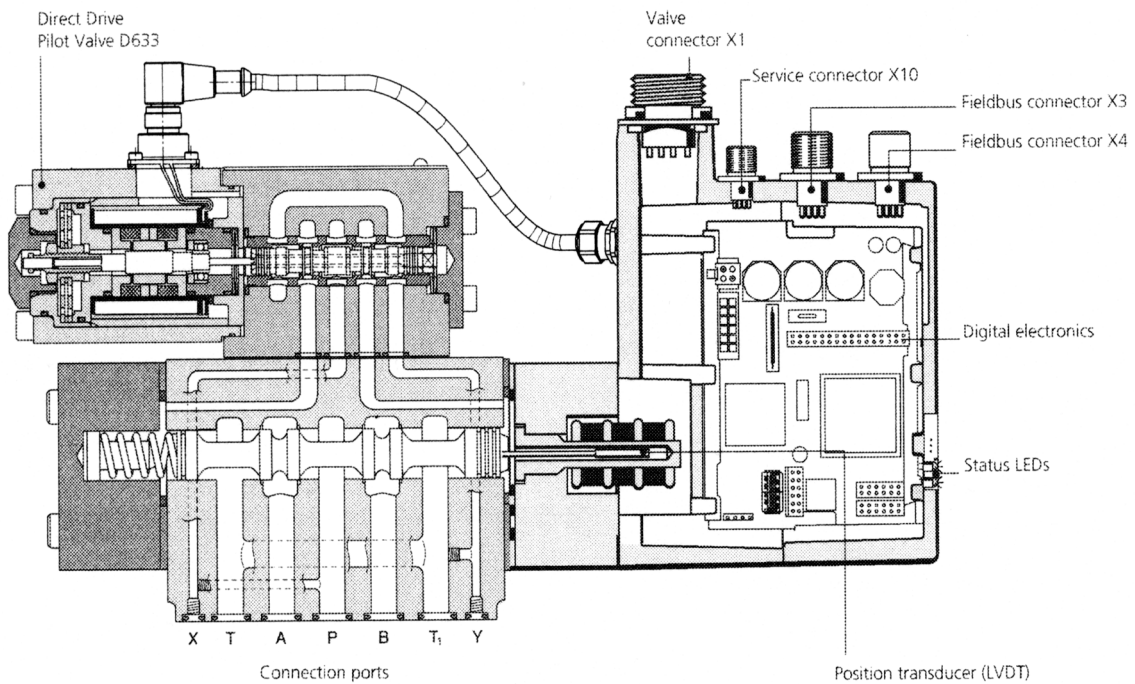


Figure 1.24 Direct drive servovalve with return springs [www.moog.com]

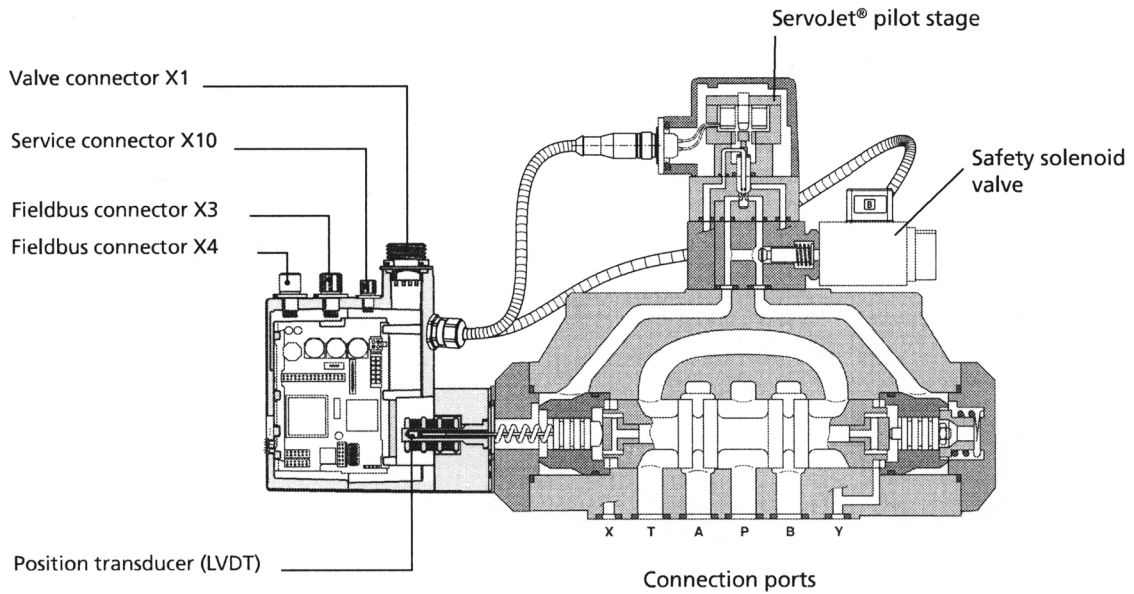
For more advanced applications for example requiring higher flow rates than from a single-state servovalve, distributed control via fieldbus, or with added control functions then there are many other servovalves available. For example figure 1.25 shows just a few that illustrate a multi-stage valve, digital electronics and field bus facilities, and the addition of safety facilities.



a) Three-stage digital servovalve with servo-jet pilot valve and spool position feedback



b) Two-stage digital servovalve with direct drive servo-jet pilot valve, spool position feedback, digital electronics and field bus facility



c) Two-stage proportional servovalve with servo-jet pilot valve, spool position feedback, field bus management and with safety requirements

Figure 1.25 Some more advanced servovalves for different applications [www.moog.com]

Pressures up to typically 350bar are standard but flow rates up to 3500l/min can now be generated, of course with very large diameter spools, with an indication from one manufacturer that this value can be increased for special applications. This does indicate how progress has been made in servovalve control technology since its introduction in the early 1950s.

2 Servovalve flow characteristics

2.1 Aim

This chapter aims to introduce the reader to the basic servovalve flow rate characteristics for steady-state behaviour by introducing a number of objectives as follows:

- to consider the origin of the basic flow rate equations
- to consider the different types of common spool lands
- to develop the linearised flow rate equations for later use in systems dynamic analysis
- to illustrate performance by worked examples

2.2 Servovalve flow characteristics, critically-lapped spool

To understand the flow rate characteristic it is necessary to consider the steady-state flow rate through each port. Consider therefore a cross section through a servovalve shown as figure 2.1. The spool is *critically-lapped* such that the smallest spool movement causes the ports to open.

To determine the flow characteristics in practice the output ports are connected via a restrictor valve that may be manually adjusted. Notice the flow meter placed in the load line to measure the flow rate.



American online
LIGS University
is currently enrolling in the
Interactive Online **BBA, MBA, MSc,**
DBA and PhD programs:

- ▶ enroll **by September 30th, 2014** and
- ▶ **save up to 16%** on the tuition!
- ▶ pay in 10 installments / 2 years
- ▶ Interactive Online education
- ▶ visit www.ligsuniversity.com to find out more!

Note: LIGS University is not accredited by any nationally recognized accrediting agency listed by the US Secretary of Education. More info [here](#).



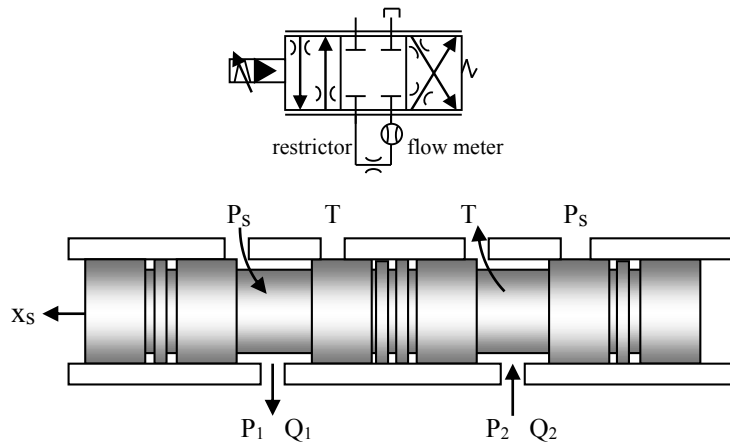


Figure 2.1 A servovalve with critically-lapped ports having equal flow rates

Each port around the spool bush that houses the spool is machined as a group of rectangular slots, typically four, and equally-spaced around the spool bush periphery. Because the spool movement is usually very small then the flow rate equation across the ostensibly-matched ports obeys the Bernoulli form of flow equation.

$$Q = C_f \text{ area} \sqrt{\frac{2 \Delta p}{\rho}} \tag{2.1}$$

where C_f is a flow coefficient to represent losses, ρ is the fluid density and Δp is the pressure drop across the port. Given that the flow area is proportional to spool displacement, which is also designed to be proportional to servovalve current, then equation (2.1) may be written:

$$Q = k_f i \sqrt{\Delta P} \tag{2.2}$$

In practice spool displacement cannot respond immediately to a change in current; there must be a dynamic effect which may have to be considered in some applications and will be discussed further in Chapter 4.

Considering figure 2.1 then from equation (2.2) the steady-state flow rate equations for a servovalve become:

$$\begin{aligned} Q_1 &= k_f i \sqrt{P_s - P_1} & Q_2 &= k_f i \sqrt{P_2} & i > 0 \\ & & & & (2.3) \\ Q_1 &= k_f i \sqrt{P_1} & Q_2 &= k_f i \sqrt{P_s - P_2} & i < 0 \end{aligned}$$

If the ports are connected via a load restrictor, as shown in figure 2.1, then $Q_1 = Q_2$ and from equation (2.3):

$$P_1 + P_2 = P_s \tag{2.4}$$

The **load pressure differential** is defined as:

$$P_\ell = P_1 - P_2 \quad (2.5)$$

It then follows that for **connected ports**, or for **ports with equal flows** into and out of the load actuator, then:

$$Q = Q_1 = Q_2 = k_f i \sqrt{\frac{P_s - P_\ell}{2}} \quad (2.6)$$

$$P_1 = \frac{P_s + P_\ell}{2} \quad P_2 = \frac{P_s - P_\ell}{2}$$

That is, as the load is increased then side 1 pressure increases and side 2 pressure decreases by the same amount. With no load then the pressures on either side are equal to half the supply pressure. This is a good practical test to see how the actual servovalve varies from the ideal design. Developing the non-dimensional form of (2.6) then gives:

$$\bar{Q} = \frac{Q}{k_f i_{\max} \sqrt{P_s/2}} = \bar{i} \sqrt{1 - \bar{P}_\ell} \quad \bar{i} = \frac{i}{i_{\max}} \quad \bar{P}_\ell = \frac{P_\ell}{P_s} \quad (2.7)$$

A plot of equation (2.7) is shown as figure 2.2 for a positive current and a positive load pressure differential only. For negative currents then the flow rate is reversed. Also shown is a typical operating point at a particular flow rate, current and load pressure differential.

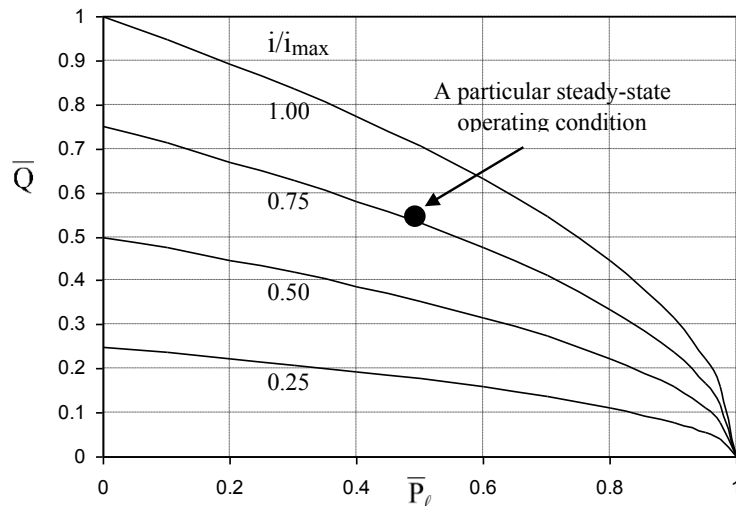


Figure 2.2 Flow characteristic for a critically-lapped spool


It can be seen from figure 2.2 or equation (2.7) that the flow rate increases with increasing current but decreases with increasing load pressure.

One way of looking at the non-linear flow characteristic is to consider **small variations about a particular steady-state operating point** $i(o)$, $P_\ell(o)$, $Q(o)$ and the process is called **linearisation** of the non-linear flow rate equation into a linear equation. This is useful when considering system dynamics, as will be pursued later. For small variations of current, δi , and small variations in load pressure, δP_ℓ , then using the first two linear terms of the Taylor series expansion of equation (2.6) gives the approximate small change in flow rate δQ as follows:

$$Q(o) + \delta Q = Q(o) + \frac{\partial Q}{\partial i} \delta i + \frac{\partial Q}{\partial P_\ell} \delta P_\ell \quad (2.8)$$

$$\delta Q = k_{qi} \delta i - k_{qp} \delta P_\ell$$

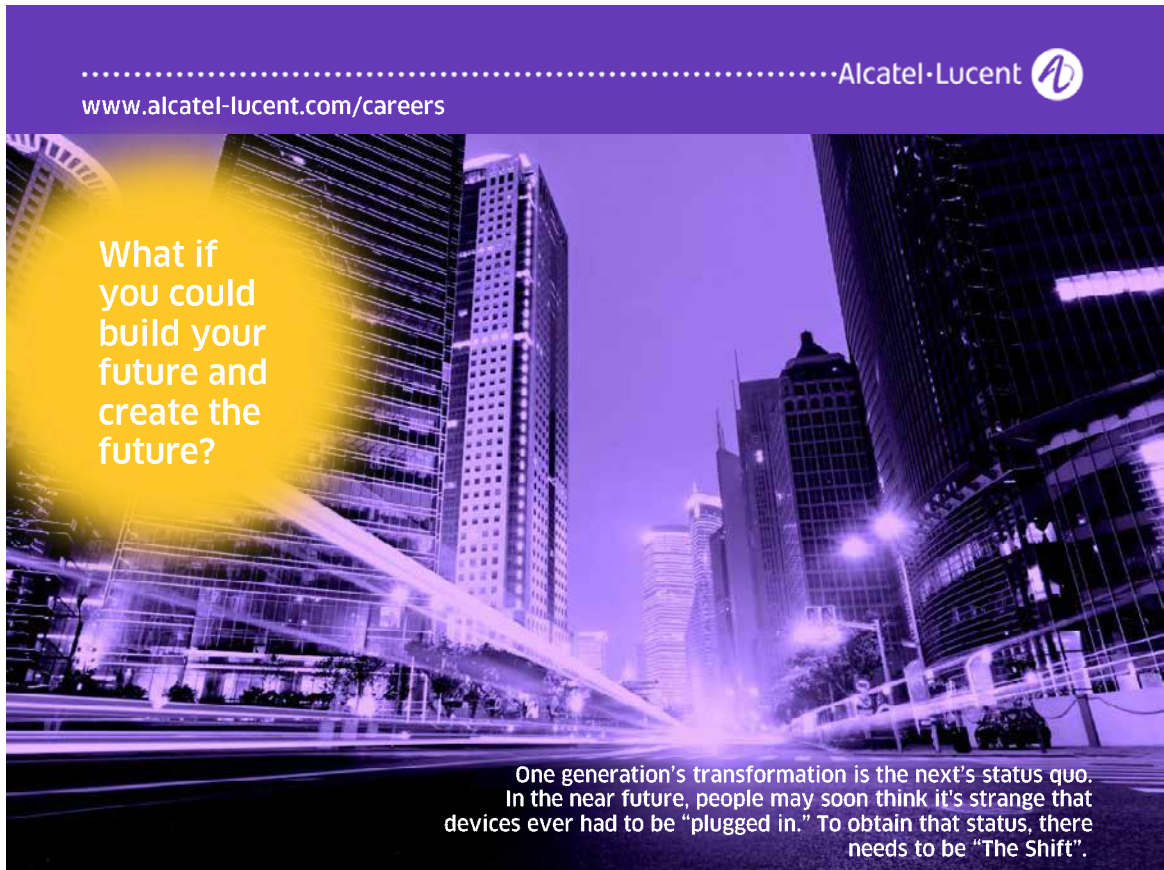
k_{qi} is the flow gain and k_{qp} is the pressure gain.

.....Alcatel-Lucent 

www.alcatel-lucent.com/careers

What if you could build your future and create the future?

One generation's transformation is the next's status quo. In the near future, people may soon think it's strange that devices ever had to be "plugged in." To obtain that status, there needs to be "The Shift".



These linearised coefficients k_{qi} and k_{qp} are determined from the partial differentials evaluated at the operating point $i(o)$, $P_\ell(o)$, $Q(o)$:

$$\text{flow gain } k_{qi} = \frac{\partial Q}{\partial i} = k_f \sqrt{\frac{P_s - P_\ell(o)}{2}} = \frac{Q(o)}{i(o)} \tag{2.9}$$

$$\text{pressure gain } k_{qp} = -\frac{\partial Q}{\partial P_\ell} = \frac{k_f i(o)}{2\sqrt{2[P_s - P_\ell(o)]}} = \frac{Q(o)}{2[P_s - P_\ell(o)]} \tag{2.10}$$

$$\text{servovalve resistance } R_{sv} = \frac{1}{k_{qp}} \tag{2.11}$$

A further coefficient that is useful is the pressure sensitivity k_{pi} defined as:

$$\text{pressure sensitivity } k_{pi} = \frac{\partial P}{\partial i} = -\frac{\frac{\partial Q}{\partial i}}{\frac{\partial Q}{\partial P_\ell}} = \frac{k_{qi}}{k_{qp}} = \frac{2[P_s - P_\ell(o)]}{i(o)} \tag{2.12}$$

At the **null condition** $i(o) = 0$, $P_\ell(o) = 0$ and the linearised coefficients become:

$$\begin{aligned} \text{flow gain } k_{qi} &= k_f \sqrt{\frac{P_s}{2}} \\ \text{pressure gain } k_{qp} &= 0 \end{aligned} \tag{2.13}$$

$$\text{servovalve resistance } R_{sv} = \infty$$

From a practical test on a servovalve, its flow/current characteristic at the null condition may be used to determine the valve flow constant k_f from the measured flow gain.

2.3 Servovalve flow characteristics, under-lapped spool

Now consider the **symmetrically under-lapped spool** shown as figure 2.3 with a spool small displacement within the region of under-lap.

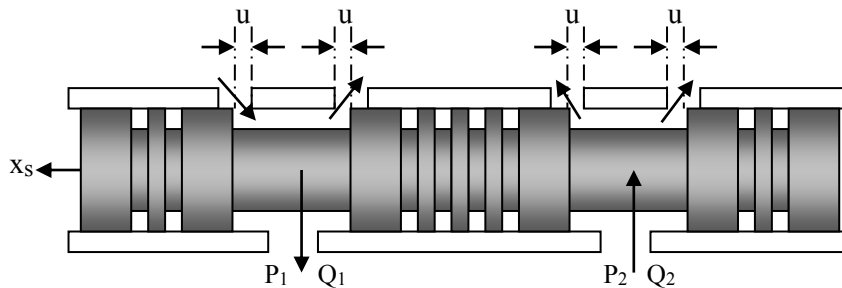


Figure 2.3 A symmetrically under-lapped spool with a small spool displacement within the under-lap region

Each port now has three paths, in, out, and leakage back to tank. As with the previous case of a critically-lapped spool, each port is assumed to have identical flow rate characteristics for each port. The flow rate equations *within the under-lap region only* are now as follows for a positive current and the direction convention shown:

$$Q_1 = k_f(i_u + i)\sqrt{P_s - P_1} - k_f(i_u - i)\sqrt{P_1} \quad (2.14)$$

$$Q_2 = k_f(i_u + i)\sqrt{P_2} - k_f(i_u - i)\sqrt{P_s - P_2}$$

It will be clear from (2.14) that when $Q_1 = Q_2$ then the sum of line pressure equals the supply pressure, just as in the case for a critically-lapped spool. The flow rate equation then becomes:

$$Q = k_f(i_u + i)\sqrt{\frac{P_s - P_\ell}{2}} - k_f(i_u - i)\sqrt{\frac{P_s + P_\ell}{2}} \quad (2.15)$$

$$P_1 + P_2 = P_s$$

In non-dimensional terms equation (2.15) becomes:

$$\bar{Q} = \frac{Q}{k_f i_u \sqrt{P_s/2}} = (1 + \bar{i})\sqrt{1 - \bar{P}_\ell} - (1 - \bar{i})\sqrt{1 + \bar{P}_\ell} \quad \bar{i} = \frac{i}{i_u} \quad \bar{P}_\ell = \frac{P_\ell}{P_s} \quad (2.16)$$

This non-dimensional flow characteristic is shown as figure 2.4, again for positive current and for spool displacements only within the underlap region. Beyond the region of underlap then the flow equation obeys the conventional critically-lapped form previously discussed. Given that in reality any inherent, or deliberately-machined, under-lap will be very small then flow rates given by equation (2.16) will also be very small.

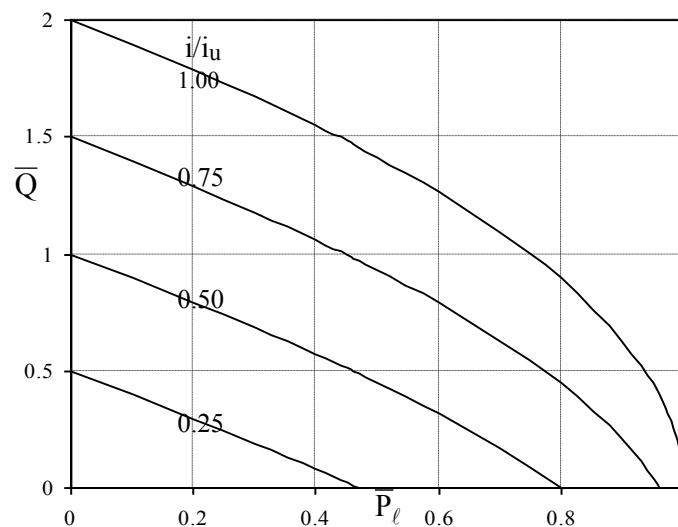


Figure 2.4 Flow characteristic for a symmetrically under-lapped spool servovalve and for spool displacements within the region of under-lap

Note that the flow rate may be zero for a finite load pressure and a finite servovalve current. This leads to the conclusion that:

“A position control system can have a steady-state error if the servovalve spool is symmetrically under-lapped. It can be made zero, or significantly minimised, by the selection of an appropriate load condition”

This will be pursued later. The linearised coefficients may be easily be derived for the under-lapped spool by considering the appropriate partial differentials of equation (2.15) in the same way as for the critically-lapped spool. These are not presented here in full but at the the **null condition** $i(o) = 0$, $P_e(o) = 0$, the linearised coefficients are compared for the two types of spool lands:

<i>critically-lapped spool</i>	<i>under-lapped spool</i>
flow gain $k_{qi} = k_f \sqrt{\frac{P_s}{2}}$	flow gain $k_{qi} = 2k_f \sqrt{\frac{P_s}{2}}$
pressure gain $k_{qp} = 0$	pressure gain $k_{qp} = \frac{k_f i_u}{\sqrt{2P_s}}$
pressure sensitivity $k_{pi} = \infty$	pressure sensitivity $k_{pi} = \frac{2P_s}{i_u}$



**Join the best at
the Maastricht University
School of Business and
Economics!**

Top master's programmes

- 33rd place Financial Times worldwide ranking: MSc International Business
- 1st place: MSc International Business
- 1st place: MSc Financial Economics
- 2nd place: MSc Management of Learning
- 2nd place: MSc Economics
- 2nd place: MSc Econometrics and Operations Research
- 2nd place: MSc Global Supply Chain Management and Change

Sources: Keuzegids Master ranking 2013; Elsevier 'Beste Studies' ranking 2012; Financial Times Global Masters in Management ranking 2012

Maastricht University is the best specialist university in the Netherlands
(Elsevier)

Visit us and find out why we are the best!
Master's Open Day: 22 February 2014

www.mastersopenday.nl



Two important conclusions arise as follows:

- the pressure gain and pressure sensitivity are now finite and note that the **flow gain is double that for a critically-lapped valve** as given earlier by equation (2.13). This may be practically used to identify whether or not a servovalve spool has under-lap
- a servovalve will have a flow rate loss at the null condition and therefore a **servovalve with under-lap has a finite resistance at the null condition**. A finite resistance implies damping and advantageous during dynamic operation, although in practice it may only have a minor effect

The three types of land laps may now be compared using the idealised flow/current graph shown schematically in figure 2.5. The flow characteristics are idealised since the transition from under/over-lap to critical-lap is smooth in practice, but any change around zero current is usually identifiable. Note that in figure 2.5 the under-lap/over-lap region is not to a realistic scale.

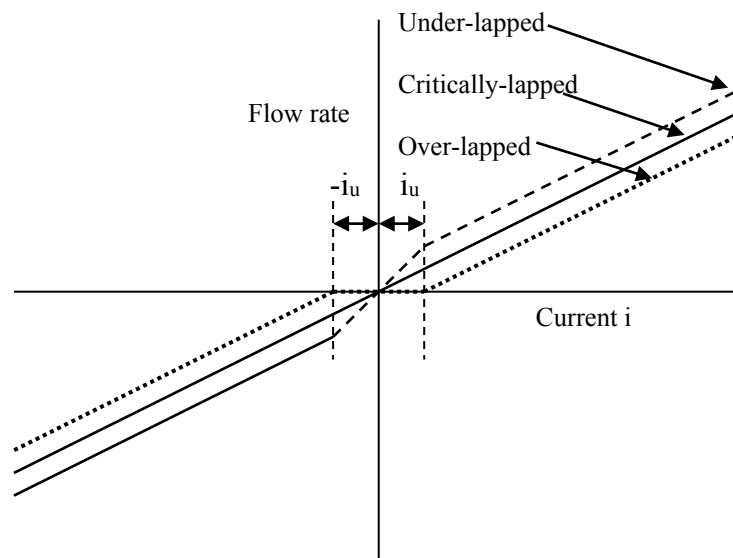


Figure 2.5 A comparison of land laps on the flow characteristic

2.4 Valve rating

A servovalve manufacturer will specify the steady-state flow rate capability of a servovalve in terms of the **rated flow**, Q_{rated} . This is specified in relation to the **rated current**, i_{rated} , and for a **valve total pressure drop of $\Delta p = 70\text{bar}$** across the two ports.

Total pressure drop across the two ports $\Delta P = (P_s - P_1) + (P_2 - 0)$

$$\Delta P = P_s - P_\ell \quad (2.18)$$

where $P_\ell = P_1 - P_2$ is the load pressure. But by definition of valve rating then $\Delta P = 70\text{bar}$ and therefore:

$$\text{At the valve rating } P_s - P_\ell = 70\text{bar} \quad (2.19)$$

Using the valve rated flow specified by the manufacturer then the flow at any other supply pressure, load pressure and current is obtained from equation (2.6), for a critically-lapped valve, to give:

$$\frac{Q}{Q_{\text{rated}}} = \frac{i}{i_{\text{rated}}} \sqrt{\frac{P_s - P_\ell}{70}} \quad (2.20)$$

2.5 Servo valve specification by the manufacturer

A consideration of the way a manufacturer specifies servo valve performance is now appropriate. The data provided will be typically as follows:

General

- class of protection
- temperature range, for example $-30^\circ\text{C} \rightarrow 130^\circ\text{C}$
- recommended fluid and viscosity
- filtration, filter rating, cleanliness including ISO class
- installation and vibration data, for example up to 30g at all axes

Specific, steady-state

- operating pressure, for example 14bar \rightarrow 315bar
- proof pressure, for example 470bar at P port or 310bar at T port
- type of pilot stage and optional connection
- rated flow @ 70bar valve pressure drop
- rated flow tolerance, for example $\pm 10\%$
- symmetry, for example $< 10\%$
- threshold, for example $< 0.5\%$ typically measure at a supply pressure of 210bar
- hysteresis, for example $< 3\%$ typically measure at a supply pressure of 210bar
- null shift, typically $< 2\%$ and temperature specified
- dimensions
- electrical connection data
- internal leakage data, for example $< 4\%$ of the rated flow rate

Specific, dynamic

- frequency response in graphical form and for two different signal amplitudes, for example at rated current and 40% rated current
- step response in graphical form for different flow rates



> Apply now

REDEFINE YOUR FUTURE
**AXA GLOBAL GRADUATE
PROGRAM 2015**

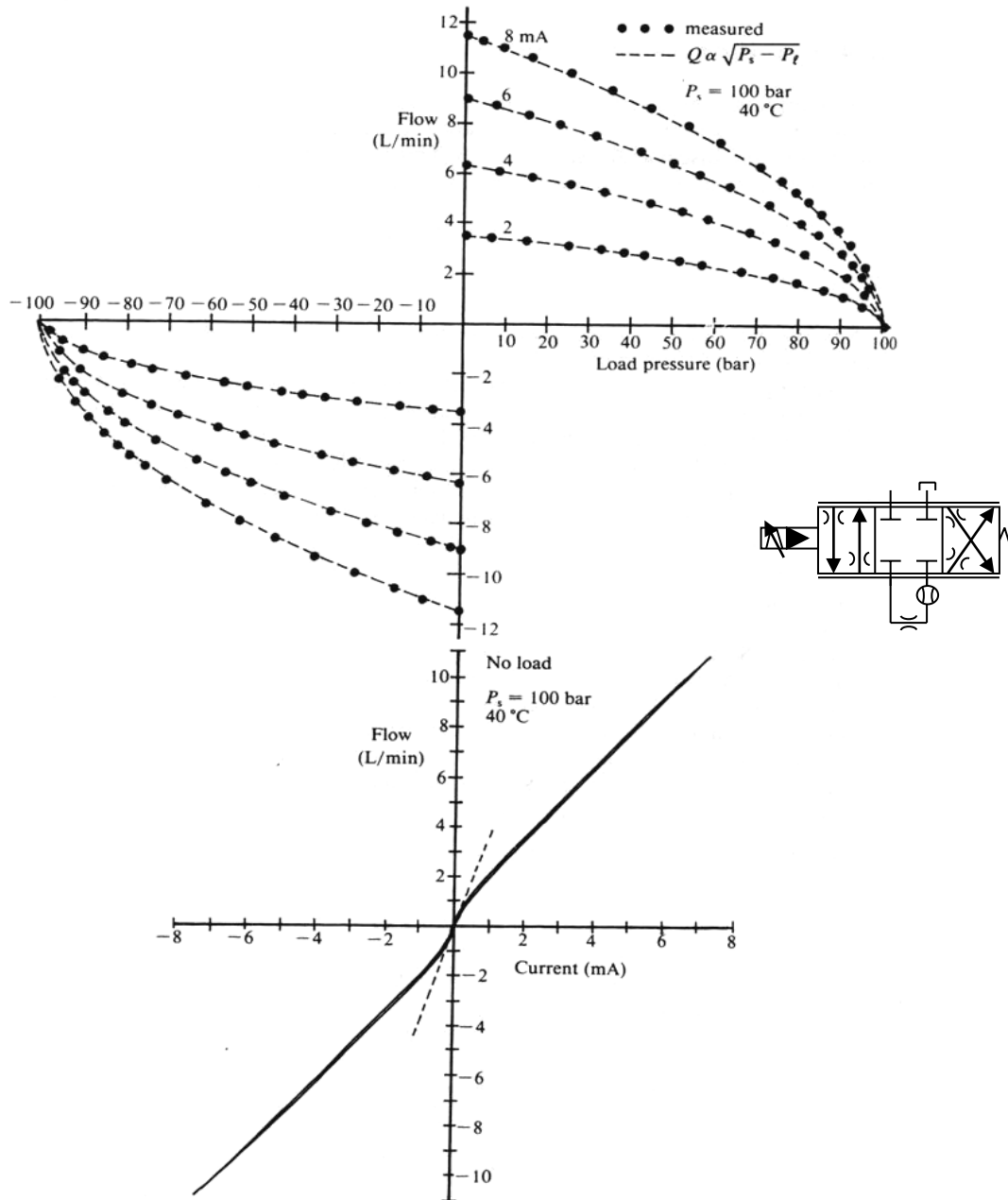
redefining / standards 

agence.cdg © Photonostop



Example 2.1

A servovalve flow characteristic for a flapper/nozzle and force feedback servovalve with ports connected using a variable restrictor, and measured by the author, is as shown.



Notice how the fitted square root characteristic matches extremely well over the measurement range although measurements at very low current is difficult in practice due to the resolution of the flow meter electronic measuring sensor used at the correspondingly-low flow rates.

It can be seen that the characteristic around zero current is not linear. The doubling of flow gain compared with higher currents shows that the spool lands have a small under-lap.

From the data the flow gain k_{qi} when $P_\ell = 0$ may be used to determine the flow constant k_f . Note that away from the very small under-lap zone the valve spool behaves like a critically-lapped spool and the appropriate flow gain must be used.

i) From the first graph at zero load and assuming data out of the under-lap region:

$$Q = Q_1 = Q_2 = k_f i \sqrt{\frac{P_s - P_\ell}{2}}$$

$$k_{qi} = \frac{\partial Q}{\partial i} = k_f \sqrt{\frac{P_s}{2}} \quad @ P_\ell = 0$$

$$\frac{(11.6 - 0)}{(8 - 0)} = k_f \sqrt{\frac{100}{2}} \rightarrow k_f = 0.21$$

ii) This is more accurate than using the second graph which gives approximately:

$$\text{For the range } 0 \rightarrow 10\text{mA} \quad k_{qi} = k_f \sqrt{\frac{P_s}{2}} \quad \frac{(10 - 0)}{(6.5 - 0)} = k_f \sqrt{\frac{100}{2}}$$

$$k_f \approx 0.22$$

$$\text{For the range } 4 \rightarrow 10\text{mA} \quad k_{qi} = k_f \sqrt{\frac{P_s}{2}} \quad \frac{(10 - 4)}{(6.5 - 2.4)} = k_f \sqrt{\frac{100}{2}}$$

$$k_f \approx 0.21$$

Accept that $k_f = 0.21$ under-lap $i_u \approx \pm 0.33\text{mA}$

2.6 Maximum power transfer to the load and selection of supply pressure


Maximum power to the load means that the load may be accelerated at its maximum value, if this is desired. Since hydraulic power is defined as flow rate multiplied by pressure then, assuming that the flow into the load actuator is the same as the flow out of the load actuator and also a critically-lapped spool, then equation (2.6) applies giving:

$$\text{Power to load } W = P_\ell Q = [P_\ell] \left[k_f i \sqrt{\frac{P_s - P_\ell}{2}} \right] \quad (2.21)$$

This power transfer is independent of the actuator speed for an ideal system with no flow losses and mechanical losses. It can be seen from equation (2.21) that the power at a particular current varies from zero when $P_\ell = 0$ through to a maximum value and then back to zero when the load pressure equals supply pressure $P_\ell = P_s$. Differentiating (2.21) with respect to load pressure and equating to zero to find the condition of maximum power transfer gives:

$$P_s = 1.5 P_\ell \quad Q = k_f i \sqrt{\frac{P_s}{6}} \quad (2.22)$$

So, select a supply pressure 50% higher than the load pressure to give maximum steady-state power transfer. In practice this rule is generally used to also provide sufficient supply power to overcome the load steady-state and dynamic requirement.



Empowering People. Improving Business.

BI Norwegian Business School is one of Europe's largest business schools welcoming more than 20,000 students. Our programmes provide a stimulating and multi-cultural learning environment with an international outlook ultimately providing students with professional skills to meet the increasing needs of businesses.

BI offers four different two-year, full-time Master of Science (MSc) programmes that are taught entirely in English and have been designed to provide professional skills to meet the increasing need of businesses. The MSc programmes provide a stimulating and multi-cultural learning environment to give you the best platform to launch into your career.

- MSc in Business
- MSc in Financial Economics
- MSc in Strategic Marketing Management
- MSc in Leadership and Organisational Psychology

BI NORWEGIAN BUSINESS SCHOOL

EFMD **EQUIS ACCREDITED**

www.bi.edu/master

Example 2.2

Select a servo valve for an application with a linear actuator size and speed requiring a flow rate of 20 litres/min at a load pressure differential of 120 bar. A particular servo valve model has a range of sizes defined by the following rated flows:

- a) 4 litres/min
- b) 10 litres/min
- c) 19 litres/min
- d) 38 litres/min
- e) 63 litres/min

The rated current is ± 20 mA for series connected coils.

Minimum supply pressure 14 bar

Maximum supply pressure 315 bar

Select a supply pressure to ensure optimum power transfer such that $P_s = 1.5P_\ell$.

$$P_s = 1.5 \times 120 = 180 \text{ bar}$$

Comparing the flow rate to the rated flow rate at the same rated current gives:

$$\frac{Q}{Q_{\text{rated}}} = \sqrt{\frac{P_s - P_\ell}{70}}$$

$$\frac{20}{Q_{\text{rated}}} = \sqrt{\frac{180 - 120}{70}} \rightarrow Q_{\text{rated}} = 21.6 \text{ litres/min}$$

Therefore it is possible to select:

- Servo valve c) is just less than the flow required
- Servo valve d) may be used at around 57% of the rated current
- Servo valve e) may also be used at around 34% of the rated current.

It is better to use as much current as possible over the maximum flow range experienced. Therefore use servo valve c) but change the supply pressure to maximise current while maintaining optimum power transfer such that $P_s = 1.5P_\ell$.

$$\frac{Q}{Q_{\text{rated}}} = \sqrt{\frac{P_s - P_\ell}{70}} = \sqrt{\frac{P_s - 2P_\ell / 3}{70}} = \sqrt{\frac{P_s}{210}}$$

$$\frac{20}{19} = \sqrt{\frac{P_s}{210}} \rightarrow P_s = 233\text{bar}$$

Therefore the supply pressure has increased from 180bar \rightarrow 233bar.

Need help with your dissertation?

Get in-depth feedback & advice from experts in your topic area. Find out what you can do to improve the quality of your dissertation!

Get Help Now



Go to www.helpmyassignment.co.uk for more info



Helpmyassignment



Click on the ad to read more

3 Connecting a servovalve to an actuator, steady-state behaviour

3.1 Aim

This aim of this chapter is to introduce the reader to the basic servovalve/actuator combinations and to understand their steady-state behaviour via a number of objectives as follows:

- to present the actuator ideal flow rate and force/torque equations
- to determine the ideal performance of various servovalve/actuator combinations
- to introduce the basic practical losses and show their effect on performance
- to illustrate performance through worked examples
- to demonstrate the practical use of a Programmable Servo Controller to improve steady-state performance

3.2 Connecting a servovalve to a cylinder, the open-loop steady-state behaviour

Consider first the general case of a single-rod actuator and in *open-loop* control mode as shown in figure 3.1. The application of an input voltage to the controller/servoamplifier causes the actuator to either extend or retract depending on the sign of the voltage. In the absence of any variation such as temperature, supply pressure or load conditions then a fixed voltage will create a fixed velocity.

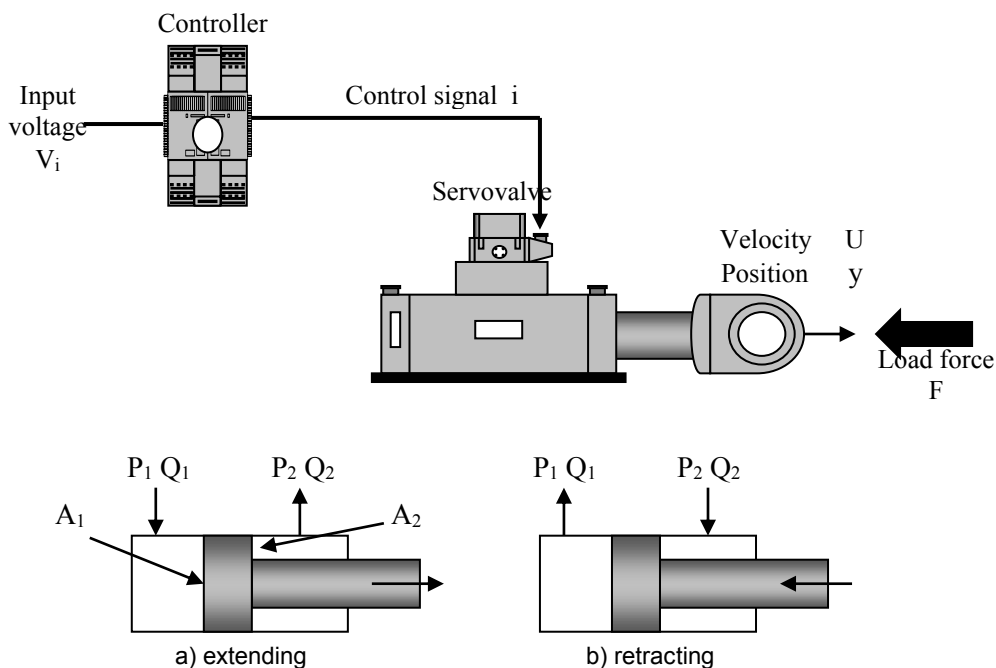


Figure 3.1 An open-loop servodrive, single-rod linear actuator

Assuming a critically-lapped servovalve spool then the flow from the servovalve output port into the actuator and the flow out of the actuator into the servovalve return port must be equal to the actuator velocity multiplied by actuator cross-sectional-area. Also the net hydraulic force must balance the load force. It then follows that:

Actuator extending

$$\begin{aligned} Q_1 &= k_f i \sqrt{P_s - P_1} = A_1 U \\ Q_2 &= k_f i \sqrt{P_2} = A_2 U \\ P_1 A_1 - P_2 A_2 &= F \end{aligned} \quad (3.1)$$

Combining these equations then gives:

$$P_1 = \frac{P_s + \gamma^2 P_\ell(o)}{(1 + \gamma^3)} \quad P_2 = \frac{\gamma P_s - P_\ell(o)}{(1 + \gamma^3)} \quad P_\ell(o) = \frac{F}{A_2} \quad \gamma = \frac{A_1}{A_2} \quad (3.2)$$

$$U_e = \frac{k_f i}{A_2} \sqrt{\frac{\gamma P_s - P_\ell(o)}{(1 + \gamma^3)}}$$

Actuator retracting

$$\begin{aligned} Q_1 &= k_f i \sqrt{P_1} = A_1 U \\ Q_2 &= k_f i \sqrt{P_s - P_2} = A_2 U \\ P_1 A_1 - P_2 A_2 &= F \end{aligned} \quad (3.3)$$

Combining these equations then gives:

$$P_1 = \frac{\gamma^2 P_s + \gamma^2 P_\ell(o)}{(1 + \gamma^3)} \quad P_2 = \frac{\gamma^3 P_s - P_\ell(o)}{(1 + \gamma^3)} \quad P_\ell(o) = \frac{F}{A_2} \quad \gamma = \frac{A_1}{A_2} \quad (3.4)$$

$$U_r = \frac{k_f i}{A_2} \sqrt{\frac{P_s + P_\ell(o)}{(1 + \gamma^3)}}$$

The ratio of retracting velocity to extending velocity is given by:

$$\frac{U_r}{U_e} = \sqrt{\frac{P_s + P_\ell(o)}{\gamma P_s - P_\ell(o)}} \quad (3.5)$$

The retracting velocity is greater than the extending velocity providing:

$$\frac{U_r}{U_e} > 1 \quad \text{giving} \quad P_\ell(o) > \frac{\gamma - 1}{2} P_s \quad (3.6)$$

If a supply pressure is selected such that $P_s = 1.5P_\ell(o)$ then from (3.6):

$$\frac{U_r}{U_e} > 1 \quad \text{when} \quad \gamma < 2.133 \quad (3.7)$$

This is usually the case in practice and it is concluded that, with the same servovalve current applied in each direction, the **retracting velocity will probably be greater than the extending velocity** for an open-loop linear servodrive with optimum supply pressure setting.

An interesting feature of a single-rod actuator is that the **extending speed and the retracting speed can be made equal** from (3.5) to give:

$$U_r = U_e \quad \text{when} \quad F = \frac{P_s A_{\text{rod}}}{2} \quad (3.8)$$



Brain power

By 2020, wind could provide one-tenth of our planet's electricity needs. Already today, SKF's innovative know-how is crucial to running a large proportion of the world's wind turbines.

Up to 25 % of the generating costs relate to maintenance. These can be reduced dramatically thanks to our systems for on-line condition monitoring and automatic lubrication. We help make it more economical to create cleaner, cheaper energy out of thin air.

By sharing our experience, expertise, and creativity, industries can boost performance beyond expectations. Therefore we need the best employees who can meet this challenge!

The Power of Knowledge Engineering

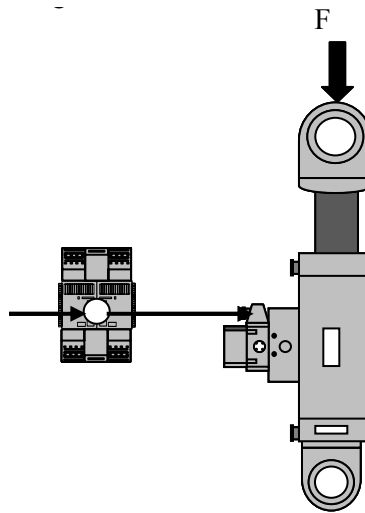
Plug into The Power of Knowledge Engineering.
Visit us at www.skf.com/knowledge

SKF

where A_{rod} is the cross-sectional-area of the rod. Selecting such a design would appear to make intuitive sense from a closed-loop control systems design point of view although there may be some cases for simple extend/retract systems where it is desirable to retract, for example, as quickly as possible.

Example 3.1

An *open-loop* servodrive with a *single-rod cylinder* operates vertically to lift a platform. Determine the extending and retracting speeds using the following data:



Actuator bore diameter 50mm, rod diameter 28mm

Actuator stroke 2.5m

Servovalve flow constant $k_f = 0.2$, rated flow @20mA

Supply pressure $P_s = 210\text{bar}$

Platform mass $M = 2200\text{kg}$

$$\text{Bore area } A_1 = \frac{\pi (2500)10^{-6}}{4} = 19.64 \times 10^{-4} \text{ m}^2$$

$$\text{Actuator annulus area } A_2 = \frac{\pi (1716)10^{-6}}{4} = 13.5 \times 10^{-4} \text{ m}^2$$

$$\text{Area ratio } \gamma = A_1/A_2 = 1.45$$

Actuator extending

$$U_e = \frac{k_f i}{A_2} \sqrt{\frac{\gamma P_s - P_\ell(o)}{(1 + \gamma^3)}} \quad P_1 = \frac{P_s + \gamma^2 P_\ell(o)}{(1 + \gamma^3)} \quad P_2 = \frac{\gamma P_s - P_\ell(o)}{(1 + \gamma^3)} \quad P_\ell(o) = \frac{F}{A_2}$$

$$P_\ell(o) = \frac{F}{A_2} = \frac{2200(9.81)}{13.5 \times 10^{-4}} = 160 \times 10^5 \text{ N/m}^2 \text{ (160bar)}$$

Selecting the rated flow gives $U_e = \frac{k_f i}{A_2} \sqrt{\frac{\gamma P_s - P_\ell(o)}{(1 + \gamma^3)}} = \frac{(0.2)(20)}{13.5 \times 10^{-4}} \sqrt{\frac{144.5}{4.05}} \left(\frac{10^{-3}}{60}\right) = 0.29 \text{ m/s}$

$$P_1 = 134.9 \text{ bar} \quad P_2 = 35.7 \text{ bar}$$

Actuator retracting

$$U_r = \frac{k_f i}{A_2} \sqrt{\frac{P_s + P_\ell(o)}{(1 + \gamma^3)}} \quad P_1 = \frac{\gamma^2 P_s + \gamma^2 P_\ell(o)}{(1 + \gamma^3)} \quad P_2 = \frac{\gamma^3 P_s - P_\ell(o)}{(1 + \gamma^3)}$$

Selecting the rated flow gives $U_r = \frac{k_f i}{A_2} \sqrt{\frac{P_s + P_\ell(o)}{(1 + \gamma^3)}} = \frac{(0.2)(20)}{13.5 \times 10^{-4}} \sqrt{\frac{370}{4.05}} \left(\frac{10^{-3}}{60}\right) = 0.47 \text{ m/s}$

$$P_1 = 192.1 \text{ bar} \quad P_2 = 118.6 \text{ bar}$$

The extending speed is 0.29m/s and the retracting speed is 0.47m/s

3.3 Connecting a servovalve to a motor, the open-loop steady-state behaviour

The open-loop servodrive is shown in figure 3.2. In this servodrive the equations are similar to a linear actuator with a double-rod.

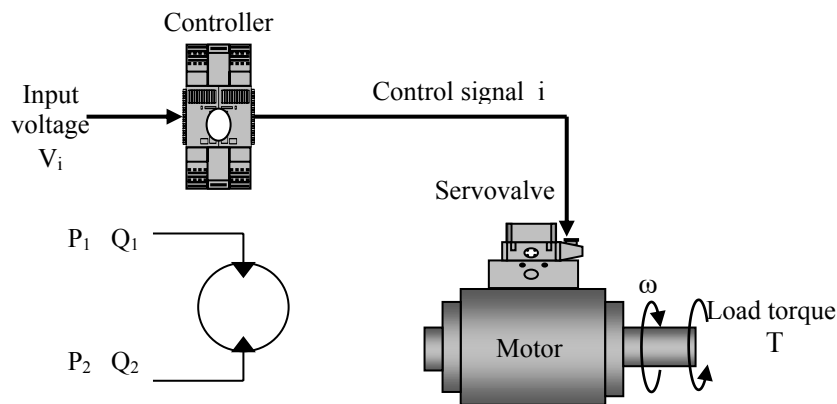


Figure 3.2 An open-loop servodrive, motor actuator

The flow rate for a positive displacement motor is given by multiplying its displacement, $D_m \text{ m}^3/\text{rad}$, by the angular velocity, $\omega \text{ rad/s}$, and therefore the flow equations are now:

$$Q_1 = k_f i \sqrt{P_s - P_1} = D_m \omega \quad (3.9)$$

$$Q_2 = k_f i \sqrt{P_2} = D_m \omega$$

Due to displacement symmetry for a motor, these equations apply for the other direction of rotation with pressures interchanged. The load equation for a motor is derived from the shaft load torque T and it can be shown that:

$$T = D_m (P_1 - P_2) \quad (3.10)$$

Consequently for the ideal system then equating the two flows gives similar conclusions than for a linear actuator with a double-rod, that is:

$$Q = Q_1 = Q_2 = k_f i \sqrt{\frac{P_s - P_\ell(o)}{2}} = D_m \omega \quad (3.11)$$

$$P_1 = \frac{P_s + P_\ell(o)}{2} \quad P_2 = \frac{P_s - P_\ell(o)}{2} \quad P_\ell(o) = \frac{T}{D_m}$$



What do you want to do?

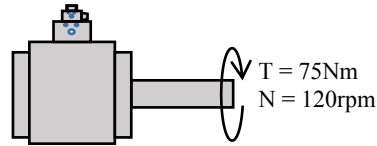
No matter what you want out of your future career, an employer with a broad range of operations in a load of countries will always be the ticket. Working within the Volvo Group means more than 100,000 friends and colleagues in more than 185 countries all over the world. We offer graduates great career opportunities – check out the Career section at our web site www.volvogroup.com. We look forward to getting to know you!

VOLVO
AB Volvo (publ)
www.volvogroup.com

VOLVO TRUCKS | RENAULT TRUCKS | MACK TRUCKS | VOLVO BUSES | VOLVO CONSTRUCTION EQUIPMENT | VOLVO PENTA | VOLVO AERO | VOLVO IT
VOLVO FINANCIAL SERVICES | VOLVO 3P | VOLVO POWERTRAIN | VOLVO PARTS | VOLVO TECHNOLOGY | VOLVO LOGISTICS | BUSINESS AREA ASIA

Example 3.2

Determine the servovalve supply pressure and servovalve current for an open-loop motor servodrive given the following information:



Motor displacement $D_m = 6 \times 10^{-6} \text{ m}^3/\text{rad}$

Load torque $T = 75 \text{ Nm}$

Servovalve flow coefficient $k_f = 0.3$ (current mA, pressure bar, flow rate litres/min)

Servovalve rated current $\pm 20 \text{ mA}$

Required load speed 120rpm

A speed reduction gearbox of 2:1 is available

Without a gearbox

$$\text{Load pressure } P_\ell(o) = \frac{T}{D_m} = \frac{75}{6 \times 10^{-6}} = 12.5 \times 10^6 \text{ N/m}^2 = 125 \text{ bar}$$

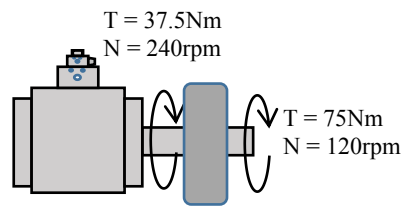
Select a servovalve supply pressure $P_s = 1.5P_\ell(o)$ $P_s = 188 \text{ bar}$

Using the required motor speed of 120rpm (12.57rad/s) the motor current is given by:

$$Q = k_f i \sqrt{\frac{P_s - P_\ell(o)}{2}} = D_m \omega$$

$$0.3 \times i \sqrt{\frac{63}{2}} \frac{10^{-3}}{60} = (6 \times 10^{-6})(12.57) \quad i = 2.69 \text{ mA}$$

This current is within the servovalve current rating of $\pm 20 \text{ mA}$ but is low.

With a gearbox

Gearbox speed at the load is 120rpm and the torque is 75Nm

The motor speed is now 240rpm and the torque is 37.5Nm

$$\text{Load pressure } P_{\ell}(o) = \frac{T}{D_m} = \frac{37.5}{6 \times 10^{-6}} = 6.25 \times 10^6 \text{ N/m}^2 = 62.5 \text{ bar}$$

$$\text{Select a servovalve supply pressure } P_s = 1.5P_{\ell}(o) \quad P_s = 94 \text{ bar}$$

This supply pressure is now halved but acceptable. Using the motor speed of 240rpm (25.14rad/s) the motor current is given by:

$$Q = k_f i \sqrt{\frac{P_s - P_{\ell}(o)}{2}} = D_m \omega$$

$$0.3 \times i \sqrt{\frac{31.5}{2}} \frac{10^{-3}}{60} = (6 \times 10^{-6})(25.14) \quad i = 7.6 \text{ mA}$$

Increasing the motor speed x2, using a gearbox, has increased the required current by a factor >2. The supply pressure has been decreased by a factor x2.

3.4 Connecting a servovalve to a motor, the closed-loop steady-state behaviour

A speed sensor is now secured to the motor drive shaft, as shown in figure 3.3, and produces a voltage proportional to speed. The motor speed sensor voltage is subtracted from the demanded speed equivalent voltage as shown to form a closed-loop speed control system.

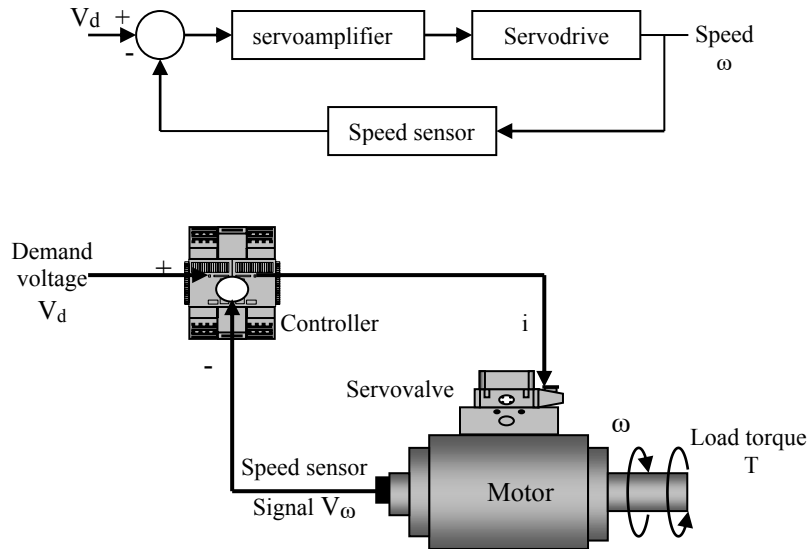


Figure 3.3 An closed-loop motor servodrive

The equations for this basic system with no losses or dynamic effects are as follows:

$$\text{error signal } i = G_a [V_d - H_\omega \omega] \tag{3.12}$$

where V_d is the demanded voltage equivalent of the demanded position, G_a mA/V is the servoamplifier gain and H_ω V/rad s^{-1} is the speed sensor gain. At the demanded speed ω_d then the demanded voltage equivalent is given by:

$$\text{Demand voltage } V_d = H_\omega \omega_d \tag{3.13}$$

$$\text{and therefore } i = G_a H_\omega [\omega_d - \omega] \tag{3.14}$$

Since the steady-state condition with no motor losses is being considered then the servovalve flow rate into and out of the actuator must equal motor speed ω multiplied by displacement D_m .

$$Q = k_f i \sqrt{\frac{P_s - P_\ell(o)}{2}} = D_m \omega \quad P_\ell(o) = \frac{T}{D_m} \tag{3.15}$$

Combining these equations allows the motor speed ω to be expressed as a ratio of its no-load speed $\omega(o)$, when $P_l(o) = 0$, as follows:

$$\frac{\omega}{\omega(o)} = \frac{(1 + K) \sqrt{1 - \frac{P_l(o)}{P_s}}}{1 + K \sqrt{1 - \frac{P_l(o)}{P_s}}} \quad \omega(o) = \frac{k_f i}{D_m} \sqrt{\frac{P_s}{2}} \quad K = \frac{k_f G_a H_\omega}{D_m} \sqrt{\frac{P_s}{2}} \quad (3.16)$$

The effect of increasing the system **closed-loop gain** K can be seen from figure 3.4 as the load pressure is increased.

gaiteye
Challenge the way we run

EXPERIENCE THE POWER OF FULL ENGAGEMENT...

.....

**RUN FASTER.
RUN LONGER..
RUN EASIER...**

**READ MORE & PRE-ORDER TODAY
WWW.GAITEYE.COM**



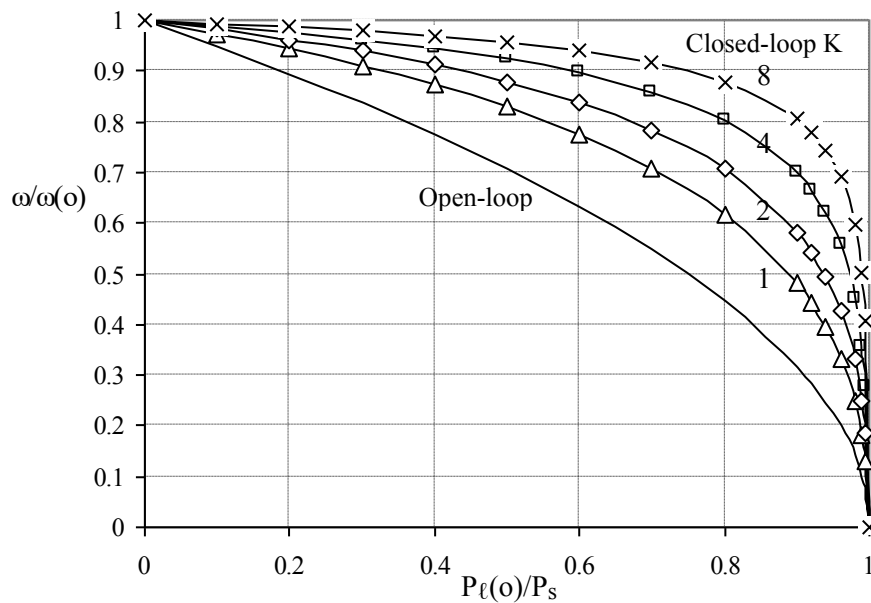


Figure 3.4 Comparison of open-loop and closed-loop control of a motor speed, no motor losses or dynamics

Some interesting points arise from this steady-state analysis:

- the effect of simply closing the loop is clear from figure 3.4 since the speed drop is less pronounced with increasing load pressure, and for any closed-loop gain
- closed-loop control does not prevent the speed falling to zero at maximum load pressure
- the speed drop characteristic can be further improved by increasing the closed-loop gain K but in practice the effect of inherent system dynamics will cause the motor speed to eventually oscillate. This is a dangerous condition for a motor having a number of internal pistons/vanes that can bounce and cause severe damage.

3.5 Connecting a servovalve to a cylinder, the closed-loop position transient response

Consider now a closed-loop servodrive using a linear actuator as shown in figure 3.5. Due to the integration from velocity to position, this position control system behaves in a transient manner when position change is demanded, even in absence of system dynamics. For this preliminary look at closed-loop control the following conditions are set:

- a double-rod type having a net cross-sectional-area A
- the load pressure is constant, for example due to a constant resisting force F
- no load mass and actuator fluid compressibility, no servovalve dynamics
- a critically-lapped servovalve spool

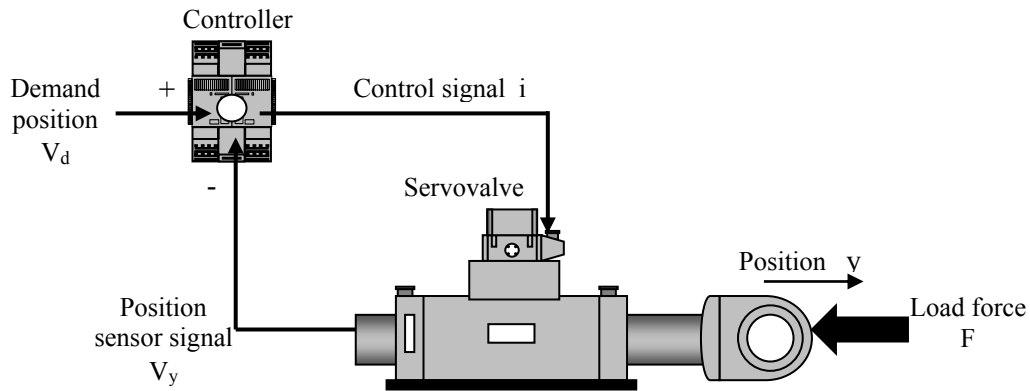


Figure 3.5 A servodrive closed-loop control system with a double-rod actuator

The equations for this basic system with no dynamics or losses are as follows:

$$\text{error signal } i = G_a [V_d - H_p y] \tag{3.17}$$

V_d is the demanded voltage equivalent of the demanded position, G_a mA/V is the servoamplifier gain and H_p V/mm is the position sensor gain. Since the demanded position is given by y_d then:

$$\text{demand voltage } V_d = H_p y_d \tag{3.18}$$

$$\text{and therefore } i = G_a H_p [y_d - y] \tag{3.19}$$

Since actuator dynamic effects are neglected then the servovalve flow rate into and out of the actuator must equal actuator speed U multiplied by cross-sectional-area A :

$$Q = k_f i \sqrt{\frac{P_s - P_\ell(o)}{2}} = AU = A \frac{dy}{dt} \tag{3.20}$$

$$P_\ell(o) = \frac{F}{A} \tag{3.21}$$

Combining these equations then results in the system differential equation:

$$y + \frac{dy}{dt/\tau} = y_d \quad \tau = \frac{A}{k_f G_a H_p \sqrt{\frac{P_s - P_\ell(o)}{2}}} \tag{3.22}$$

This is a **first-order differential equation** with a system **time constant τ** seconds. The solution to this standard first-order differential equation, assuming a zero initial displacement, speed and a constant load pressure $P_\ell(o)$, is given by:

$$y = y_d [1 - e^{-t/\tau}] \tag{3.23}$$

The position increases in an exponential manner from zero to the steady state value y_d as shown in figure 3.6 and such a plot is known as the system *transient response*.

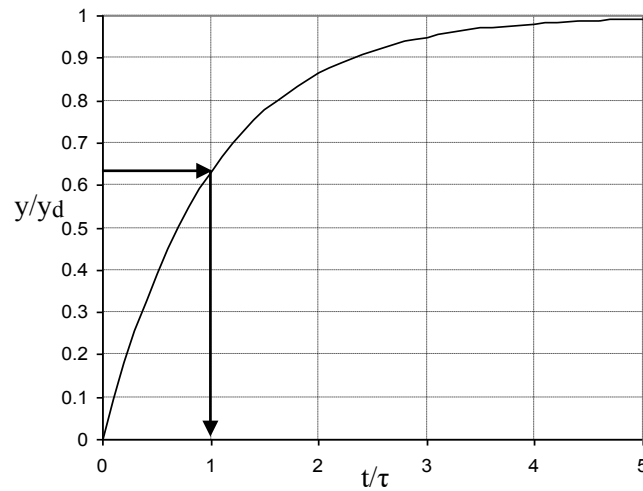


Figure 3.6 The transient response of a first-order system

Information on system parameters, one perhaps unknown, may be determined by noting that when the position has achieved 63% of the steady-state value then the time elapsed has a value equal to the time constant τ as shown in figure 3.6.

This e-book
is made with
SetaPDF



SETASIGN

PDF components for PHP developers

www.setasign.com



Clearly to make the response faster the time constant τ must be reduced which may be achieved by reducing the numerator of τ in (3.22) and/or increasing the denominator. The response may be made faster, if feasible in practice, by:

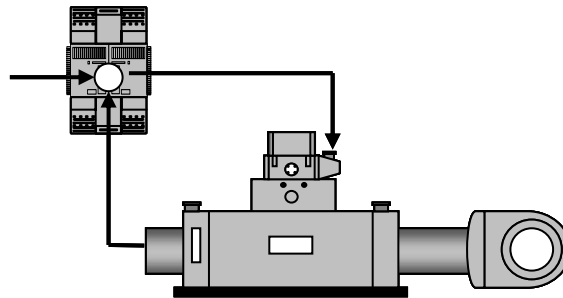
- reducing the actuator cross-sectional-area A , that is using a smaller cylinder
- increasing k_f , that is increasing the servovalve flow rating
- reducing $P_\ell(o)$, that is reducing the load force F
- increasing the supply pressure P_s at a fixed load
- increasing the gains G_a and/or H_p .

In practice increasing the gains G_a and H_p will eventually lead to closed-loop instability due to other dynamic aspects not considered here such as servovalve dynamics and load dynamics. When this occurs in actuator position control systems, sometimes pressure oscillations are more evident than position oscillations.

If the load mass is very small then often the transient response of a real position control system will probably be dominated by this first-order characteristic.

Example 3.3

Consider a closed-loop servodrive with a double-rod cylinder. Determine the transient response as the servoamplifier gain G_a is varied and using the following data:



Bore diameter 50mm, rod diameter 28mm

Actuator stroke 150mm

Servovalve flow constant $k_f = 0.2$, rated flow @20mA

Supply pressure $P_s = 140\text{bar}$

Position sensor gain $H_p = 10\text{V/m}$

No load $F = 0$

$$\text{Actuator annulus area } A = A = \frac{\pi (1716 \times 10^{-6})}{4} = 13.5 \times 10^{-4} \text{ m}^2$$

$$\text{Rated flow} = k_f i_{\text{rated}} \sqrt{\frac{P_s - P_\ell(0)}{2}} = 0.2(20) \sqrt{70} = 33.47 \text{ l/min}$$

For full stroke the voltage generated by the position sensor is $(10)(0.15) = 1.5\text{V}$

The maximum voltage error $V_{\text{error}} = 1.5\text{V}$

The current generated $i = G_a V_{\text{error}}$

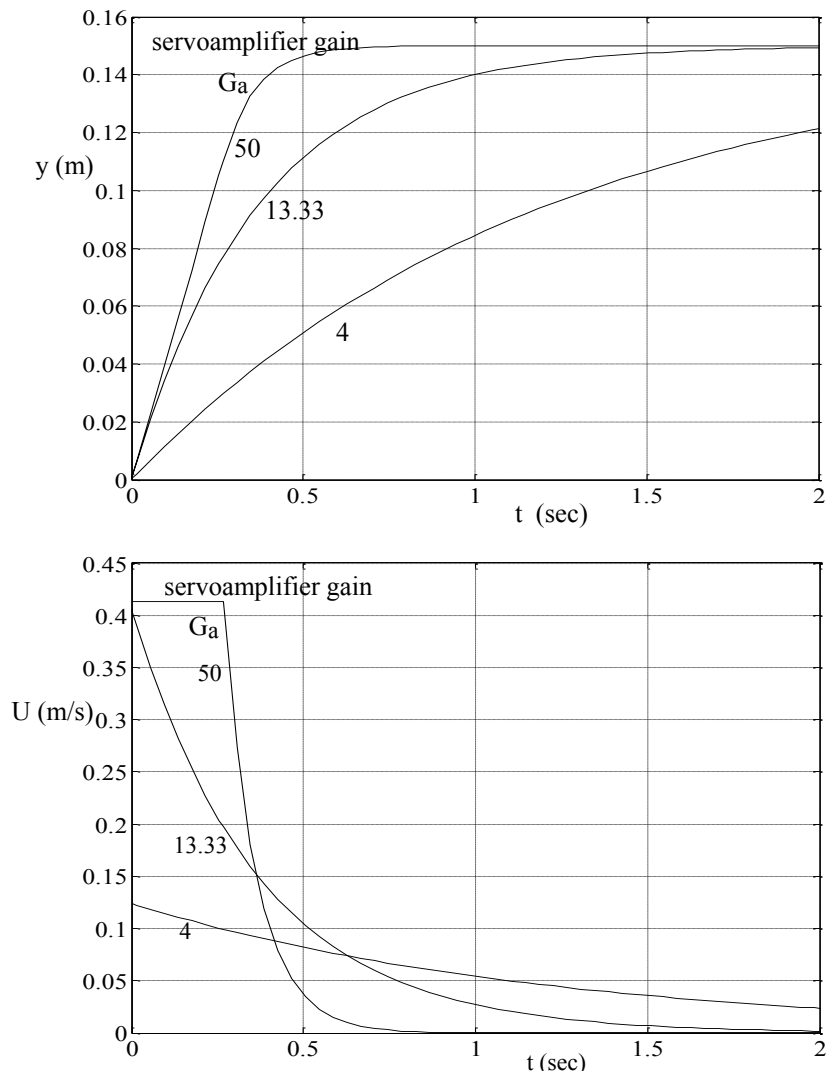
Therefore at the rated current of 20mA the servoamplifier gain $G_a = 20/1.5 = 13.33\text{mA/V}$

Servoamplifier gains above this value will cause servovalve flow saturation and the actuator will move at a constant speed. At the working supply pressure $P_s = 140\text{bar}$ and no load:

$$\begin{aligned} \text{Maximum speed} &= \frac{Q}{A} = \frac{33.47 \times 10^{-3}}{60 \times (13.5 \times 10^{-4})} = 0.41 \text{ m/s} \\ \tau &= \frac{A}{k_f G_a H_p \sqrt{\frac{P_s - P_\ell(0)}{2}}} = \frac{13.5 \times 10^{-4}}{(0.2)(13.33)(10) \sqrt{70} \frac{10^{-3}}{60}} = 0.36 \text{ sec} \end{aligned}$$

The closed-loop time constant at the point of flow saturation $\tau = 0.36\text{sec}$

A servoamplifier gain $G_a > 13.33\text{mA/V}$ will cause the servovalve flow rate to just saturate. Computer simulation results are shown for a servoamplifier gain $G_a = 13.33$ and also for $G_a = 4$ and 50 . Note velocity saturation at the highest gain shown.



Up to a servoamplifier gain of $G_a=13.33\text{mA/V}$ the response behaves in a linear exponential manner as expected. Higher gains are not detrimental since initial velocity saturation moves the cylinder at its highest velocity and actually improves the transient response.

3.6 Servodrive damping, leakage and friction losses, efficiency

The main contribution to system damping are:

- leakages at the actuator
- viscous resistance due to actuator motion within the working fluid
- servovalve flow leakage
- actuator and load mechanical stiction/Coulomb friction
- connecting line fluid flow resistance

First consider leakages at the actuator. These are due to the inherent clearances that must exist due to internal motion between components that experience a pressure differential across them. Leakages are usually assumed to be proportional to the pressure difference across the leakage path. Leakage across a linear actuator piston tends to be low but leakages usually cannot be neglected for a motor which has many internal leakage flow paths.

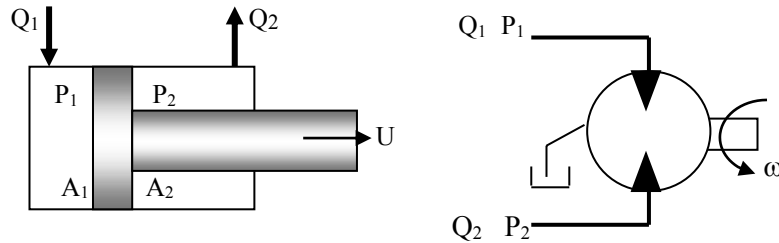


Figure 3.7 Flow rates into and out of hydraulic actuators

www.sylvania.com

We do not reinvent the wheel we reinvent light.

Fascinating lighting offers an infinite spectrum of possibilities: Innovative technologies and new markets provide both opportunities and challenges. An environment in which your expertise is in high demand. Enjoy the supportive working atmosphere within our global group and benefit from international career paths. Implement sustainable ideas in close cooperation with other specialists and contribute to influencing our future. Come and join us in reinventing light every day.

Light is OSRAM



The flow continuity equations, considering figure 3.7, are modified as follows:

$$\begin{array}{ll}
 \textbf{Linear actuator} & \textbf{Motor} \\
 Q_1 = A_1 U + \frac{(P_1 - P_2)}{R_i} & Q_1 = D_m \omega + \frac{(P_1 - P_2)}{R_i} + \frac{P_1}{R_e} \\
 Q_2 = A_2 U + \frac{(P_1 - P_2)}{R_i} & Q_2 = D_m \omega + \frac{(P_1 - P_2)}{R_i} - \frac{P_2}{R_e}
 \end{array} \tag{3.24}$$

The concept of **resistance** is again used where now R_i is the leakage series resistance across the linear actuator piston, R_i and R_e are the motor internal and external resistances due to cross-port and other leakages. Clearly a correctly functioning linear actuator has no significant external leakage from the rod seals but piston motors do have external leakage via the case drain connection to tank.

The motor equations used here are those established by the author from measurements on just two motors of the same design and they may vary slightly for other designs. Also the relative importance of different leakages for a motor is difficult to pre-judge in practice since it is not possible to obtain detailed loss data for every motor commercially available. To get a feel for the probable system equations the mean flow rate may be used as follows:

$$\begin{array}{ll}
 \text{Linear actuator} & Q = \frac{(A_1 + A_2)}{2} U + \frac{P_\ell}{R_{act}} \\
 \text{Motor} & Q = D_m \omega + \frac{P_\ell}{R_{act}}
 \end{array} \tag{3.25}$$

where R_{act} is a general leakage term for either actuator.

The **force and torque equations** must also be modified to **include viscous and mechanical losses**. The first loss component, the **viscous friction loss**, is due to the motion of internal components within the viscous working fluid. It is usually assumed that this loss is proportional to velocity as follows:

$$\text{Viscous friction force loss for a cylinder} = B_v U \tag{3.26}$$

$$\text{Viscous friction torque loss for a motor} = B_v \omega$$

Now consider the **mechanical friction loss** which can be affected by both speed and pressure, and is generally considered to have two dominant components. The first component is the **zero-speed stiction** component and the second component is a **constant Coulomb friction** component that is independent of speed. This combined stiction/Coulomb friction characteristic is shown in figure 3.8.

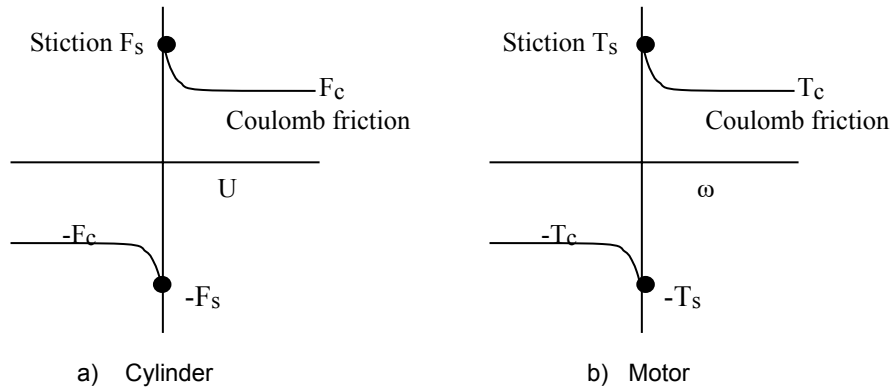


Figure 3.8 Stiction/Coulomb friction characteristic F_f or T_f .

The stiction component, F_s or T_s , drops rapidly to the Coulomb friction component, F_c or T_c , as motion begins, is difficult to measure in practice, and the characteristic around zero speed does provide a small de-stabilising damping component for control systems. For general motion a simple friction term, F_f or T_f is often added to the load force F and load torque T equations which become:

$$\text{Linear actuator} \quad P_1 A_1 - P_2 A_2 = F + F_f + B_v U \tag{3.27}$$

$$\text{Motor} \quad D_m (P_1 - P_2) = T + T_f + B_v \omega$$

A *viscous resistance* term is now defined as:

$$\text{Viscous resistance } R_{\text{visc}} = \frac{B_v}{A_1 A_2} \quad \text{or} \quad \frac{B_v}{D_m^2} \tag{3.28}$$

Hence, when a servovalve is connected to either a linear actuator or a motor then the actual linear velocity or angular velocity is reduced due to both fluid and mechanical losses. An initial assessment of velocity may then be made as follows, **assuming a double-rod linear actuator**, and a motor for the purpose of example:

$$\text{Linear actuator} \quad AU = k_f i \sqrt{\frac{P_s - \frac{(F + F_f + B_v U)}{A}}{2}} - \frac{(F + F_f + B_v U)}{A R_{\text{act}}} \tag{3.29}$$

$$\text{Motor} \quad D_m \omega = k_f i \sqrt{\frac{P_s - \frac{(T + T_f + B_v \omega)}{D_m}}{2}} - \frac{(T + T_f + B_v \omega)}{D_m R_{\text{act}}}$$

It will be seen that these are non-linear equations and may be solved by further re-arrangement into quadratic equation form to solve for the speed U or ω . Alternatively they may be solved by iteration beginning with the no-loss velocity which may be directly calculated from (3.29).

The *overall efficiency of a servodrive* is defined as:

$$\text{Efficiency } \eta = \frac{\text{Output power}}{\text{Input power}} \quad (3.30)$$

For a double-rod linear actuator servodrive:

$$\eta = \frac{FU}{P_s Q} \quad \eta = \frac{P_\ell}{P_s} \text{ for no losses}$$

$$P_\ell A = F + F_f + B_v U \quad P_\ell = P_1 - P_2 \quad (3.31)$$

$$Q = k_f i \sqrt{\frac{P_s - P_\ell}{2}} = AU + \frac{P_\ell}{R_{\text{act}}}$$



Discover the truth at www.deloitte.ca/careers

Deloitte.

© Deloitte & Touche LLP and affiliated entities.



Click on the ad to read more

For a motor servodrive:

$$\eta = \frac{T\omega}{P_s Q} \quad \eta = \frac{P_\ell}{P_s} \text{ for no losses}$$

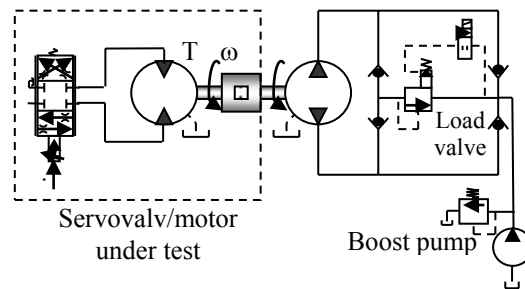
$$P_\ell D_m = T + T_f + B_v \omega \quad P_\ell = P_1 - P_2 \quad (3.32)$$

$$Q = k_f i \sqrt{\frac{P_s - P_\ell}{2}} = D_m \omega + \frac{P_\ell}{R_{act}}$$

For a real motor servodrive with losses, the efficiency will reach a maximum value for a pressure differential P_ℓ typically $0.7P_s < P_\ell < P_s$.

Example 3.4

Consider a real open-loop motor servodrive built and studied by the author. A motor/pressure relief valve/check valve bridge is used to load the motor. Determine the variation in efficiency and motor speed as the load pressure is varied and using the following measured data:



mineral oil @ 40°C

Motor displacement $D_m = 1.68 \times 10^{-6} \text{ m}^3/\text{rad}$

Supply pressure $P_s = 100 \text{ bar}$

$R_{act} = 1.6 \times 10^{12} \text{ Nm}^{-2}/\text{m}^3 \text{ s}^{-1}$

Coulomb friction loss negligible

Viscous friction loss coefficient $B_v = 0.014 \text{ Nm/rads}^{-1}$

Servovalve flow constant $k_f = 1.07 \times 10^{-8}$ (pressure in N/m^2)

Nominal speed at no-load = 234rpm (24.5rad/s) @ $i = 1.72\text{mA}$

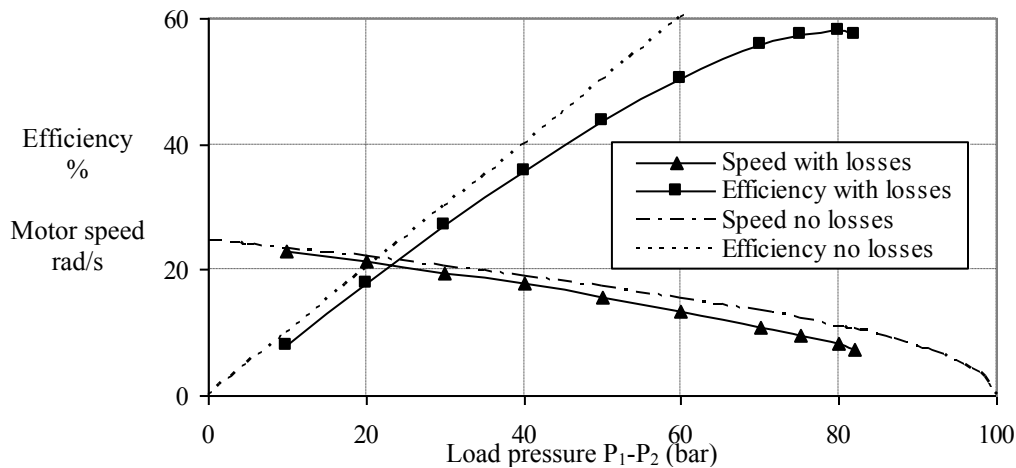
Servovalve flow rate $Q = k_f i \sqrt{\frac{P_s - P_\ell}{2}} = 1.07 \times 10^{-8} (1.72) \sqrt{\frac{10^7 - P_\ell}{2}} \text{ m}^3/\text{s}$

Motor speed $Q = D_m \omega + \frac{P_\ell}{R_{act}} \quad \omega = 0.6 \times 10^6 Q - 0.37 \times 10^{-6} P_\ell \text{ rad/s}$

Motor torque $P_\ell D_m = T + T_f + B_v \omega \quad T = 1.68 \times 10^{-6} P_\ell - 0.014 \omega \text{ Nm}$

Efficiency $\eta = \frac{T \omega}{P_s Q}$

The following figure shows the results up to a load pressure differential of 82bar. The maximum efficiency achieved is 57.8% at a pressure differential of 80bar. The ideal efficiency, that is, with no losses, at this load pressure differential would of course be 80%. The drop in speed from the no-loss case is small and only becomes noticeable at high load pressure differentials beyond maximum efficiency.



The measured data fits well with the theoretical model illustrating its validity over the load pressure differential range. Notice the minimum speed at a finite load pressure differential and the difficulty in obtaining measurements at a high load pressure differential due to the low motor speed and its fluctuation due to the piston pumping effect of the (motor + load pump).

3.7 Improving the steady-state performance of an open-loop motor servodrive using a Programmable Servo Controller

This is particularly useful for open-loop motor drives where an increasing load pressure differential inherently reduces motor speed due to the square root effect of the servovalve. Attempting to change the square-root characteristic to a linear characteristic will continually drive the servovalve current to a new value to minimise the square-root effect on motor speed. In addition the supply pressure may be continually varied to optimise the drive efficiency.

Consider a practical validation by the author on a uni-directional motor drive with a commercially-available proportional servovalve having just one control port active, that is one side of the motor is pressurised and the other side is returned to tank at a very low, and constant, pressure of $\approx 9\text{bar}$. This means that only one active pressure has to be measured with a pressure sensor. The motor is loaded with a pump whose output pressure is varied using a proportional pressure relief valve with electrical control. Therefore both steady-state and dynamic testing could be undertaken. The actual supply pressure was also measured using a pressure sensor and this was useful for other dynamic improvements that will be discussed in the section on dynamic behaviour. The open-loop drive is shown as figure 3.9. First consider *servovalve linearisation*.

SIMPLY CLEVER

ŠKODA



We will turn your CV into
an opportunity of a lifetime



Do you like cars? Would you like to be a part of a successful brand?
We will appreciate and reward both your enthusiasm and talent.
Send us your CV. You will be surprised where it can take you.

Send us your CV on
www.employerforlife.com



Click on the ad to read more

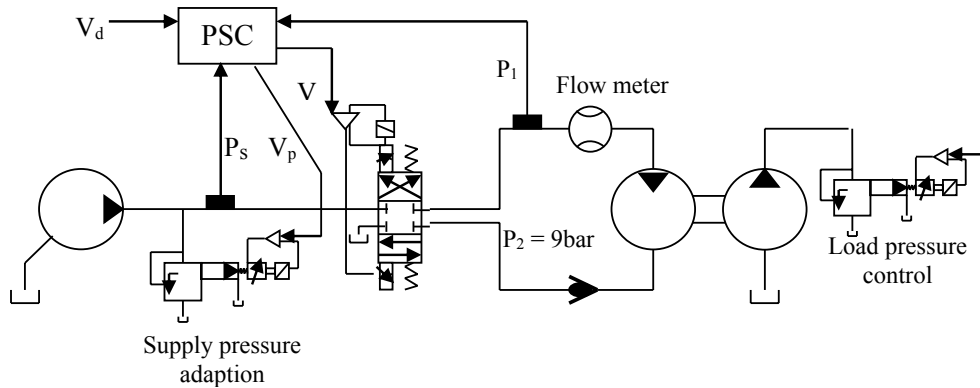


Figure 3.9 Linearisation of a servovalve flow characteristic and supply pressure adaption using a Programmable Servo Controller (PSC)

A flow meter was placed in the inlet line to determine the servovalve flow characteristic in detail and both load and supply pressures can be varied electrically using electrohydraulic proportional pressure relief valves (two PRV's).

A Moog two-axis Programmable Servo Controller (PSC) card, as introduced in Chapter 1, was used to monitor the signals, carry out the on-line computations and provide the corrective control voltages. The servovalve flow characteristic was experimentally-determined to be as follows:

$$Q = (2.48V - 2.25)\sqrt{P_s - P_1} \tag{3.33}$$

V is the applied voltage. Linearisation attempts to create a “virtual servovalve” by electronically generating a flow characteristic that is independent of load pressure as follows:

$$Q = 2.48V_d\sqrt{P_{ref}} \tag{3.34}$$

P_{ref} can be any chosen reference pressure, usually supply pressure P_s . From (3.33) and (3.34) it follows that:

$$V = V_d\sqrt{\frac{P_{ref}}{P_s - P_1}} + 0.91 \tag{3.35}$$

This process of linearisation therefore requires a multiplication factor on V_d that increases $\rightarrow \infty$ as the load pressure $P_1 \rightarrow P_s$. There must be a finite limit that can be achieved by the programmable controller and hence the servovalve flow characteristic cannot be linearised over its entire pressure differential range in practice, in fact for small values of $(P_s - P_1)$. In this application a maximum voltage of 6V was set for the PSC. Figure 3.10 shows the effect of linearisation on the flow rate.

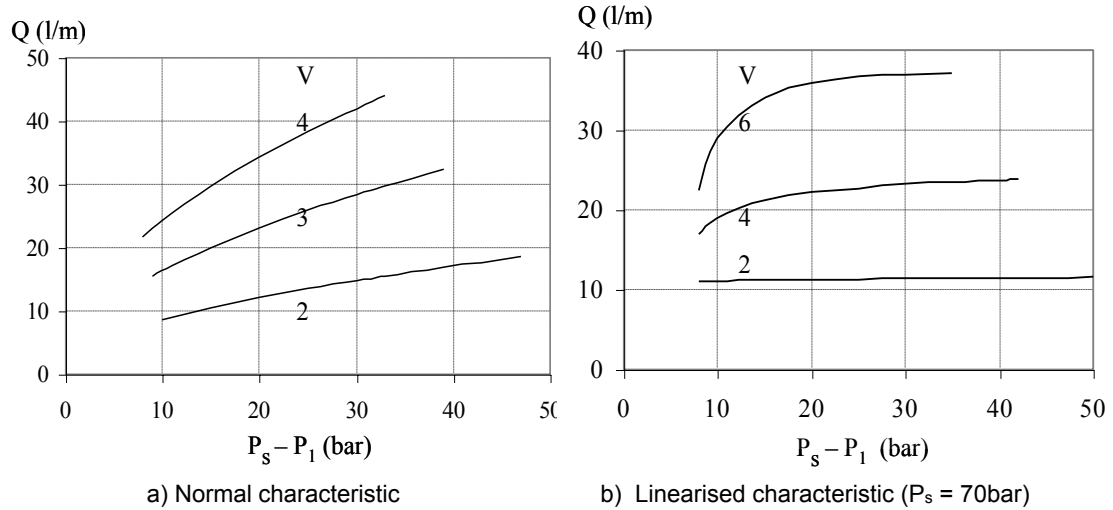


Figure 3.10 Flow characteristics for a servovalve without and with linearisation

The linearisation process works sufficiently well above a pressure differential of $\approx 15\text{bar}$ and particularly for lower flow rates and hence lower motor speeds. These are real results and show that an idealised linearization cannot be achieved in practice.

Now consider supply pressure adaption to maintain optimum efficiency using a PRV to continually adjust supply pressure as shown in figure 3.9. The efficiency of the drive and the supply pressure PRV characteristic were measured and are shown as figure 3.11.

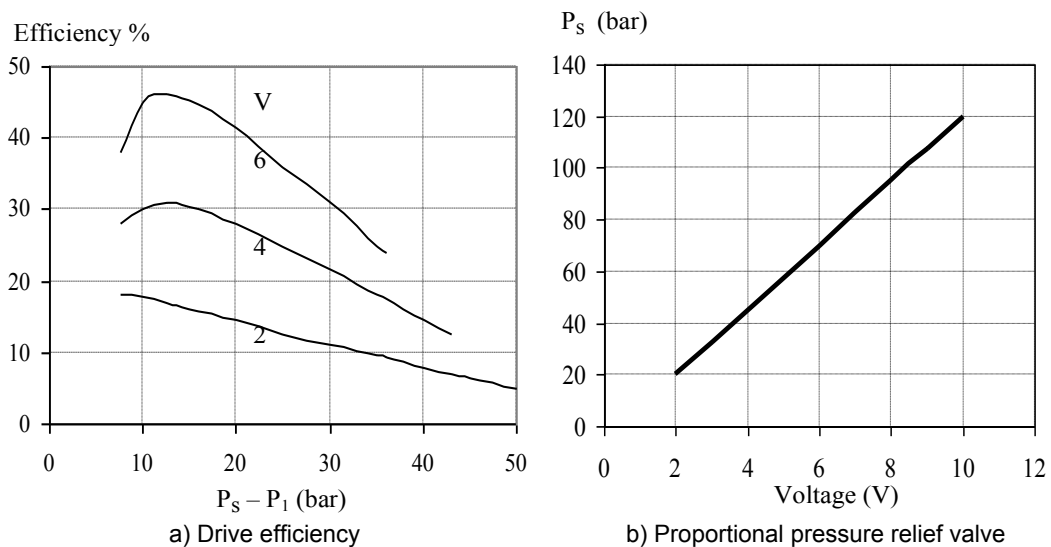


Figure 3.11 Efficiency and proportional pressure relief valve characteristics

Efficiency is defined in this example as the power being delivered to the motor compared with the supply power as follows:

$$\text{Efficiency} = \frac{(P_1 - P_2)Q}{P_s Q_s} \quad (3.36)$$

where Q_s is the pump supply fixed flow rate. It can be seen for this particular servodrive that the drive efficiency is a maximum for a reasonably-constant pressure differential across the servovalve of $(P_s - P_1) \approx 15\text{bar}$ for most of its operating voltage range.

The appropriate conditions are therefore:

$$\text{Optimum drive efficiency } (P_s - P_1) = 15\text{bar} \quad (3.37)$$

$$\text{Supply pressure PRV } P_s = -4 + 12.5 V_p \text{ bar} \quad (3.38)$$

$$\text{Combining these two equations gives } V_p = 1.52 + 0.08 P_1 \quad (3.39)$$

Applying both servovalve flow rate linearisation and supply pressure adaption then results in the motor speed and drive efficiency characteristics shown as figure 3.12 for a nominal motor speed of 515rpm at minimum load pressure differential.

I joined MITAS because
I wanted **real responsibility**

The Graduate Programme
for Engineers and Geoscientists
www.discovermitas.com





Month 16

I was a construction supervisor in the North Sea advising and helping foremen solve problems

Real work
International opportunities
Three work placements





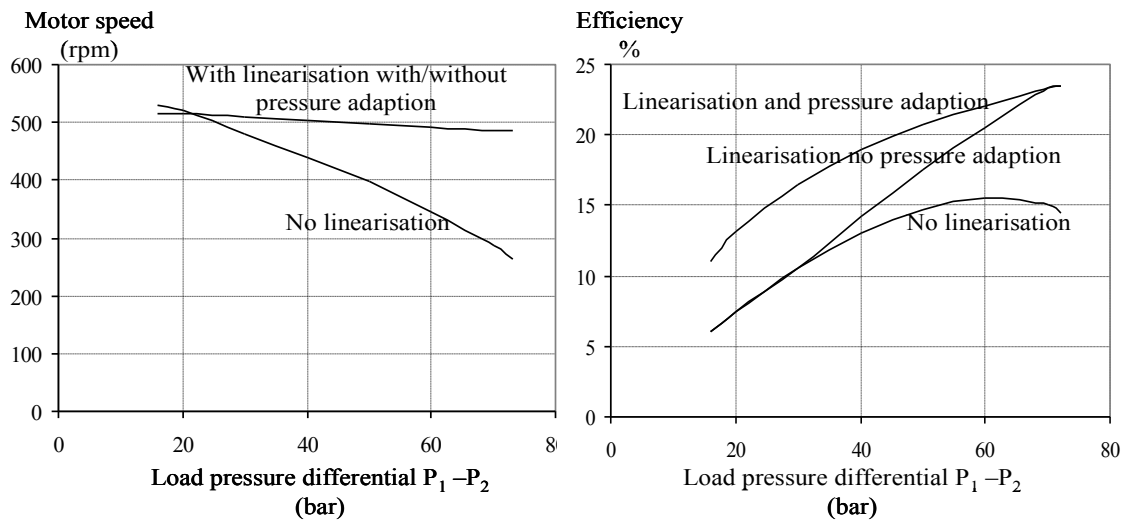


Figure 3.12 Motor open-loop servodrive speed and drive efficiency characteristics for a nominal motor speed of 53.94rad/s (515rpm) [Davies RM and Watton J. Intelligent Control of an Electrohydraulic Motor Drive System. Journal of Mechatronics, Vol 5, No 5, 1995, 527–540]

The efficiency is generally low because the supply pump flow is high and fixed. However, the principle of the approach is demonstrated. A more advanced approach would also include supply flow rate adaption but within fixed limits. It can be seen from figure 3.12 that:

- flow rate linearisation has a significant effect on motor speed over the range of operation and on drive efficiency for higher load pressure differentials
- the addition of pressure adaption has no effect on motor speed, as preferred
- the addition of pressure adaption does improve the drive efficiency as designed

The negative aspects of this approach to performance improvement are:

- the use of a PRV for both supply pressure control and servovalve linearisation has added more system dynamics which have not been presented here. In other words, the dynamic behaviour deteriorates
- servovalve linearisation has significantly reduced system damping by the servovalve, which has not been addressed at this stage. Damping may be improved using the PSC to generate dynamic pressure feedback, as will be discussed in Chapter 7

4 System dynamics and computer simulation

4.1 Aim

The aim of this chapter is to introduce more realistic system models by adding dynamic effects, together with losses, and via the following objectives:

- to introduce the interaction between fluid compressibility and moving mass/inertia
- to show how to calculate the actuator/load fundamental resonant frequency
- to introduce the linearisation method to give a feel for the probable dynamic behaviour
- to introduce the role of computer simulation using Matlab Simulink
- to illustrate the performance of servodrives using worked examples

4.2 Fluid compressibility and its effect on flow rate

In reality a fluid power system has moving mass and the combination of this with fluid compressibility results in system dynamics that usually cannot be neglected. Also a servovalve spool cannot move immediately to its commanded position and it therefore contributes to dynamic behaviour. Whether or not the servovalve dynamics should be included depends usually on the magnitude of the moving mass for a linear actuator or the rotary inertia for a motor combined with actuator size. In practice damping is fortuitously provided by losses due to viscous and leakage effects but a closed-loop control system will almost certainly become unstable as the servoamplifier gain is increased due to dynamic effects. Instability can lead to disastrous consequences if severe pressure oscillations occur, for example in motor servodrives.

Consider first the effect of *fluid compressibility* for an arbitrary control volume which has a flow rate Q_i into it and a flow rate Q_o out of it as shown in figure 4.1.

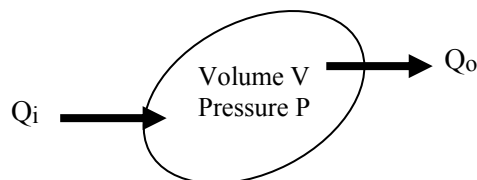


Figure 4.1 Flow into and out of a control volume

Considering mass flow continuity including fluid compressibility and the equation of state it can be shown that:

$$Q_i - Q_o = \frac{dV}{dt} + \frac{V}{\beta} \frac{dP}{dt} \quad (4.1)$$

The fluid bulk modulus is β and varies with pressure, temperature, and fluid type and it is very important to refer to manufacturers data sheets when considering fluid properties. Most of the author's work with mineral oil uses ISO 32 mineral oil, that is, a mineral oil with a viscosity of 32cSt at a temperature of 40°C (1centiStoke = 10^{-6} m²/s). At typical servodrive pressures around 100→240bar the fluid bulk modulus is $\beta \approx 1.6 \times 10^9$ N/m². Considering a very small inherent air content in practice reduces this value to typically $\beta \approx 1.4 \times 10^9$ N/m².

If flexible hose is used then the effective bulk modulus of the fluid/hose combination is drastically reduced. Measurements by the author has indicated a value typically half that for a rigid steel line of the same length.

ie business school

#1 EUROPEAN BUSINESS SCHOOL
FINANCIAL TIMES 2013

#gobeyond

MASTER IN MANAGEMENT

Because achieving your dreams is your greatest challenge. IE Business School's Master in Management taught in English, Spanish or bilingually, trains young high performance professionals at the beginning of their career through an innovative and stimulating program that will help them reach their full potential.

- Choose your area of specialization.
- Customize your master through the different options offered.
- Global Immersion Weeks in locations such as London, Silicon Valley or Shanghai.

Because you change, we change with you.

www.ie.edu/master-management | mim.admissions@ie.edu |

For a combination of different lines and volumes connected together, V_1, V_2, V_3 etc. and each having a bulk modulus $\beta_1, \beta_2, \beta_3$ etc, the following equation may be used to calculate the effective bulk modulus β_e :

$$\frac{1}{\beta_e} = \frac{V_1}{V_t} \frac{1}{\beta_1} + \frac{V_2}{V_t} \frac{1}{\beta_2} + \frac{V_3}{V_t} \frac{1}{\beta_3} + \dots \quad (4.2)$$

$$V_t = V_1 + V_2 + V_3 + \dots$$

Returning to equation (4.1), the difference between the input flow rate Q_i and the output flow rate Q_o is equal to the rate of change of the boundary volume plus an additional flow rate due to fluid compressibility. It is crucial to appreciate here that the dynamic fluid compressibility effect can only occur if pressure is varying with time. For steady state conditions the compressibility flow rate term is zero but there could still be a moving boundary such as a piston moving with a constant velocity. Considering the actuators shown in figure 4.2 the flow rate continuity equation may be applied to the appropriate control volume:

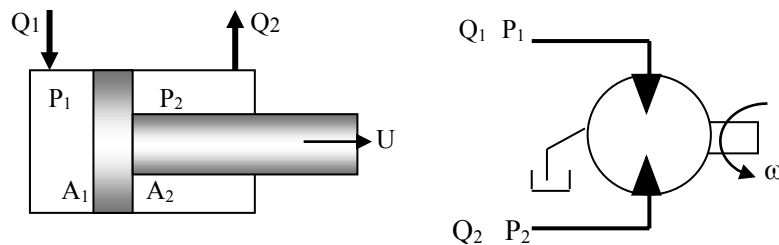


Figure 4.2 Flow rates into and out of hydraulic actuators

$$Q_i - Q_o = \frac{dV}{dt} + \frac{V}{\beta} \frac{dP}{dt}$$

Linear actuator

Motor

in	$Q_1 = A_1 U + \frac{V_1}{\beta} \frac{dP_1}{dt}$	in	$Q_1 = D_m \omega + \frac{V_1}{\beta} \frac{dP_1}{dt}$	(4.3)
out	$Q_2 = A_2 U - \frac{V_2}{\beta} \frac{dP_2}{dt}$	out	$Q_2 = D_m \omega - \frac{V_2}{\beta} \frac{dP_2}{dt}$	

V_1 and V_2 are the total fluid volumes on either side of the actuator. Volumes are a combination of line and actuator volumes, the latter also varying with time for a linear actuator during motion. Usually pressure transients occur very rapidly and within a small movement for a linear actuator. For this reason, particularly when using transfer functions as introduced in Chapter 5, it is common to assume a constant actuator volume on either side and at the particular steady-state condition selected.

Considering the electrical analogy where pressure is analogous to voltage $P \rightarrow V$ and flow rate is analogous to current $Q \rightarrow i$ then fluid compressibility is sometimes referred to as fluid capacitance:

$$\text{Capacitance } C = \frac{V}{\beta} \tag{4.4}$$

4.3 Force and torque equations for actuators with moving mass or rotary inertia

Consider both a linear actuator and a motor as shown in figure 4.3. In the absence of losses the applied hydraulic force or moment has to overcome any load force or torque and load inertia effects due to actuator acceleration.

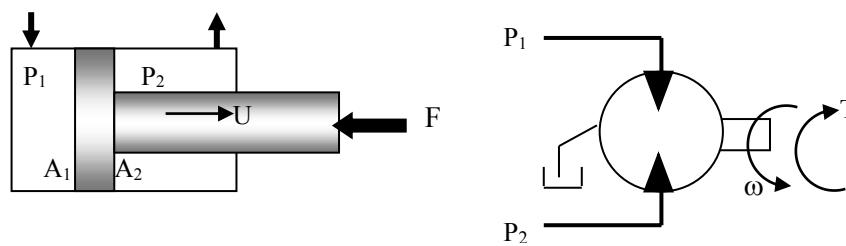


Figure 4.3 Force and torque on hydraulic actuators

From Newton’s second law of motion:

$$\begin{aligned} \text{Linear actuator} \quad P_1 A_1 - P_2 A_2 &= F + M \frac{dU}{dt} \\ \text{Motor} \quad D_m (P_1 - P_2) &= T + J \frac{d\omega}{dt} \end{aligned} \tag{4.5}$$

M is the load mass, J is the rotary inertia, F and T are the load force and torque. Again considering the electrical analogy then gives rise to the concept of mechanical inductance:

$$\text{Inductance } L = \frac{M}{A_1^2 A_2^2} \quad \text{or} \quad \frac{J}{D_m^2} \tag{4.6}$$

4.4 Undamped natural frequency of an actuator

The natural frequency is not affected by the input, load conditions and losses and therefore equations (4.3) and (4.5) may be combined and letting $Q_1 = Q_2 = F = T = 0$. Servovalve dynamics are neglected since they are very weakly connected to the actuator by flow reaction forces that are not discussed here. Considering a linear actuator, since the motor equivalent may be derived from this, then gives the servodrive speed differential equation by combining equations (4.3) and (4.5) as follows:

$$U + \frac{M}{\left(\frac{A_1^2 \beta}{V_1}\right) + \left(\frac{A_2^2 \beta}{V_2}\right)} \frac{d^2 U}{dt^2} = 0 \tag{4.7}$$

This is an undamped 2nd order differential equation, because there is no 1st order differential term dU/dt , and is often written in the following standard form:

$$U + \frac{1}{\omega_n^2} \frac{d^2U}{dt^2} = 0 \tag{4.8}$$

ω_n is called the undamped natural frequency.

$$\begin{aligned} \text{Cylinder } \omega_n &= \sqrt{\frac{k}{M}} \text{ rad/s} & \text{hydraulic spring stiffness } k &= \frac{A_1^2\beta}{V_1} + \frac{A_2^2\beta}{V_2} \text{ N/m} \\ \text{Motor } \omega_n &= \sqrt{\frac{t}{J}} \text{ rad/s} & \text{hydraulic torque stiffness } t &= \frac{D_m^2\beta}{V_1} + \frac{D_m^2\beta}{V_2} \text{ Nm} \end{aligned} \tag{4.9}$$



no.1
nine years
in a row

STUDY AT A TOP RANKED INTERNATIONAL BUSINESS SCHOOL

Reach your full potential at the Stockholm School of Economics, in one of the most innovative cities in the world. The School is ranked by the Financial Times as the number one business school in the Nordic and Baltic countries.

Visit us at www.hhs.se





Some interesting points arise by considering the undamped natural frequency equation:

- for a double-rod linear actuator $A_1 = A_2 = A$. If the volumes are dominated by the actuator only, that is line volumes are negligible, then it is a simple matter to show that the minimum undamped natural frequency occurs with the actuator in its mid-position with $V_1 = V_2 = V$.

This frequency is given by:

$$\omega_n = \sqrt{\frac{2A^2\beta}{MV}} = \sqrt{\frac{2}{LC}} \text{ rad/s} \quad L = \frac{M}{A^2} \quad C = \frac{V}{\beta} \quad (4.10)$$

- for a single rod actuator where $A_1 \neq A_2$, and again if line volumes are negligible, it can also be shown that the minimum undamped natural frequency occurs very close to the central position, even for area ratios up to $\gamma = A_1/A_2 = 2$
- a high undamped natural frequency requires a low mass and/or a high stiffness. The latter may be achieved using a large cross-sectional-area and small volumes

It is possible that *steel pipes may contribute to the effective bulk modulus*. The pipe material bulk modulus β_p may be determined from the theory of elasticity assuming a pipe of internal diameter d_i and external diameter d_o :

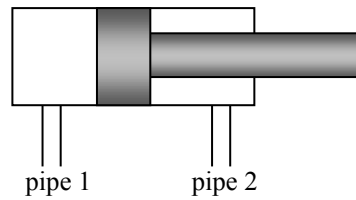
$$\frac{1}{\beta_p} = \frac{2}{E} \left[\frac{d_o^2 + d_i^2}{d_o^2 - d_i^2} + \mu \right] \quad (4.11)$$

E is the modulus of elasticity for the material and μ is Poisson's ratio for the material, typically $\mu = 0.3$ and $E = 2 \times 10^{11} \text{ N/m}^2$ for steel. For a pipe with a wall thickness $t \ll d_i$ then $d_i \approx d_o$ and equation (4.11) can be approximated by:

$$\frac{1}{\beta_p} \approx \frac{d}{tE} \quad (4.12)$$

The effective bulk modulus for a pipe β_e is then obtained by combining the pipe effect β_p with the fluid volume effect β_{ef} :

$$\frac{1}{\beta_e} = \frac{1}{\beta_p} + \frac{1}{\beta_{ef}} \quad (4.13)$$

Example 4.1

Consider the single-rod actuator shown.

Pipes 1 and 2 are flexible hose 7mm diameter 2m long

Hose bulk modulus $\beta_h = 0.7 \times 10^9 \text{ N/m}^2$

Oil bulk modulus $\beta = 1.4 \times 10^9 \text{ N/m}^2$

Bore diameter 50mm, rod diameter 28mm, actuator stroke 150mm

Load and actuator mass 550kg.

Assume the actuator is in its mid-position

Side 1

$$\text{Pipe volume} = \frac{\pi (49 \times 10^{-6}) \times 2}{4} = 7.7 \times 10^{-5} \text{ m}^3$$

$$\text{Actuator area } A_1 = \frac{\pi (2500 \times 10^{-6})}{4} = 19.64 \times 10^{-4} \text{ m}^2$$

$$\text{Actuator volume} = (19.64 \times 10^{-4}) (0.075) = 14.7 \times 10^{-5} \text{ m}^3$$

$$\text{Total volume } V_1 = 22.4 \times 10^{-5} \text{ m}^3$$

Effective bulk modulus:

$$\frac{1}{\beta_{e1}} = \left(\frac{7.7}{22.4} \right) \frac{1}{0.7 \times 10^9} + \left(\frac{14.7}{22.4} \right) \frac{1}{1.4 \times 10^9} \quad \frac{1}{\beta_{e1}} = \frac{0.49}{10^9} + \frac{0.47}{10^9}$$

$$\beta_{e1} = 1.04 \times 10^9 \text{ N/m}^2$$

Side 2

$$\text{Pipe volume} = 7.7 \times 10^{-5} \text{ m}^3$$

$$\text{Actuator area } A_2 = \frac{\pi (1716 \times 10^{-6})}{4} = 13.5 \times 10^{-4} \text{ m}^2$$

$$\text{Actuator volume} = (13.5 \times 10^{-4}) (0.075) = 10.1 \times 10^{-5} \text{ m}^3$$

$$\text{Total volume } V_2 = 17.8 \times 10^{-5} \text{ m}^3$$

Effective bulk modulus:

$$\frac{1}{\beta_{e2}} = \left(\frac{7.7}{17.8}\right) \frac{1}{0.7 \times 10^9} + \left(\frac{10.1}{17.8}\right) \frac{1}{1.4 \times 10^9} \quad \frac{1}{\beta_{e2}} = \frac{0.62}{10^9} + \frac{0.41}{10^9}$$

$$\beta_{e2} = 0.97 \times 10^9 \text{ N/m}^2$$

$$\text{stiffness } k = \frac{A_1^2 \beta_{e1}}{V_1} + \frac{A_2^2 \beta_{e2}}{V_2} = \frac{(385.7 \times 10^{-8})(1.04 \times 10^9)}{22.4 \times 10^{-5}} + \frac{(182.3 \times 10^{-8})(0.97 \times 10^9)}{17.8 \times 10^{-5}}$$

$$k = 17.9 \times 10^6 + 9.9 \times 10^6$$

$$k = 27.8 \times 10^6 \text{ N/m}$$

$$\text{undamped natural frequency } \omega_n = \sqrt{\frac{k}{M}} = \sqrt{\frac{27.8 \times 10^6}{550}} = 225 \text{ rad/s (35.8 Hz)}$$

- note in this example that the much smaller-volume hose, compared with actuator volumes, significantly influences the effective bulk modulus on each side due to the hose flexibility when compared with a rigid steel pipe
- also note that the hydraulic stiffness at side 1 is almost double that on side 2 due to the area ratio effect.



#1
in eco-friendly attitude

**STUDY AT
LINKÖPING UNIVERSITY, SWEDEN**
RANKED AMONG TOP 50 UNIVERSITIES UNDER 50

Interested in Strategy and Management in International Organisations? Kick-start your career with a master's degree from Linköping University, Sweden.

→ **Click here!**

 **Linköping University**

4.5 Actuator equations with losses and dynamics

The steady-state losses were discussed in Chapter 3 where it will be recalled that the main contribution to system damping are:

- leakages at the actuator
- viscous resistance due to actuator motion within the working fluid
- actuator and load stiction/Coulomb friction
- fluid friction due to long connecting lines in some applications

Considering now linear and rotary actuators shown in figure 4.4 with load mass M and rotary inertia J and losses. The flow continuity equations (4.3) are again stated and include leakage and compressibility as follows:

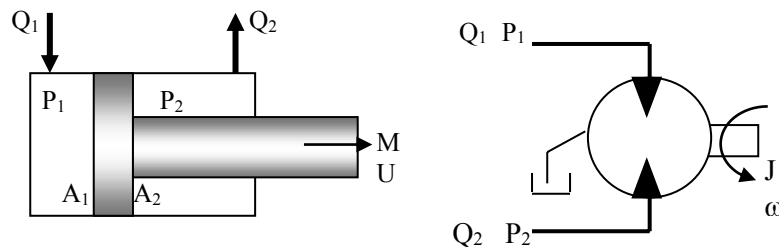


Figure 4.4 Flow rates into and out of hydraulic actuators

Linear actuator

Motor

$$\begin{aligned}
 Q_1 &= A_1 U + \frac{(P_1 - P_2)}{R_i} + \frac{V_1}{\beta} \frac{dP_1}{dt} & Q_1 &= D_m \omega + \frac{(P_1 - P_2)}{R_i} + \frac{P_1}{R_e} + \frac{V_1}{\beta} \frac{dP_1}{dt} \\
 Q_2 &= A_2 U + \frac{(P_1 - P_2)}{R_i} - \frac{V_2}{\beta} \frac{dP_2}{dt} & Q_2 &= D_m \omega + \frac{(P_1 - P_2)}{R_i} - \frac{P_2}{R_e} - \frac{V_2}{\beta} \frac{dP_2}{dt}
 \end{aligned}
 \tag{4.14}$$

It will be recalled that R_i is the leakage series resistance across the linear actuator piston, R_i and R_e are the motor internal and external resistances due to cross-port and other leakages. A correctly functioning linear actuator has no significant external leakage from the rod seals but a motor does have external leakage via the case drain connection to tank.

To get a reasonable initial feel for the probable system dynamic equations the mean flow rate may be used. Also, it may be assumed that for most applications that the volumes on either side are equal. This is probably correct for a motor and a reasonable approximation for a linear actuator, particularly with a double rod. Hence the dynamic flow continuity equations may be written as follows:

$$\text{Linear actuator} \quad Q = \frac{(A_1 + A_2)}{2} U + \frac{P_\ell}{R_{\text{act}}} + \frac{V}{2\beta} \frac{dP_\ell}{dt} \quad (4.15)$$

$$\text{Motor} \quad Q = D_m \omega + \frac{P_\ell}{R_{\text{act}}} + \frac{V}{2\beta} \frac{dP_\ell}{dt}$$

where R_{act} is a general leakage term for either actuator and $P_\ell = P_1 - P_2$.

It will be recalled from Chapter 3 that there will be a viscous friction loss which may be written as follows:

$$\text{Viscous friction loss} = B_v U \quad \text{or} \quad B_v \omega \quad (4.16)$$

where B_v is the viscous damping coefficient. The other friction losses are due to the stiction/friction characteristic of the actuator, also discussed in Chapter 3. A single stiction/Coulomb friction value, F_f or T_f , is usually added to the true viscous component for an estimate of system behaviour. The force and torque equations (4.5) therefore now become:

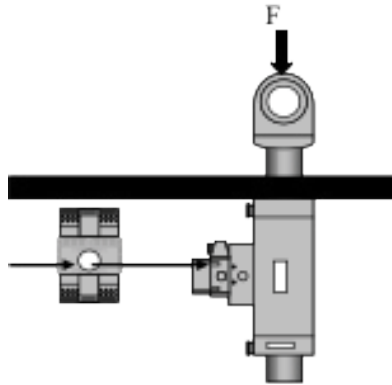
$$\text{Linear actuator} \quad P_1 A_1 - P_2 A_2 = F + F_f + B_v U + M \frac{dU}{dt} \quad (4.17)$$

$$\text{Motor} \quad D_m (P_1 - P_2) = T + T_f + B_v \omega + J \frac{d\omega}{dt}$$

where F is the load force for a linear actuator and T is the load torque for a motor.

Example 4.2

Consider an *open-loop* servodrive with a *double-rod actuator* with the servovalve directly mounted on the actuator. Determine the maximum velocity using the following data that includes losses:



Bore diameter 50mm, rod diameter 28mm

Actuator is vertical, stroke 150mm

Load and actuator mass 550kg

Actuator viscous damping coefficient $B_v = 2750 \text{ N/ms}^{-1}$

Negligible friction damping

“I studied English for 16 years but...
...I finally learned to speak it in just six lessons”
Jane, Chinese architect

ENGLISH OUT THERE

Click to hear me talking before and after my unique course download

Actuator leakage resistance $R_{act} = 5 \times 10^{11} \text{Nm}^{-2}/\text{m}^3\text{s}^{-1}$

Servovalve flow constant $k_f = 0.2$, rated flow @20mA

Supply pressure $P_s = 140\text{bar}$

Actuator annulus area $A = \frac{\pi(1716)10^{-6}}{4} = 13.5 \times 10^{-4} \text{m}^2$

Force steady-state equation $P_{\ell}(o) A = F + B_v U$

Flow steady-state flow continuity $Q = k_f i \sqrt{\frac{P_s - P_{\ell}(o)}{2}} = AU + \frac{P_{\ell}(o)}{R_{act}}$

The solution will be obtained using an iterative approach as follows:

i) **Step 1**, determine the steady-state velocity with the static load only:

$$P_{\ell}(o) (13.5 \times 10^{-4}) = 550(\text{g}) = 5396\text{N}$$

$$P_{\ell}(o) = 40\text{bar} \quad [P_1(o) = 90\text{bar} \quad P_2(o) = 50\text{bar}]$$

$$(0.2)(20) \sqrt{\frac{100}{2}} \frac{10^{-3}}{60} = (13.5 \times 10^{-4})U(o) + \frac{40 \times 10^5}{5 \times 10^{11}}$$

$$0.47 \times 10^{-3} - 0.008 \times 10^{-3} = (13.5 \times 10^{-4})U(o)$$

$$U(o) = 0.342\text{m/s}$$

ii) **Step 2**, now add the viscous effect:

$$P_{\ell}(o) (13.5 \times 10^{-4}) = 550(\text{g}) + 2750(0.342)$$

$$= 5396 + 941 = 6337\text{N}$$

$$P_{\ell}(o) = 46.9\text{bar}$$

$$(0.2)(20) \sqrt{\frac{93.1}{2}} \frac{10^{-3}}{60} = (13.5 \times 10^{-4})U(o) + \frac{46.9 \times 10^5}{5 \times 10^{11}}$$

$$0.455 \times 10^{-3} - 0.009 \times 10^{-3} = (13.5 \times 10^{-4})U(o)$$

$$U(o) = 0.33\text{m/s}$$

iii) **Step 3**, now modify the viscous effect:

$$P_{\ell}(o) (13.5 \times 10^{-4}) = 550(\text{g}) + 2750(0.33)$$

$$= 5396 + 908 = 6304\text{N}$$

$$P_{\ell}(o) = 46.7\text{bar}$$

$$(0.2)(20) \sqrt{\frac{93.3}{2}} \frac{10^{-3}}{60} = (13.5 \times 10^{-4})U(o) + \frac{46.7 \times 10^5}{5 \times 10^{11}}$$

$$0.455 \times 10^{-3} - 0.009 \times 10^{-3} = (13.5 \times 10^{-4})U$$

$$U(o) = 0.33 \text{ m/s}$$

The load pressure and velocity have barely changed so the iteration can cease with the assumption that $P_t(o) \approx 47 \text{ bar}$. The maximum actuator velocity $U_{\max} = 0.33 \text{ m/s}$. Note that the static load pressure alone gives $P_t(o) \approx 40 \text{ bar}$.

4.6 Linearisation of the system equations

An understanding of system dynamics can be achieved by the use of transfer functions, discussed later, which for a set of non-linear equations requires that all the equations must be linearised. This means that the analysis applies to small dynamic variations about a particular operating point. Consider a general second-order linear differential equation and linearise about an operating condition $y(o)$, $Y(o)$ by adding small increments δy and δY :

$$y + a \frac{dy}{dt} + b \frac{d^2 y}{dt^2} = Y$$

$$[y(o) + \delta y] + a \frac{d[y(o) + \delta y]}{dt} + b \frac{d^2 [y(o) + \delta y]}{dt^2} = [Y(o) + \delta Y] \quad (4.18)$$

$$\text{but } y(o) = Y(o) \quad \frac{dy(o)}{dt} = 0 \quad \frac{d^2 y(o)}{dt^2} = 0$$

$$\delta y + a \frac{d \delta y}{dt} + b \frac{d^2 \delta y}{dt^2} = \delta Y$$

The original differential equation is unchanged in its form but with y replaced by δy and Y replaced by δY .

Therefore the **servodrive flow rate linearised equations** may be developed from (4.15) by combining the servovalve linearised coefficients, (2.9), (2.10) and (2.11) to become:

$$\text{Linear actuator} \quad k_{qi} \delta i = \frac{(A_1 + A_2)}{2} \delta U + \delta P_\ell \left(\frac{1}{R_{\text{act}}} + \frac{1}{R_{\text{sv}}} \right) + \frac{V}{2\beta} \frac{d \delta P_\ell}{dt} \quad (4.19)$$

$$\text{Motor} \quad k_{qi} \delta i = D_m \delta \omega + \delta P_\ell \left(\frac{1}{R_{\text{act}}} + \frac{1}{R_{\text{sv}}} \right) + \frac{V}{2\beta} \frac{d \delta P_\ell}{dt}$$

$$k_{qi} = k_f \sqrt{\frac{P_s - P_\ell(o)}{2}} = \frac{Q(o)}{i(o)}$$

$$R_{sv} = \frac{1}{k_{qp}} = \frac{2\sqrt{2[P_s - P_\ell(o)]}}{k_f i(o)} = \frac{2[P_s - P_\ell(o)]}{Q(o)} \quad (4.20)$$

The *linearised force and torque equations* using (4.17) now become:

$$\text{Linear actuator} \quad \delta P_1 A_1 - \delta P_2 A_2 = \delta F + \delta F_f + B_v \delta U + M \frac{d \delta U}{dt} \quad (4.21)$$

$$\text{Motor} \quad D_m (\delta P_1 - \delta P_2) = \delta T + \delta T_f + B_v \delta \omega + J \frac{d \delta \omega}{dt}$$

Often the δ notation is dropped for convenience so that δP_1 is simply written as P_1 etc. However, it should be made clear in any analysis that a linearised approach is being used.

Note that the linearised steady-state relationship between actuator speed and current is exactly the same as the true relationship. This is another reason why a linearised approximation to system dynamics is useful as a good starting point in understanding both steady-state and dynamic behaviour of servodrives.

Excellent Economics and Business programmes at:



university of
groningen



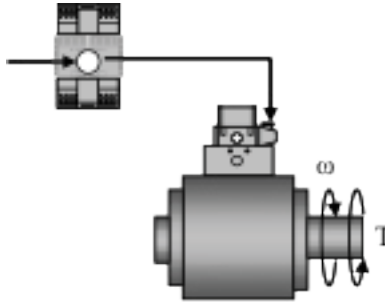

“The perfect start
of a successful,
international career.”

CLICK HERE
to discover why both socially
and academically the University
of Groningen is one of the best
places for a student to be

www.rug.nl/feb/education

Example 4.3

A motor is required to accelerate from zero to 120rpm in 2 seconds. Calculate the servovalve supply pressure required. If the motor is to be driven at a steady-state speed of 120rpm, calculate the power and flow rate needed. Data are as follows:



Load torque $T = 128.4\text{Nm}$, Coulomb friction $T_{cf} = 12\text{Nm}$

Displacement $D_m = 12 \times 10^{-6} \text{ m}^3/\text{rad}$

motor and load inertia $J = 0.5\text{kg m}^2$

Viscous coefficient $B_v = 0.04\text{Nm/rad s}^{-1}$

Flow loss = 1.5 litres/min @ the load pressure

i) Torque equation $D_m P_\ell = T + (T_f + B_v \omega) + J \frac{d\omega}{dt}$

Considering the worst condition for losses, that is the highest speed:

$$120\text{rpm} = 12.57\text{rad/s}$$

$$12 \times 10^{-6} P_\ell(o) = 128.4 + (12 + 0.04 \times 12.57) + 0.5 \frac{12.57}{2}$$

$$12 \times 10^{-6} P_\ell(o) = 128.4 + 12 + 0.5 + 3.14 = 144 \text{ Nm}$$

$$P_\ell(o) = 120\text{bar}$$

Choose a supply pressure $1.5 \times P_\ell(o)$ $P_s = 180\text{bar}$

Without the losses and inertia effect the load pressure would be 107 bar and the supply pressure would be 161bar, a difference of 19bar.

ii) The steady-state hydraulic torque required = 140.9Nm

$$\text{Power} = T\omega = (140.9)(12.57) = 1.77\text{kW}$$

$$\text{Flow rate } Q = D_m \omega + Q_{\text{loss}} \approx (12 \times 10^{-6})(12.57) + \frac{1.5 \times 10^{-3}}{60} \text{ m}^3/\text{sec}$$

$$Q = (0.151 \times 10^{-3} + 0.035 \times 10^{-3}) \text{ m}^3/\text{s}$$

$$Q = 0.186 \times 10^{-3} \text{ m}^3/\text{s} \text{ (11.2 litres/min)}$$

4.7 Pipe resistance, compressibility and inertia

Pipe friction losses can be extremely significant in large diameter/high flow rate systems such as steel processing operations where the power supply has to be remote from the actuators due to both noise and safety considerations. In such applications the power loss can be extremely high and cannot be overcome. For most conventional applications pipe friction is often negligible and clearly so when the servovalve is mounted on the actuator. However, each application must be assessed on its own merits.

The pressure drop Δp down a smooth pipe is calculated using the following well-established equation:

$$\text{Pipe pressure drop } \Delta p = 4f \left(\frac{1}{2} \rho U_{\text{mean}}^2 \right) \left(\frac{\ell}{d} \right) \quad (4.22)$$

where $4f$ is known as the friction factor, U_{mean} is the fluid mean velocity, ρ is the fluid density, ℓ is the pipe length and d is the pipe diameter. The friction factor may be calculated by determining the type of flow regime, laminar flow or turbulent flow. These regimes are calculated, for a smooth pipe, by first determining the Reynolds Number:

$$\text{Reynolds Number } R_e = \frac{\rho U_{\text{mean}} d}{\mu} \quad (4.23)$$

where μ is the fluid absolute viscosity. Note that fluid density varies slightly with temperature and pressure and it is important to check the fluid manufacturer's data. The friction factor $4f$ is then calculated using the sufficiently acceptable approximations as follows:

$$\begin{aligned} \text{laminar flow} \quad 4f &= \frac{64}{R_e} & R_e < 2000 \\ \text{turbulent flow} \quad 4f &= \frac{0.316}{R_e^{1/4}} & R_e > 2000 \end{aligned} \quad (4.24)$$


For laminar flow the relationship between pressure drop and flow rate is linear and combining equations (4.23) and (4.24) gives:

$$\begin{aligned} \Delta p &= R_p Q \\ \text{Resistance } R_p &= \frac{128 \mu \ell}{\pi d^4} \end{aligned} \quad (4.25)$$

The flow regime around $Re = 2000$ is actually quite complex and the transition zone from laminar to turbulent flow is not quite matched at $Re = 2000$. However this fluid mechanics detail is not too important for servodrive applications where the flow is usually well defined as either laminar for low-power applications or turbulent for high-power applications. For turbulent flow conditions a linear resistance is not applicable but the use of a non-linear resistance is easy to implement if computer simulation is used. For large flow, large diameter and long pipe applications, such as forging presses, the use of a laminar flow resistance rather than a turbulent flow resistance can give serious errors in system damping

Example 4.4

Consider a forging press as shown below and similar in concept to two industrial systems analysed by the author for the manufacturer.



In the past four years we have drilled

89,000 km

That's more than **twice** around the world.

Who are we?
We are the world's largest oilfield services company¹. Working globally—often in remote and challenging locations—we invent, design, engineer, and apply technology to help our customers find and produce oil and gas safely.

Who are we looking for?
Every year, we need thousands of graduates to begin dynamic careers in the following domains:

- Engineering, Research and Operations
- Geoscience and Petrotechnical
- Commercial and Business

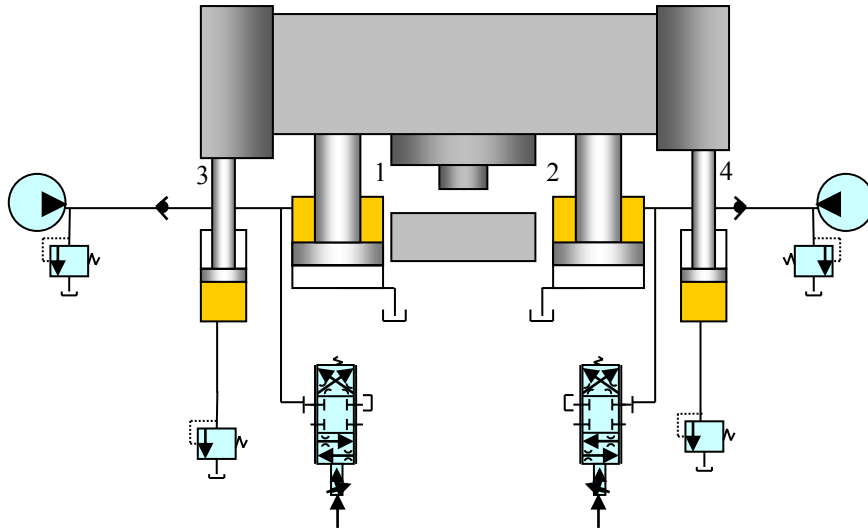
What will you be?

careers.slb.com

Schlumberger

¹Based on Fortune 500 ranking 2011. Copyright © 2015 Schlumberger. All rights reserved.





One half of the press is shown where cylinders 3 and 4 (plus two others) are used for lowering the press into position and cylinders 1 and 2 (plus two others) are used for pressing. The servovalves shown are used to bleed flow for rotation control when the press is operating off-centre. Determine the line pressure drop when forging and the total power dissipated by friction when forging. Data for the lines are as follows:

Pressing cylinder net cross-sectional-area = 2.5m^2

Line length $\ell = 150\text{m}$ Line diameter $d = 80\text{mm}$

Full flow rate when pressing 4000litres/min

Fluid viscosity $\mu = 0.02\text{Ns/m}^2$ Fluid density $\rho = 860\text{kg/m}^3$

$$\text{Flow rate when pressing} \quad Q = \frac{(4000)10^{-3}}{60} = 66.7 \times 10^{-3} \text{ m}^3/\text{s}$$

$$\text{Pressing speed} \quad U_p = \frac{66.7 \times 10^{-3}}{2.5} = 27 \text{ mm/s}$$

$$\text{Pipe cross-sectional-area} \quad a = \frac{\pi(6400 \times 10^{-6})}{4} = 5.03 \times 10^{-3} \text{ m}^2$$

$$\text{Pipe mean velocity} \quad U_{\text{mean}} = \frac{66.7 \times 10^{-3}}{5.03 \times 10^{-3}} = 13.3 \text{ m/s}$$

$$\text{Reynolds Number} \quad R_e = \frac{\rho U_{\text{mean}} d}{\mu} = \frac{(860)(13.3)(0.08)}{0.02} = 45,752$$

Hence the flow is highly turbulent and therefore the friction factor is given by;

$$4f = \frac{0.316}{R_e^{1/4}} = \frac{0.316}{45752^{1/4}} = 0.0216$$

The pressure drop is then given by $\Delta p = 4f \left(\frac{1}{2} \rho U_{\text{mean}}^2 \right) \left(\frac{\ell}{d} \right)$

$$\Delta p = 0.0216 \left(\frac{(860)(176.9)}{2} \right) \left(\frac{150}{0.08} \right) = 30.8 \times 10^5 \text{ N/m}^2 \text{ (30.8bar)}$$

Power dissipated down one line only when pressing:

$$(\Delta p)(Q) = (30.8 \times 10^5)(66.7 \times 10^{-3}) = 205 \times 10^3 \text{ W (205kW)}$$

The total power loss is extremely large and explains why large-force forging presses require a substantial electrical power supply to drive the array of pumps to overcome friction losses and provide the high flow rate at the high pressure required during operation.

Fluid compressibility for a pipe has already been dealt with since it is no different to that defined earlier for a general fluid volume. However the problem is how the compressibility is handled if it is significant for a long line and this will be considered after fluid inertia has been discussed. **Fluid inductance** for a pipe is defined as follows:

$$\text{Pipe fluid inductance } L_p = \frac{m}{a^2} = \frac{\rho \ell}{a} \quad (4.26)$$

$$\text{Pipe total capacitance } C_p = \frac{V}{\beta} \quad (4.27)$$

Therefore for laminar flow the pressure drop down a pipe has resistive and inductive components. The compressibility flow and pressure drop are given symbolically by:

$$\Delta Q = C_p \frac{dP}{dt} \quad (4.28)$$

$$\Delta p = R_p Q + L_p \frac{dQ}{dt} \quad (4.29)$$

Now having defined fluid resistance, capacitance and inductance the important question is how are these fluid properties distributed along a line? The true answer is that a distributed parameter analysis applies and there are well-established ways of modelling a line using this approach. For the present study, given the context of this book, just one of several approximations is used, sometimes called a lumped approximation, and actually can be a good representation of a line as a first-estimate. A common lumped approximation is a π network as shown in figure 4.5.

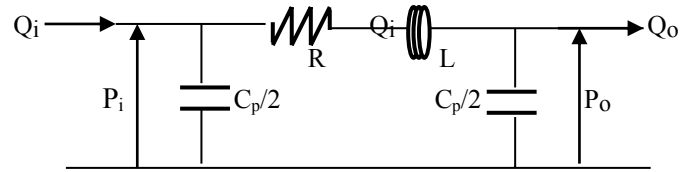


Figure 4.5 A π network approximation for a line

In this approximating network half the line capacitance is lumped at each end with the total resistance and total inductance being lumped in series in the middle. Two networks may be connected with each R, L, C elements halved for each network. This aspect of line modelling will be pursued later when a servodrive undamped natural frequency is considered.

4.8 Servodrive open-loop linearised differential equation with losses and dynamics

Bringing together flow rate equations (4.19) and load equations (4.21) then allows the equations relating speed and input current to be established. **For a linear actuator a double-rod will be used such that $A_1 = A_2 = A$** and only the dynamic terms will be included since constant terms such as load force/torque and friction do not influence the dynamic behaviour. It will also be assumed that the volumes on either side of the actuator are equal $V_1 = V_2 = V$. Therefore with no line dynamics the open-loop system linearised equations of motion become:

For a linear actuator:

$$\left[1 + \frac{R_{\text{visc}}}{R} \right] \delta U + \left[\frac{L}{R} + \frac{CR_{\text{visc}}}{2} \right] \frac{d \delta U}{dt} + \frac{LC}{2} \frac{d^2 \delta U}{dt^2} = \frac{k_{qi}}{A} \delta i$$

$$k_{qi} = k_f \sqrt{\frac{P_s - P_\ell(o)}{2}} \quad R_{sv} = \frac{1}{k_{qp}} = \frac{2[P_s - P_\ell(o)]}{Q(o)} \tag{4.30}$$

$$R_{\text{visc}} = \frac{B_v}{A^2} \quad \frac{1}{R} = \frac{1}{R_{\text{act}}} + \frac{1}{R_{sv}} \quad L = \frac{M}{A^2} \quad C = \frac{V}{\beta}$$

For a motor:

$$\text{replace } A \rightarrow D_m \text{ and } M \rightarrow J \tag{4.31}$$

It can be seen that the open-loop system has damping, as expected, due to the presence of the $d\delta U/dt$ term in (4.31). In practice the second factor in the δU term will probably be negligible. Dropping the δ notation for representational convenience only, this 2nd order differential equation may now be written in standard notation:

$$U + \frac{2\zeta}{\omega_n} \frac{dU}{dt} + \frac{1}{\omega_n^2} \frac{d^2U}{dt^2} = U_{ss} \quad (4.32)$$

$$U_{ss} = \frac{k_{qi}i}{A\alpha} \quad \omega_n = \sqrt{\frac{2\alpha}{LC}} \quad \frac{2\zeta}{\omega_n} = \frac{L}{R\alpha} + \frac{CR_{visc}}{2\alpha} \quad \alpha = \left[1 + \frac{R_{visc}}{R} \right]$$

ω_n is the undamped natural frequency and ζ is the damping ratio

In practice the terms involving R_{visc} are often negligible thus simplifying the evaluation of undamped natural frequency and damping ratio. Usually $\alpha \approx 1$, but whatever data applies the transient response to a step change in demand will be as shown in figure 4.6 for different values of damping ratio.

American online

LIGS University

is currently enrolling in the
Interactive Online **BBA, MBA, MSc,**
DBA and PhD programs:

- ▶ enroll **by September 30th, 2014** and
- ▶ **save up to 16%** on the tuition!
- ▶ pay in 10 installments / 2 years
- ▶ Interactive **Online** education
- ▶ visit www.ligsuniversity.com to find out more!

Note: LIGS University is not accredited by any nationally recognized accrediting agency listed by the US Secretary of Education. More info [here](http://www.ligsuniversity.com).





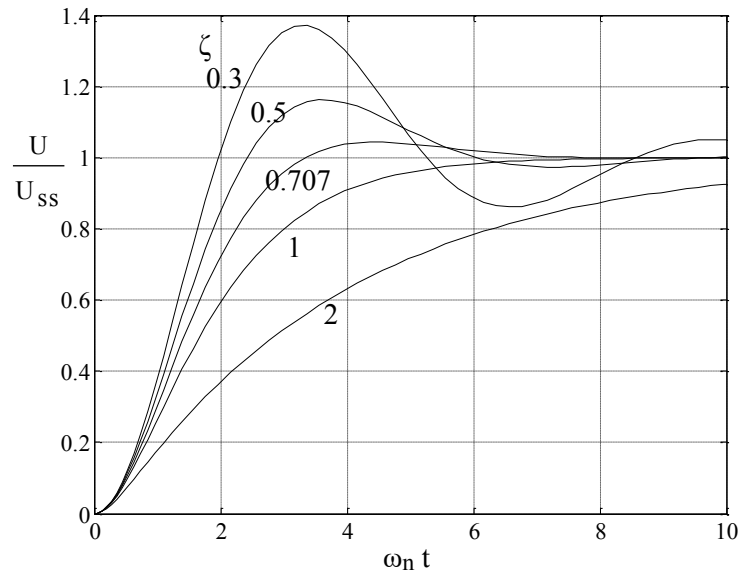


Figure 4.6 Time response to a step input of a second-order transfer function

The damping ratio is equally important as the undamped natural frequency since it determines whether or not the system response is oscillatory as follows:

under-damped (oscillatory) $\zeta < 1$

critically-damped $\zeta = 1$ (4.33)

over-damped $\zeta > 1$

In practice a good design would achieve a damping ratio $0.7 < \zeta < 1$. If a response is oscillatory then the actual frequency of oscillation, the **damped frequency** ω_d , is given by:

$$\omega_d = \omega_n \sqrt{1 - \zeta^2} \quad (4.34)$$

If the viscous friction effect is negligible then the damping ratio is given by:

$$\zeta = \frac{1}{R} \sqrt{\frac{2L}{C}} = \left[\frac{1}{R_{act}} + \frac{1}{R_{sv}} \right] \sqrt{\frac{2L}{C}} \quad (4.35)$$

For very small servovalve currents and hence low speeds under open-loop control, and certainly under closed-loop position control, the servovalve resistance R_{sv} is extremely high and will contribute little damping. Inherent damping is then provided by actuator resistance R_{act} . From the author's experience, two power regimes of control may be considered.

- low-power servodrives will have small-diameter actuators and hence a relatively high undamped natural frequency which is desirable
- high-power servodrives will have large-diameter actuators and hence will tend to provide actuator damping albeit with a low undamped natural frequency
- this may well explain, to some extent, why servodrive dynamics in practice do not seem to present major control issues

4.9 Servovalve dynamics

Clearly the sudden application of a current to a servovalve will not result in the spool moving instantaneously to its commanded position. Servovalve dynamics originate from the electromagnetic circuit of the torque motor, fluid dynamics within the hydraulic first stage, viscous and inertia effects due to the spool. These effects have been studied over many years but the applicability of a general theory to the many servovalve designs available is not possible or even fruitful in the context of this book.

A second-order spool dynamics characteristic is often used but a higher-order approximation may be used if necessary. Considering a second order differential equation for servovalve spool motion then the undamped natural frequency ω_{nsv} and damping ratio ζ_{sv} may be estimated from the manufacturer's data or from measurements by the user. Hence recalling definitions in Chapter 2, the dynamic flow rate for a particular port may be determined by including a spool dynamics function f as follows:

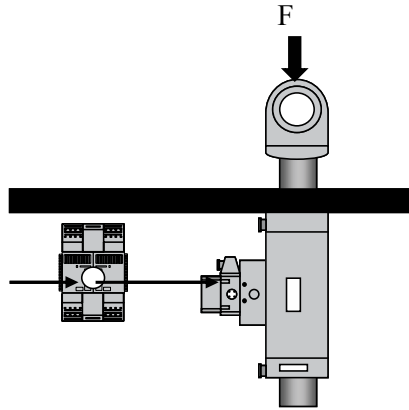
$$Q = f \sqrt{\Delta P} \quad (4.36)$$

$$f + \frac{2\zeta_{sv}}{\omega_{nsv}} \frac{df}{dt} + \frac{1}{\omega_{nsv}^2} \frac{d^2f}{dt^2} = k_f i \quad (4.37)$$

It should also be realised that the damping ratio will vary greatly with servovalve type and also the magnitude of the current applied to the servovalve. For larger current changes the damping tends to increase and this variation may readily be assessed from the manufacturer's data where the effect is usually presented. In practical work by the author, the manufacturer's data for a common industrial servovalve showed an undamped natural frequency $\omega_{nsv} = 140\text{Hz}$ and a damping ratio $\zeta_{sv} = 1$, and averaged over a wide range of servovalve currents. Very-high response servovalves are available but the performance does depend upon the servovalve type, design and rated flow.

Example 4.5

Consider Example 4.2. Determine the probable open-loop transient behaviour when the actuator is extending from zero to maximum speed given the following data:



- Fluid bulk modulus $\beta = 1.4 \times 10^9 \text{N/m}^2$
- Bore diameter 50mm, rod diameter 28mm, actuator stroke 150mm
- Load and actuator mass 550kg, the actuator is vertical
- Assume the actuator is in its mid-position
- Servo valve flow constant $k_f = 0.2$, rated flow @20mA

.....Alcatel-Lucent 

www.alcatel-lucent.com/careers

What if you could build your future and create the future?

One generation's transformation is the next's status quo. In the near future, people may soon think it's strange that devices ever had to be "plugged in." To obtain that status, there needs to be "The Shift".

 [Click on the ad to read more](#)

Supply pressure $P_s = 140\text{bar}$

Actuator leakage resistance $R_{\text{act}} = 5 \times 10^{11} \text{Nm}^{-2}/\text{m}^3\text{s}^{-1}$

Viscous damping coefficient $B_v = 2750 \text{N/ms}^{-1}$

Actuator friction is negligible due to low-friction seals

Actuator annulus area $A = \frac{\pi(1716)10^{-6}}{4} = 13.5 \times 10^{-4} \text{m}^2$

Actuator volume $V = 13.50 \times 10^{-4}(0.075) = 10.1 \times 10^{-5} \text{m}^3$

Pressure differential required is $P_\ell A = F + B_v U + M \text{d}U/\text{d}t$

A linearised analysis assumes steady-state conditions in which case the acceleration is zero. For this example the load force and viscous losses only will be used to determine the load pressure as used in Example 4.2. From the steady-state conditions at the maximum servovalve current of 20mA:

$$P_\ell(o)A = F + B_v U(o)$$

$$U = \frac{k_{qi} i}{A} = \frac{k_f i \sqrt{\frac{P_s - P_\ell(o)}{2}}}{A} = \frac{k_f i \sqrt{\frac{P_s - [F + B_v U]/A}{2}}}{A}$$

Using an iterative approach the steady-state velocity is found to be $U(o) = 0.33\text{m/s}$

Steady-state flow rate $Q(o) = (0.33)(13.5 \times 10^{-4}) = 45 \times 10^{-5} \text{m}^3/\text{s}$

During motion $P_\ell(o) \approx 47\text{bar}$ $P_1(o) = 93.5\text{bar}$ $P_2(o) = 46.5\text{bar}$

At rest $P_\ell(o) \approx 40\text{bar}$ $P_1(o) = 90\text{bar}$ $P_2(o) = 50\text{bar}$

Now consider the transient response from zero to maximum velocity. The linearised differential equation of motion is given by:

$$\left[1 + \frac{R_{\text{visc}}}{R}\right]U + \left[\frac{L}{R} + \frac{CR_{\text{visc}}}{2}\right]\frac{\text{d}U}{\text{d}t} + \frac{LC}{2}\frac{\text{d}^2 U}{\text{d}t^2} = \frac{k_{qi} i}{A}$$

$$R_{\text{visc}} = \frac{B_v}{A^2} \quad \frac{1}{R} = \frac{1}{R_{\text{act}}} + \frac{1}{R_{\text{sv}}} \quad L = \frac{M}{A^2} \quad C = \frac{V}{\beta}$$

$$R_{\text{sv}} = \frac{1}{k_{qp}} = \frac{2[P_s - P_\ell(o)]}{Q(o)}$$

Evaluating all the resistances:

$$R_{\text{visc}} = \frac{2750}{182.3 \times 10^{-8}} = 0.15 \times 10^{10} \text{ Nm}^{-2}/\text{m}^3 \text{ s}^{-1}$$

$$R_{\text{sv}} = \frac{(2)(93 \times 10^5)}{45 \times 10^{-5}} = 4.1 \times 10^{10} \text{ Nm}^{-2}/\text{m}^3 \text{ s}^{-1}$$

$$R_{\text{act}} = 50 \times 10^{10} \text{ Nm}^{-2}/\text{m}^3 \text{ s}^{-1}$$

$$\frac{1}{R} = \frac{1}{R_{\text{act}}} + \frac{1}{R_{\text{sv}}} = \frac{1}{50 \times 10^{10}} + \frac{1}{4.1 \times 10^{10}} = 0.26 \times 10^{-10}$$

$$\frac{R_{\text{visc}}}{R} = 0.15 \times 10^{10} (0.26 \times 10^{-10}) = 0.04 \quad \alpha = 1 + \frac{R_{\text{visc}}}{R} \approx 1$$

$$\frac{L}{R} = \frac{(550)(0.26 \times 10^{-10})}{182.3 \times 10^{-8}} = 78.4 \times 10^{-4} \text{ s}$$

For the damping terms

$$\frac{CR_{\text{visc}}}{2} = \frac{(10.1 \times 10^{-5})(0.15 \times 10^{10})}{1.4 \times 10^9 (2)} = 0.54 \times 10^{-4} \text{ s}$$

$$\frac{L}{R} + \frac{CR_{\text{visc}}}{2} = 78.4 \times 10^{-4} + 0.54 \times 10^{-4} = 79 \times 10^{-4} \text{ s}$$

So, the mechanical time constant L/R dominates over the fluid time constant $CR_{\text{visc}}/2$

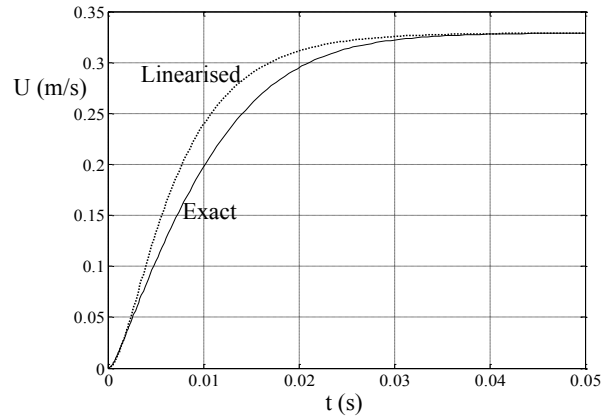
$$\omega_n = \sqrt{\frac{2}{LC}} = \sqrt{\frac{2(182.3 \times 10^{-8})(1.4 \times 10^9)}{(550)(10.1 \times 10^{-5})}} = 303 \text{ rad/s (48.2 Hz)}$$

The linearised differential equation of motion is:

$$U + 79 \times 10^{-4} \frac{dU}{dt} + \frac{1}{(303)^2} \frac{d^2U}{dt^2} = 0.33$$

$$\text{since } \frac{2\zeta}{\omega_n} = 79 \times 10^{-4} \rightarrow \zeta = 1.2$$

The open-loop transient behaviour is therefore predicted to be over-damped and there will be no oscillation in velocity based on the steady-state speed specified. A comparison of the linearised estimation and the exact motion obtained from computer simulation is shown.



A linearised transient analysis strictly speaking only applies for small variations about the steady-state condition. However a linearised analysis is usually extrapolated to the large-signal response, in this case from zero velocity to its steady-state velocity. The following points arise from this example:

- the steady-state velocity is correctly predicted by the linearised equation of motion
- it can be seen that the linearised solution has a lower predicted damping which is usually the case for a second-order servodrive system and is a good, fortuitous, design feature
- a linearised approach based upon steady-state conditions can give a good feel for the transient response that might be expected



Join the best at
the Maastricht University
School of Business and
Economics!

Top master's programmes

- 33rd place Financial Times worldwide ranking: MSc International Business
- 1st place: MSc International Business
- 1st place: MSc Financial Economics
- 2nd place: MSc Management of Learning
- 2nd place: MSc Economics
- 2nd place: MSc Econometrics and Operations Research
- 2nd place: MSc Global Supply Chain Management and Change

Sources: Keuzegids Master ranking 2013; Elsevier 'Beste Studies' ranking 2012; Financial Times Global Masters in Management ranking 2012

Maastricht University is the best specialist university in the Netherlands (Elsevier)

Visit us and find out why we are the best!
Master's Open Day: 22 February 2014

www.mastersopenday.nl



4.10 The role of computer simulation

In many cases, with easily-defined hydraulic elements and loads, it may only be necessary to use a linearised approach and the assessment of dynamic behaviour is then not too difficult, as will be seen later. However the reality of more complex processes means that non-linear computer simulation is essential. It is now commonplace that a simulation model incorporating the non-linear equations and higher-order dynamics is used to assess the most probable system behaviour, particularly for complex processes such as metal working or aerospace applications.

Hydraulic systems users are demanding that the control promise of the system manufacturer can be met and the only way this can be done is by computer simulation if a similar system has not previously been built. It therefore makes sense for the system manufacturer to build up good system sub-models along the way such that future contracts can be more readily assessed. In the author's experience of modelling the dynamic behaviour of high-power manufacturing processes prior to manufacture, the issues of concern have been:

- determination of actuator damping and leakage, particularly for very large diameter actuators
- joint friction in large structures
- suitable, useable, pipeline models for larger diameter pipes with turbulent flow
- dynamic models for very high flow rate flow control valves and pressure relief valves

For modest power applications component testing can be undertaken in the fluid power laboratory and/or data can be supplied by the manufacturer. Whatever the approach, an agreement has to be reached between the manufacture and the system analyst regarding any possible limitations of a computer simulation and its predictions.

There are many simulation packages used by different fluid power groups, some of them developed in-house, but in this book Matlab software is used, the Control System Toolbox for linear systems and Simulink for non-linear systems. A servoactuator and control system is built using the software library but the final model does not look like a fluid power circuit. Appropriate mathematical functions are dragged onto the computer screen from the Library using the mouse, the function placed wherever appropriate in the block diagram and then connected. The package is easy to work with, extremely flexible and allows a library of hydraulic and control sub-models to be developed that may then be easily integrated into new control systems.

Where appropriate in this book the “*exact model*” for a servovalve-controlled linear actuator system is as follows:

Servovalve dynamic flow rates:

$$\begin{aligned} Q_1 &= f \sqrt{P_s - P_1} & Q_2 &= f \sqrt{P_2} & i > 0 \\ Q_1 &= f \sqrt{P_1} & Q_2 &= f \sqrt{P_s - P_2} & i < 0 \end{aligned} \quad (4.38)$$

Servovalve spool dynamics:

$$f + \frac{2\zeta_{sv}}{\omega_{nsv}} \frac{df}{dt} + \frac{1}{\omega_{nsv}^2} \frac{d^2f}{dt^2} = k_f i \quad (4.39)$$

$$\text{Actuator volume changes:} \quad V_1 = V_1(o) + A_1 y \quad V_2 = V_2(o) - A_2 y \quad (4.40)$$

Flow rate dynamic equations:

$$\begin{aligned} Q_1 &= A_1 U + \frac{(P_1 - P_2)}{R_{act}} + \frac{V_1}{\beta} \frac{dP_1}{dt} \\ Q_2 &= A_2 U + \frac{(P_1 - P_2)}{R_{act}} - \frac{V_2}{\beta} \frac{dP_2}{dt} \end{aligned} \quad (4.41)$$

$$\text{Actuator/load dynamic equation:} \quad P_1 A_1 - P_2 A_2 = F + B_v U + M \frac{dU}{dt} \quad (4.42)$$

Building the Matlab Simulink model is relatively straightforward, each differential equation being re-arranged such that the highest differential term is placed on the left hand side. For the system being considered here this means that dP_1/dt , dP_2/dt , dU/dt and d^2f/dt^2 are then created allowing them to be integrated to produce P_1 , P_2 , U , df/dt and f which are then used to complete each appropriate block diagram.

From the modelling experience of the author, the following points may be useful for the beginner:

- limit appropriate parameters to their practical values such as servovalve current and actuator maximum stroke in each direction from the initial condition
- do not allow negative pressures following integration. This is a simplified approach, rarely needed, but does avoid simulation failure by trying to calculate the square root of a negative number in some operational conditions
- select a relative tolerance of 10^{-6} and use the ode23 [bogacki-Shampine] solver as a starting point
- do not include closed-loops that are algebraic only

- create sub-models for self-contained elements of the simulation to both simplify the screen layout and to allow transfer of standard sub-models to other simulations. Annotate each sub-model as much as possible to aid later understanding
- try and make sub-models as general as possible, for example include both actuator areas A_1 and A_2 as separate input parameters. They may be made equal for a double-rod actuator
- use scopes to view the simulation results and save data to Workspace using the Array format. Include a clock to Workspace so that the simulation time is available for the plotting requirement
- use the Simulink command window to plot the results, for example `plot(t,y)` will plot the computed position y against time t which may be annotated using the graphics routines within this facility. If the symbols P_1 and P_2 for pressures are used in the simulation, then to plot the pressures use `plot(t,P1,t,P2)`
- note that later versions of the software not used by the author may well have significant updates

The general Matlab Simulink block diagram for an open-loop linear actuator system is now shown as figure 4.7 and is exactly as appears on the computer screen. Outputs position, y , and velocity, U , are monitored via Scopes and also stored via Workspace 1 and Workspace 2. The time t is stored using Workspace 3.

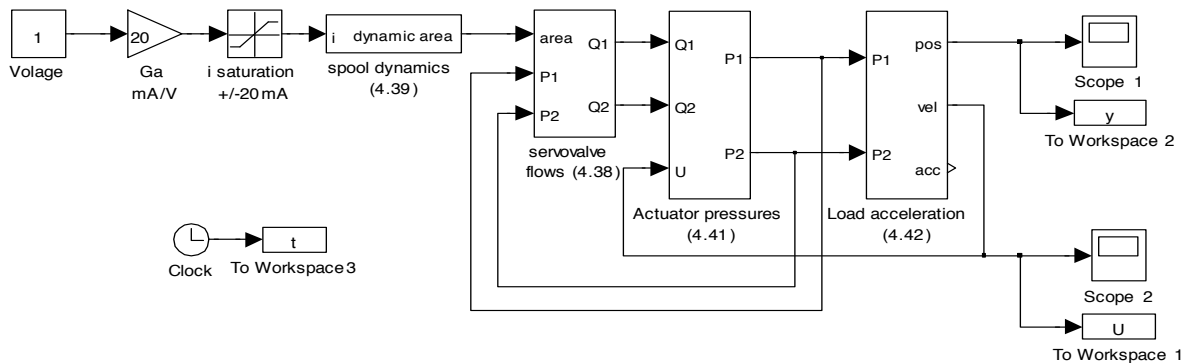
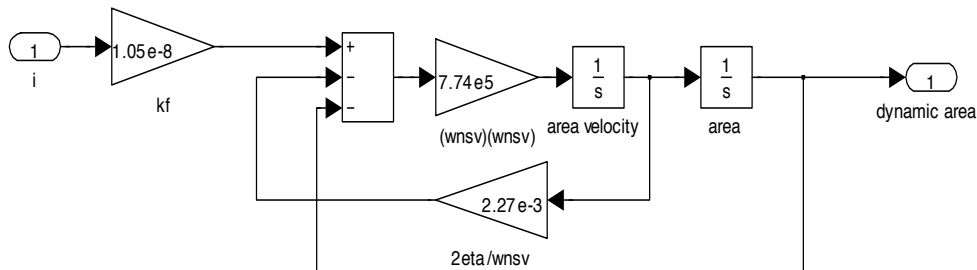


Figure 4.7 Matlab Simulink open-loop block diagram for a linear actuator

It can be seen that four sub-models have been created for servovalve spool dynamics, servovalve flows, actuator pressures and actuator acceleration which is integrated twice to determine velocity and position.

Example 4.6

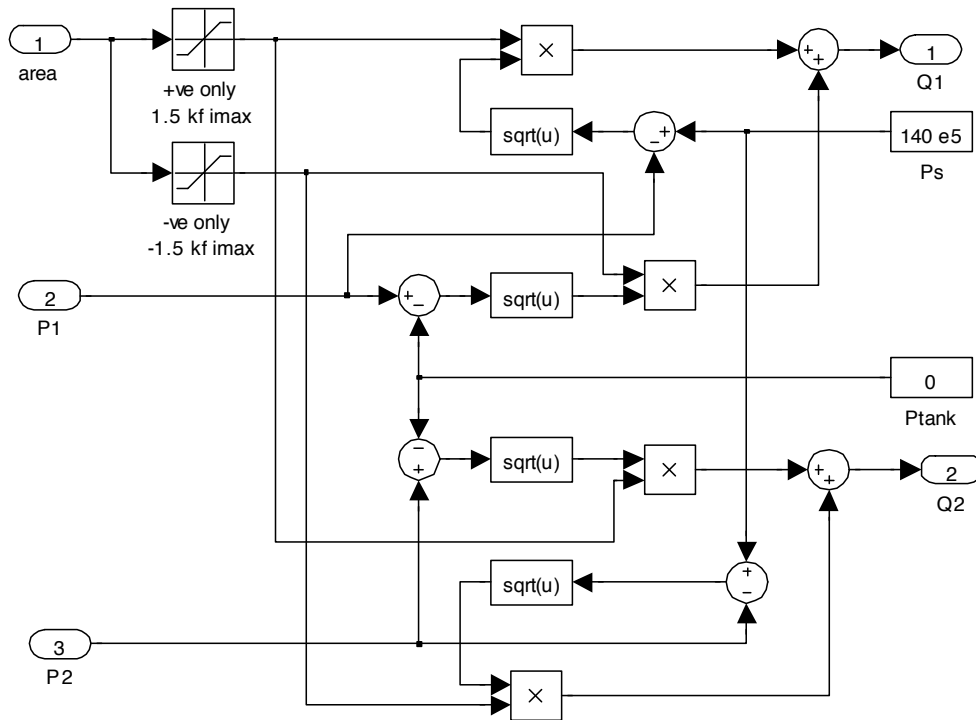
Consider the previous Example 4.5 with the addition of servovalve dynamics. The same data applies together with servovalve dynamics characterised by an undamped natural frequency $\omega_{nsv} = 140\text{Hz}$ and a damping ratio $\zeta_{sv} = 1$. The block diagram is the same as figure 4.7 and the sub-blocks to determine servovalve flow rates are now shown.



a) Dynamic build-up of the servovalve area function

agence.cdg. © Photonistop

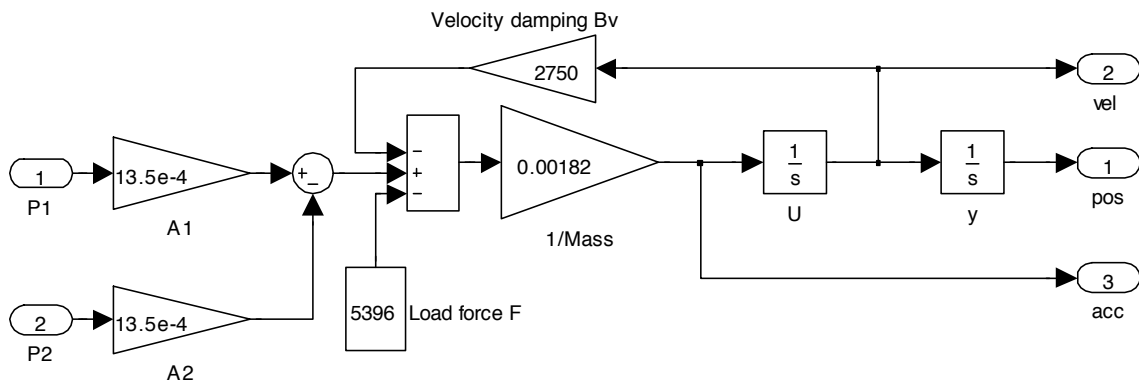




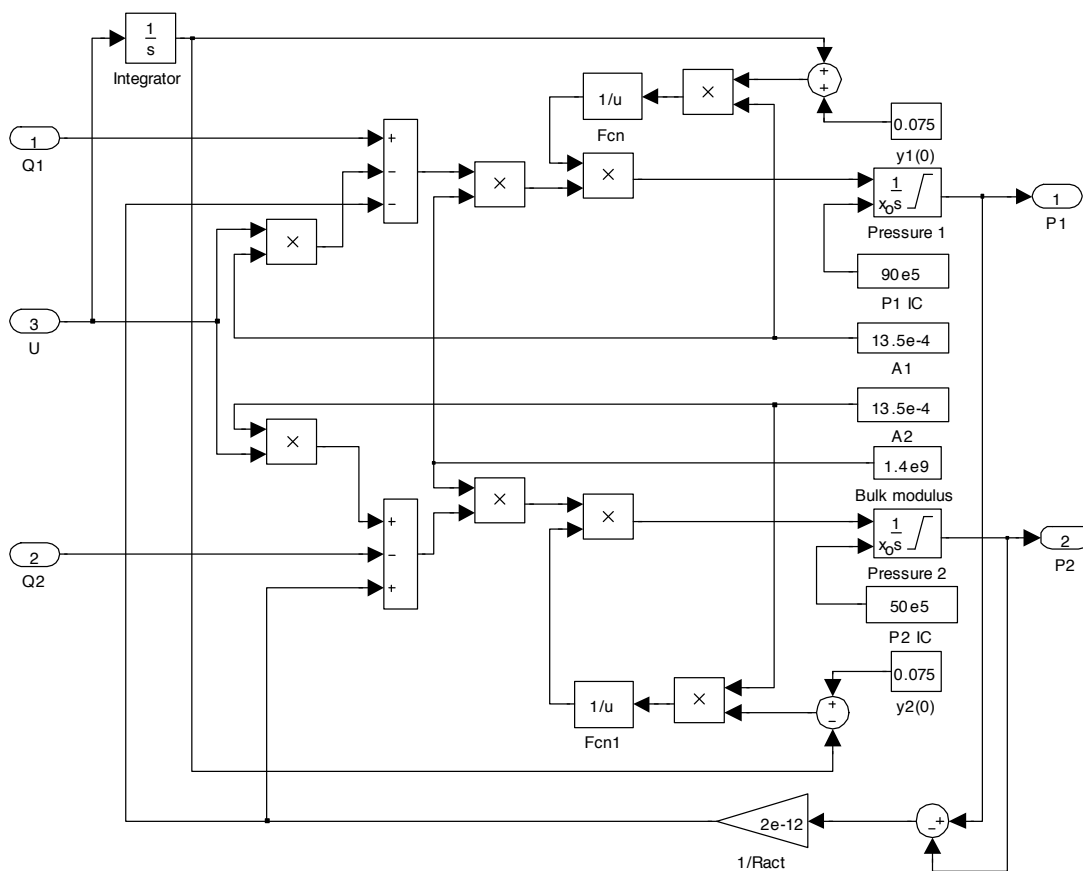
b) Calculation of the flow rates Q_1 and Q_2

An integrator has the symbol $1/s$, where s is the Laplace operator that is discussed further in Chapter 5. Saturation blocks are used to select port flow direction and maintain the correct notation for each pressure, although in this example for the actuator extending case only the servovalve current does not change sign. The range of each saturation blocks is set to $0 \rightarrow +1.5kf i_{max}$ and $-1.5kf i_{max} \rightarrow 0$.

The sub-models for obtaining the load position y and the two pressures P_1 and P_2 are built in a similar way, the only significant addition being that the mathematical function $1/u$, is required to determine the inverse of the time varying volumes either side of the actuator. Note the output limitations on each integrator to determine pressures. The static pressures $P_1 = 90\text{bar}$ and $P_2 = 50\text{bar}$ are used as initial conditions.



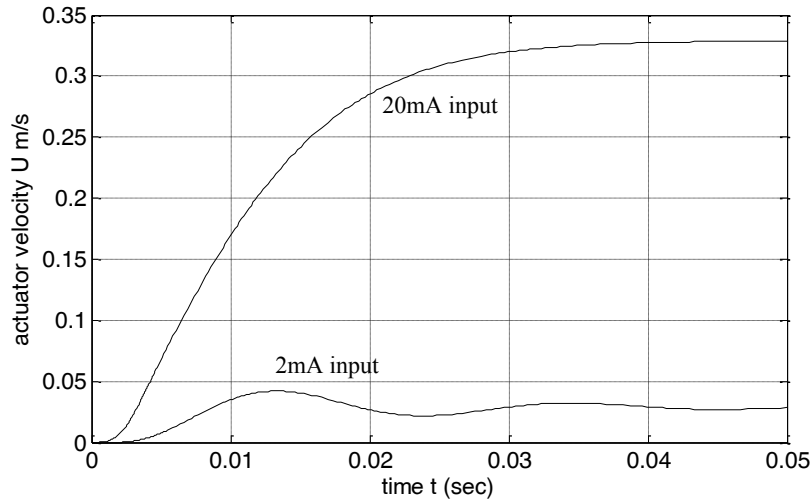
c) Calculation of the velocity U and the position y



d) Calculation of the pressures P_1 and P_2

The time to run this basic simulation is difficult to assess since it is completed almost as soon as the mouse click, to initiate execution, has been released. It is therefore a very fast and efficient approach that allows system changes to be easily made and their effects observed.

Results are now shown using Example 4.5 data and for servovalve currents of 2mA and 20mA. The latter was shown in Example 4.5 together with the prediction using a linearised transfer function.



Servodrive open-loop velocity response for sudden changes in applied current of 2mA and 20mA. Actuator initially at rest

As predicted by the linearised analysis, the response becomes more oscillatory as the magnitude of the applied current is decreased. It is recalled here that from earlier work presented that the servovalve resistance is given by:

$$R_{sv} = \frac{1}{k_{qp}} = \frac{2[P_s - P_\ell(o)]}{Q(o)}$$

Empowering People. Improving Business.

BI Norwegian Business School is one of Europe's largest business schools welcoming more than 20,000 students. Our programmes provide a stimulating and multi-cultural learning environment with an international outlook ultimately providing students with professional skills to meet the increasing needs of businesses.

BI offers four different two-year, full-time Master of Science (MSc) programmes that are taught entirely in English and have been designed to provide professional skills to meet the increasing need of businesses. The MSc programmes provide a stimulating and multi-cultural learning environment to give you the best platform to launch into your career.

- MSc in Business
- MSc in Financial Economics
- MSc in Strategic Marketing Management
- MSc in Leadership and Organisational Psychology

www.bi.edu/master



At high steady-state flow rates the servovalve resistance is finite and dominant but as the flow rate approaches zero then the servovalve resistance approaches infinity and damping is then dominated by leakage and viscous friction effectively producing low effective damping.

Over the range of operation one of the pressures may transiently approach zero, implying undesirable cavitation in practice. This is a common dichotomy in open-loop electrohydraulic servodrives:

- small signals may produce large fluctuations in velocity but small fluctuations in pressures
 - larger signals produce less oscillations in velocity yet higher fluctuations in pressures
-

The use of Matlab Control System Toolbox is valuable for the analysis of linear systems and may easily be used to determine both transient response and frequency response, the latter being extremely useful for understanding the effect of control techniques and the conditions for closed-loop instability. The use of this Toolbox will be demonstrated later following the introduction of block diagrams for linear systems.

5 Laplace transforms, transfer functions, block diagrams, transient and frequency response

5.1 Aim

The aim of this chapter is to show how a fluid power circuit can be analysed in a way that is common within the fluid power industry and via objectives as follows:

- to introduce Laplace transforms for linear, or linearised, system equations and to use the method to generate transfer functions and block diagrams
- to develop common block diagrams for servodrives
- to use a transfer function approach to get a preliminary feel for natural frequency with significant connecting lines
- to compare the relationship between transient response and frequency response and to introduce the use of Matlab Control System Toolbox
- to demonstrate the use of transfer functions and block diagrams via worked examples

5.2 Laplace transforms

Differential equations that describe system dynamics are not in a form often used by fluid power control engineers, unless computer simulation is to be undertaken. Block diagrams are a useful way of representing a control system and Laplace transforms are merely a way of changing linear differential equations into algebraic equations to facilitate this process. For the purpose of this book Laplace transforms are used in their simplest form, notwithstanding the powerful mathematical process of the technique used in many aspects of control theory. The process of Laplace transformation of all elements of a linear differential equations changes it to an algebraic equation and operates on time domain functions as follows:

$$\text{Laplace transform of a function } \mathbf{L}f(t) = F(s) = \int_0^{\infty} f(t)e^{-st} dt \quad (5.1)$$

where $f(t)$ is the time varying function and s is the Laplace operator. Some common Laplace transforms are shown in Table 1. Consider first an arbitrary differential equation for position control relating output y with its demanded value y_d as follows:

$$y + a \frac{dy}{dt} + b \frac{d^2y}{dt^2} = y_d \quad (5.2)$$

To solve this differential equation then transform each element using the appropriate Laplace transforms from Table 1. Also for the complete solution any initial conditions, $y(0)$ and $dy(0)/dt$ will have to be specified. The (s) notation is used to signify Laplace transformation as follows:

$$y(s) + a[s y(s) - y(0)] + b[s^2 y(s) - s y(0) - \frac{dy(0)}{dt}] = y_d(s) \tag{5.3}$$

[entry 15] [entry 16]

$$[1 + as + bs^2]y(s) = [a y(0) + s b y(0) + b \frac{dy(0)}{dt}] + y_d(s)$$

$$y(s) = \frac{[a y(0) + s b y(0) + b \frac{dy(0)}{dt}] + y_d(s)}{[1 + as + bs^2]} \tag{5.4}$$

The complete solution is then obtained by inserting any initial conditions and also applying the Laplace transform of the input signal $y_d(s)$. The resulting function is then transformed back into the time domain by choosing appropriate inverse Laplace transforms from Table 1. For a system starting from rest then all the initial conditions are zero and the relationship between the output and the input is now given by:

$$y(s) = \frac{y_d(s)}{[1 + as + bs^2]} \tag{5.5}$$

Need help with your dissertation?

Get in-depth feedback & advice from experts in your topic area. Find out what you can do to improve the quality of your dissertation!

Get Help Now



Go to www.helpmyassignment.co.uk for more info





f(t)	F(s)	f(t)	F(s)
1 Unit impulse	1	8 $\frac{1}{a^2}[at - (1 - e^{-at})]$	$\frac{1}{s^2(s+a)}$
2 Step h	$\frac{h}{s}$	9 $\frac{1}{(b-a)}[e^{-at} - e^{-bt}]$ b ≠ a	$\frac{1}{(s+a)(s+b)}$
3 t^n n = 1,2,3,---	$\frac{n!}{s^{n+1}}$	10 $\sin \omega t$	$\frac{\omega}{(s^2 + \omega^2)}$
4 e^{-at}	$\frac{1}{(s+a)}$	11 $\cos \omega t$	$\frac{s}{(s^2 + \omega^2)}$
5 $t e^{-at}$	$\frac{1}{(s+a)^2}$	12 $1 - \cos \omega t$	$\frac{\omega^2}{s(s^2 + \omega^2)}$
6 $\frac{1}{(n-1)!} t^{n-1} e^{-at}$	$\frac{1}{(s+a)^n}$	13 $e^{at} \sin \omega t$	$\frac{\omega}{(s+a)^2 + \omega^2}$
7 $\frac{1}{a}(1 - e^{-at})$	$\frac{1}{s(s+a)}$	14 $e^{-at} \cos \omega t$	$\frac{(s+a)}{(s+a)^2 + \omega^2}$
15 $\frac{df(t)}{dt}$	$sF(s) - f(0)$		
16 $\frac{d^2f(t)}{dt^2}$	$s^2F(s) - sf(0) - \frac{df(0)}{dt}$		
17 Delay $f(t - T)$	$e^{-sT}f(t)$		
18 Final value theorem	$\text{Lim}_{t \rightarrow \infty} f(t) = sF(s) \Big _{s=0}$		
19 Initial value theorem	$\text{Lim}_{t \rightarrow 0} f(t) = sF(s) \Big _{s=\infty}$		

Table 1 Some common Laplace transforms

5.3 Transfer functions and block diagrams

The concept of a **transfer function** may now be introduced. A transfer function relates “output” to “input”. For example, neglecting the initial condition, then from (5.5) the transfer function relating position $y(s)$ to demanded position $y_d(s)$ becomes:

$$\frac{y(s)}{y_d(s)} = \frac{1}{(1 + as + bs^2)} \tag{5.6}$$

A transfer function may then be represented by a **block diagram** and this is of great value when describing a control system. For example a simple block diagram for (5.6) may be constructed as shown in figure 5.1.

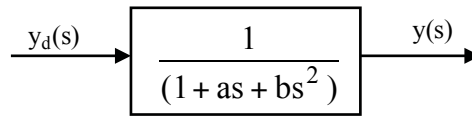


Figure 5.1 Block diagram representation of a transfer function

It should now be noticed that time differential terms in a differential equation are simply transformed into algebraic terms, when initial conditions are neglected, with a suitable power of the Laplace operator s . The transformations are as follows:

$$\frac{dy}{dt} \rightarrow sy(s) \quad \frac{d^2y}{dt^2} \rightarrow s^2y(s) \quad \frac{d^3y}{dt^3} \rightarrow s^3y(s) \quad \int ydt \rightarrow \frac{y(s)}{s} \quad (5.7)$$

It is important to realise at this stage that the nature of the transient response and the stability of a linear closed-loop system do not depend upon initial conditions and load conditions. For this reason transfer functions such as that shown as figure 5.1 tend not to include initial condition terms when analysing control systems response and stability.

Now consider a **closed-loop position control system** as shown in figure 5.2, in this case for a servodrive with a double-rod linear actuator, and with losses and significant dynamics. **Servo valve dynamics are neglected here**, that is they are much faster than the system dynamics.

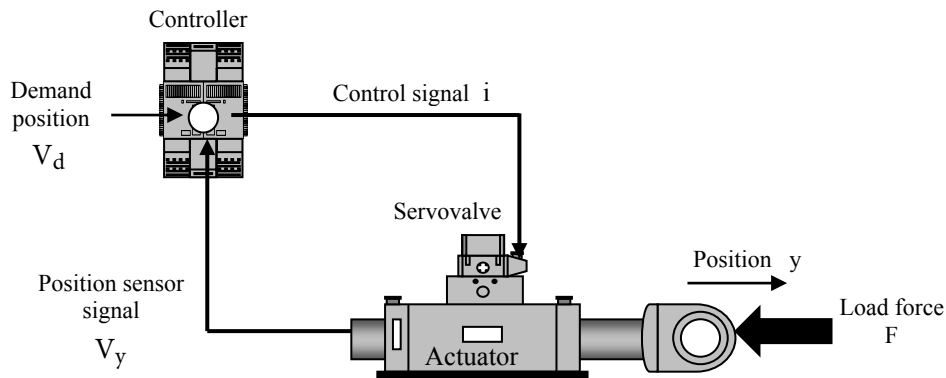


Figure 5.2 A servodrive closed-loop control system

The differential equation for the servodrive is reproduced as follows *in linearised form* but without the $\delta U(s)$ and $\delta i(s)$ notation for convenience:

$$\left[1 + \frac{R_{\text{visc}}}{R}\right]U + \left[\frac{L}{R} + \frac{CR_{\text{visc}}}{2}\right]\frac{dU}{dt} + \frac{LC}{2}\frac{d^2U}{dt^2} = \frac{k_{qi}i}{A} \quad (5.8)$$

$$R_{\text{visc}} = \frac{B_v}{A^2} \quad \frac{1}{R} = \frac{1}{R_{\text{act}}} + \frac{1}{R_{\text{sv}}} \quad L = \frac{M}{A^2} \quad C = \frac{V}{\beta}$$

It was also discussed earlier that the second term of U will probably be negligible in practice and therefore (5.8) may be represented with sufficient accuracy as follows:

$$U + \left[\frac{L}{R} + \frac{CR_{\text{visc}}}{2}\right]\frac{dU}{dt} + \frac{LC}{2}\frac{d^2U}{dt^2} = \frac{k_{qi}i}{A} \quad (5.9)$$

Brain power

By 2020, wind could provide one-tenth of our planet's electricity needs. Already today, SKF's innovative know-how is crucial to running a large proportion of the world's wind turbines.

Up to 25 % of the generating costs relate to maintenance. These can be reduced dramatically thanks to our systems for on-line condition monitoring and automatic lubrication. We help make it more economical to create cleaner, cheaper energy out of thin air.

By sharing our experience, expertise, and creativity, industries can boost performance beyond expectations. Therefore we need the best employees who can meet this challenge!

The Power of Knowledge Engineering

Plug into The Power of Knowledge Engineering.
Visit us at www.skf.com/knowledge

SKF

Taking Laplace transforms and neglecting initial conditions then gives the following transfer function relating velocity to applied current:

$$\frac{U(s)}{i(s)} = \frac{k_{qi}/A}{(1 + \frac{2\zeta}{\omega_n}s + \frac{s^2}{\omega_n^2})} \tag{5.10}$$

$$\omega_n = \sqrt{\frac{2}{LC}} \quad \frac{2\zeta}{\omega_n} = \frac{L}{R} + \frac{CR_{visc}}{2}$$

The *undamped natural frequency* is ω_n and ζ is the *damping ratio*. Recalling the process of integration to obtain position from velocity, using its Laplace transform, then results in the closed-loop block diagram shown as figure 5.3. The feedback signal is obtained from a position sensor, gain H_p V/m, and the closed-loop system must have *negative feedback* to function in a stable manner.

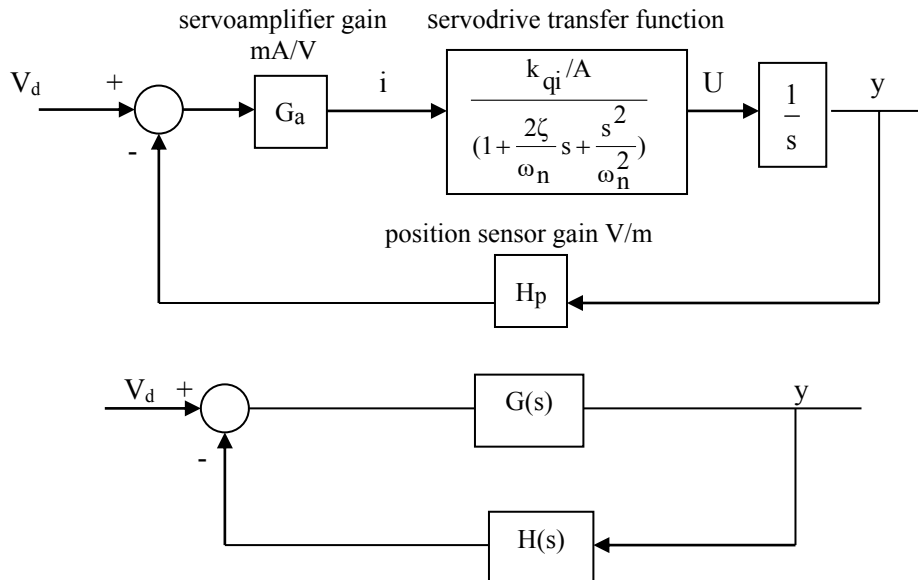


Figure 5.3 Block diagram for a servodrive position control system

The blocks in the forward loop are usually combined into a common block called the *forward gain* $G(s)$. In control theory any feedback block, or product of blocks, is referred to as the *feedback gain* $H(s)$. The **open-loop transfer function** (OLTF) is the product $G(s)H(s)$.

This very basic introduction to block diagram representation should indicate the simplicity of adding extra dynamics. For example if it is necessary to include *servovalve dynamics*, then from Chapter 4 the 2nd order differential equation approximation results in a 2nd order transfer function which is then simply added into the forward loop as shown in figure 5.4.

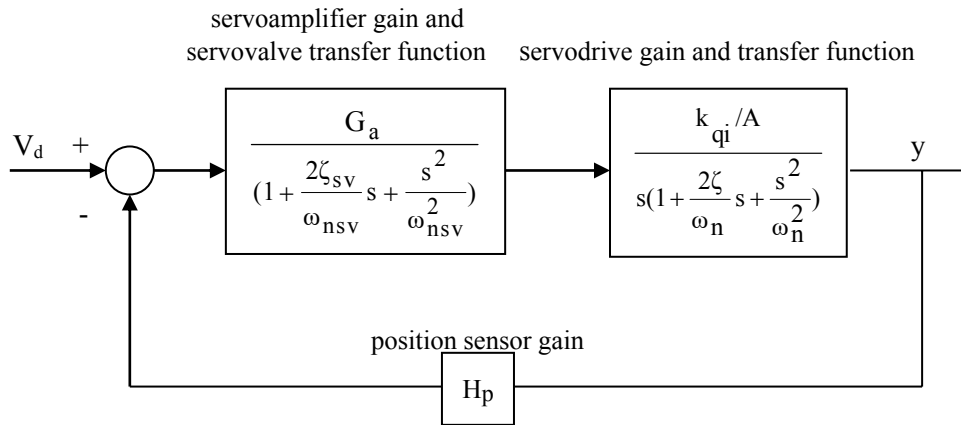


Figure 5.4 Block diagram for a servodrive position control system with servovalve dynamics included

Now the closed-loop dynamics are 5th order, the highest power of s in the denominator of the OLTF, and the dynamic behaviour can really only be assessed via computer analysis or simulation, a straightforward process given the various simulation packages commercially available. If computer simulation is used then it makes sense to model the correct servovalve non-linear flow characteristic.

The servovalve transfer function is known as *type 0* since it has no free integrator term in the denominator, the servodrive transfer function is known as *type 1* due to the single integrator, the combined servovalve and servodrive transfer function therefore also being *type 1*.

5.4 Undamped natural frequency with connecting line effects

An initial estimate on whether or not line dynamics are significant may be made by comparing line and load inductances. From Chapter 4 it was stated that:

$$\begin{aligned}
 \text{Line inductance } L_{\text{line}} &= \frac{\rho \ell}{a} \\
 \text{Load inductance } L &= \frac{M}{A_1 A_2} \text{ or } \frac{J}{D_m^2}
 \end{aligned}
 \tag{5.11}$$

If the two values are similar then line dynamics will probably have to be included. An additional aid is to determine the line fundamental frequency by considering the time for a wave travelling at the speed of sound to travel along the line. This pure delay is given by:

$$T = \frac{\ell}{C_o} \qquad C_o = \sqrt{\frac{\beta}{\rho}}
 \tag{5.12}$$

Assuming typical values of $\beta \approx 1.4 \times 10^9 \text{ Nm}^{-2}/\text{m}^3\text{s}^{-1}$ and $\rho \approx 860 \text{ kg/m}^3$ for a mineral oil then the velocity of sound $C_o = 1276 \text{ m/s}$ and the pure delay is 0.78 ms per metre length of pipe. The frequency to travel along a line, and back, is then given by:

$$f_n = \frac{1}{2T} = \frac{C_o}{2\ell} \text{ Hz} \rightarrow \omega_n = \pi \frac{C_o}{\ell} \text{ rad/s} \quad (5.13)$$

This gives a line frequency of 638 Hz/m , 319 Hz/2m etc which may be compared with the actuator undamped natural frequency already discussed.

The influence of the connecting lines between the servovalve and actuator can easily be deduced using Laplace transforms but is restricted here to a **double-rod actuator**. Consider figure 5.5 and a first-estimate of line dynamics using a simple approximation.

What do you want to do?

No matter what you want out of your future career, an employer with a broad range of operations in a load of countries will always be the ticket. Working within the Volvo Group means more than 100,000 friends and colleagues in more than 185 countries all over the world. We offer graduates great career opportunities – check out the Career section at our web site www.volvogroup.com. We look forward to getting to know you!

VOLVO
AB Volvo (publ)
www.volvogroup.com

VOLVO TRUCKS | RENAULT TRUCKS | MACK TRUCKS | VOLVO BUSES | VOLVO CONSTRUCTION EQUIPMENT | VOLVO PENTA | VOLVO AERO | VOLVO IT
VOLVO FINANCIAL SERVICES | VOLVO 3P | VOLVO POWERTRAIN | VOLVO PARTS | VOLVO TECHNOLOGY | VOLVO LOGISTICS | BUSINESS AREA ASIA

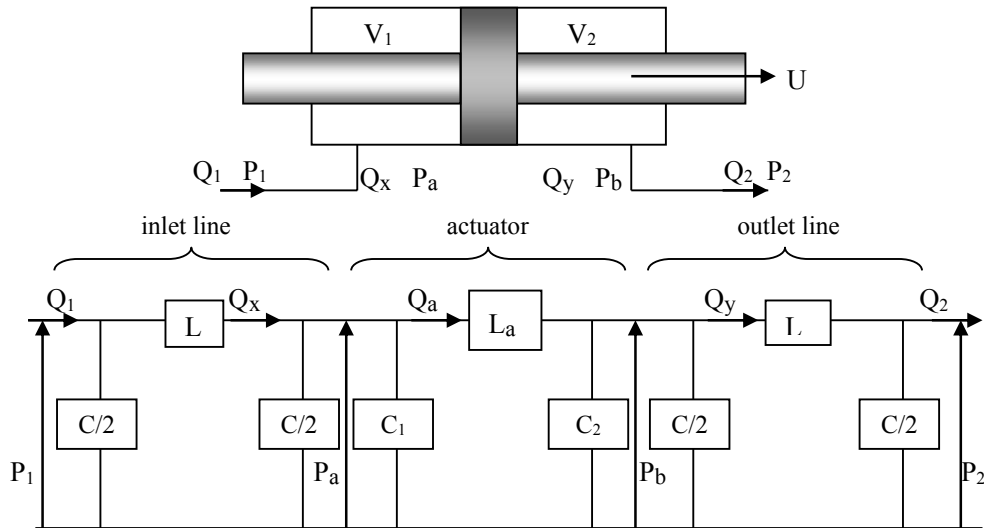


Figure 5.5 Electrical analogy for actuator and lines with losses neglected

The model is built up as follows:

- to determine the system undamped natural frequency then losses do not need to be included. Hence compressibility and inertia terms only are needed to construct the circuit representation shown as figure 5.5
- a **single π lump approximation** has been used for each line as a first-estimate, and is just one of many approximations that may be used. Half the line total compressibility effect, $C/2$, has been placed at each line end with each line total inductance L placed between them
- it will be noticed that the actuator compressibility effects C_1 and C_2 have to be added with each line $C/2$ where appropriate at two circuit points
- the load inductance due to moving mass is given by L_a . Assume equal volumes on either side of the actuator, $C_1 = C_2 = C_{act}$

The Laplace transformed equations, with zero initial conditions, are as follows:

$$\begin{aligned} \text{Inlet line} \quad Q_1 - Q_x &= s \frac{C}{2} P_1(s) \\ P_1 - P_a &= sLQ_x(s) \end{aligned}$$

$$\begin{aligned} \text{Actuator} \quad Q_x(s) - Q_a(s) &= sC_a P_a(s) & C_a &= \frac{C}{2} + C_{act} \\ P_a(s) - P_b(s) &= sL_a Q_a(s) & Q_a(s) &= AU(s) \end{aligned}$$

$$Q_a(s) - Q_y(s) = sC_b P_b(s) \quad C_b = \frac{C}{2} + C_{act}$$

$$\text{Outlet line} \quad P_b(s) - P_2(s) = sLQ_y(s)$$

$$Q_y(s) - Q_2(s) = s \frac{C}{2} P_2(s)$$

Combining the system equations then gives:

$$Q_a(s) = AU(s) = \frac{(Q_1 + Q_2)(s)}{1 + s^2 \left(\frac{LC}{2} + \frac{L_a C}{2} + \frac{L_a C_{act}}{2} \right) + s^4 \frac{LL_a C \left(\frac{C}{2} + C_{act} \right)}{4}}{2} \quad (5.14)$$

The roots of the denominator of (5.14) give an approximation to the two coupled undamped natural frequencies, one representative of line dynamics and the other representative of actuator dynamics. These two frequencies are easily determined by the solution of two quadratic equations by letting $s = j\omega$ and then equating the denominator of (5.14) to zero. Two useful solutions are readily obtained for the uncoupled cases as follows:

i) *If the actuator dynamics are negligible*, $L_a = C_{act} = 0$, then:

$$Q_a(s) = AU(s) = \frac{(Q_1 + Q_2)(s)}{1 + s^2 \frac{LC}{2}} \quad (5.15)$$

Hence the undamped natural frequency is due to the lines alone. The undamped natural frequency is given by:

$$\omega_n = \sqrt{\frac{2}{LC}} = \sqrt{2} \frac{C_o}{\ell}$$

$$\text{where } C_o \text{ is the velocity of sound propagation } C_o = \sqrt{\frac{\beta}{\rho}} \quad (5.16)$$

Considering a lossless line in isolation then the undamped natural frequency for two coupled lines of total length 2ℓ is given by:

$$f_n = \frac{C_o}{4\ell} \rightarrow \omega_n = \frac{\pi C_o}{2\ell} \quad (5.17)$$

It can be seen that equation (5.16) has a numerical factor of 1.41 whereas equation (5.17) has a numerical factor of 1.57. For servodrives that have lines that create little damping then the lumped parameter approximation gives an estimate of the undamped natural frequency similar to that estimated using wave transmission theory. These two similar solutions are sufficient to give a “feel” for the magnitude of expected line dynamic effects.

ii) If line dynamics are negligible, $L = C = 0$, then:

$$Q_a(s) = AU(s) = \frac{(Q_1 + Q_2)(s)}{1 + s^2 \frac{L_a C_{act}}{2}} \tag{5.18}$$

This is the same as for the actuator alone. The undamped natural frequency now is given by:

$$\omega_n = \sqrt{\frac{2}{L_a C_{act}}} = \sqrt{\frac{2A^2 \beta}{MV}} = \sqrt{\frac{k}{M}} \tag{5.19}$$

k is the hydraulic stiffness $k = \frac{2A^2 \beta}{V}$

Example 5.1

Consider a real example, studied by the author, of a servovalve connected to the actuator by a pair of similar lines, each line being a combination of steel pipe and flexible hose. This is typical of what happens in practice where a short hose is often used to minimise vibration coupling between components and with a steel pipe to minimise air-borne noise.

gaiteye
Challenge the way we run

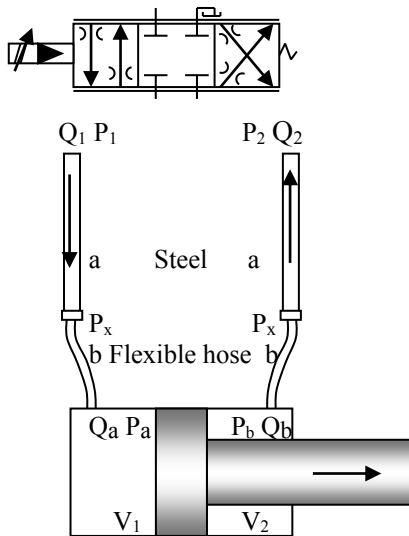
EXPERIENCE THE POWER OF FULL ENGAGEMENT...

.....

**RUN FASTER.
RUN LONGER..
RUN EASIER...**

READ MORE & PRE-ORDER TODAY
WWW.GAITEYE.COM





Fluid density $\rho = 860\text{kg/m}^3$
 Fluid viscosity $\mu = 0.032\text{Ns/m}^2$
 Velocity damping $B_v = 2 \times 10^4\text{N/ms}^{-1}$
 $\beta_{\text{hose}} = 0.7 \times 10^9\text{Nm}^{-2}$
 $\beta_{\text{oil}} = 1.4 \times 10^9\text{Nm}^{-2}$

Moving mass $m = 25\text{kg}$
 Cylinder bore diameter = 76.2mm
 Cylinder rod diameter = 38.1mm
 Total stroke = 0.254mm
 Piston initially centralised

Steel lines (a) 0.9m long, 13mm diameter
 Flexible hose (b) 0.6m long, 7mm diameter

Servovalve flow constant $k_f = 0.212$
 current mA, pressure drop bar

The actuator is horizontal, with no load force F and is not connected to its load mechanism, hence having its minimum mass m . The cylinder is a high quality product designed for precision control applications and having low friction seals. Consequently the stiction/friction force was found to be negligible.

a) areas and volumes

$A_1 = 4.56 \times 10^{-3}\text{m}^2$	$a_a = 1.33 \times 10^{-4}\text{m}^2$	$a_b = 0.38 \times 10^{-4}\text{m}^2$
$V_1 = 0.58 \times 10^{-3}\text{m}^3$	$V_a = 0.12 \times 10^{-3}\text{m}^3$	$V_b = 0.023 \times 10^{-3}\text{m}^3$
$A_2 = 3.42 \times 10^{-3}\text{m}^2$	$a_a = 1.33 \times 10^{-4}\text{m}^2$	$a_b = 0.38 \times 10^{-4}\text{m}^2$
$V_2 = 0.43 \times 10^{-3}\text{m}^3$	$V_a = 0.12 \times 10^{-3}\text{m}^3$	$V_b = 0.023 \times 10^{-3}\text{m}^3$

Total volume on side 1 $V_{t1} = 0.72 \times 10^{-3}\text{m}^3$

Total volume on side 2 $V_{t2} = 0.57 \times 10^{-3}\text{m}^3$

b) system parameters

The effective bulk modulus for each side of the actuator is developed using the three components in parallel as follows:

inlet line $\frac{1}{\beta} = \frac{0.12/0.72}{0.7 \times 10^9} + \frac{0.023/0.72}{1.4 \times 10^9} + \frac{0.58/0.72}{1.4 \times 10^9} \rightarrow \beta = 1.2 \times 10^9\text{N/m}^2$

outlet line $\frac{1}{\beta} = \frac{0.12/0.57}{0.7 \times 10^9} + \frac{0.023/0.57}{1.4 \times 10^9} + \frac{0.43/0.57}{1.4 \times 10^9} \rightarrow \beta = 1.2 \times 10^9\text{N/m}^2$

Considering the various inductance values:

$$\text{Line a} \quad L = \frac{\rho \ell_a}{a_a} = \frac{(860)(0.9)}{1.33 \times 10^{-4}} = 5.8 \times 10^6 \text{ kg/m}^4$$

$$\text{Line b} \quad L = \frac{\rho \ell_b}{a_b} = \frac{(860)(0.6)}{0.38 \times 10^{-4}} = 13.6 \times 10^6 \text{ kg/m}^4$$

$$\text{Line total } L = 19.4 \times 10^6 \text{ kg/m}^4$$

An approximate load mechanical inductance is calculated using both actuator areas:

$$L_a = \frac{m}{A_1 A_2} = \frac{25}{(4.56 \times 10^{-3})(3.42 \times 10^{-3})} = 1.6 \times 10^6 \text{ kg/m}^4$$

Notice how each line inductance is significantly greater than the actuator inductance and it might be expected even at this stage that line dynamics are dominant and must be included in the analysis. The various capacitances become:

$$C_1 = \frac{0.58 \times 10^{-3}}{1.2 \times 10^9} = 0.483 \times 10^{-12} \text{ m}^5/\text{N}$$

$$\text{Actuator} \quad C_2 = \frac{0.43 \times 10^{-3}}{1.2 \times 10^9} = 0.358 \times 10^{-12} \text{ m}^5/\text{N}$$

$$\text{mean value } C_{\text{act}} = 0.42 \times 10^{-12} \text{ m}^5/\text{N}$$

$$\text{Line a + line b} \quad C = \frac{0.14 \times 10^{-3}}{1.2 \times 10^9} = 0.12 \times 10^{-12} \text{ m}^5/\text{N}$$

The uncoupled undamped natural frequencies

a) actuator only:

$$\omega_n = \sqrt{\frac{\frac{A_1^2 \beta_{e1}}{V_{t1}} + \frac{A_2^2 \beta_{e2}}{V_{t2}}}{m}}$$

$$\omega_n = \sqrt{\frac{(4.56 \times 10^{-3})^2 (1.2 \times 10^9)}{(0.72 \times 10^{-3})(25)} + \frac{(3.42 \times 10^{-3})^2 (1.2 \times 10^9)}{(0.57 \times 10^{-3})(25)}}$$

$$\omega_n = 1544 \text{ rad/s (246 Hz)}$$

b) lines only:

$$\omega_n = \sqrt{\frac{2}{LC}} = \sqrt{\frac{2}{(19.4 \times 10^6)(0.12 \times 10^{-12})}}$$

$$\omega_n = 927 \text{ rad/s (148 Hz)}$$

The coupled undamped natural frequencies assuming equal volumes either side and taken as the mean volume:

$$\frac{LC}{2} = \frac{(19.4 \times 10^6)(1.2 \times 10^{-13})}{2} = 116 \times 10^{-8}$$

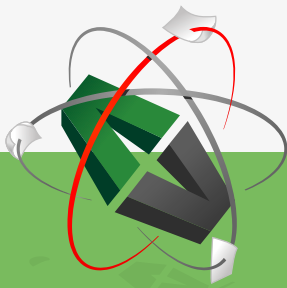
$$\frac{L_a C}{2} = \frac{(1.6 \times 10^6)(1.2 \times 10^{-13})}{2} = 9.6 \times 10^{-8} \quad \frac{LC}{2} + \frac{L_a C}{2} + \frac{L_a C_{act}}{2} = 160 \times 10^{-8}$$

$$\frac{L_a C_{act}}{2} = \frac{(1.6 \times 10^6)(0.42 \times 10^{-12})}{2} = 34 \times 10^{-8}$$

$$\frac{LL_a C \left(\frac{C}{2} + C_{act} \right)}{4} = \frac{LCL_a C}{8} + \frac{LCL_a C_{act}}{4} = 557 \times 10^{-16} + 3335 \times 10^{-16} = 3944 \times 10^{-16}$$

$$AU(s) = \frac{(Q_1 + Q_2)(s)}{1 + 160 \times 10^{-8} s^2 + 3944 \times 10^{-16} s^4}$$

This e-book
is made with
SetaPDF



PDF components for PHP developers

www.setasign.com



The roots of this transfer function 4th order denominator are determined to be:

288Hz, the effect of actuator

140Hz, the effect of the lines

Hence it is concluded at this stage that ***the transient response is dominated by line dynamics rather than by actuator dynamics.***

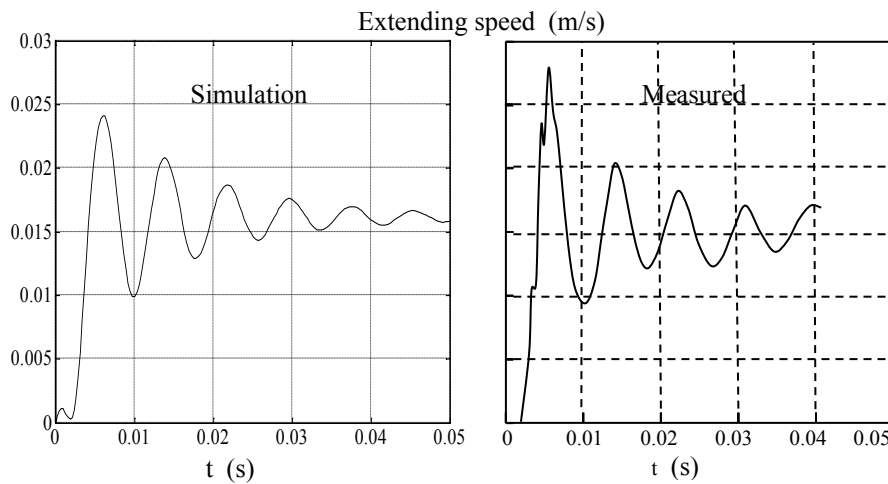
Computer simulation of the system equations

The servovalve dynamic response is represented by the manufacturer’s recommended second-order transfer function with an undamped natural frequency $\omega_{ns} = 110\text{Hz}$ and a damping ratio $\zeta_s = 1$. Note that this has no effect on the system natural frequency. Each line resistance is as follows:

$$R_a = \frac{128\mu\ell}{\pi d_a^4} = \frac{128(0.032)(0.9)}{\pi(0.013)^4} = 0.42 \times 10^8 \text{ Nm}^{-2}/\text{m}^3 \text{ s}^{-1}$$

$$R_b = \frac{128\mu\ell}{\pi d_b^4} = \frac{128(0.032)(0.6)}{\pi(0.007)^4} = 3.26 \times 10^8 \text{ Nm}^{-2}/\text{m}^3 \text{ s}^{-1}$$

Simulation results and measured results for the actuator extending are shown.



The response of a servovalve/cylinder open-loop drive, unloaded and with short lines

Simulation

damped frequency 127Hz

Measured

damped frequency 120Hz

Transfer function model, uncoupled solution

line-dominated *undamped* natural frequency is **148Hz**
 actuator-dominated **undamped** natural frequency is 246Hz

Transfer function model, coupled solution

line-dominated **undamped** natural frequency is **140Hz**
 actuator-dominated **undamped** natural frequency is 288Hz

The main conclusions from this example are:

- the simulation transient response prediction is good given that only a single π lump approximation is used for each line
- the simulation prediction for the damped frequency is 127Hz and close to the measured value of 120Hz. The transfer function coupled prediction for the undamped natural frequency is 140Hz and therefore higher than the damped frequency
- the transfer function two uncoupled solutions indicate that line dynamics dominate although the actuator effect can just be seen at the initial part of the measured transient response

5.5 Transient response and its specification

Having now considered transfer functions and block diagrams, the response of open-loop and closed-loop systems may be pursued further in the time domain and in the frequency domain. The time response of a **1st order system**, following a sudden demand to change its “output”, experiences a system output that increases in an exponential manner with increasing time. Considering figure 5.6 and a step input of magnitude y_d then the time response is readily deduced from the Laplace transform Table 1 and is as shown.

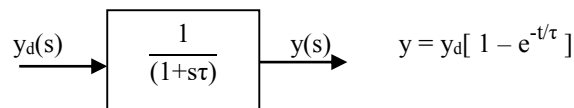


Figure 5.6 Transfer function of a 1st order system

The time response solution for a **2nd order system** is a little more complicated because it depends upon the damping ratio ζ of the system. Consider a second-order transfer function shown in figure 5.7.

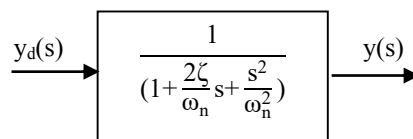


Figure 5.7 Transfer function of a 2nd order system

The time response to a unit step input demand was presented in Chapter 4 shown and is repeated as figure 5.8.

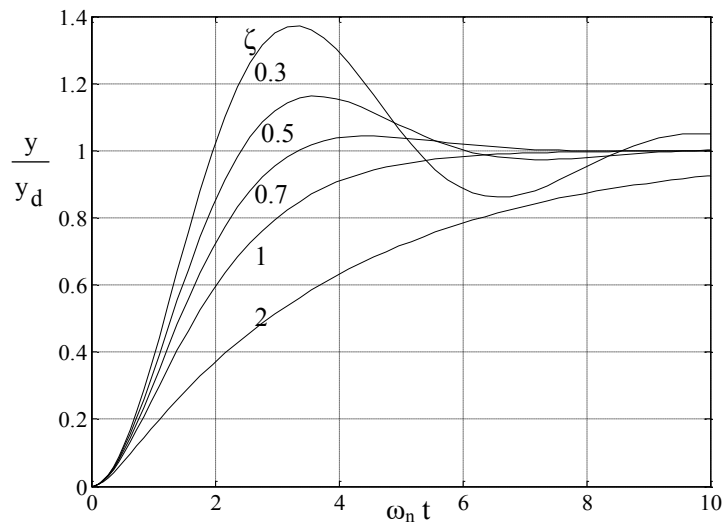


Figure 5.8 Time response to a step input of a 2nd order transfer function

www.sylvania.com

We do not reinvent the wheel we reinvent light.

Fascinating lighting offers an infinite spectrum of possibilities: Innovative technologies and new markets provide both opportunities and challenges. An environment in which your expertise is in high demand. Enjoy the supportive working atmosphere within our global group and benefit from international career paths. Implement sustainable ideas in close cooperation with other specialists and contribute to influencing our future. Come and join us in reinventing light every day.

Light is OSRAM

OSRAM
SYLVANIA



The response can be one of three forms as follows:

under-damped (oscillatory)	$\zeta < 1$
critically-damped	$\zeta = 1$
over-damped	$\zeta > 1$

when oscillatory, the damped frequency $\omega_d = \omega_n \sqrt{1 - \zeta^2}$ (5.20)

The output eventually settles down to the demanded value of 1 and a good design will have a damping ratio between $0.5 < \zeta < 1.0$ and with a selection of $\zeta \approx \sqrt{2}/2$ being suitable.

The time response solution for a **3rd order system** is further complicated because of the different forms that the denominator can take as dictated by its three roots. The denominator of the transfer function can be a combination of three 1st order terms or a combination of one 1st order term together with a 2nd order term. Consider the 3rd order transfer function, figure 5.9, with the denominator written in the specific form shown:

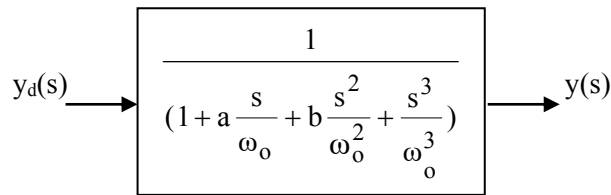


Figure 5.9 Transfer function of a 3rd order system

One way of designing a 3rd order system is to consider the response to a step input and use the Integral of Time multiplied by Absolute Error criterion, the **ITAE criterion**. The ITAE value from $t = 0$ to $t = \infty$ is then minimised as the parameters a and b are varied. This results in values of $a = 2.15$ and $b = 1.75$.

The resulting response to a step input demand is shown as figure 5.10.

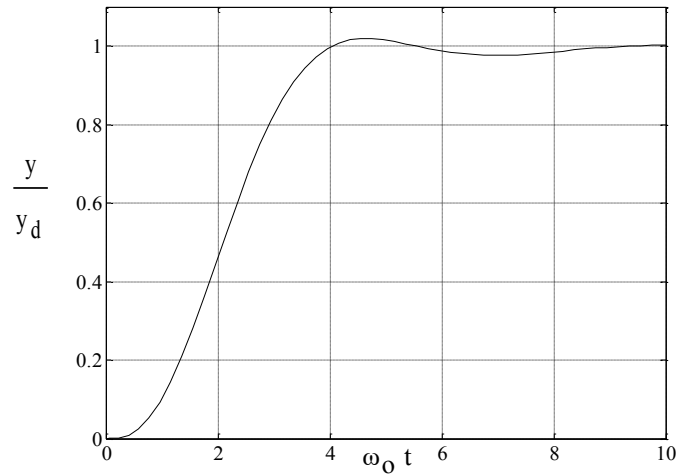


Figure 5.10 Transient response to a step input for a 3rd order transfer function satisfying the ITAE criterion

The result of the ITAE third-order criterion is actually to simplify the 3rd order transfer function into:

a 1st order transfer function with a time constant of $\tau = 1.41/\omega_0$

a 2nd order transfer function with $\omega_n = 0.84\omega_0$ and $\zeta = 0.31$

In practice it may not be possible to achieve the 3rd order criterion since it places restraints on system parameters that may not be possible to change to achieve the desired solution.

When *specifying a desired transient performance in practice* the realities of hydraulic and measurement noise together with friction and servovalve static and dynamic behaviour means that idealised transfer functions do not quite hold but are often a very good estimate of probable performance. A servodrive user will specify preferred characteristics as shown schematically in figure 5.11.

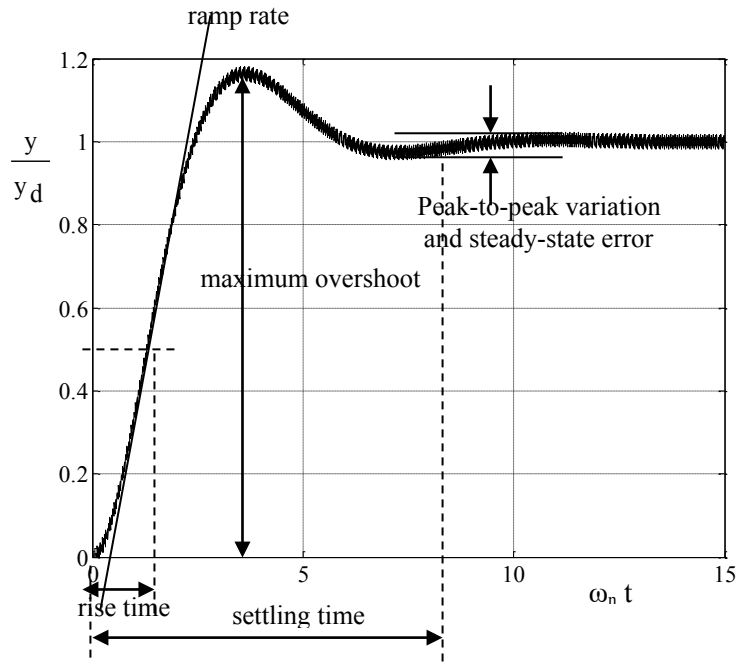


Figure 5.11 Transient response design specification



Discover the truth at www.deloitte.ca/careers

Deloitte.

© Deloitte & Touche LLP and affiliated entities.

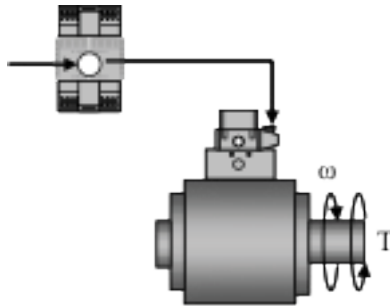


A design will probably require a number of performance parameters to be achieved such as:

- maximum overshoot
- maximum ramp rate
- peak-to-peak variation and steady-state error
- rise time interval to achieve a specific output
- settling time to achieve a specific output value

Example 5.2

Determine the linearised open-loop transfer function for a motor servodrive given the following system data:



Supply pressure = 210bar

Load pressure @ 240rpm = 120bar

Displacement $D_m = 12 \times 10^{-6} \text{ m}^3/\text{rad}$

motor and load inertia $J = 0.5 \text{ kg m}^2$

Volume either side = $2 \times 10^{-4} \text{ m}^3$

Maximum steady-state motor speed = 240rpm

Viscous coefficient $B_v = 0.04 \text{ Nm/rad s}^{-1}$

Motor flow losses are negligible

Fluid bulk modulus $\beta = 1.4 \times 10^9 \text{ N/m}^2$

Servo valves available, $k_f = 0.15, 0.30, 0.45, 0.6$

Maximum servovalve current = 20mA

$$\text{Servovalve flow gain } k_{qi} = k_f \sqrt{\frac{P_s - P_\ell(o)}{2}} = \frac{Q(o)}{i(o)}$$

$$\text{Servovalve resistance } R_{sv} = \frac{1}{k_{qp}} \quad k_{qp} = \frac{k_f i(o)}{2\sqrt{2[P_s - P_\ell(o)]}} = \frac{Q(o)}{2[P_s - P_\ell(o)]}$$

The servodrive linearised transfer function may be derived from (5.8) and (5.9) by replacing $A \rightarrow D_m$ and $M \rightarrow J$ to give:

$$\frac{\omega(s)}{i(s)} = \frac{k_{qi}/D_m}{\left[1 + \frac{R_{\text{visc}}}{R}\right] + \left[\frac{L}{R} + \frac{CR_{\text{visc}}}{2}\right]s + \frac{LC}{2}s^2}$$

$$R_{\text{visc}} = \frac{B_v}{D_m^2} \quad \frac{1}{R} = \frac{1}{R_{\text{act}}} + \frac{1}{R_{\text{sv}}} \quad L = \frac{J}{D_m^2} \quad C = \frac{V}{\beta}$$

Evaluating the flow rate at 240rpm = 25.1rad/s:

$$Q(o) = D_m \omega = (12 \times 10^{-6})(25.1) = 0.3 \times 10^{-3} \text{ m}^3/\text{s}$$

$$Q(o) = k_f i(o) \sqrt{\frac{P_s - P_\ell(o)}{2}}$$

$$0.3 \times 10^{-3} = k_f (20) \sqrt{\frac{210 - 120}{2}} \frac{10^{-3}}{60} \rightarrow k_f = 0.134$$

Therefore consider the servovalve with $k_f = 0.15$. Evaluating the resistance terms gives:

$$R_{\text{visc}} = \frac{B_v}{D_m^2} = \frac{0.04}{144 \times 10^{-12}} = 0.28 \times 10^9 \text{ Nm}^{-2}/\text{m}^3 \text{ s}^{-1}$$

$$\frac{1}{R} = \frac{1}{R_{\text{act}}} + \frac{1}{R_{\text{sv}}}$$

$$R_{\text{act}} = \infty \quad R_{\text{sv}} = \frac{2[P_s - P_\ell(o)]}{Q(o)} = \frac{2 \times 90 \times 10^5}{0.3 \times 10^{-3}} = 60 \times 10^9 \text{ Nm}^{-2}/\text{m}^3 \text{ s}^{-1}$$

$$\frac{R_{\text{visc}}}{R} = 0.28 \times 10^9 [0.0166 \times 10^{-9}] = 0.0047 \ll 1 \text{ and negligible}$$

$$\frac{L}{R} = \frac{0.5}{144 \times 10^{-12} (60 \times 10^9)} = 0.059 \text{ s}$$

$$\frac{CR_{\text{visc}}}{2} = \frac{(2 \times 10^{-4}) 0.28 \times 10^9}{(1.4 \times 10^9) 2} = 0.2 \times 10^{-4} \text{ s}$$

So, the servovalve flow resistance is more dominant than viscous friction resistance.

$$\frac{L}{R} + \frac{CR_{\text{visc}}}{2} \approx \frac{L}{R} = 0.059 \text{ seconds} \qquad \frac{LC}{2} = \frac{0.5(2 \times 10^{-4})}{(2)144 \times 10^{-12} (1.4 \times 10^9)} = 2.48 \times 10^{-4}$$

Selecting the servovalve with $k_f = 0.15$ then $\frac{k_{qi}}{D_m} = \frac{0.15 \sqrt{45} \times 10^{-3}}{60(12 \times 10^{-6})} = 1.4$

$$\frac{\omega(s)}{i(s)} = \frac{1.4}{[1 + 0.059s + 2.48 \times 10^{-4} s^2]} = \frac{1.4}{[1 + \frac{2\zeta}{\omega_n} s + \frac{s^2}{\omega_n^2}]}$$

The undamped natural frequency $\omega_n = 63.5 \text{ rad/s}$ (10.1 Hz) and the damping ratio $\zeta = 1.87$ and therefore the response is over-damped. Hence the motor transient speed will not overshoot and therefore not exceed the steady-state speed demanded. The steady-state motor speed is 240 rpm @ $i = 17.9 \text{ mA}$.

If an improved transient response is desired then a change in motor displacement could be considered but the load pressure will have to be re-calculated and the supply pressure re-assessed.

SIMPLY CLEVER

ŠKODA



We will turn your CV into an opportunity of a lifetime



Do you like cars? Would you like to be a part of a successful brand? We will appreciate and reward both your enthusiasm and talent. Send us your CV. You will be surprised where it can take you.

Send us your CV on www.employerforlife.com



Click on the ad to read more

5.6 Frequency response

Now consider the *frequency response* technique for characterising and designing servodrives. A transient response test is easier to undertake than a frequency response test but the former gives little information on the dynamic structure of the component or system being analysed. For example a transient response test might show overshoot of the parameter being measured but is the dynamic structure 2nd order, 3rd order, etc.? A frequency response test can provide this information providing the test can be carried out up to a sufficiently-high frequency to embrace the dynamic structure.

The frequency response method of analysing the system considers the steady-state condition with a sinusoidal excitation of fixed amplitude and a varying frequency applied to the input. Consider figure 5.12, an open-loop position control system, to determine the dynamics of the servovalve and actuator. A sinusoidal voltage of appropriate amplitude is applied and initially the output position will fluctuate and then settle down also to a steady-state sine wave for a linear system, or a close representation of a sine wave for a non-linear system, but with a phase difference compared with the input. The phase difference and amplitude of the output will change as the input frequency changes.

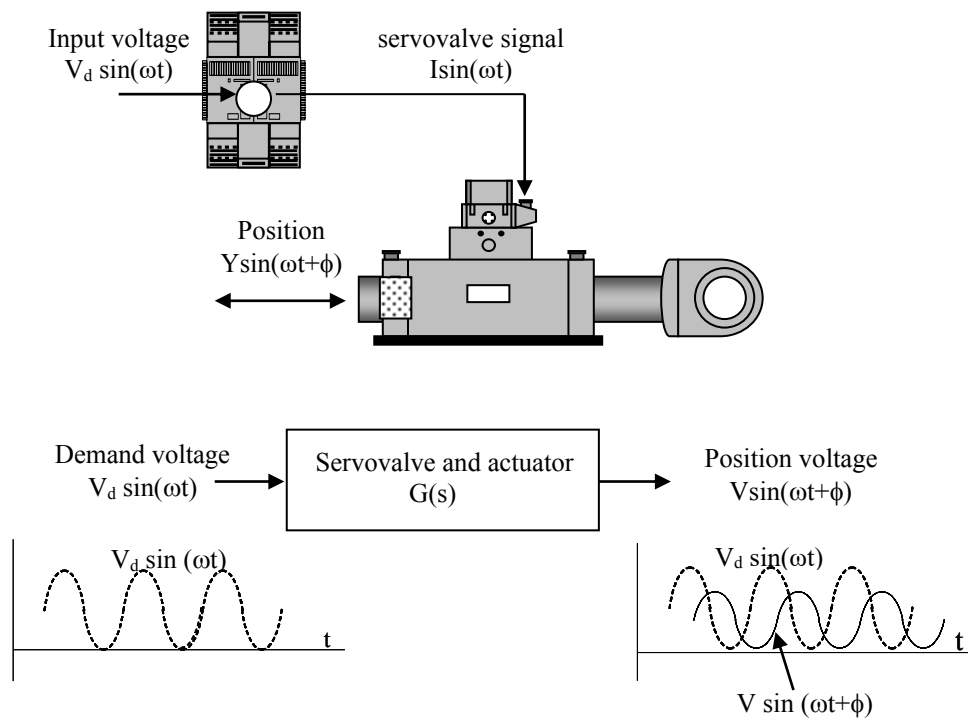


Figure 5.12 Frequency response of a servodrive

Note that *when attempting this experimentally* two important issues arise:

- for an open-loop servodrive the actuator will drift for a single-rod actuator due to different speeds when extending and retracting in the open-loop mode; this drift will also inevitably occur for a double-rod actuator. In practice therefore it will be necessary to add a small bias voltage to the input sinusoid to correct for drift and maintain the actuator in the desired mean position
- as the frequency is increased then the output position voltage amplitude will eventually reduce and will become impossible to determine due to both its low magnitude and superimposed hydraulic and sensor noise.

It can be shown using Laplace transform theory that for steady-state conditions the amplitude ratio and the phase angle of the transfer function, as indicated in figure 5.12, are given by:

$$\begin{aligned} \text{Amplitude ratio } \frac{V}{V_d} &= |G(s)|_{s=j\omega} \\ \text{Phase angle } \phi &= \angle G(s)|_{s=j\omega} \end{aligned} \quad (5.21)$$

So, if the transfer functions is known then the substitution $s = j\omega$ will result in a complex function having Real and Imaginary parts:

$$\begin{aligned} G(j\omega) &= A + jB \\ \text{Amplitude ratio } \frac{V}{V_d} &= \sqrt{A^2 + B^2} \\ \text{Phase angle } \phi &= \tan^{-1}B/A \end{aligned} \quad (5.22)$$

Frequency response is usually shown with frequency plotted on a logarithmic scale. Two parts are used, one for magnitude ratio/frequency and the other for phase angle/frequency. The amplitude ratio is converted to decibels (dB) as follows:

$$\text{Amplitude ratio (dB)} = 20 \log \frac{V}{V_d} = 20 \log |G(s)|_{s=j\omega} \quad (5.23)$$

Such a logarithmic representation of magnitude ratio is often referred to as a **Bode diagram**, although strictly speaking a Bode diagram is a collection of straight line approximations to the actual magnitude ratio.

When the magnitude is considered it will be evident that common transfer functions will have asymptotic approximations over some parts of the frequency range and this can help in deciding the probable form of a transfer function when experimentally measured. Note also that a product of transfer functions become additive when a frequency response is considered on a logarithmic basis.

i) Consider an integrator $G(s) = \frac{1}{s} \rightarrow G(j\omega) = \frac{1}{j\omega}$ (5.24)

It can be seen that the magnitude ratio and phase angle become:

$$\text{Magnitude ratio} = 20 \log \frac{1}{\omega} \text{ dB} \quad \text{Phase angle } \phi = -90^\circ \quad (5.25)$$

The frequency response plot is shown as figure 5.13.

I joined MITAS because
I wanted **real responsibility**

The Graduate Programme
for Engineers and Geoscientists
www.discovermitas.com





Month 16
I was a construction supervisor in the North Sea advising and helping foremen solve problems

Real work
International opportunities
Three work placements







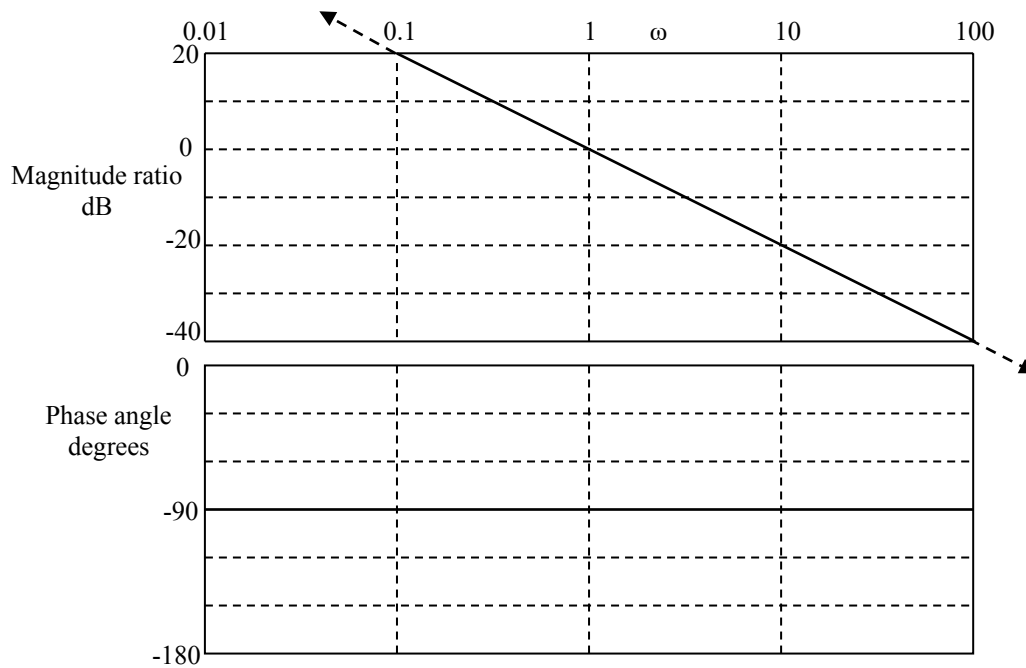


Figure 5.13 Frequency response for an integrator

Some observations may be made:

- the phase angle is constant at -90°
- at the frequency $\omega = 1 \text{ rad/s}$ the magnitude ratio is 0 dB
- the slope of the magnitude ratio is always -20 dB/decade

ii) Consider a 1st order transfer function $G(s) = \frac{K}{(1 + s\tau)} \rightarrow G(j\omega) = \frac{K}{(1 + j\omega\tau)}$ (5.26)

This generalised 1st order transfer function has a gain K and a time constant τ . The frequency response diagram is constructed using the transformation $s \rightarrow j\omega$ and the magnitude ratio and phase angle become:

$$\text{Magnitude ratio} = 20 \log \frac{K}{\sqrt{1 + (\omega\tau)^2}} \text{ dB} \quad \text{Phase angle } \phi = -\tan^{-1} \omega\tau \quad (5.27)$$

The frequency response plot is shown as figure 5.14 for a gain $K = 1$. Any other gain K simply lifts the whole magnitude plot by $+20 \log K \text{ dB}$.

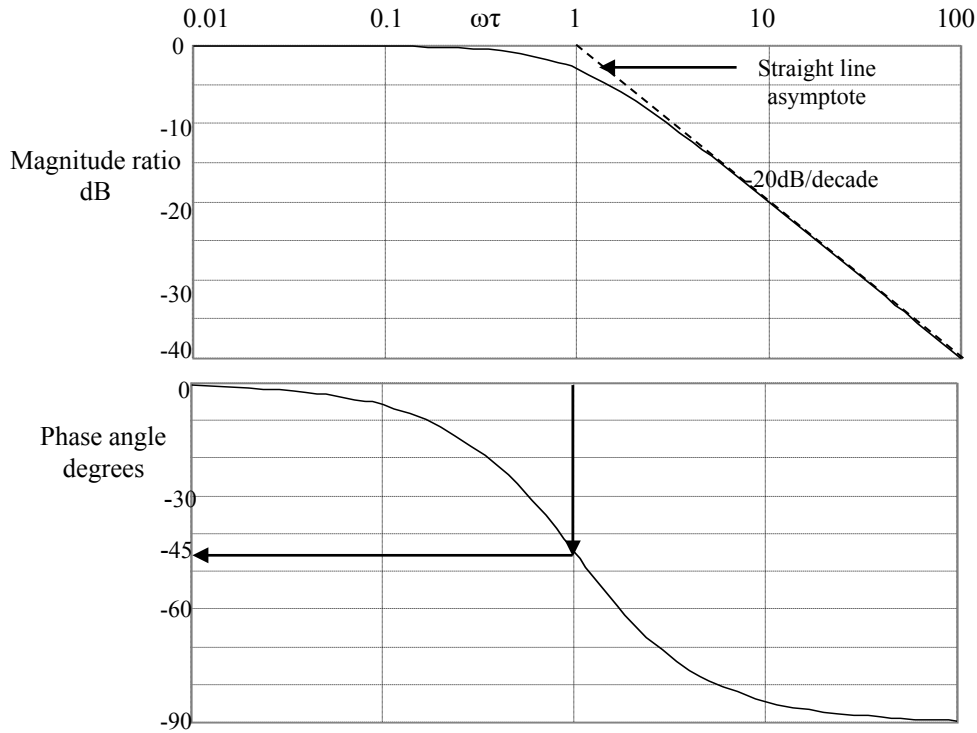


Figure 5.14 Frequency response for a 1st order transfer function, K = 1

Some observations may be made:

- the **break frequency** is defined when $\omega\tau = 1$ and when $\omega = 1/\tau$ the phase angle $\phi = -45^\circ$
- as the frequency becomes large the phase angle $\phi \rightarrow -90^\circ$
- drawing a straight line from 0dB magnitude at the break frequency, $\omega\tau = 1$, and at a slope of -20dB/decade becomes asymptotic to the exact magnitude ratio at higher frequencies. This is the Bode approximation
- at the break frequency, $\omega\tau = 1$, the exact magnitude ratio is 3dB down from the Bode approximation. In other words where the measured magnitude ratio drops 3dB from the low-frequency constant magnitude ratio gives the system break frequency. Hence $\tau = 1/\omega$

This information may be used to identify a 1st order transfer function from practical data, should the plot suggest a 1st order transfer function.

iii) Consider a 2nd order transfer function:

$$G(s) = \frac{1}{1 + \frac{2\zeta}{\omega_n} s + \frac{1}{\omega_n^2} s^2} \quad \rightarrow \quad G(j\omega) = \frac{1}{1 - \frac{\omega^2}{\omega_n^2} + j \frac{2\zeta\omega}{\omega_n}} \quad (5.28)$$

The magnitude ratio and phase angle are now given by:

$$\text{Magnitude ratio} = 20 \log \frac{1}{\sqrt{\left(1 - \frac{\omega^2}{\omega_n^2}\right)^2 + \left(\frac{2\zeta\omega}{\omega_n}\right)^2}} \text{ dB}$$

$$\text{Phase angle } \phi = -\tan^{-1} \frac{\frac{2\zeta\omega}{\omega_n}}{1 - \frac{\omega^2}{\omega_n^2}} \tag{5.29}$$

The frequency response plot is now more complicated because of the varying damping ratio ζ and a plot for a few values of damping ratio is shown as figure 5.15.

ie business school

#1 EUROPEAN BUSINESS SCHOOL
FINANCIAL TIMES 2013

#gobeyond

MASTER IN MANAGEMENT

Because achieving your dreams is your greatest challenge. IE Business School's Master in Management taught in English, Spanish or bilingually, trains young high performance professionals at the beginning of their career through an innovative and stimulating program that will help them reach their full potential.

- Choose your area of specialization.
- Customize your master through the different options offered.
- Global Immersion Weeks in locations such as London, Silicon Valley or Shanghai.

Because you change, we change with you.

www.ie.edu/master-management | mim.admissions@ie.edu | Facebook | Twitter | LinkedIn | YouTube | Instagram



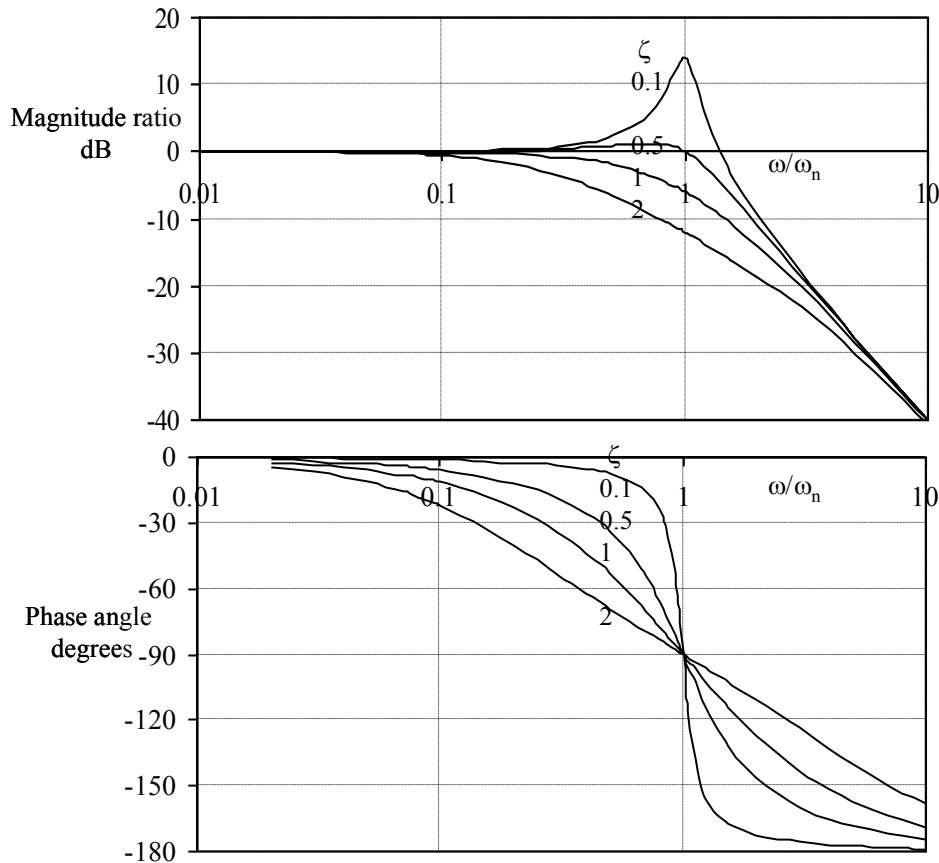


Figure 5.15 Frequency response for a 2nd order transfer function

Some observations may be made:

- as the frequency is increased the phase angle becomes asymptotic to -180°
- at the undamped natural frequency $\omega = \omega_n$
 the phase angle is -90° the magnitude ratio is $1/2\zeta$ (5.30)
- as the frequency is increased the slope of the magnitude ratio approaches -40dB/decade
- the peak magnitude occurs when:

$$\omega = \omega_n \sqrt{1 - 2\zeta^2} \quad \text{Magnitude ratio} = 20\log \frac{1}{2\zeta\sqrt{1 - \zeta^2}} \text{ dB} \quad (5.31)$$

It should be realised that there is a pattern to the overall “shape” of a frequency response plot and some general points may be made as follows:

- the order, n , of a transfer function denominator indicates the asymptotic phase angle which is $(n) \times (-90^\circ)$. The order of a transfer function numerator, m , indicates the asymptotic phase angle which is $(m) \times (+90^\circ)$. The net asymptotic phase angle is the addition of the two
- the high-frequency slope of the magnitude ratio plot is $(n-m) \times (-20) \text{ dB/decade}$

- each free s term in the denominator has a phase angle of -90° and a slope of -20dB/decade
- each free s term in the numerator has a phase angle of $+90^\circ$ and a slope of $+20\text{dB/decade}$
- the low frequency asymptote can give information on the transfer function gain

For example, consider the following transfer function:

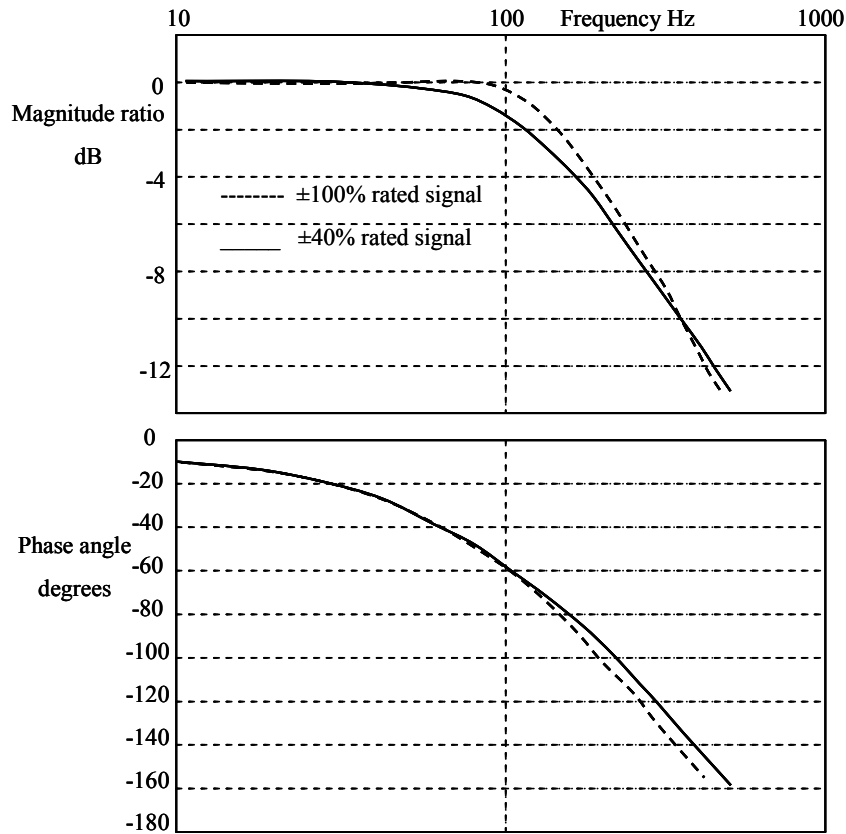
$$G(s) = \frac{1 + s\tau}{s\left(1 + \frac{2\zeta}{\omega_n}s + \frac{s^2}{\omega_n^2}\right)} \quad (5.32)$$

- the asymptotic magnitude ratio slope at low frequency is -20dB/decade due to the dominant integrator
- the asymptotic magnitude ratio slope at high frequency approaches -60dB/decade for the denominator and $+20\text{dB/decade}$ for the numerator giving a net value of -40dB/decade
- the phase angle has a low frequency value of -90° due to the integrator
- as the frequency increases then the phase contribution from the denominator approaches -270° and the phase contribution from the numerator approaches $+90^\circ$ resulting in a net phase angle of -180°

This type of information greatly assists identification of the dynamic shape of a servovalve or servodrive transfer function. When the transfer function is not known with any satisfaction then the deduction of terms such as those in (5.32) is difficult to assess from experimental data. However, there are commercial identification software packages available that can be used to best match data with a chosen transfer function.

Example 5.3

A *measured transfer function plot for a servovalve* is shown and is just one of many depending on the servovalve type and rating selected. Determine a possible transfer function.



no.1
 nine years
 in a row



STUDY AT A TOP RANKED INTERNATIONAL BUSINESS SCHOOL

Reach your full potential at the Stockholm School of Economics, in one of the most innovative cities in the world. The School is ranked by the Financial Times as the number one business school in the Nordic and Baltic countries.

Visit us at www.hhs.se



Click on the ad to read more

It can be seen that the data is applicable up to a frequency of about 500Hz, a high value and most probably beyond many industrial servodrive frequencies. Notice that the plot changes with input signal amplitude.

The magnitude plot shows a high-frequency slope of typically -20dB/decade and indicative of a 1st order transfer function. However, the phase angle is moving beyond -180° indicating at least a 2nd order or possibly a 3rd order transfer function; the servovalve dynamic response is certainly very fast.

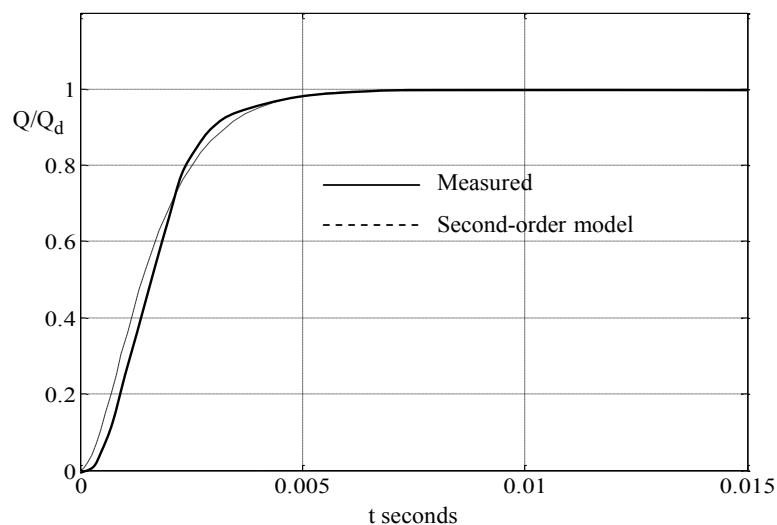
Assuming a 2nd order transfer function approximation as a starting point and considering the average of the two sets of data then:

- the phase angle is -90° at a frequency of about 190Hz and this is the undamped natural frequency ω_n
- at the undamped natural frequency the magnitude ratio is about -4.2dB $\rightarrow 1/2\zeta$. Hence the damping ratio $\zeta \approx 0.81$. This suggests under-damping since $\zeta < 1$
- however, the servovalve is possibly overdamped as is evident from the magnitude ratio plot so increase the damping ratio to $\zeta = 1$

The 2nd order approximation is therefore:

$$G(s) \approx \frac{1}{1 + 1.68 \times 10^{-3} s + \frac{s^2}{1194^2}}$$

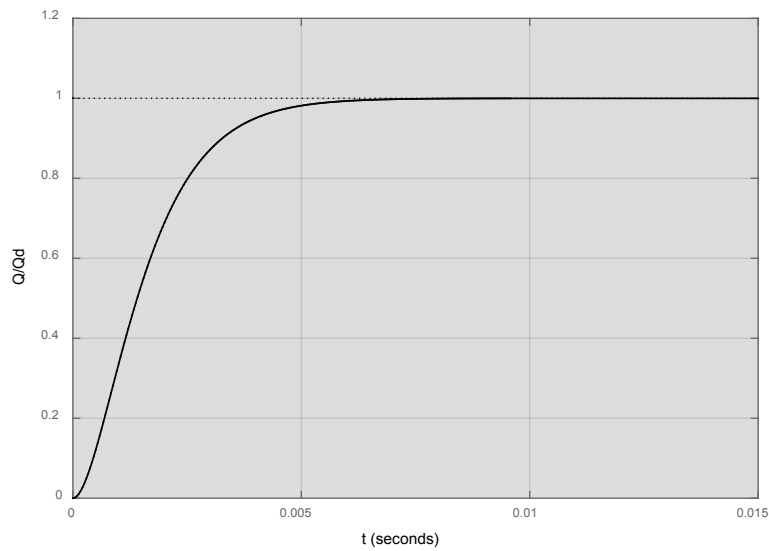
A comparison of the manufacturer's measured transient response with the transfer function approximation is shown, where the response may be considered as the ratio of actual flow rate to the demanded steady-state flow rate.



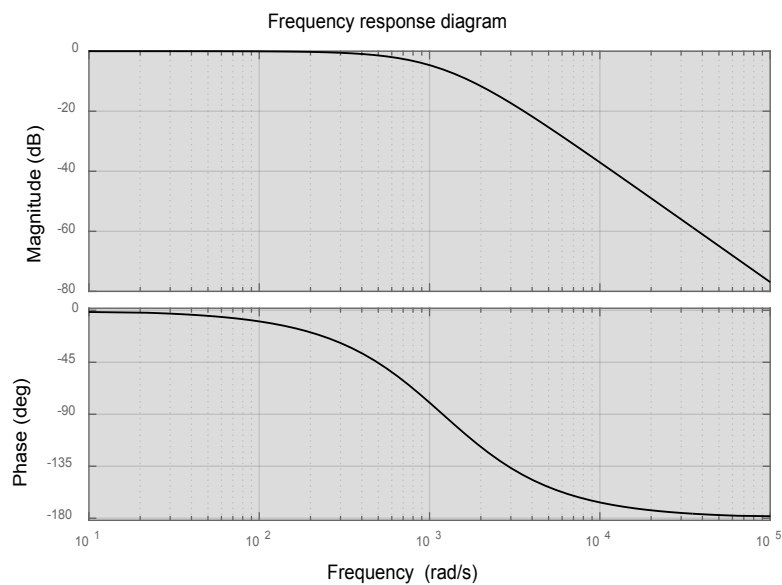
This pragmatic approach gives an approximation that is good for a first estimate and further analysis might consider different transfer function forms, for example a combination of a 1st order term and a 2nd order term.

If the Matlab Control System Toolbox is available then both the transient response and the frequency response of the assumed transfer function may be evaluated as follows:

```
G = tf([0 0 1],[7.01e-7 1.68e-3 1]);
stepplot(G);
```

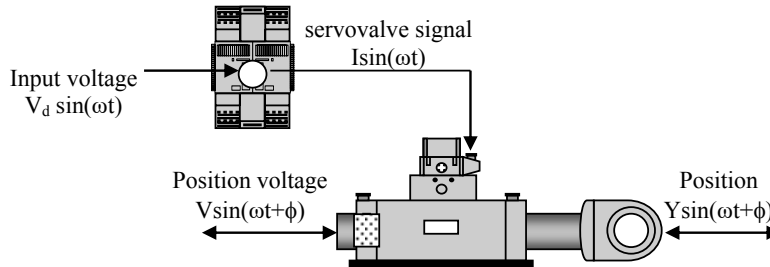


```
G = tf([0 0 1],[7.01e-7 1.68e-3 1]);
bodeplot(G);
```



Example 5.4

An open-loop frequency response test, using a transfer function analyser, on a servodrive resulted in data for frequencies up to 160Hz. Determine a possible transfer function with the following additional system data.



Fluid bulk modulus $\beta = 1.4 \times 10^9 \text{N/m}^2$

Bore diameter 80mm, rod diameter 45mm, actuator stroke 250mm

Load and actuator mass 820kg, actuator is horizontal

Assume the double-rod actuator is in its mid-position

The servovalve spool is critically-lapped, $k_f = 0.2$, rated flow @20mA

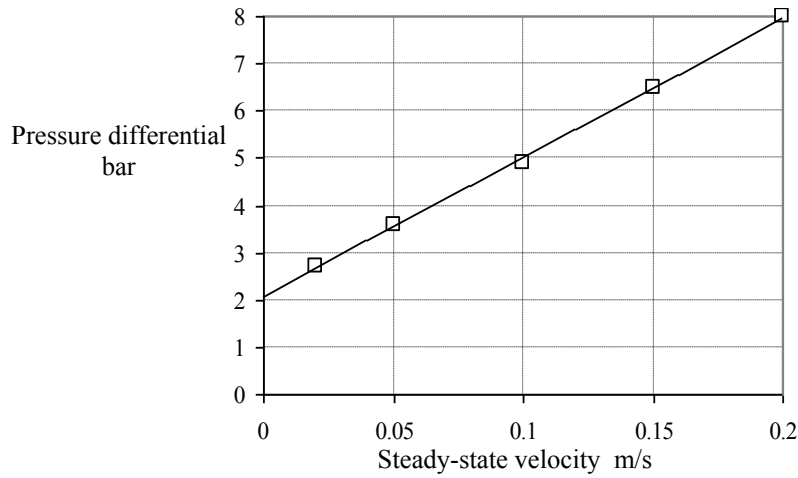
Servoamplifier gain $G_a = 2 \text{mA/V}$, position sensor gain $H_p = 10 \text{V/m}$

Supply pressure $P_s = 210 \text{bar}$

Actuator leakage resistance R_{act} unknown



Friction and viscous damping was determined from an open-loop test as follows:



From this data it is concluded that the Coulomb friction force is equivalent to $\approx 2\text{bar}$ and the viscous friction coefficient may be estimated from the slope of the graph:

$$\text{Actuator annulus area } A = \frac{\pi(6400 - 2025)10^{-6}}{4} = 34.4 \times 10^{-4} \text{ m}^2$$

$$B_v = \frac{(\Delta P)(A)}{\Delta U} = \frac{(6 \times 10^5)(34.4 \times 10^{-4})}{0.2} = 1.03 \times 10^4 \text{ N/ms}^{-1}$$

Before analysing the data it is appropriate to consider the expected transfer function. From earlier work the best modelling estimate of the OLTF, **neglecting servovalve dynamics**, is as follows:

$$\text{For open-loop velocity } \frac{U(s)}{V_d(s)} = \frac{G_a k_{qi}/A}{[1 + \frac{R_{\text{visc}}}{R}] + [\frac{L}{R} + \frac{CR_{\text{visc}}}{2}]s + \frac{LC}{2}s^2}$$

For open-loop position

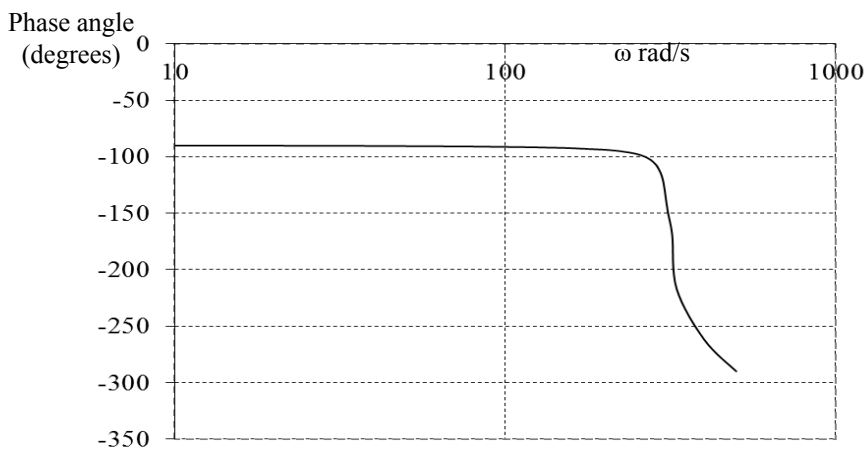
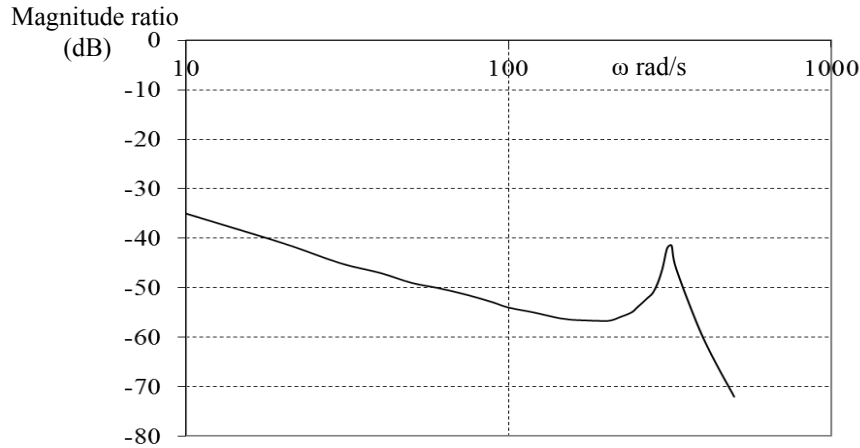
$$\frac{V}{V_d} = \frac{y(s)}{y_d(s)} = \frac{H_p G_a k_{qi}/A}{s \left[[1 + \frac{R_{\text{visc}}}{R}] + [\frac{L}{R} + \frac{CR_{\text{visc}}}{2}]s + \frac{LC}{2}s^2 \right]}$$

$$R_{\text{visc}} = \frac{B_v}{A^2} \quad \frac{1}{R} = \frac{1}{R_{\text{act}}} + \frac{1}{R_{\text{sv}}} \quad L = \frac{M}{A^2} \quad C = \frac{V}{\beta}$$

$$k_{qi} = k_f \sqrt{\frac{P_s - P_\ell(o)}{2}} = \frac{Q(o)}{i(o)}$$

$$k_{qp} = \frac{k_f i(o)}{2\sqrt{2}[P_s - P_\ell(o)]} = \frac{Q(o)}{2[P_s - P_\ell(o)]} \quad R_{sv} = \frac{1}{k_{qp}}$$

The measured open-loop frequency response plot for position is now shown and demonstrates how typical data will “run-away” at higher frequencies due to both hydraulic and signal noise signal resolution and the effect of the integrator attenuation effect. The frequency response test is carried out at the actuator central position which is maintained during the open-loop test using a bias current that has to be continually adjusted as the actuator tends to drift during this type of test.



The servovalve resistance $R_{sv} = \infty$ for a critically-lapped spool, but only at its true zero position. Since a finite amplitude of oscillation in current has to be used when testing then an average finite resistance will probably be indicated and it is often difficult to assess the true zero spool position resistance. In this example it will be assumed that damping is dominated by viscous friction, $R = \infty$, and the OLF first-estimate transfer function then becomes:

$$\frac{V}{V_d} = \frac{y(s)}{y_d(s)} = \frac{H_p G_a k_{qi}/A}{s \left[1 + \frac{CR_{visc}}{2} s + \frac{LC}{2} s^2 \right]} = \frac{K}{s \left[1 + \frac{CR_{visc}}{2} s + \frac{LC}{2} s^2 \right]}$$

Now consider the measured data.

- as expected the measured transfer function has a low-frequency magnitude having a slope of -20dB/decade and a constant phase angle of -90^0 due to the integrator term for position measurement
- the 2nd order contribution is evident but appears to be very lightly damped. This means that the peak magnitude occurs at a frequency close to its undamped natural frequency. From the magnitude plot:

$$\omega_n \approx 320\text{rad/s}$$

- at the lowest frequency used, $10\text{rad/s} \ll 320\text{rad/s}$, the magnitude is dominated by the integrator term and therefore:

- Magnitude ratio = $20\log \frac{K}{\omega} = 20\log \frac{K}{10} \approx -35\text{dB} \rightarrow K \approx 0.18$

- at the undamped natural frequency the magnitude ratio is given by:

- Magnitude ratio = $20\log \frac{K}{2\zeta\omega_n} = 20\log \frac{0.18}{2\zeta(320)} \approx -41\text{dB} \rightarrow \zeta \approx 0.032$



"I studied English for 16 years but...
...I finally learned to speak it in just six lessons"

Jane, Chinese architect

ENGLISH OUT THERE

Click to hear me talking before and after my unique course download

It must be stated that these calculations are subject to error since it is difficult to experimentally determine the peak magnitude conditions accurately at the undamped natural frequency for a very lightly damped 2nd order transfer function.

Now consider validating the assumed transfer function model.

The actuator volume on either side is $V = (34.4 \times 10^{-4})(0.125) = 4.3 \times 10^{-4} \text{ m}^3$

$$L = \frac{M}{A^2} = \frac{820}{34.4^2 \times 10^{-8}} = 0.69 \times 10^8 \quad C = \frac{V}{\beta} = \frac{4.3 \times 10^{-4}}{1.4 \times 10^9} = 3.07 \times 10^{-13}$$

$$R_{\text{visc}} = \frac{B_v}{A^2} = \frac{1.03 \times 10^4}{34.4^2 \times 10^{-8}} = 8.7 \times 10^8 \text{ Nm}^{-2} / \text{m}^3 \text{ s}^{-1}$$

The **undamped natural frequency** is calculated to be:

$$\omega_n = \sqrt{\frac{2}{LC}} = \sqrt{\frac{2}{(0.69 \times 10^8)(3.07 \times 10^{-13})}} = 307 \text{ rad/s}$$

This is close to the value of 320 rad/s assessed from measurement.

The **damping ratio** may now be calculated from $\frac{2\zeta}{\omega_n} = \frac{CR_{\text{visc}}}{2}$

$$\frac{(2)(\zeta)}{307} = \frac{(3.07 \times 10^{-13})(8.7 \times 10^8)}{2} = 1.34 \times 10^{-4} \rightarrow \zeta = 0.021$$

The assessed damping ratio from tests gave a value of $\zeta = 0.032$ and illustrates the problem of determining its value experimentally when the second-order component of the open-loop transfer function has little-to-no damping.

The **transfer function gain** is given by:

$$K = \frac{H_p G_a k_{qi}}{A} \quad k_{qi} = k_f \sqrt{\frac{P_s - P_\ell(o)}{2}} \quad P_\ell(o) \approx 2 \text{ bar}$$

$$K = \frac{(10)(2)(0.2 \times \sqrt{104})(10^{-3})}{(34.4 \times 10^{-4})(60)} = 0.2$$

This compares with the measured value, using the theoretical transfer function, of $K = 0.18$.

5.7 The effect of a pure delay

Sometimes it is found in published work that a servoactuator transfer function includes a pure delay term. The reason for a significant pure delay is not always justifiable and is often attributed to:

- an electromagnetic effect when building up the servovalve coil current
- the building up of pressure differential across the servovalve spool to overcome the small amount of spool friction
- additional higher-order fluid and mechanical dynamic effects within the servovalve not discussed in this book
- The servoactuator may have a line effect

These effects may be significant for multi-stage servovalves and the user must make an assessment in conjunction with manufacturers' data. In terms of transfer function analysis, a pure delay is represented by its Laplace transform as follows:

$$\text{Pure delay transfer function } G(s) = e^{-sT} \rightarrow G(j\omega) = e^{-j\omega T} \quad (5.33)$$

The magnitude ratio and phase angle are given by:

$$|G(j\omega)| = 1 \quad \text{phase angle } \phi = -\omega T \quad (5.34)$$

The effect of a pure delay is therefore to give an increasing phase lag with increasing frequency and is therefore de-stabilising. For computer simulation, for example using Matlab Simulink, a pure delay may be used in its exact form given by equation (5.33). However, in some published work using transfer function analysis, particularly for practical identifications, then linear approximations to equation (5.33) have been used. For example, one approximation is the bilinear approximation using the linear terms of the Taylor series expansion which gives:

$$G(s) = e^{-sT} = \frac{e^{-sT/2}}{e^{+sT/2}} \approx \frac{1 - sT/2}{1 + sT/2} \quad (5.35)$$

Consequently the open-loop transfer function relating position, y , to current, i , for a linear position servoactuator with a pure delay is now modified as follows:

$$\frac{y}{i} = \frac{K e^{-sT}}{s(1 + \frac{2\zeta}{\omega_n} s + \frac{s^2}{\omega_n^2})} \approx \frac{K(1 - \frac{sT}{2})}{s(1 + \frac{sT}{2})(1 + \frac{2\zeta}{\omega_n} s + \frac{s^2}{\omega_n^2})} \quad K = \frac{k_{qi}}{A} \quad (5.36)$$

If a computer package is used to identify a transfer function such as (5.36) using experimental data then the computed value of T may be different to the expected value of T . Also, if the 2nd order denominator term in (5.36) is changed, for example to 3rd order, then the computed value of T may also change. In other words, the identification approach computes the best coefficients to match the transfer function specified without any consideration of the physical reality.

Excellent Economics and Business programmes at:



university of
 groningen



“The perfect start
 of a successful,
 international career.”

CLICK HERE
 to discover why both socially
 and academically the University
 of Groningen is one of the best
 places for a student to be

www.rug.nl/feb/education



6 Closed-loop stability

6.1 Aim

To understand the dynamic stability of closed-loop systems via the following objectives:

- to become further familiar with closed-loop block diagram terminology
- to determine the conditions for closed-loop stability
- to become familiar with frequency response techniques
- to demonstrate concepts via worked examples

6.2 Closed-loop stability

Any closed-loop system, particularly type 1 systems such as position control systems, will become unstable if the open-loop gain is increased without bound. A closed-loop position control system is shown in block diagram form as figure 6.1.

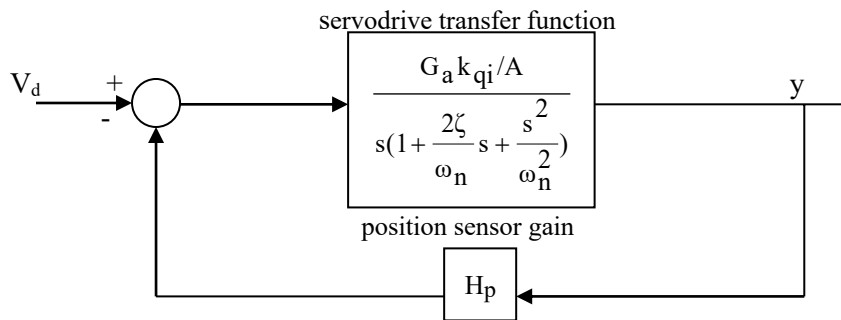


Figure 6.1 Block diagram for a servodrive position control system

It will be recalled from Chapter 5 that in general a closed-loop system is represented by the block diagram shown as figure 6.2 with a *forward transfer function* $G(s)$ and a *feedback loop transfer function* $H(s)$.

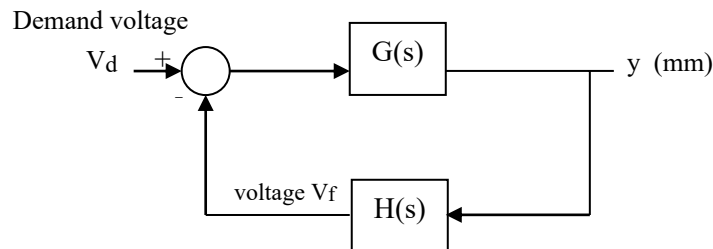


Figure 6.2 General block diagram for a control system

This leads to two important fundamental definitions in control theory:

$$\text{Open-loop transfer function OLTF} = G(s)H(s)$$

$$\text{Closed-loop transfer function CLTF} = \frac{G(s)}{1 + G(s)H(s)} \quad (6.1)$$

The closed-loop characteristic equation is given by:

$$1 + G(s)H(s) = 0 \quad (6.2)$$

$$G(s)H(s) = -1$$

The response and stability of a closed-loop control system is critically linked to the roots of the characteristic equation.

For the *servodrive position control system* shown in figure 6.1, and neglecting servovalve dynamics, the OLTF $G(s)H(s)$ is given by:

$$G(s)H(s) = \frac{K}{s(1 + \frac{2\zeta}{\omega_n}s + \frac{s^2}{\omega_n^2})} \quad K = \frac{H_p G_a k_{qi}}{A} \quad (6.3)$$

The characteristic equation then becomes:

$$1 + G(s)H(s) = 0$$

$$\frac{s^3}{\omega_n^2} + \frac{2\zeta}{\omega_n}s^2 + s + K = 0 \quad (6.4)$$

$$b_3 s^3 + b_2 s^2 + b_1 s + b_0 = 0$$

At the onset of closed-loop instability it can be shown that **in the frequency domain let $s = j\omega$** and substitute into the characteristic equation. Hence from equation (6.4) the Real and Imaginary parts may be separated as follows:

$$\text{Let } s = j\omega, s^2 = -\omega^2, s^3 = -j\omega^3 \quad -jb_3\omega^3 - b_2\omega^2 + jb_1\omega + b_0 = 0$$

$$\begin{array}{cc} \text{Re} & \text{Im} \\ [b_0 - b_2\omega^2] + j[b_1\omega - b_3\omega^3] = 0 & \end{array}$$


Equating both the Real and Imaginary terms to zero and combining then gives the condition for the onset of closed-loop stability:

$$b_1 b_2 = b_0 b_3 \quad \omega = \sqrt{b_1 / b_3} \quad (6.5)$$

For the position control example $K = 2\zeta\omega_n$ $\omega = \omega_n$

At the onset of instability, when the open-loop gain $K = 2\zeta\omega_n$, then the frequency of oscillation is the OLTf undamped natural frequency ω_n .

Stability is of course ensured if $K < 2\zeta\omega_n$, and a good starting point is to select a gain typically $1/4$ of the critical value, $K = \zeta\omega_n/2$.



In the past four years we have drilled

89,000 km

That's more than **twice** around the world.

Who are we?
We are the world's largest oilfield services company¹. Working globally—often in remote and challenging locations—we invent, design, engineer, and apply technology to help our customers find and produce oil and gas safely.

Who are we looking for?
Every year, we need thousands of graduates to begin dynamic careers in the following domains:

- Engineering, Research and Operations
- Geoscience and Petrotechnical
- Commercial and Business

What will you be?

careers.slb.com

Schlumberger

¹Based on Fortune 500 ranking 2011. Copyright © 2015 Schlumberger. All rights reserved.



6.3 The use of frequency response

The use of the *frequency response diagram approach*, introduced in Chapter 5, is a useful technique for understanding the effect of the interaction between different open-loop transfer functions providing that the transfer function of the electrohydraulic system is sufficiently accurate. If the open-loop transfer function $G(j\omega)H(j\omega)$ is considered then to ensure closed-loop stability the concept of *gain and phase margins* is useful. It will be recalled that at the onset of closed-loop instability the OLTF satisfies the following condition:

$$G(j\omega)H(j\omega) = -1$$

$$G(j\omega)H(j\omega) \text{ has a magnitude ratio of } 1 \text{ (0dB)} \quad (6.6)$$

$$G(j\omega)H(j\omega) \text{ has a phase angle of } -180^\circ$$

The avoidance of instability is easy, in principle, by selecting a *desired gain margin* or *phase margin*. Consider figure 6.3 which illustrates an OLTF $G(j\omega)H(j\omega)$ that has a stable closed-loop system. The gain and phase margins are defined and both are positive numbers.

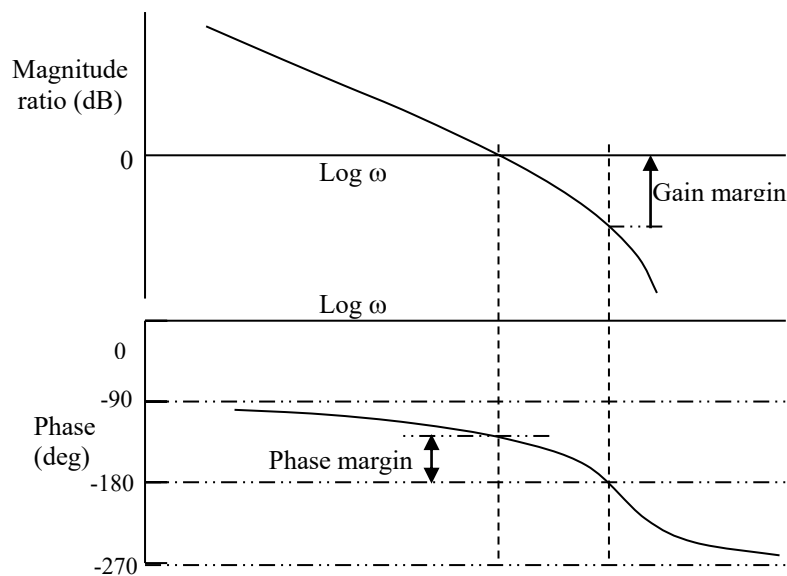


Figure 6.3 Gain and phase margins in the frequency domain

- the phase margin is defined when the magnitude ratio is 0dB. The gain margin is defined when the phase is -180°
- for the closed-loop system to be stable the magnitude ratio must have a negative dB value when the phase angle is -180° . This is the case shown
- suppose in figure 6.3 the magnitude ratio is -20dB when the phase angle is -180° then the gain margin is 20dB. This means that the OLTF gain can be increased by 20dB before closed-loop instability occurs.
- suppose the magnitude ratio was +20dB when the phase angle is -180° then the phase margin is -20dB. This means that the closed-loop would be unstable and the OLTF gain must be decreased by 20dB to avoid closed-loop instability
- in practice seek a phase margin around 45°

American online LIGS University

is currently enrolling in the
Interactive Online **BBA, MBA, MSc,**
DBA and PhD programs:

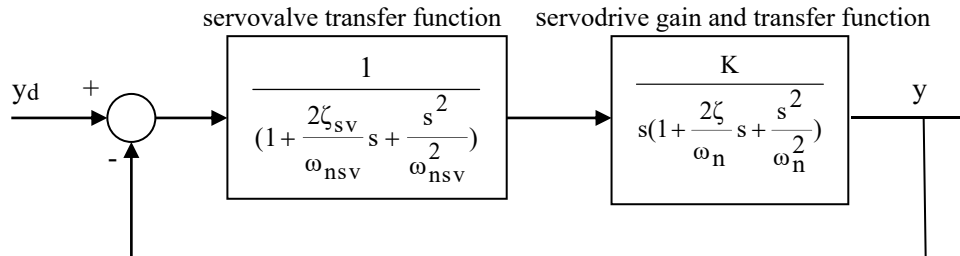
- ▶ enroll **by September 30th, 2014** and
- ▶ **save up to 16%** on the tuition!
- ▶ pay in 10 installments / 2 years
- ▶ Interactive Online education
- ▶ visit www.ligsuniversity.com to find out more!

Note: LIGS University is not accredited by any nationally recognized accrediting agency listed by the US Secretary of Education. More info [here](#).



Example 6.1

The block diagram of a position control system is shown with both servovalve dynamics and system dynamics considered important. Determine the gain to cause closed-loop instability and suggest a suitable gain value.



The following data applies:

servovalve $\zeta = 1 \quad \omega_{nsv} = 628.4\text{rad/s (100Hz)}$

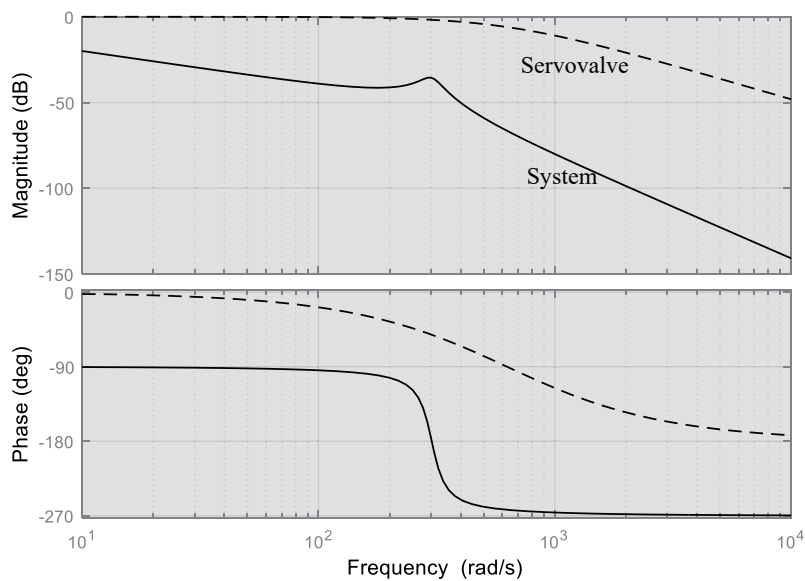
system $\zeta = 0.1 \quad \omega_n = 301.6\text{rad/s (48Hz)}$

The OLTf may then be established as follows:

$$G(s)H(s) = \frac{K}{s(1 + 3.18 \times 10^{-3}s + 2.53 \times 10^{-6}s^2)(1 + 6.63 \times 10^{-4}s + 1.1 \times 10^{-5}s^2)}$$

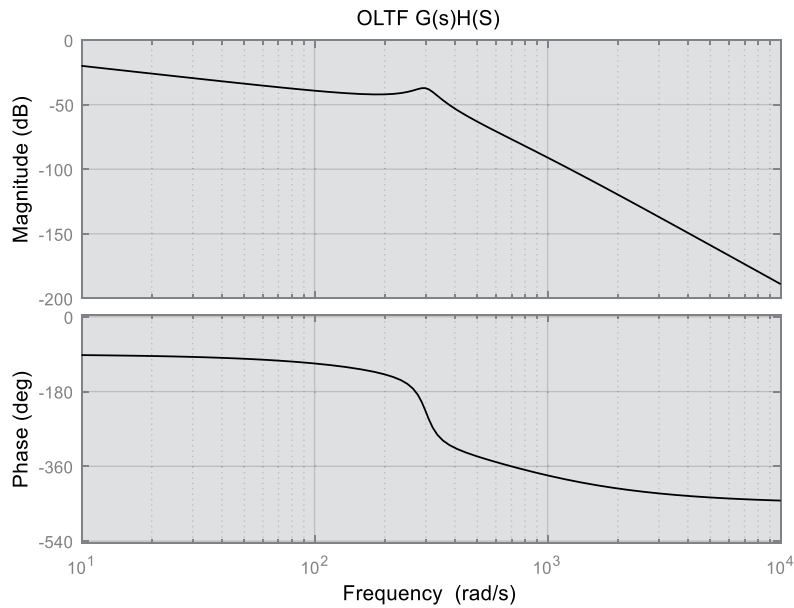
Using Matlab Control System Toolbox results in the following frequency responses for the servovalve and the system, and with unity gains for each transfer function.

```
G1=tf([0 0 1],[2.53e-6 3.18e-3 1]);
G2=tf([0 0 0 1],[1.11e-5 6.63e-4 1 0]);
bodeplot(G1,G2);
```



It can be seen that the servovalve contributes phase angle to the OLF around the condition where the phase angle for the system only is -180° . The servovalve magnitude contributes little to the overall magnitude at this phase angle, but it is concluded at this stage that both servovalve and system dynamics must be considered. The OLF is next shown.

```
G=G1*G2;
bodeplot(G);
```



By zooming into the phase angle diagram at a frequency between 260rad/s and 280rad/s it is deduced that the phase angle is -180° when $\omega = 270\text{rad/s}$ (**43Hz**). The magnitude ratio is then read from the graph as -38.6dB and therefore the condition for the onset of closed-loop instability is determined as follows:

$$+38.6\text{dB} = 20\log K \rightarrow K = 85$$

Now considering the direct calculation approach, the closed-loop characteristic equation is:

$$1 + G(s)H(s) = 0$$

$$s\left(1 + \frac{2\zeta_{sv}}{\omega_{nsv}}s + \frac{s^2}{\omega_{nsv}^2}\right)\left(1 + \frac{2\zeta}{\omega_n}s + \frac{s^2}{\omega_n^2}\right) + K = 0$$

Substituting the numerical values then gives:

$$2.78 \times 10^{-11} s^5 + 3.67 \times 10^{-8} s^4 + 1.56 \times 10^{-5} s^3 + 3.84 \times 10^{-3} s^2 + s + K = 0$$

At the point of instability let $s = j\omega$ to give:

$$(K - 3.84 \times 10^{-3} \omega^2 + 3.67 \times 10^{-8} \omega^4) + j(\omega - 1.56 \times 10^{-5} \omega^3 + 2.78 \times 10^{-11} \omega^5) = 0$$

Considering first the Imaginary term gives the solutions for ω :

$$\omega = 0 \quad \text{or} \quad 1 - 1.56 \times 10^{-5} \omega^2 + 2.78 \times 10^{-11} \omega^4 = 0$$


Taking the lowest finite frequency gives $\omega = 272 \text{ rad/s}$ (**43Hz**)

Considering the Real term from the characteristic equation and substituting $\omega = 272 \text{ rad/s}$ then gives the gain **K = 84**.

The solution using the frequency response plot is sufficiently close to the analytical solution, allowing for rounding off and accuracy of graphical analysis. The simulation result for the position response to a step demand of 1mm is now shown for a stable gain $K = 20$ and $K = 40$.

$$\text{CLTF} = \frac{K}{2.78 \times 10^{-11} s^5 + 3.67 \times 10^{-8} s^4 + 1.56 \times 10^{-5} s^3 + 3.84 \times 10^{-3} s^2 + s + K}$$

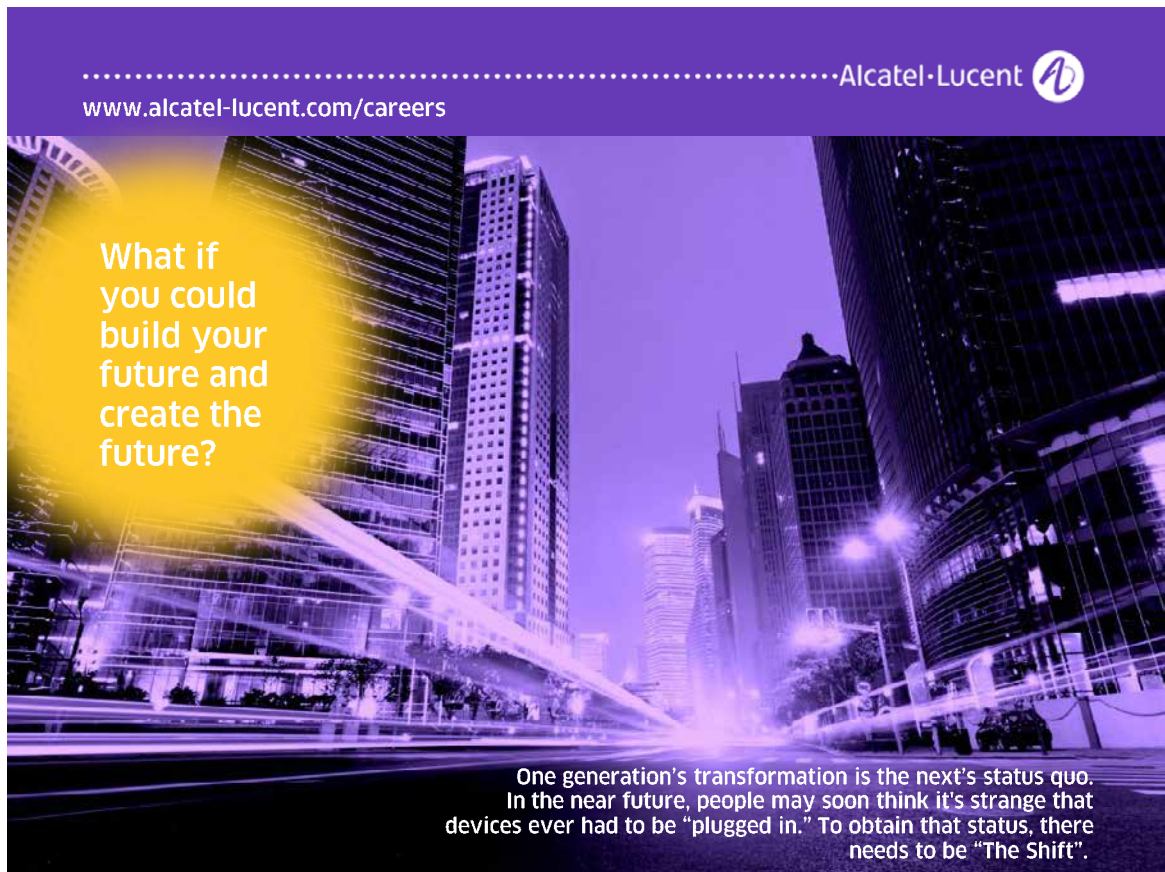
```
GC1=tf([0 0 0 0 0 20],[2.78e-11 3.67e-8 1.56e-5 3.84e-3 1 20]);
GC2=tf([0 0 0 0 0 40],[2.78e-11 3.67e-8 1.56e-5 3.84e-3 1 40]);
stepplot(GC1,GC2);
```

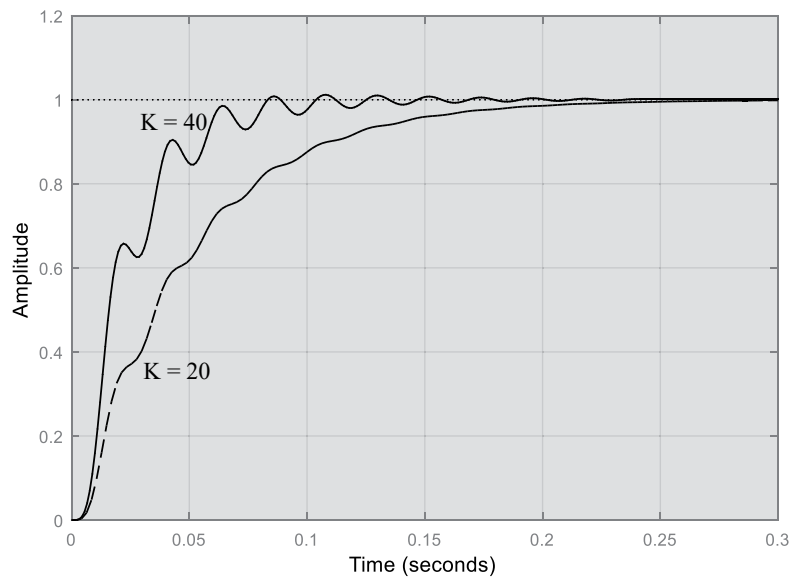
.....Alcatel-Lucent 

www.alcatel-lucent.com/careers

What if you could build your future and create the future?

One generation's transformation is the next's status quo. In the near future, people may soon think it's strange that devices ever had to be "plugged in." To obtain that status, there needs to be "The Shift".





The oscillatory component from the system dynamics is evident from the closed-loop system step response, under proportional control, and some form of improvement is probably necessary.

In general, the conditions for the onset of closed-loop stability for two common characteristic equations may be determined as follows:

i) *for a 3rd order characteristic equation*

$$b_3 s^3 + b_2 s^2 + b_1 s + b_o = 0$$

$$b_1 b_2 = b_o b_3 \quad \omega = \sqrt{b_1 / b_3} \quad (6.7)$$

ii) *for a 4th order characteristic equation*

$$b_4 s^4 + b_3 s^3 + b_2 s^2 + b_1 s + b_o = 0$$

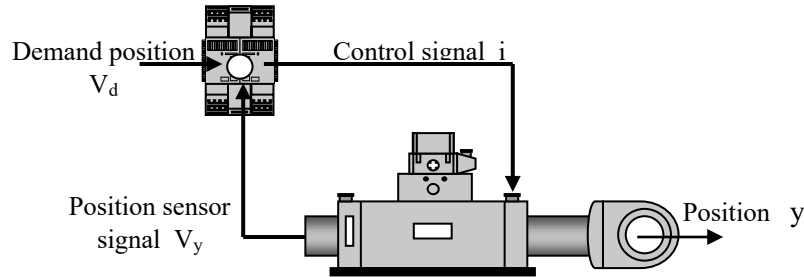
$$b_1^2 b_4 - b_1 b_2 b_3 + b_o b_3^2 = 0 \quad \omega = \sqrt{b_1 / b_3} \quad (6.8)$$

From a more rigorous control theory point of view closed-loop stability of electrohydraulic control systems, which usually have stable open-loop transfer functions, requires that the roots of the closed-loop characteristic equation must not have positive real parts.

There is a simple method of determining whether or not a characteristic equation has roots with positive real parts, known as **Routh's stability criterion**, and more details may be found in the many standard reference books on control theory.

Example 6.2

Consider a previous example with a servoactuator damping ratio $\zeta = 0.021$ and an undamped natural frequency $\omega_n = 307\text{rad/s}$. Investigate the behaviour of the closed-loop position control system using the linearised OLTf assuming that the servoamplifier gain G_a is the design variable.



$$\text{OLTf } G(s)H(s) = \frac{K}{s(1 + 1.34 \times 10^{-4}s + \frac{s^2}{307^2})} \quad K = \frac{H_p G_a k_{qi}}{A} = 0.1G_a$$

The characteristic equation is given by:

$$1 + G(s)H(s) = 0 \rightarrow s(1 + 1.34 \times 10^{-4}s + \frac{s^2}{307^2}) + 0.1G_a = 0$$

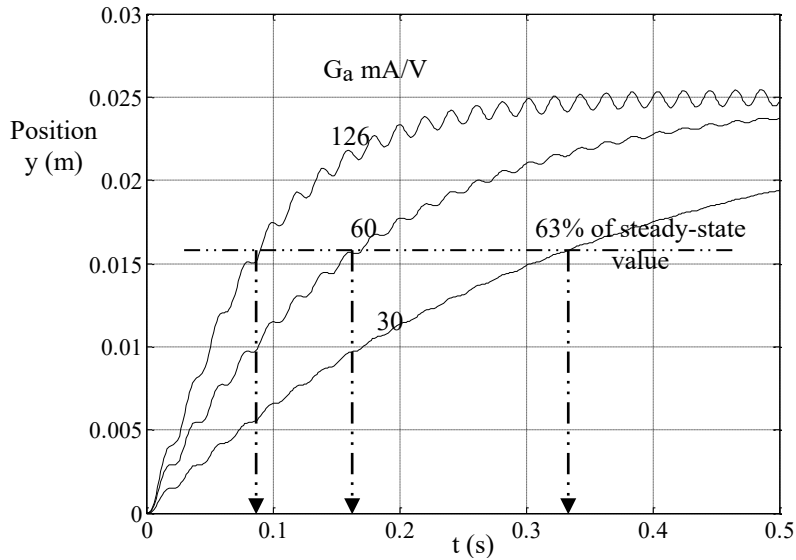
$$\frac{s^3}{307^2} + 1.34 \times 10^{-4}s^2 + s + 0.1G_a = 0$$

Stability is ensured providing: $b_1 b_2 > b_0 b_3$

$$(1.34 \times 10^{-4})(1) > (\frac{1}{307^2})(0.1G_a)$$

$$G_a < 126\text{mA/V} \quad (K < 12.6)$$

A comparison of transient responses to a step input demand of 25mm is shown for various servoamplifier gains.



The 2nd order lightly-damped component may be seen superimposed on each transient response from the actuator mid-position to an extension of 25mm. It can also be seen that the response is dominated by a 1st order component.



Join the best at
**the Maastricht University
 School of Business and
 Economics!**

Top master's programmes

- 33rd place Financial Times worldwide ranking: MSc International Business
- 1st place: MSc International Business
- 1st place: MSc Financial Economics
- 2nd place: MSc Management of Learning
- 2nd place: MSc Economics
- 2nd place: MSc Econometrics and Operations Research
- 2nd place: MSc Global Supply Chain Management and Change

Sources: Keuzegids Master ranking 2013; Elsevier 'Beste Studies' ranking 2012; Financial Times Global Masters in Management ranking 2012

Maastricht University is the best specialist university in the Netherlands
 (Elsevier)

Visit us and find out why we are the best!
Master's Open Day: 22 February 2014

www.mastersopenday.nl



When the servoamplifier gain is set to its maximum value of 126mA/V then a steady-state small oscillation in position is observed. Although there is no large-scale position fluctuation, a large fluctuation in velocity/pressure differential occurs, and this is often the case with position control systems.

For a servodrive that has an appearance of *a dominant over-damped transient response* then the OLTf is dominated by a 1st order time constant effect:

$$\text{OLTf} = \frac{K}{s(1 + \frac{2\zeta}{\omega_n}s + \frac{s^2}{\omega_n^2})} \approx \frac{K}{s}$$

$$\text{CLTF} = \frac{1}{1 + s\tau} \quad \tau = \frac{1}{K} = \frac{1}{0.1G_a}$$

So the approximate time constant τ is given by:

G_a (mA/V)	τ (s)
30	0.333
60	0.167
126	0.079

These values are evident from the transient response diagram at the time when the output achieves approximately 63% of its steady-state value.

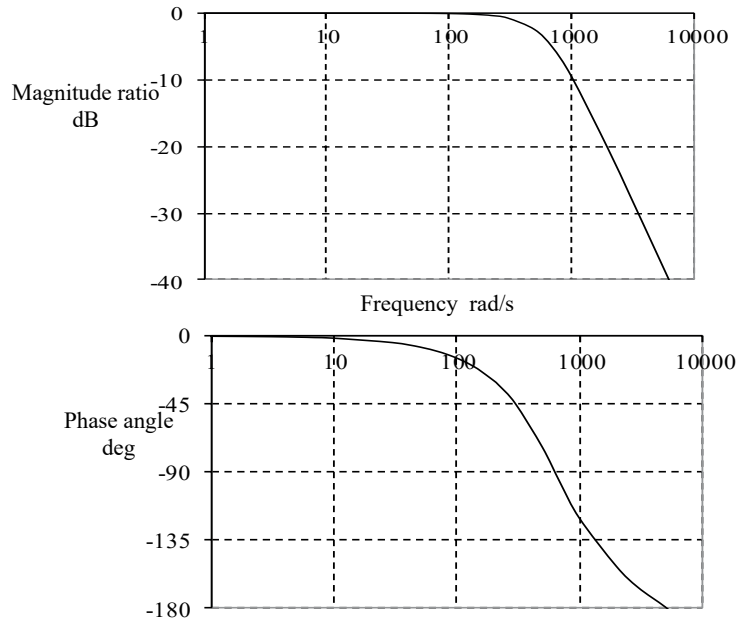
The *linearised transfer function is only valid in the absence of servoamplifier saturation*, ± 20 mA in this example, and this has been included in the results shown. Current saturation occurs for $G_a > 80$ mA/V and so the concept of a linear 1st order closed-loop response is only valid for gains below this value.

Comparing the linearised prediction with the exact simulation, not presented here, it turns out for this example that:

- the transient responses are almost identical in overall shape.
- the exact solution does not exhibit the oscillatory component in the position response as evident from the linearised results shown.
- when the servoamplifier gain is set to the value of 126mA/V then instability still occurs for the exact model but significant oscillations in position are not evident. However there are very significant oscillations in pressure differential.

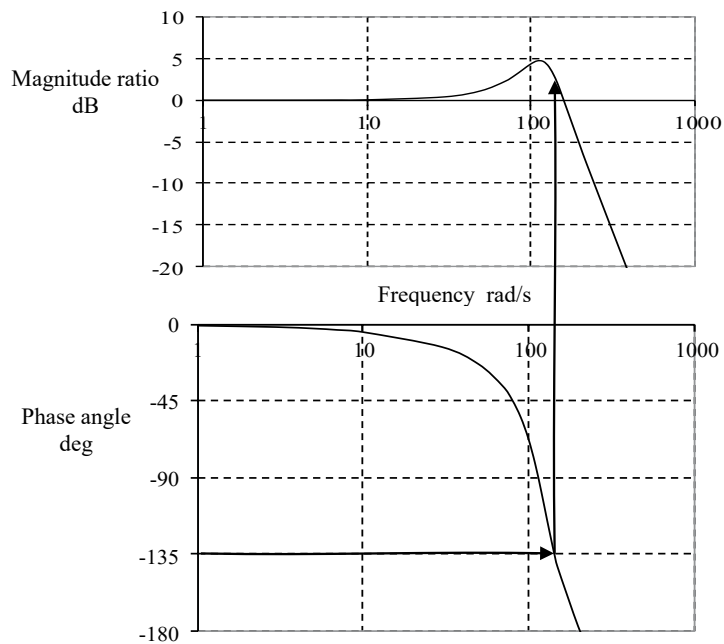
Example 6.3

The small-signal frequency response of a servovalve taken from the manufacturer’s data sheet is shown.



The OLTF of a motor speed control system was estimated to be 2nd order with a damping ratio $\zeta = 0.3$ and an undamped natural frequency $\omega_n = 126 \text{ rad/s}$ ($\approx 20\text{Hz}$). Determine a suitable open-loop gain to give a phase margin of 45° and deduce the significance of its value.

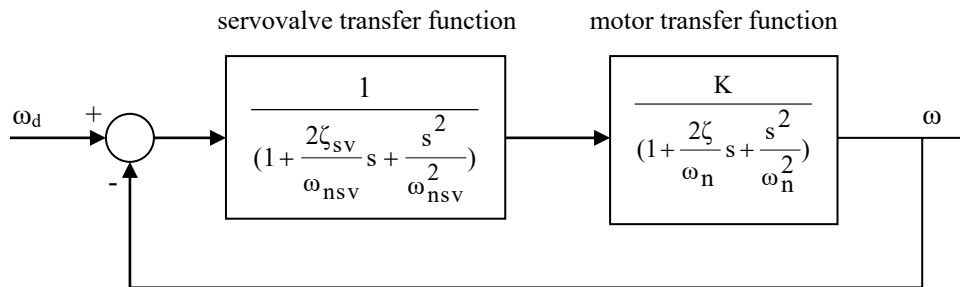
Adding the motor frequency response to the servovalve frequency response then gives the OLTF for the servovalve and the motor as follows:



This open-loop frequency response is based on a gain of 1. To achieve a phase margin of -45° then the magnitude ratio must be 0dB when the phase angle is -135° . From the OLF data the actual magnitude ratio is $\approx +2.4$. Therefore the added gain K must be equivalent to -2.4 dB to give:

$$20\log K = -2.4 \quad K = 0.76$$

The block diagram of the motor speed control system with proportional control only is now shown.



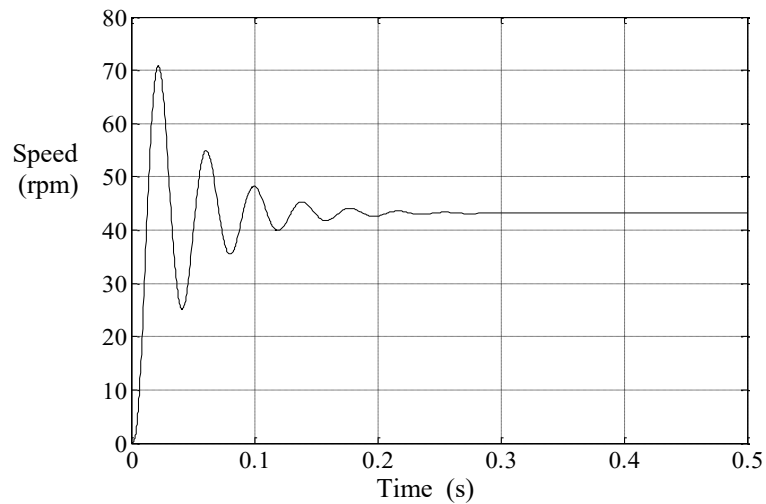
The servovalve is represented by a 2nd order transfer function approximation and from the data presented it is assessed to have a damping ratio $\zeta_{sv} \approx 0.8$ with an undamped natural frequency $\omega_{nsv} = 628$ rad/s (≈ 100 Hz).



The steady-state relationship between speed and demanded speed, the closed-loop gain, is given by:

$$\frac{\omega}{\omega_d} = \frac{K}{1+K} = 0.43$$

However, this is only a calibration issue since to achieve any steady-state speed it is only necessary to select the appropriate input voltage. The transient response to a step demand of 100rpm is now shown, and evaluated from the estimated transfer functions.



The transient response is too oscillatory and a further consideration of the gain is necessary or perhaps an improved control strategy beyond just proportional control. Reducing the open-loop gain K will improve the response but the closed-loop steady-state gain will also be reduced. This example will be pursued further in Chapter 7.

7 Improving closed-loop behaviour

7.1 Aim

To understand how to improve closed-loop behaviour via the following objectives:

- to first consider some methods of improving steady-state behaviour
- to then consider some basic methods of improving dynamic performance
- to introduce the use of a Programmable Servo Controller (PSC)

7.2 Some preliminary comments

There are several different types of control systems such as velocity control, position control, force control, pressure control and pressure differential control. For each type of control system the servovalve dynamics may be significant or may not be significant depending on the dynamics of the system and its load. It is therefore beyond the scope of this book to investigate all the combinations together with the many different types of methods that may be used to improve system performance and meet design objectives. In addition, the published literature on electrohydraulic control systems abounds with “modern” methods of control that are interesting, yet often mathematically defined in a way that cannot be practically implemented and also present issues of robustness to changing system conditions. These advanced methods must be pursued but this chapter considers just a few examples of the common methods that seem to be implemented by industry.

7.3 The use of servoamplifier dither to improve steady-state error drift for a position control system

High-frequency, low amplitude current dither is used to improve the small variations in position steady-state error that inevitably occurs in practice. Consider a position servodrive with a servovalve having a small amount of under-lap and has its optimum load to give ostensibly a zero steady-state error in position, and an actual system studied by the author. The demanded position is $y = 0.4$ mm and a low-frequency triangular input voltage is applied and having an amplitude of 18.5 mV. This means that ideally the cylinder position/input voltage graph should be a straight line where the cylinder moves from -0.048 mm to +0.448 mm. Results are shown in figure 7.1 for 3 cycles.

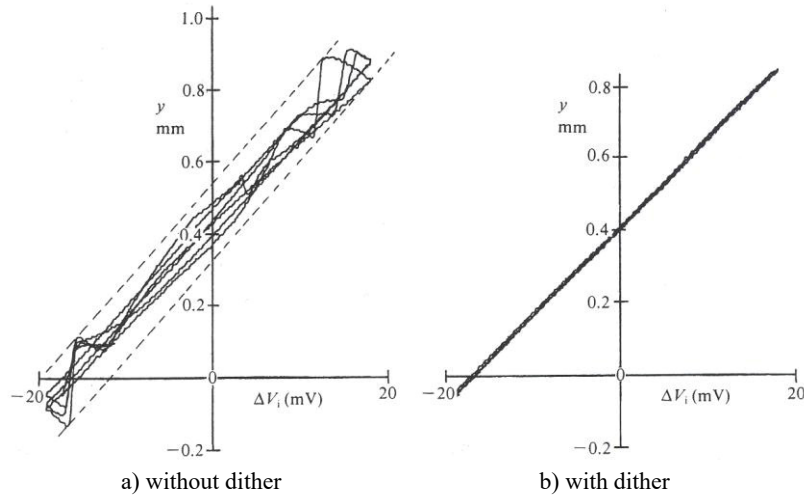


Figure 7.1 The effect of dither on steady-state position

Empowering People. Improving Business.

BI Norwegian Business School is one of Europe's largest business schools welcoming more than 20,000 students. Our programmes provide a stimulating and multi-cultural learning environment with an international outlook ultimately providing students with professional skills to meet the increasing needs of businesses.

BI offers four different two-year, full-time Master of Science (MSc) programmes that are taught entirely in English and have been designed to provide professional skills to meet the increasing need of businesses. The MSc programmes provide a stimulating and multi-cultural learning environment to give you the best platform to launch into your career.

- MSc in Business
- MSc in Financial Economics
- MSc in Strategic Marketing Management
- MSc in Leadership and Organisational Psychology

BI NORWEGIAN BUSINESS SCHOOL

EFMD **EQUIS ACCREDITED**

www.bi.edu/master



Figure 7.1a) is an interesting result in that it displays a position error variation that could be explained qualitatively in terms of hysteresis, drift etc. Note also that as the triangular voltage input slope changes sign then the actuator momentarily moves in the wrong direction. However it is dramatically clear that when servovalve dither is introduced a much superior performance is achieved as shown in figure 7.1b). Servovalve dither is added to the input signal at the servoamplifier. In this example the dither frequency is 150Hz and the amplitude is the same as the triangular demanded variation voltage, i.e. 18.5mV. This amplitude produces a servovalve current amplitude of 0.19mA and within the under-lap equivalent current of 0.27mA.

A typical manufacturer's specification would indicate hysteresis as being less than 3% of rated current with the threshold less than 0.5% of rated current without dither. If dither is used then the amplitude should be less than 10% of rated current.

7.4 The effect of spool under-lap on the steady-state error for a position control system

Whatever the type of intentional spool lap, a servodrive will always have a very small position error. It was briefly discussed earlier that a servovalve spool may be symmetrically critically-lapped, over-lapped or under-lapped. While a critically-lapped spool should give a zero position error, for the idealised servovalve performance characteristic, this will not be so for over-lapped and under-lapped spools. For an over-lapped spool the position can be any value within the over-lap region equivalent to a current value of $\pm i_o$ mA.

Position error for an under-lapped spool may not be so obvious and is now worth pursuing. Recalling the flow rate equations, Chapter 2, for a servovalve with a symmetrically under-lapped spool, the under-lap being equivalent to $\pm i_u$ mA:

$$Q_1 = k_f (i_u + i) \sqrt{P_s - P_1} - k_f (i_u - i) \sqrt{P_1} \quad (7.1)$$

$$Q_2 = k_f (i_u + i) \sqrt{P_2} - k_f (i_u - i) \sqrt{P_s - P_2}$$

Also recalling the steady-state force equation for a *single-rod actuator* with load force only:

$$P_1 A_1 - P_2 A_2 = F \quad (7.2)$$

Under closed-loop position control then $Q_1 = Q_2 = 0$ and therefore from (7.1) it follows that the sum of line pressures must equal supply pressure. This gives:

$$Q = k_f (i_u + i) \sqrt{\frac{\gamma P_s - P_\ell(o)}{(1 + \gamma)}} - k_f (i_u - i) \sqrt{\frac{P_s + P_\ell(o)}{(1 + \gamma)}} \quad (7.3)$$

$$P_1 + P_2 = P_s \quad P_\ell(o) = \frac{F}{A_2} \quad P_1 = \frac{P_s + P_\ell(o)}{1 + \gamma} \quad P_2 = \frac{\gamma P_s - P_\ell(o)}{1 + \gamma}$$

For the flow rate within the region of under-lap to be zero then from (7.3):

$$\frac{i}{i_u} = \frac{\sqrt{P_s + P_\ell(o)} - \sqrt{\gamma P_s - P_\ell(o)}}{\sqrt{P_s + P_\ell(o)} + \sqrt{\gamma P_s - P_\ell(o)}} \quad (7.4)$$

This means that a finite servovalve current may exist, will vary with load force, and hence a steady-state position error is given by:

$$y_{\text{error}} = \frac{i}{G_a H_p} \quad (7.5)$$

From (7.4) the steady-state error can be made zero by ensuring that:

$$P_s + P_\ell(o) = \gamma P_s - P_\ell(o) \rightarrow P_\ell(o) = \frac{(\gamma - 1)}{2} P_s \quad (7.6)$$

$$F = \frac{P_s A_{\text{rod}}}{2} \quad A_{\text{rod}} = A_1 - A_2 \quad P_1 = P_2 = P_s / 2$$

This analysis leads to some important points:

- the supply pressure may be matched to the load to produce a zero position error. At this condition $P_1 = P_2 = P_s/2$. Looking at this in another way, if it is practically feasible to adjust the supply pressure until both line steady-state pressures are equal then the position error should be minimum, ideally zero
- at the optimum condition with $P_1 = P_2 \approx P_s/2$, the pressure differential across the actuator piston will be close to zero thus minimising leakage across the piston
- at the matched load condition the open-loop extending velocity is the same as the retracting velocity, that is, the open-loop gain does not change with direction of motion. This is preferable from a closed-loop control point of view
- it is important to now realise that for a double rod actuator, $\gamma = 1$, a zero position error can only occur for zero load, $F = 0$
- higher loads can be positioned with zero error and will be aided by an increased area ratio
- the sensitivity of steady-state error to variations in load around the zero position error point is improved for increased area ratios, although the effect is small for area ratios up to $\gamma = 2$

Example 7.1

Consider some *experimental evidence taken from a 3-axis manipulator project* undertaken by the author. This small manipulator used three low-friction servo cylinders and the one examined here, the second axis, had the following data:

Actuator bore 50.8mm diameter, rod 28.6mm diameter

Position sensor gain $H_p = 0.0413\text{V/mm}$

Servoamplifier gain $G_a = 10\text{mA/V}$

Servo valve supply pressure $P_s = 50\text{bar}$

Servo valve under-lap equivalent to $\pm 0.27\text{mA}$

The low supply pressure is chosen here to avoid compression of the results at the lower end of the scale.

$$A_1 = 20.27 \times 10^{-4} \text{m}^2 \quad A_2 = 13.84 \times 10^{-4} \text{m}^2 \quad A_{\text{rod}} = 6.43 \times 10^{-4} \text{m}^2$$

Optimum load occurs when $F = P_s A_{\text{rod}} / 2 = (50 \times 10^5) (6.43 \times 10^{-4}) / 2 = 1608\text{N}$

$$\text{or } F / P_s A_2 = (1608) / (50 \times 10^5) (13.84 \times 10^{-4}) = 0.23$$

Results for current error are shown and it can be seen that the theory match the measurements reasonably well with the measured pressures being a little lower than the theoretical values. The condition for zero steady-state position error matches the predicted value. The result of the cylinder position error at no-load is that the manipulator end error would be 0.23mm.

Need help with your dissertation?

Get in-depth feedback & advice from experts in your topic area. Find out what you can do to improve the quality of your dissertation!

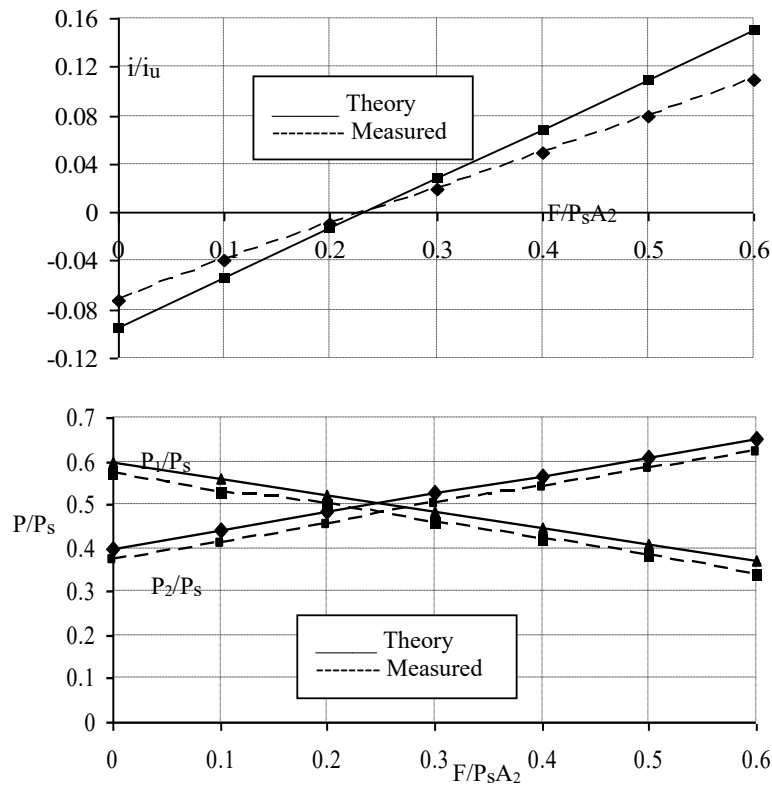
Get Help Now



Go to www.helpmyassignment.co.uk for more info



Helpmyassignment



A possible design guide for setting under-lap at the null condition may be derived by considering the leakage flow back to tank, that is with no position error and each line pressure at half supply pressure at the matched load condition. The leakage flow back to tank, $Q_{leakage}$, may be deduced and compared with the rated flow as follows:

$$Q_{leakage} = 2k_f i_u \sqrt{\frac{P_s}{2}} \quad Q_{rated} = k_f i_{rated} \sqrt{35} \quad (7.7)$$

Now it is desirable that the leakage flow to tank is minimised since it also represents a power loss and hence drop in efficiency. As a first step **assume that the leakage flow is to be less than 10% of the rated flow**. It then follows from equation (7.7) that:

$$\frac{i_u}{i_{rated}} < \frac{0.42}{\sqrt{P_s}} \quad P_s \text{ bar} \quad (7.8)$$

For example, at a supply pressure of 210bar then $i_u < 3\% i_{rated}$. Clearly only a very small under-lap can be tolerated in practice.

Now consider the spool under-lap effect on damping. For a symmetrically-underlapped spool the resistance is given by:

$$R_{sv} = \frac{\sqrt{2P_s}}{k_f i_u} = \frac{2P_s}{Q_{leakage}} \quad (7.9)$$

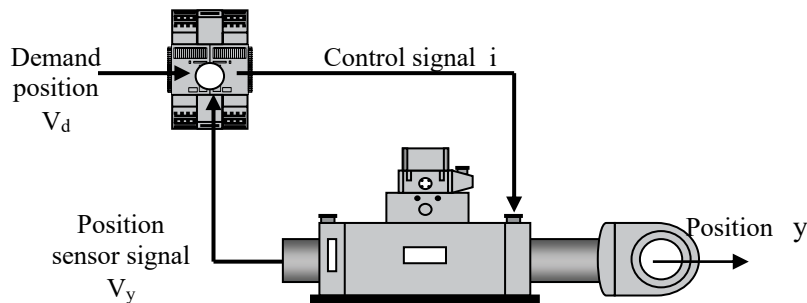
Note also that the introduction of under-lap doubles the flow gain, when compared with a critically-lapped spool, and is given by:

$$k_{qi} = 2k_f \sqrt{\frac{P_s}{2}} \tag{7.10}$$

So increasing spool leakage back to tank decreases the resistance and improves damping, although the effect may be small in reality.

Example 7.2

Consider Example 5.4 where the servoactuator is lightly damped and now investigate the introduction of servovalve spool under-lap to give increased damping.



With just viscous damping the damping ratio of the 2nd order part of the OLF was found to be $\zeta = 0.021$ and the undamped natural frequency $\omega_n = 307\text{rad/s}$.

$$\text{OLTF } \frac{V}{V_d} = \frac{y(s)}{y_d(s)} = \frac{K}{s \left[1 + \left[\frac{L}{R} + \frac{CR_{\text{visc}}}{2} \right] s + \frac{LC}{2} s^2 \right]} \quad K = \frac{H_p G_a k_{qi}}{A}$$

Since the actuator leakage resistance $R_{act} = \infty$ the overall resistance R is now the servovalve resistance and given by:

$$\frac{1}{R} = \frac{1}{R_{act}} + \frac{1}{R_{sv}} = \frac{1}{R_{sv}} \quad R_{sv} = \frac{\sqrt{2P_s}}{k_f i_u} = \frac{2P_s}{Q_{leakage}}$$

Also that the flow gain has doubled, when compared with a critically-lapped spool, and is now given by:

$$k_{qi} = 2k_f \sqrt{\frac{P_s}{2}}$$

The servovalve rated flow is $Q_{rated} = k_f i_{rated} \sqrt{35} = (0.2)(20) \sqrt{35} = 23.7 \text{ litres/min}$

Now assume the leakage flow is 10% of the rated flow then $Q_{\text{leakage}} = 2.37$ litres/min and the leakage resistance @ a supply pressure of 210bar is:

$$R_{sv} = \frac{(2)(210 \times 10^5)60}{2.37 \times 10^{-3}} = 1.06 \times 10^{12} \text{ Nm}^{-2}/\text{m}^3 \text{ s}^{-1}$$

$$\text{New damping term} \quad \frac{L}{R} = \frac{L}{R_{sv}} = \frac{0.69 \times 10^8}{1.06 \times 10^{12}} = 0.65 \times 10^{-4} \text{ s}$$

$$\text{Existing damping term} \quad \frac{CR_{\text{visc}}}{2} = \frac{(3.07 \times 10^{-13})(8.7 \times 10^8)}{2} = 1.34 \times 10^{-4} \text{ s}$$

$$\text{The new damping ratio becomes } \zeta = 0.021 \frac{(0.65 + 1.34)}{1.34} = 0.031$$

So, spool under-lap will only marginally improve the damping ratio from $\zeta = 0.021$ to 0.031. Increasing spool under-lap has little value for this example since the increased leakage flow will be unacceptable.



Brain power

By 2020, wind could provide one-tenth of our planet's electricity needs. Already today, SKF's innovative know-how is crucial to running a large proportion of the world's wind turbines.

Up to 25 % of the generating costs relate to maintenance. These can be reduced dramatically thanks to our systems for on-line condition monitoring and automatic lubrication. We help make it more economical to create cleaner, cheaper energy out of thin air.

By sharing our experience, expertise, and creativity, industries can boost performance beyond expectations. Therefore we need the best employees who can meet this challenge!

The Power of Knowledge Engineering

Plug into The Power of Knowledge Engineering.
Visit us at www.skf.com/knowledge

SKF

7.5 Steady-state tracking error in response to a velocity demand for a position control system

Now consider a linear position servodrive which is demanded to track at a particular velocity for part of its duty cycle by applying a ramp voltage at the input. This is a common design specification, so consider figure 7.2.

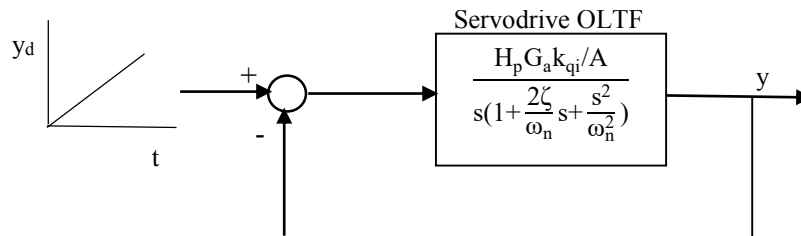


Figure 7.2 A linear servodrive position control system

The position error is given by:

$$y_e(s) = y_d(s) - y(s) = \frac{y_d(s)}{1 + G(s)H(s)} \tag{7.11}$$

So for a velocity demand U_d then: $y_d = U_d t$ (7.12)

From the Laplace transform Table: $y_d(s) = \frac{U_d}{s^2}$ (7.13)

Apply the input $y_e(s) = \frac{U_d}{s^2} \frac{s(1 + \frac{2zeta}{\omega_n}s + \frac{s^2}{\omega_n^2})}{s(1 + \frac{2zeta}{\omega_n}s + \frac{s^2}{\omega_n^2}) + K}$ $K = \frac{H_p G_a k_{qi}}{A}$ (7.14)

From the Laplace transform Table then using the Final Value Theorem:

$$y_e(t) \Big|_{t \rightarrow \infty} = sF(s) \Big|_{s \rightarrow 0} = s \left[\frac{U_d}{s^2} \frac{s(1 + \frac{2zeta}{\omega_n}s + \frac{s^2}{\omega_n^2})}{s(1 + \frac{2zeta}{\omega_n}s + \frac{s^2}{\omega_n^2}) + K} \right]_{s=0}$$

steady-state tracking error $y_e = \frac{U_d}{K}$ (7.15)

So, there will **always be a position error when tracking a velocity input** but it can be reduced by increasing the open-loop gain K . However there is a limit to the value of K since increasing it will eventually lead to closed-loop instability as previously discussed in Chapter 6.

One way of reducing the steady-state error for a velocity demand is to introduce **Derivative feedforward** action as shown in figure 7.3.

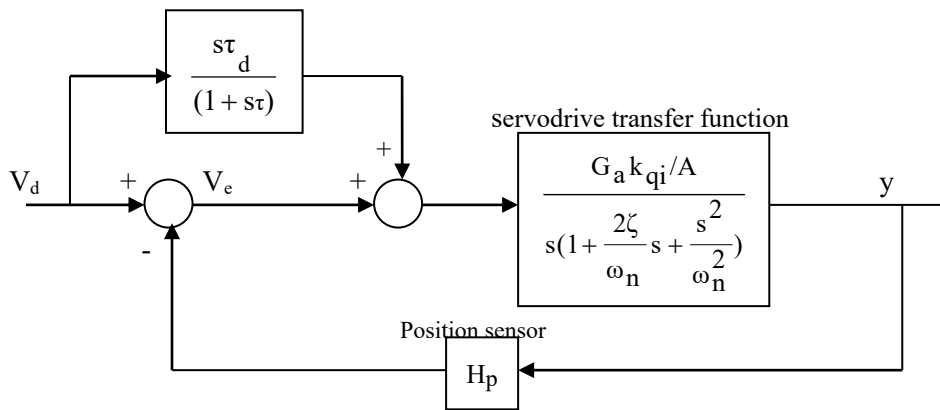


Figure 7.3 A linear servodrive position control system with feedforward control

The forward Derivative term is $s\tau_d$ and it will be seen that a **first-order filter**, with a time constant τ , has been included to indicate its necessity in practice to minimise noise effects and rapid fluctuations in demand. It is particularly important to consider the type of demands used when Derivative feedforward control is implemented. Rapid changes in demand imply high derivatives which may cause a rapid, and possibly undesirable, opening or closure of the servovalve spool.

Again applying a ramp input ($y_d = Udt$) and using the Final Value Theorem now gives the steady-state tracking error as:

$$\text{steady-state tracking error } y_e = \frac{U}{K} (1 - K\tau_d) \tag{7.16}$$

Comparing (7.16) with (7.15), for the case with no feedforward term, then it can be seen that the tracking error may now be reduced in a different way, possibly made zero by choosing the Derivative time constant to have a value of $\tau_d \approx 1/K$.

Example 7.3

Considering previous examples 6.2 and 7.2 where the linearised second-order OLF has an undamped natural frequency $\omega_n = 307\text{rad/s}$ and a damping ratio $\zeta = 0.021$. It was shown that the closed-loop system will become unstable when $K = 2\zeta\omega_n = 12.9$. For the purpose of example select $K = 5$ and investigate feedforward using the exact simulation model and a demand velocity of $U_d = 0.01\text{m/s}$.



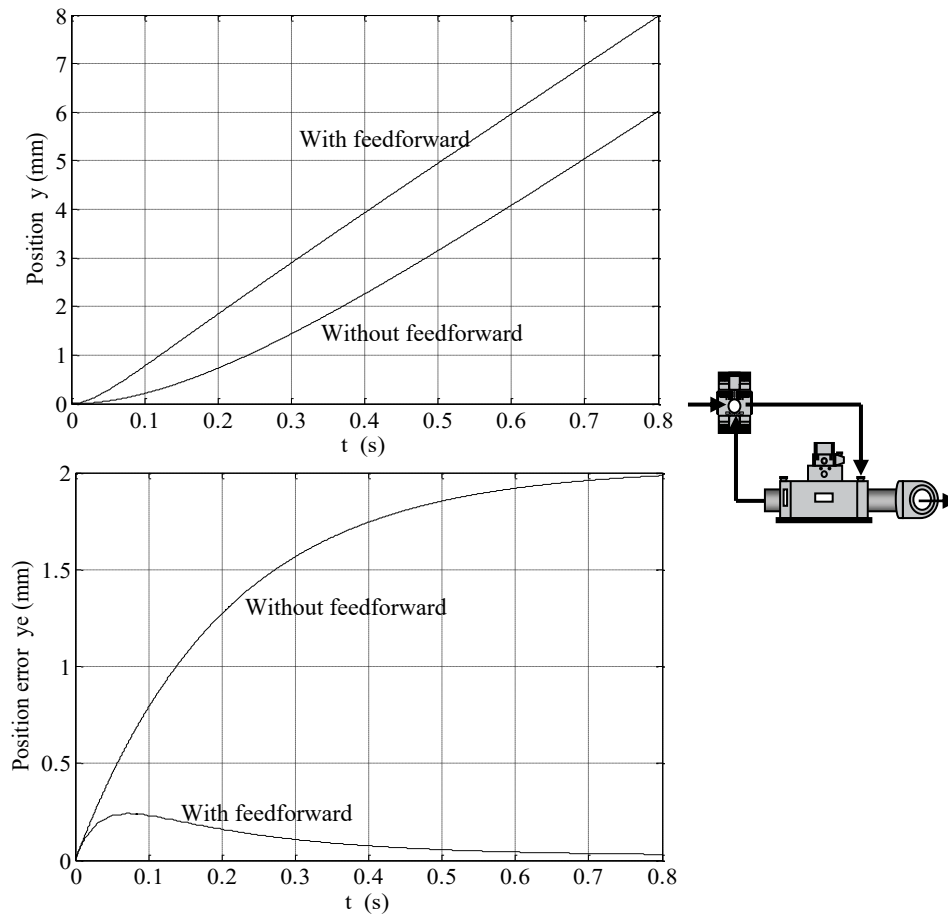
What do you want to do?

No matter what you want out of your future career, an employer with a broad range of operations in a load of countries will always be the ticket. Working within the Volvo Group means more than 100,000 friends and colleagues in more than 185 countries all over the world. We offer graduates great career opportunities – check out the Career section at our web site www.volvogroup.com. We look forward to getting to know you!

VOLVO
AB Volvo (publ)
www.volvogroup.com

VOLVO TRUCKS | RENAULT TRUCKS | MACK TRUCKS | VOLVO BUSES | VOLVO CONSTRUCTION EQUIPMENT | VOLVO PENTA | VOLVO AERO | VOLVO IT
VOLVO FINANCIAL SERVICES | VOLVO 3P | VOLVO POWERTRAIN | VOLVO PARTS | VOLVO TECHNOLOGY | VOLVO LOGISTICS | BUSINESS AREA ASIA

Select $\tau_d = 1/K = 0.2s$ select $\tau = 10/\omega_n = 0.033s$



For an ideal system the output should achieve 8mm after 0.8 seconds. With no feedforward the linearised analysis predicts a steady-state position error given by:

$$y_e = U_d/K = 0.01/5 = 0.002m = 2mm$$

The exact simulation validates this prediction. With a feedforward Derivative time constant of $\tau_d = 1/K = 0.2s$ then the linearised analysis predicts zero steady-state position error. The exact simulation showed a very small error of 0.024mm and changing the time constant from 0.2s to 0.202s produced a zero steady-state error. The closed-loop velocity tracking error performance is therefore very sensitive to the feedforward gain setting in this example.

The pressure differential results show that a very low amplitude oscillation occurs close to the servodrive undamped natural frequency and could not be damped using feedforward control for this system. However, the maximum pressure differential was only around 1.5bar for the input condition tested and would probably not be detected in practice.

7.6 Optimising the closed-loop transient response

In some cases, a control system transient response may be optimised using the Integral of Time multiplied by Absolute Error criterion, the *ITAE criterion* as briefly discussed in Chapter 5. For a 3rd order transfer function, with a unity gain only in the numerator, then the required form is as follows:

$$\text{ITAE closed-loop transfer function} = \frac{1}{1 + \frac{2.15s}{\omega_o} + \frac{1.75s^2}{\omega_o^2} + \frac{s^3}{\omega_o^3}} \quad (7.17)$$

The transient response to a step input produces a very small overshoot. The idea is to match the actual closed-loop transfer function with (7.17) which may not always be possible in practice.

For example consider the following OLF:

$$G(s)H(s) = \frac{K}{s(1 + \frac{2\zeta}{\omega_n}s + \frac{s^2}{\omega_n^2})} \quad (7.18)$$

$$\text{CLTF} = \frac{1}{1 + s\tau + \frac{2\zeta\tau s^2}{\omega_n} + \frac{\tau s^3}{\omega_n^2}} \quad \tau = \frac{1}{K} \quad (7.19)$$

Equating terms in (7.17) and (7.19) and combining gives:

$$\omega_o = 0.68\omega_n \quad K = 0.32\omega_n \quad \zeta = 0.6 \quad (7.20)$$

Considering example 7.3 where $\omega_n = 307\text{rad/s}$ and $\zeta = 0.021$ then the ITAE criterion cannot be achieved for this particular system unless damping can be significantly increased in some way. Increasing viscous damping by changing the fluid viscosity or deliberately introducing leakage damping are usually not an option. Under-lapping the servovalve spool might be considered as an option but probably again not achievable due to the large under-lap inevitably required with its inherent leakage flow and power loss.

Using additional feedback sensor terms or adding a compensating network is usually required to improved closed-loop performance and will be discussed later in this chapter.

7.7 Velocity sensing or Derivative computation

Linear velocity sensors are usually of the type that induce a voltage proportional to velocity via an electromagnetic circuit that does not require an external power supply. Other types are available such as optical grating sensors but tend to be more expensive. For rotary actuators then an optical or brush-type tachogenerator is either directly attached or geared to the motor output shaft, or acoustic wave technology sensors may be connected in-line. Self-generating linear sensors, optical and brush-type tachogenerator have been used by the author although the brush-type tachogenerator does suffer from added noise generation.

Velocity may be directly measured, or computed, and used as additional feedback signal. In addition Derivative computation may be used in the forward loop, and commonly known as Proportional plus Derivative control, PD control. Both aspects are shown in figure 7.4 for a linear position servodrive example.



gaiteye
Challenge the way we run

EXPERIENCE THE POWER OF FULL ENGAGEMENT...

**RUN FASTER.
RUN LONGER..
RUN EASIER...**

**READ MORE & PRE-ORDER TODAY
WWW.GAITEYE.COM**

The advertisement features a background image of a person running on a path during a sunrise or sunset. The Gaiteye logo is in the top left. The main text is in the middle left. A dotted line separates the headline from the benefits. A hand cursor icon is positioned over the call-to-action button in the bottom right. Technical diagrams, including a circle with intersecting lines, are overlaid on the runner's feet.

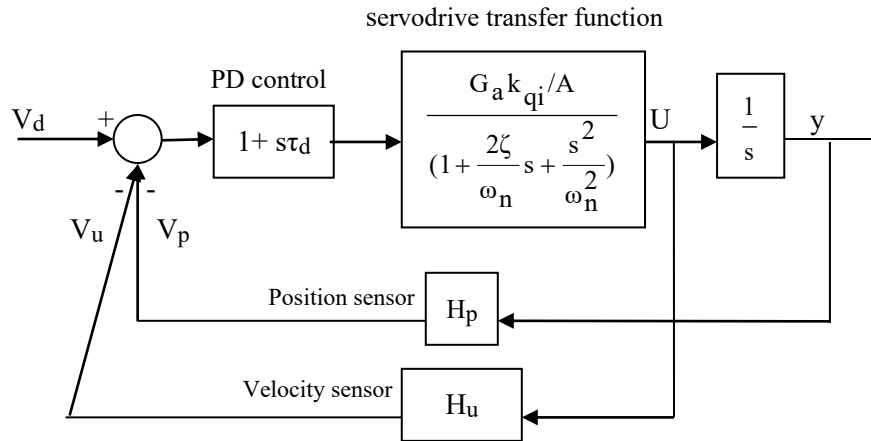


Figure 7.1 A linear servodrive position control system with additional derivative terms

Again it is pointed out that should PD be used in the forward loop then a filter should be included with the Derivative term to minimise sudden changes in input conditions and also to minimise any noise that will inevitably occur in practice. An initial analysis will neglect this filter.

$$\text{The velocity sensor voltage is given by } V_u = H_u \frac{dy}{dt} \tag{7.21}$$

$$\text{Taking the Laplace transform } V_u(s) = H_u sy(s) \tag{7.22}$$

The OLTF becomes:

$$G(s)H(s) = \frac{K(1 + s\tau_d)(1 + s\tau_{up})}{s(1 + \frac{2\zeta}{\omega_n}s + \frac{s^2}{\omega_n^2})} \quad \tau_{up} = \frac{H_u}{H_p} \quad K = \frac{H_p G_a k_{qi}}{A} \tag{7.23}$$

Two important points arise from this analysis:

- the effect of adding a velocity term is the same whether it is in the forward loop or in the feedback loop
- in terms of frequency response, both placements give phase advance to the OLTF which is stabilising

Considering just one placement with a time constant τ then the CLTF becomes:

$$\frac{y(s)}{y_d(s)} = \frac{(1 + s\tau)K}{K + s(1 + K\tau) + \frac{2\zeta}{\omega_n}s^2 + \frac{s^3}{\omega_n^2}} \tag{7.24}$$

The closed-loop characteristic equation is:

$$\frac{s^3}{\omega_n^2} + \frac{2\zeta}{\omega_n} s^2 + (1 + K\tau)s + K = 0 \tag{7.25}$$

This 3rd order closed-loop system will be stable providing:

$$K < 2\zeta\omega_n + 2\zeta\omega_n K\tau \tag{7.26}$$

It was shown earlier that this position control system without velocity feedback is stable providing $K < 2\zeta\omega_n$. If this is ensured then the closed-loop system with velocity or derivative action is inherently stable in the absence of servovalve dynamics. It may be found in reality that velocity damping may not improve the closed-loop transient response but may help to aid closed-loop stability, depending upon the nature of the system dynamics.

7.8 Additional acceleration, or pressure, feedback

An **accelerometer** may be used for improving the closed-loop response. This is an expensive approach but does offer a way forward in some advanced control systems applications.

A measure of acceleration feedback may be obtained using **two pressure transducers** but the signal must be filtered, using a high-pass filter, to remove the bias voltage due to the load force, or torque, effect. In addition a single-rod cylinder will require unequal area gain correction by the pressure sensors.

Figure 7.5 shows the system block diagram with the acceleration determined using an acceleration sensor. If it digitally-computed from position using a Programmable Servo Controller then, as with computed derivative action, an additional filter is desirable in practice.

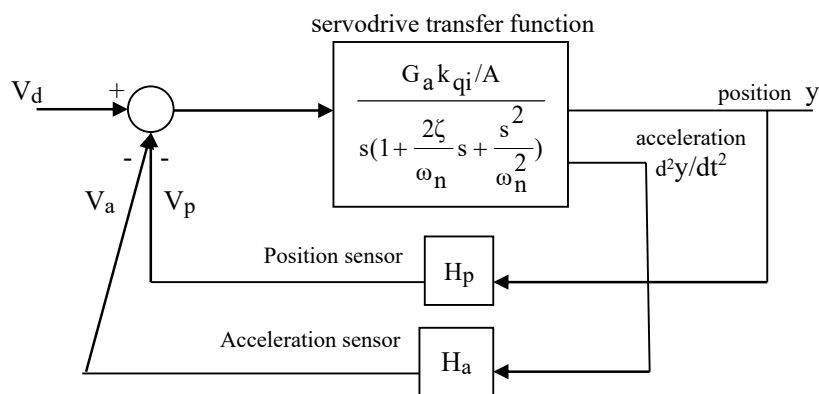


Figure 7.5 A linear servodrive position control system with added acceleration feedback

$$\text{The accelerometer voltage is given by } V_a = H_a \frac{d^2y}{dt^2} \tag{7.27}$$

$$\text{Taking the Laplace transform } V_a(s) = H_a s^2 y(s) \tag{7.28}$$

The OETF becomes:

$$G(s)H(s) = \frac{K(1 + s^2\tau^2)}{s(1 + \frac{2\zeta}{\omega_n}s + \frac{s^2}{\omega_n^2})} \quad \tau^2 = \frac{H_a}{H_p} \quad K = \frac{H_p G_a k_{qi}}{A} \quad (7.29)$$

$$\text{The CLTF is given by: } \frac{y(s)}{y_d(s)} = \frac{(1 + s^2\tau^2)K}{\frac{s^3}{\omega_n^2} + (\frac{2\zeta}{\omega_n} + K\tau^2)s^2 + s + K} \quad (7.30)$$

The closed-loop characteristic equation is given by:

$$\frac{s^3}{\omega_n^2} + (\frac{2\zeta}{\omega_n} + K\tau^2)s^2 + s + K = 0 \quad (7.31)$$

This third-order closed-loop system will be stable providing:

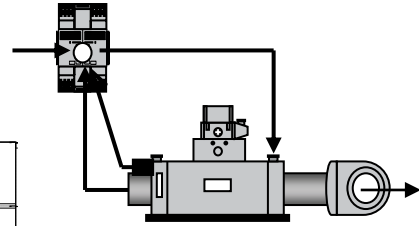
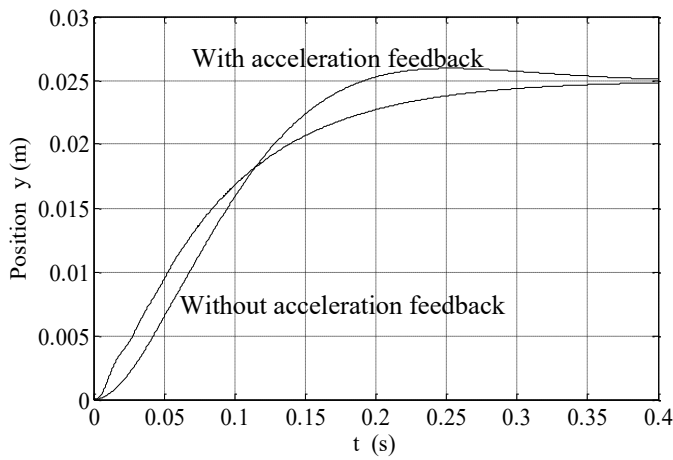
$$K < 2\zeta\omega_n + K\omega_n^2\tau^2 \quad (7.32)$$

It was shown earlier that without acceleration feedback then the requirement for stability is that $K < 2\zeta\omega_n$. It follows that if the closed-loop is stable without acceleration feedback then it will be inherently stable with the inclusion of acceleration feedback.

Example 7.4

Consider the linear double-rod actuator, example 6.2, and where a linearised analysis suggested that the transient response will become unstable at the point when the servoamplifier gain $G_a = 126\text{mA/V}$, $K = 12.6$. Investigate the use of additional acceleration feedback using the exact simulation model and selecting the critical gain $G_a = 126\text{mA/V}$, $K = 12.6$.

A value of $H_a = 0.03V/ms^{-2}$ gave just a small position overshoot as shown.



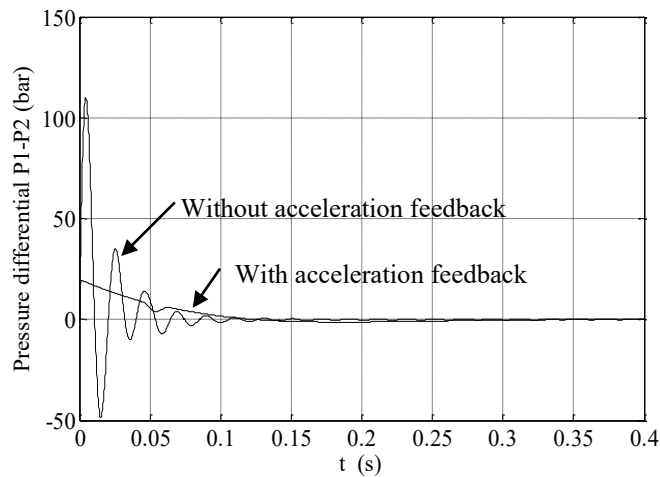
This e-book
is made with
SetaPDF



PDF components for PHP developers

www.setasign.com





The following points arise:

- with acceleration feedback the maximum pressure differential is around 20 bar compared with around 110bar without acceleration feedback
- the introduction of acceleration feedback has removed the high frequency oscillation in pressure differential
- the position transient behaviour might be considered as improved in an overall sense but the response cannot be made initially faster by the use of additional acceleration feedback
- increasing the accelerometer gain H_a will create a larger over-shoot and the response at the beginning will be more sluggish

7.9 Proportional+Integral+Derivative (PID) control

When there is an issue of steady-state error and/or dynamic response, particularly for process control systems with a pure delay and large time constants, it is common to consider PID control in the forward loop. Consider the general case for a servodrive shown as figure 7.6.

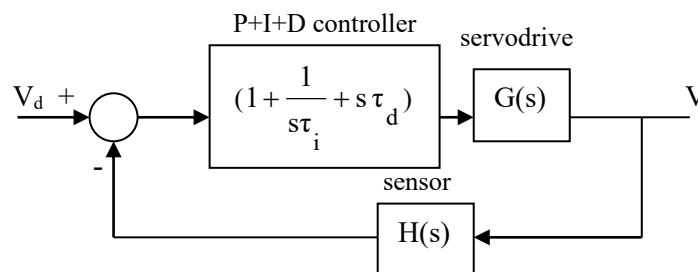


Figure 7.6 Block diagram for a control system with P+I+D control

In electrohydraulic control systems PID control is useful if a free integrator does not exist in the system forward loop transfer function, for example speed control, since by definition the integral component in PID control adds this effect. It does seem in practice that for the case of steady-state error removal it is usual to just consider PI control by adding an integral term.

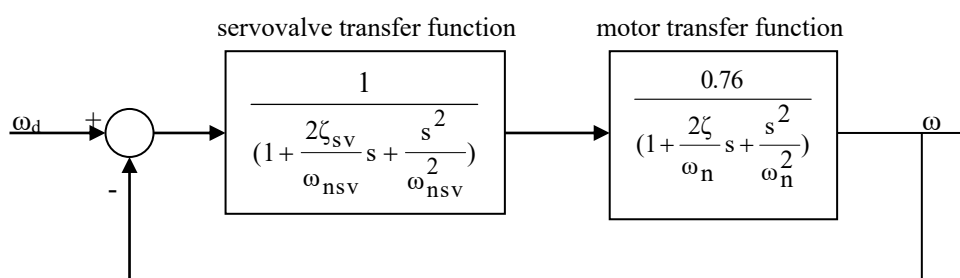
The Derivative element of PID control does not seem to be popular for many electrohydraulic control systems, particularly servodrives, one exception perhaps being for materials dynamic test machines where the load dynamics includes material stiffness. The machine manufacturer will provide design rules for setting up the controller.

In some control systems such as with a servovalve directly moving a pilot valve poppet, which then controls flow into the drive actuator, then a double integrator term dominates the OLTF. the addition of Derivative control in the forward loop, or in the feedback loop, can be considered. If derivative action is generated via a digital controller then again the signal will require bandwidth limitation to avoid higher noise frequencies being amplified.

For conventional servodrives the use of Derivative control in the forward loop has the same effect as adding it into the feedback loop. It also seems that wherever it is added it may not have any significant effect on reducing pressure oscillations.

Example 7.5

Consider the motor speed control system investigated as Example 6.3 where stability was ensured using frequency response, and an open-loop gain $K = 0.76$ was selected for proportional control only. The system is again shown.

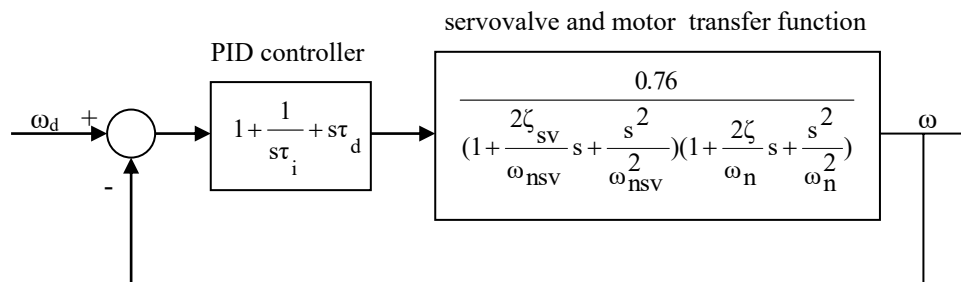


Servovalve damping ratio $\zeta_{sv} \approx 0.8$, undamped natural frequency $\omega_{nsv} = 628 \text{ rad/s} (\approx 100\text{Hz})$

Motor damping ratio $\zeta = 0.3$, undamped natural frequency $\omega_n = 126 \text{ rad/s} (\approx 20\text{Hz})$

Demanded motor speed $\omega_d = 100\text{rpm}$

PID control is now investigated to both reduce the speed fluctuations still existing in the original design and also to remove the steady-state error in achieved motor speed. The new block diagram is next shown.



- the existing gain $K = 0.76$ was retained
- derivative action was first introduced using the computer simulation and a time constant was found by trial and error, a suitable value being $\tau_d = 0.01s$ to give an acceptable transient response overshoot
- integral action was then added and a time constant selected, coincidentally, to be the same as that for derivative action and therefore $\tau_i = 0.01s$

The PID tuning then produced an acceptable transient response. Further tuning could be pursued, particularly with regard to gain selection and the tracking error in response to a ramp demand speed. This is not pursued here and the new design performance is now shown.

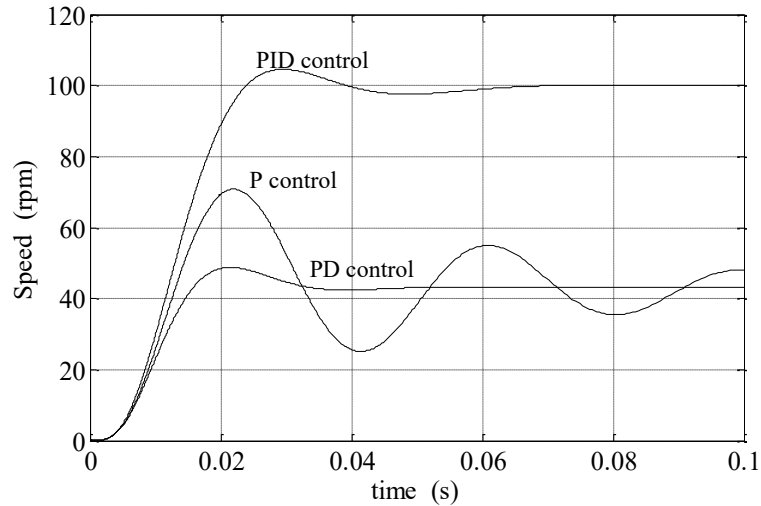
www.sylvania.com

We do not reinvent the wheel we reinvent light.

Fascinating lighting offers an infinite spectrum of possibilities: Innovative technologies and new markets provide both opportunities and challenges. An environment in which your expertise is in high demand. Enjoy the supportive working atmosphere within our global group and benefit from international career paths. Implement sustainable ideas in close cooperation with other specialists and contribute to influencing our future. Come and join us in reinventing light every day.

Light is OSRAM

OSRAM SYLVANIA



It can be seen that the addition of derivative control has adequately reduced the oscillation and the further addition of integral control has resulted in the desired steady-state speed.

7.10 Gain scheduling using a PSC

Many servodrives have different dynamic characteristics depending upon the direction of motion. Some examples are as follows:

- i) Linear actuators
 - double-rod with a load mass and vertically mounted
 - single-rod, horizontally or vertically mounted
- ii) Motors
 - with a uni-directional load torque
 - motor/winch unit, resisting load when lifting, runaway load when lowering
- iii) Pressure vessel control

It is possible to vary the gain in either direction using a Programmable Servo Controller (PSC), providing of course that the direction of motion can be deduced. The gain change required can be assessed from a linearised analysis or simply by practical trial and error. Considering the case of a **single-rod actuator** with a uni-directional load force, then it was shown in Chapter 3 that the open-loop flow gains are given by:

$$\text{Flow gain extending } k_{qi} = k_f \sqrt{\frac{\gamma P_s - P_\ell(o)}{(1 + \gamma^3)}} \quad (7.33)$$

$$\text{Flow gain retracting } k_{qi} = k_f \sqrt{\frac{P_s + P_\ell(o)}{(1 + \gamma^3)}} \quad (7.34)$$

Consequently the gain ratio, R, retracting/extending is given by:

$$R = \frac{\text{Flow gain retracting}}{\text{Flow gain extending}} = \sqrt{\frac{P_s + P_\ell(o)}{\gamma P_s - P_\ell(o)}} \quad (7.35)$$

where γ is the area ratio $A_1/A_2 > 1$ and the load-equivalent pressure $P_\ell(o) = F/A_2$. **For a double-rod actuator then let $\gamma = 1$.** The closed-loop response was then discussed in Chapter 3, neglecting actuator/load dynamics, where it was deduced that the response is first-order with a time constant given by:

$$\tau = \frac{A}{k_{qi} G_a H_p} \quad (7.36)$$

Therefore the closed-loop position transient response will be different in shape when extending and retracting due to the changing flow gain. If performance is not acceptable then a PSC can be used to match the flow gains in both directions, one could be increased or the other decreased or a combination of both.

7.11 Digital control algorithms using a PSC

The ease of using computers to control a servodrive, or the use of a more convenient Programmable Servo Controller dedicated to servodrive control, now means that a digital equivalent of an analogue controller is relatively easy to implement. In practice hydraulic noise and undesirable frequency effects, such as pump/motor speed harmonics, will probably require filtering. In addition the PSC will be accepting analogue input signals, performing digital control law generation and sending out analogue control signals.

The overall process of digital filtering and digital filter implementation is quite simple in practice. This may be illustrated when the process of time differentiation is represented by the backward step substitution method, the simplest of many possible substitutions and more 'advanced' methods. Consider the process of numerical differentiation as follows:

$$\begin{aligned} sf(s) &= \frac{df(t)}{dt} \approx \frac{\text{current sampled value} - \text{previously sampled value stored}}{\text{sampling interval}} \\ sf(s) &= \frac{f(t) - f(t-T)}{T} = \frac{f(t) - z^{-1}f(t)}{T} \end{aligned} \quad (7.37)$$

The substitution is equivalent to letting $s \rightarrow \frac{1 - z^{-1}}{T}$

T is the sampling interval selected and z^{-1} is the backward time shift operator representing one sampling interval. This transformation from the s domain to the z domain is known as the backward difference substitution. Consider then some basic transfer functions as follows:

i) Low-pass filter transfer function

This simply means that higher-frequency components are attenuated due to the characteristic of, for example, a 1st order approximation considered here.

$$\frac{V_{out}}{V_{in}} = \frac{1}{(1 + s\tau)} \rightarrow \frac{1}{(1 + \frac{\tau}{T}) - \frac{\tau}{T}z^{-1}} \quad \text{Let } A = \frac{1}{1 + \frac{\tau}{T}} \quad B = \frac{\frac{\tau}{T}}{(1 + \frac{\tau}{T})}$$

Control algorithm $V_{out} = A[V_{in}] + B[z^{-1}V_{out}]$ (7.38)

$$V_{out}(t) = AV_{in}(t) + BV_{out}(t - T)$$

Therefore the implementation of a low-pass filter requires the storage of one previously sampled output signal.



Discover the truth at www.deloitte.ca/careers

Deloitte.

© Deloitte & Touche LLP and affiliated entities.



Click on the ad to read more

ii) High-pass control law transfer function

For example it may be required to generate additional derivative of pressure feedback at lower frequencies, but frequency limited to avoid noise amplification at higher frequencies. In this case the transfer function used is as follows:

$$\frac{V_{\text{out}}}{V_{\text{in}}} = \frac{s\tau}{(1+s\tau)} \rightarrow \frac{\frac{\tau}{T}(1-z^{-1})}{(1+\frac{\tau}{T})-\frac{\tau}{T}z^{-1}}$$

$$\text{Control algorithm} \quad V_{\text{out}} = B[V_{\text{in}}] - B[z^{-1}V_{\text{in}}] + B[z^{-1}V_{\text{out}}] \quad (7.39)$$

$$V_{\text{out}}(t) = BV_{\text{in}}(t) - BV_{\text{in}}(t-T) + BV_{\text{out}}(t-T)$$

Therefore the implementation of a high-pass filter requires the storage of one previously sampled input signal and one previously sampled output signal.

iii) Proportional+Integral control law generation

$$\frac{V_{\text{out}}}{V_{\text{in}}} = 1 + \frac{1}{s\tau} \rightarrow \frac{(1+\frac{\tau}{T})-\frac{\tau}{T}z^{-1}}{\frac{\tau}{T}(1-z^{-1})} \quad \text{Let } C = \frac{1+\frac{\tau}{T}}{\frac{\tau}{T}}$$

$$\text{Control algorithm} \quad V_{\text{out}} = C[V_{\text{in}}] - [z^{-1}V_{\text{in}}] + [z^{-1}V_{\text{out}}] \quad (7.40)$$

$$V_{\text{out}}(t) = CV_{\text{in}}(t) - V_{\text{in}}(t-T) + V_{\text{out}}(t-T)$$

Therefore the implementation of a PI controller requires the storage of one previously sampled input signal and one previously sampled output signal.

These are just basic examples and have been used successfully by the author. The backward difference approach has often been found to be better than using more complicated substitutions, such as trapezoidal, which can cause closed-loop stability problems. Many more complicated, and ostensibly better, algorithms may be used as evident from control literature. Also, multi-input/output PSC's have a library of digital filter and transfer functions that may be readily included within the control loop.

7.12 Improving the dynamic performance of an open-loop motor servodrive using a PSC and pressure derivative feedback

The system is as shown in figure 7.7 and its steady-state performance improvement using a PSC was considered in Chapter 3. The servovalve flow characteristic was linearised and the supply pressure was adapted using an electrohydraulic pressure relief valve. This resulted in an improved steady-state speed characteristic and an improved steady-state efficiency.

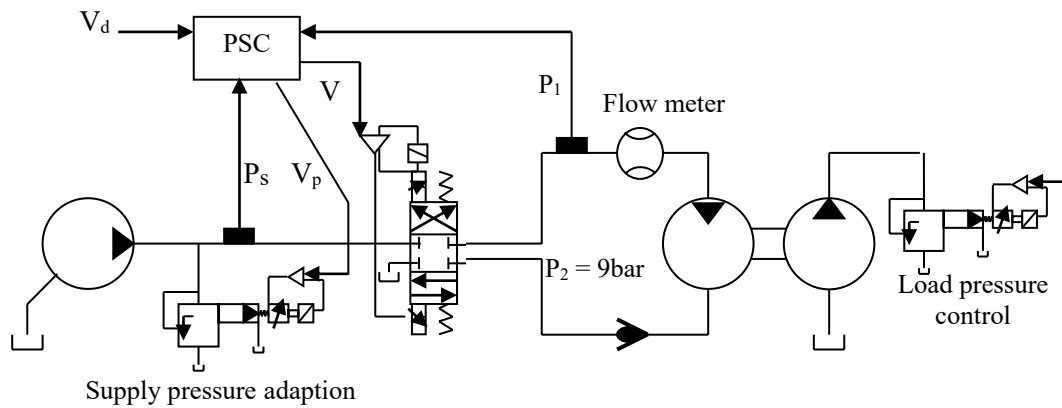


Figure 7.7 Linearisation of the servovalve flow characteristic, supply pressure adaption and dynamic improvement with dynamic pressure feedback using a PSC

Because the servovalve pressure square root characteristic has almost been removed then the servovalve adds little to no damping for the motor servodrive. It should be noted that **this is not a closed-loop control system** using speed measurement feedback, **it is an open-loop system** with performance compensation. The motor in this application is uni-directional and the commercially-available proportional control valve is designed such that only the driving port is pressure-active as described in Chapter 3.

The open-loop transfer function is dominated by fluid compressibility and motor/load inertia and therefore the servodrive has negligible damping. The system transfer function is therefore given by:

$$\frac{\omega(s)}{V_d(s)} \approx \frac{k_{qi} G_a / D_m}{(1 + \frac{s^2}{\omega_n^2})} \quad \omega_n^2 = \frac{2}{LC} \tag{7.41}$$

where D_m is the motor displacement, k_{qi} is the flow gain and G_a is the servoamplifier gain.

Without some form of system stabilisation the dynamic performance is unacceptable so the concept of **dynamic pressure feedback**, discussed earlier, is now be implemented by the PSC. Since only pressure P_1 is active in this motor control system a voltage is subtracted from V_d to provide system stabilisation, the voltage V_{pd} being:

$$V_{pd}(s) = H_{pd} \frac{s\tau P_1(s)}{(1 + s\tau)} \tag{7.42}$$

where H_{pd} is the pressure transducer gain and τ is a suitably selected time constant from a linearised analysis and, inevitably, practical testing. The open-loop transfer function now becomes:

$$\frac{\omega(s)}{V_d(s)} = \frac{k_{qi} G_a (1 + s\tau)/D_m}{[1 + s\tau + \frac{s^2}{\omega_n^2} (1 + \frac{2\tau}{\tau_{lin}}) + \frac{s^3\tau}{\omega_n^2}]} \quad \tau_{lin} = \frac{C}{k_{qi} G_a H_{pd}} \quad (7.43)$$

It then follows that:

- this 3rd order open-loop transfer function is inherently stable and independent of the choice of the time constant τ selected
- the value of the time constant τ selected does affect the speed transient behaviour, the very reason for introducing it

SIMPLY CLEVER

ŠKODA



We will turn your CV into
an opportunity of a lifetime



Do you like cars? Would you like to be a part of a successful brand?
We will appreciate and reward both your enthusiasm and talent.
Send us your CV. You will be surprised where it can take you.

Send us your CV on
www.employerforlife.com



Click on the ad to read more

There are other issues to be considered before digital implementation is introduced as follows:

- in reality the accumulation of servovalve dynamics and proportional relief valve dynamics, together with system noise, has a small but detectable effect on the system performance
- the effect of higher-order dynamics is to create a small phase shift with respect to the algebraic linearisation process and this is compounded if digital filtering is used to minimise signal noise
- signal noise arises from both fluid flow effects and the pressure ripple generated by the supply pump and the motor, and may be filtered to some extent by using the filter translator available on the PSC card
- the supply pump operates at a nominal speed of 1440 rpm and the load line pressure ripple is rich in harmonics at both the pumping frequency and the motor frequency. The time domain signal shows that the motor fundamental frequency dominates the pressure ripple and will of course vary as the motor speed is varied. The pressure ripple fundamental frequency does not present particular computation problems using the PSC card, providing higher-frequency component effects are minimised.

In practice minimising unwanted frequency components is achieved quite simply by using digital low-pass filters. The PSC card filter translator is provided to allow the user to input filter data in a high level floating point format which is then converted to low level integer form for use with the filter function block. The PSC card was set to operate with a sample time of $T = 4\text{ms}$, that is a sampling frequency of 250Hz.

Some results are shown as figure 7.8 at a constant minimum load where the motor speed was demanded to change from 500rpm to 800rpm. Comparisons are made with conventional control at a fixed supply pressure of $P_s = 90\text{bar}$ and “intelligent” control with variable supply pressure, optimum efficiency control and dynamic pressure feedback.

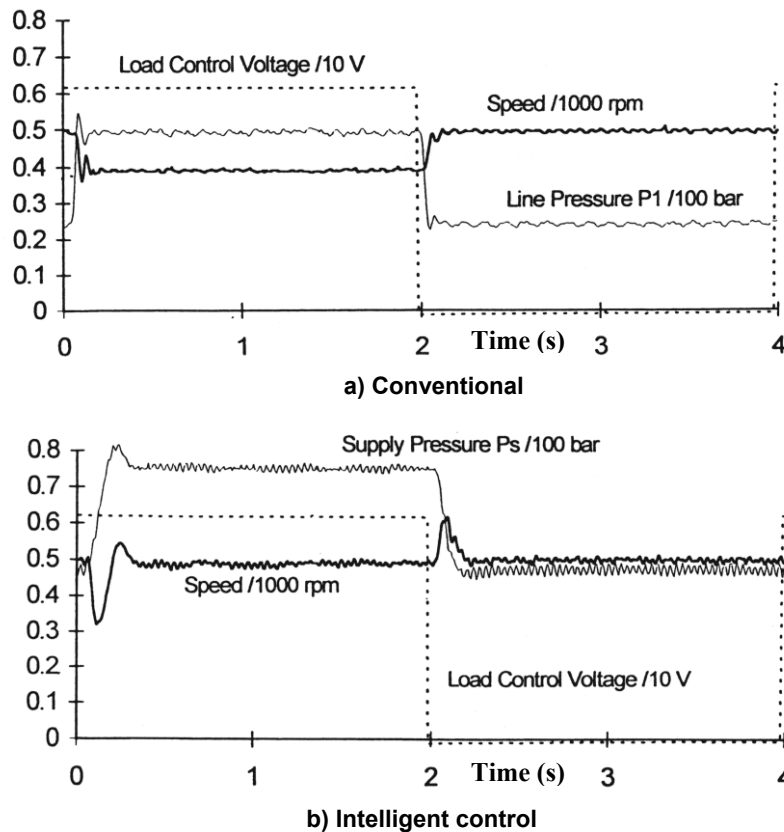


Figure 7.8 A comparison of conventional control and “intelligent” control of an openloop motor servodrive [Davies RM and Watton J. Intelligent Control of an Electrohydraulic Motor Drive System. *Journal of Mechatronics*, Vol 5, No 5, 1995, 527–540]

The major conclusions from this project are:

- the conventional dynamic behaviour is highly non-linear, the response being sluggish at high motor speeds and oscillatory at lower motor speeds as expected under conventional constant supply pressure conditions
- active control of supply pressure showed only marginal changes in steady-state values as the steady-state speed is changed
- under ‘intelligent’ control the non-linear transient speed effects are reduced, combined with a reduction in the required supply pressure when appropriate
- intelligent control has reduced the tendency of the active line pressure to cavitate, that is, fall to the fluid vapor pressure
- symmetry of dynamic behaviour at the different speeds is not exactly achieved due to the desire to also achieve optimum efficiency at a servovalve pressure drop of 15bar
- at the chosen servovalve pressure drop of 15bar the flow characteristic is not ideally linearised at higher speeds. This could be improved by moving to a higher pressure differential at the expense of a reduction in efficiency

8 Pressure and force control

8.1 Aim

To understand the behaviour of other types of electrohydraulic closed-loop systems via the following objectives:

- to consider the response, control and stability of a pressurised chamber
- to consider servodrive structural force control and stability
- to develop the concepts using worked examples

8.2 Pressure control of a fixed-volume container

Consider the case when a pressure vessel needs testing, sometimes by applying a repetitive pressure pulse. This is perhaps the simplest electrohydraulic control system and shown as figure 8.1.

I joined MITAS because
I wanted **real responsibility**

The Graduate Programme
for Engineers and Geoscientists
www.discovermitas.com



Real work
International opportunities
Three work placements



Month 16
I was a construction
supervisor in
the North Sea
advising and
helping foremen
solve problems



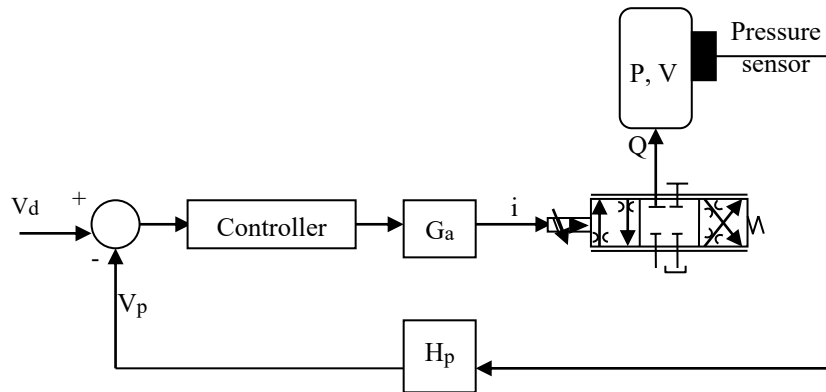


Figure 8.1 Pressure control of a vessel

A pressure sensor is needed to provide the closed-loop signal and usually its dynamics may be neglected. From what has previously been discussed it should be realised that the pressure vessel provides an integration process for the open-loop system and therefore the closed-loop system should not have a steady-state error. A 3-port servovalve is sufficient here, that is only one output port is required to charge and discharge the pressure vessel. Neglecting servovalve dynamics the system equations, for proportional control, are as follows:

$$\begin{aligned} \text{Servovalve flow rate} \quad Q &= k_f i \sqrt{P_s - P} \quad i > 0 \quad \text{charging} \\ Q &= k_f i \sqrt{P} \quad i < 0 \quad \text{discharging} \end{aligned} \tag{8.1}$$

$$\text{Pressure vessel flow rate} \quad Q = \frac{V}{\beta} \frac{dP}{dt} \tag{8.2}$$

$$\begin{aligned} \text{Proportional control} \quad i &= G_a (V_d - V_p) \\ i &= G_a H_p (P_d - P) \end{aligned} \tag{8.3}$$

H_p is the pressure sensor gain, G_a is the servoamplifier gain and P_d is pressure demand. For proportional control the servovalve current is always positive when the pressure is rising and always negative when the pressure is falling. These equations may be implicitly solved but the solutions will not be discussed here.

Note that the charging pressure may exceed the servovalve supply pressure in some cases and therefore when considering the exact simulation model this must be taken into account. This is done as follows:

$$Q = k_f i [\text{sign}(P_s - P)] \sqrt{|P_s - P|} \quad i > 0 \quad \text{charging} \tag{8.4}$$

Also in the simulation model it is important to ensure that the pressure cannot fall below zero. In reality this is a complex phenomenon when cavitation occurs but often in simulation practice a simple lower limit on pressure is introduced at the pressure integration block.

Some transient responses, when charging and discharging, are shown as figure 8.2 for different demanded pressures and using Matlab Simulink simulation software. The demanded pressure is P_d and this 1st order closed-loop system clearly demonstrates exponential-type responses when both charging and discharging.

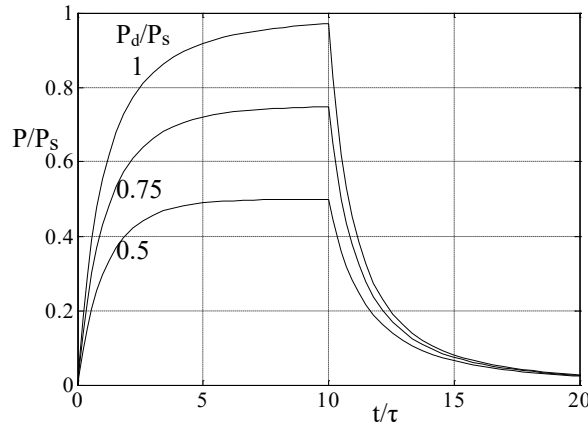


Figure 8.2 Step responses between zero pressure and various demanded pressures

The results are completely general and have been plotted in non-dimensional time with respect to the time constant τ which is given by:

$$\tau = \frac{C}{k_f G_a H_p \sqrt{P_s}} \quad C = \frac{V}{\beta} \tag{8.5}$$

The linearised open-loop transfer function will now be developed.

Charging

$$k_{qi} i = k_{qp} P + C \frac{dP}{dt} \quad i > 0 \tag{8.6}$$

$$k_{qi} = k_f \sqrt{P_s - P(o)} \quad k_{qp} = \frac{k_f i(o)}{2\sqrt{P_s - P(o)}}$$

Discharging

$$-k_{qi} i = k_{qp} P + C \frac{dP}{dt} \quad i < 0 \tag{8.7}$$

$$k_{qi} = k_f \sqrt{P(o)} \quad k_{qp} = \frac{k_f i(o)}{2\sqrt{P(o)}}$$

For both charging and discharging, $P(o)$ is the final pressure for each case, and of course not the same.

i) Proportional control, no servovalve dynamics

Since the closed-loop system has no steady-state pressure error then $i(0) = 0$ and the linearised pressure coefficient $k_{qp} = 0$ for both charging and discharging. For proportional control the linearised transfer function concept then results in the system block diagram shown in figure 8.3, and applicable for both charging and discharging.

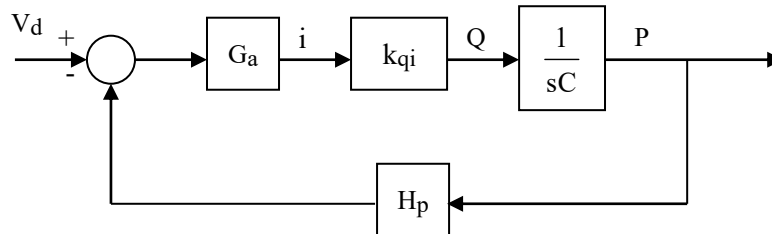


Figure 8.3 Linearised block diagram for a pressure proportional control system

The open-loop transfer function is:

$$G(s)H(s) = \frac{G_a H_p k_{qi}}{sC} \tag{8.8}$$

ie business school

#1 EUROPEAN BUSINESS SCHOOL
FINANCIAL TIMES 2013

#gobeyond

MASTER IN MANAGEMENT

Because achieving your dreams is your greatest challenge. IE Business School's Master in Management taught in English, Spanish or bilingually, trains young high performance professionals at the beginning of their career through an innovative and stimulating program that will help them reach their full potential.

- Choose your area of specialization.
- Customize your master through the different options offered.
- Global Immersion Weeks in locations such as London, Silicon Valley or Shanghai.

Because you change, we change with you.

www.ie.edu/master-management | mim.admissions@ie.edu | Facebook | Twitter | LinkedIn | YouTube | Instagram



The closed-loop transfer function is:

$$\frac{P(s)}{P_d(s)} = \frac{1}{1 + s\tau_{lin}}$$

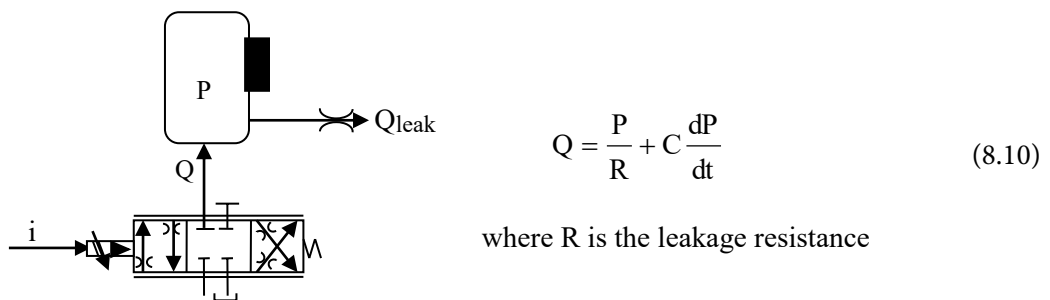
$$\text{charging } \tau_{lin} = \frac{\tau}{\sqrt{1 - P(o)/P_s}} \quad \text{discharging } \tau_{lin} = \frac{\tau}{\sqrt{P(o)/P_s}} \quad (8.9)$$

When charging from zero to supply pressure then $P(o) = P_s$ and when discharging to zero pressure then $P(o) = 0$ and some extremely important conclusions arise from the linearised theory for these particular conditions.

- the linearised pressure coefficient $k_{qp} = 0$ resulting in no servovalve resistive damping effect calculated at the steady-state condition. The linearised flow coefficient $k_{qi} = 0$ calculated at the steady-state condition
- **A transfer function cannot be derived under these conditions** even though control is clearly possible
- a linearised analysis may not give a sufficiently-accurate representation of the open-loop system under some operating conditions
- care must be taken when considering a transfer function approach for a pressure control system suggesting that computer simulation is the better approach to ensure meaningful modelling predictions

ii) **Proportional+Integral control, no servovalve dynamics**

A bleed valve, connected back to tank, may be used to ensure trapped air is released prior to testing, or deliberately introduced to provide additional damping. Also, there may be an undesirable external leakage. For these cases PI control may be used to ensure correct steady-state performance. Assuming a linear leakage characteristic for low leakage flow rates then the flow continuity equation at the load now becomes:



The linearised transfer function relating pressure to servovalve flow rate now becomes:

$$\frac{P(s)}{Q(s)} = \frac{R}{(1 + sCR)} \quad (8.11)$$

The integrator due to fluid compressibility does now no longer exist, hence the need for PI control. The linearised transfer function concept results in the system block diagram shown in figure 8.4.

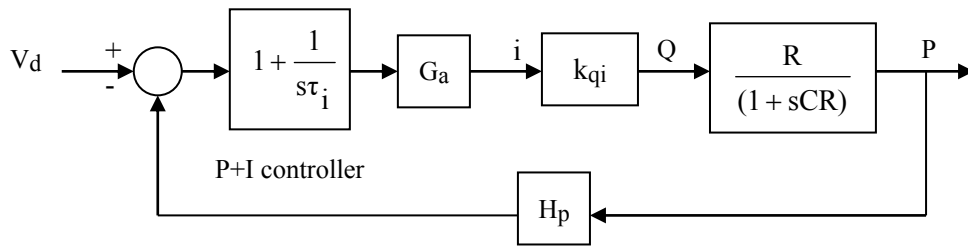


Figure 8.4 Block diagram for a vessel pressure control system with flow leakage and PI control

The linearised transfer functions now become:

$$\begin{aligned}
 \text{OLTF} \quad G(s)H(s) &= \frac{(1 + s\tau_i)\tau_{\text{leak}}}{s\tau_i\tau_{\text{lin}}(1 + s\tau_{\text{leak}})} \\
 \tau_{\text{lin}} &= \frac{C}{G_a H_p k_{qi}} \quad \tau_{\text{leak}} = CR \\
 \text{CLTF} \quad \frac{P(s)}{P_d(s)} &= \frac{(1 + s\tau_i)}{[1 + s\tau_i(1 + \frac{\tau_{\text{lin}}}{\tau_{\text{leak}}}) + s^2\tau_i\tau_{\text{lin}}]}
 \end{aligned} \tag{8.12}$$

The stable closed-loop 2nd order transfer function (8.12) has a dynamic term in its numerator so the transfer function cannot really be used in a traditional 2nd order sense for design. As a preliminary design it is better to use over-damping, for example starting with $\zeta=2$, so considering the denominator of the CLTF then gives:

$$\begin{aligned}
 \text{undamped natural frequency } \omega_n &= \frac{1}{\sqrt{\tau_i\tau_{\text{lin}}}} \\
 \text{damping ratio } \zeta &= \frac{1}{2} \sqrt{\frac{\tau_i}{\tau_{\text{lin}}}} [1 + \frac{\tau_{\text{lin}}}{\tau_{\text{leak}}}] \approx 2
 \end{aligned} \tag{8.13}$$

Given that τ_{leak} and τ_{lin} are known in advance then the integrator time constant τ_i may be calculated from equation (8.13). Again remember from earlier work that the flow coefficient k_{qi} given in (8.12) for calculating τ_{lin} is different when charging and discharging.

The overshoot when charging and undershoot when discharging may be different for different combinations of demanded pressures. An improved response may be obtained by adapting the open-loop gain for either the charging or the discharging part of the duty cycle, and which may easily be done using a Programmable Servo Controller (PSC).

iii) Proportional control with no leakage but including servovalve dynamics

The open-loop transfer function becomes as follows:

$$G(s)H(s) = \frac{K}{s[1 + \frac{2\zeta}{\omega_n}s + \frac{s^2}{\omega_n^2}]} \quad K = \frac{G_a H_p k_{qi}}{C} \quad (8.14)$$

The closed-loop transfer function is as follows:

$$\frac{P(s)}{P_d(s)} = \frac{K}{[K + s + \frac{2\zeta}{\omega_n}s^2 + \frac{s^3}{\omega_n^2}]} \quad (8.15)$$

$$\text{The closed-loop system is therefore stable providing that } K < 2\zeta\omega_n \quad (8.16)$$



no.1
nine years
in a row

Syeden
Stockholm

STUDY AT A TOP RANKED INTERNATIONAL BUSINESS SCHOOL

Reach your full potential at the Stockholm School of Economics, in one of the most innovative cities in the world. The School is ranked by the Financial Times as the number one business school in the Nordic and Baltic countries.

Visit us at www.hhs.se





Example 8.1

A pressure control system for life-cycle testing of radiators has a design requirement to achieve 95% of the steady-state charging pressure in at least 0.05sec and for a charging pressure of 180bar. The discharging pressure is 10bar.

- i) Determine an approximate servoamplifier gain G_a by first considering the linearised transfer function approximation
- ii) Then consider the exact transient response to determine a more appropriate servoamplifier gain and determine an obtainable duty cycle frequency
- iii) Investigate gain scheduling

System data are as follows:

A typical industrial mineral oil, fluid bulk modulus $\beta = 1.4 \times 10^9 \text{ N/m}^2$

The total pressurised volume $V = 2$ litres

The servovalve spool is critically-lapped, $Q = 1.05 \times 10^{-8} \sqrt{\Delta P}$ m³/s i mA, pressure N/m²

Supply pressure $P_s = 240$ bar

Servovalve damping ratio $\zeta = 1$, undamped natural frequency $f_n = 110$ Hz.

Servoamplifier rating ± 20 mA

Each pressure sensor has the range 250bar = 10V, so $H_p = 40 \times 10^{-8}$ V/Nm⁻²

The calculations proceed as follows:

$$C = \frac{V}{\beta} = \frac{2 \times 10^{-3}}{1.4 \times 10^9} = 1.43 \times 10^{-12}$$

The charging pressure is $P(o) = 180$ bar and the discharging pressure is $P(o) = 10$ bar therefore the linearised flow gains are given by:

$$k_{qi} = k_f \sqrt{P_s - P(o)} = 1.05 \times 10^{-8} \sqrt{60 \times 10^5} = 2.57 \times 10^{-5} \quad \text{charging}$$

$$k_{qi} = k_f \sqrt{P(o)} = 1.05 \times 10^{-8} \sqrt{10 \times 10^5} = 1.05 \times 10^{-5} \quad \text{discharging}$$

i) Proportional controller design with no servovalve dynamics

The linearised closed-loop transfer function is:

$$\frac{P(s)}{P_d(s)} = \frac{1}{1 + s\tau_{lin}}$$

$$\text{charging } \tau_{lin} = \frac{\tau}{\sqrt{1 - P(o)/P_s}} \quad \text{discharging } \tau_{lin} = \frac{\tau}{\sqrt{P(o)/P_s}}$$

$$\tau = \frac{C}{k_f G_a H_p \sqrt{P_s}} = \frac{1.43 \times 10^{-12}}{(1.05 \times 10^{-8})(G_a)(40 \times 10^{-8})\sqrt{240 \times 10^5}} = \frac{0.069}{G_a}$$

charging $\tau_{lin} = \frac{0.069}{G_a (0.5)} = \frac{0.138}{G_a}$

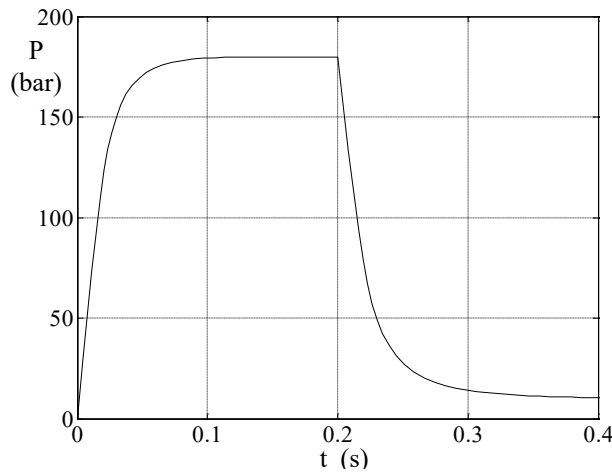
In response to step demand change in pressure, the design requirement is to achieve at least 95% of the steady-state charging pressure in 0.05 seconds. Using the linearised transfer function transient charging response to a step demand in pressure, and for a fixed servoamplifier gain, then gives:

$$\frac{P(s)}{P_d(s)} = \frac{1}{1 + s\tau_{lin}} \rightarrow P = P_d (1 - e^{-t/\tau_{lin}})$$

$$0.95(180) = 180(1 - e^{-t/\tau_{lin}}) \rightarrow \frac{t}{\tau_{lin}} = 2.94$$

$$\tau_{lin} = \frac{0.05}{2.94} = 0.017 \text{sec} = \frac{0.138}{G_a} \quad G_a \approx 8.1 \text{mA/V}$$

The exact non-linear simulation is then considered with an initial servoamplifier gain of $G_a = 8.1 \text{mA/V}$. This was then adjusted to give the charging response design requirement, resulting in a slightly reduced value of $G_a = 7.2 \text{mA/V}$ as now shown.



The design allowed a duty cycle frequency of typically 2.5Hz to be generated. The servoamplifier gain has been selected to meet the minimum design criterion and the response can be made faster by increasing the servoamplifier gain. A number of points arise:

- the response does not reveal that at the start of charging and at the start of discharging the servoamplifier saturates at $\pm 20\text{mA}$ for a short period
- increasing the servoamplifier gain will make both the charging and discharging responses faster and increase the duty cycle frequency possible. However, servovalve dynamics have been neglected at this stage
- a linearised transfer function approach can give a useful design guide but an accurate computer simulation is required to determine the correct transient behaviour

ii) Response improvement, servovalve dynamics included.

The performance is first evaluated using the exact simulation. The response is made faster by simply increasing the servoamplifier gain. In fact increasing the gain from $G_a = 7.2\text{mA/V}$ to $G_a = 22\text{mA/V}$ gave the result shown next.



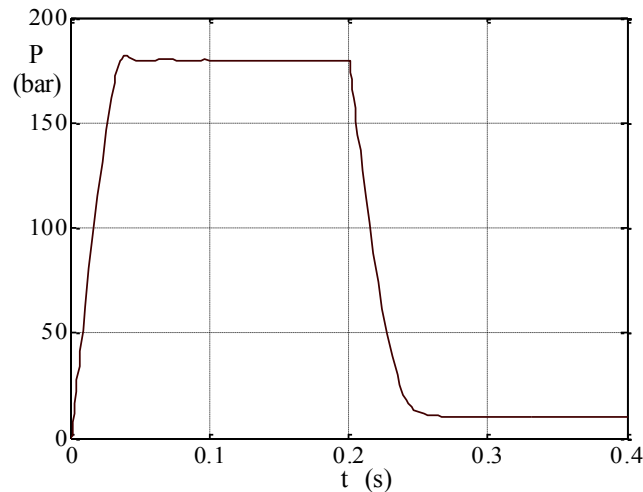
#1
in eco-friendly
attitude

**STUDY AT
LINKÖPING UNIVERSITY, SWEDEN**
RANKED AMONG TOP 50 UNIVERSITIES UNDER 50

Interested in Strategy and Management in International Organisations? Kick-start your career with a master's degree from Linköping University, Sweden.

→ **Click here!**

 **Linköping University**



Considering the conditions for instability, for proportional control with servovalve dynamics included, it was shown earlier using a linearised analysis that the system is just at the point of instability when:

$$K = \frac{G_a H_p k_{qi}}{C} = 2\zeta\omega_n \rightarrow G_a = \frac{2\zeta\omega_n C}{H_p k_{qi}}$$

$$\text{when charging} \quad G_a = \frac{2(1)(691)(1.43 \times 10^{-12})}{(40 \times 10^{-8})(2.57 \times 10^{-5})} = 192 \text{mA/V}$$

$$\text{when discharging} \quad G_a = \frac{2(1)(691)(1.43 \times 10^{-12})}{(40 \times 10^{-8})(1.05 \times 10^{-5})} = 471 \text{mA/V}$$

These are extremely high servoamplifier gains and will cause the servoamplifier to dynamically saturate and then a linearised analysis is not valid. The exact non-linear simulation, including servovalve dynamics, with servoamplifier current saturation shows that the closed-loop system is unstable at the following conditions:

$$\text{charging} \quad G_a \approx 160 \text{mA/V}$$

$$\text{discharging} \quad G_a \approx 250 \text{mA/V}$$

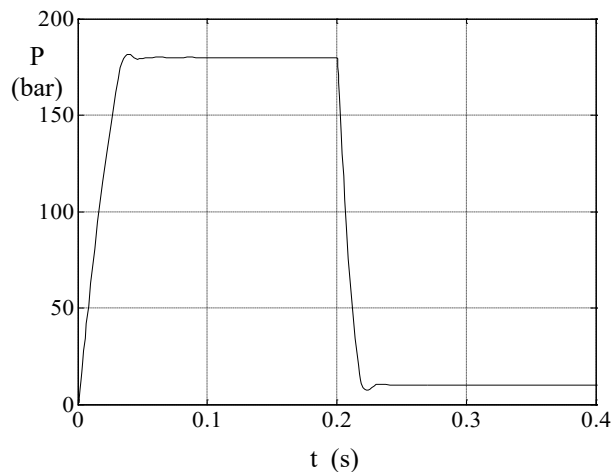
The linearised analysis therefore over-predicts the gain condition for instability when charging and significantly over-predicts the gain condition for instability when discharging.

iii) Gain scheduling

The charging response is acceptable but the discharging response is more sluggish and could be improved by increasing the gain when discharging. Now consider gain scheduling and increasing the discharging gain by the ratio of the flow gains:

$$\text{Flow gain ratio} \frac{\text{charging}}{\text{discharging}} = \sqrt{\frac{P_s - P(o)_{\text{charging}}}{P(o)_{\text{discharging}}}} = \sqrt{\frac{240 - 180}{10}} = 2.4$$

Therefore multiply the gain when discharging by a factor of 2.4, the result being as shown.



The response is now very similar for both charging and discharging, and the duty cycle frequency may be increased to at least 10Hz, which actually may be too high in practice.

8.3 Force control of a servoactuator

Now consider force control *for materials/structural testing*. A compressive load fatigue test on a structure is shown conceptually as figure 8.5. The demand signal will cause the actuator to drive the structure to its desired deflection and ostensibly match the required mean force.

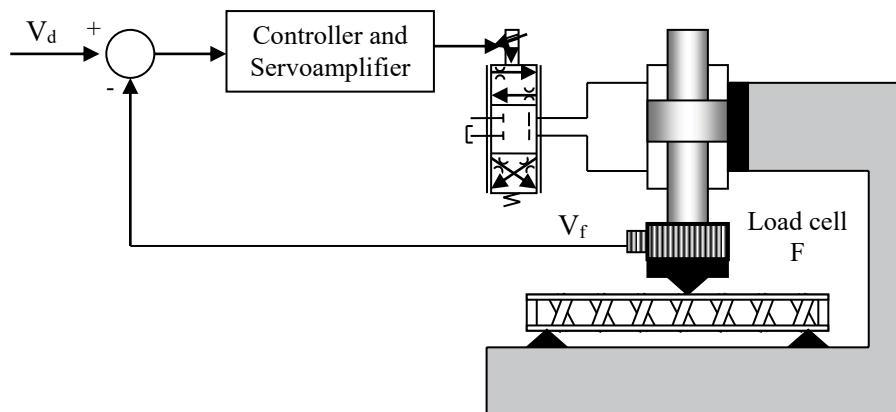


Figure 8.5 Structural testing schematic

In practice a materials testing machine servoactuator will have a load cell attached to the actuator rod and it makes better dynamic sense to use this rather than pressure differential. In the author's experience it has been more difficult to improve the closed-loop response with pressure differential control compared with force control to such an extent that even a variety of compensation techniques have proved fruitless. For a force control system the linearised equations for a servovalve/cylinder are as previously used and as follows:

$$P_{\ell} A = F + B_v U + M \frac{dU}{dt} \quad P_{\ell} = P_1 - P_2 \quad (8.17)$$

$$k_{qi} \dot{i} = AU + \frac{P_{\ell}}{R} + \frac{V}{2\beta} \frac{dP_{\ell}}{dt} \quad \frac{1}{R} = \frac{1}{R_{act}} + \frac{1}{R_{sv}} \quad (8.18)$$

$$\text{structure load force } F = k_m y \quad (8.19)$$

The material stiffness is k_m N/m and y is the structure deflection from its unloaded position. Servoactuator leakage has been included since this plays an important role in how the closed-loop system behaves.



"I studied English for 16 years but...
...I finally learned to speak it in just six lessons"
Jane, Chinese architect

ENGLISH OUT THERE

Click to hear me talking before and after my unique course download

Proportional control.

Consider the block diagram is as shown in figure 8.6.

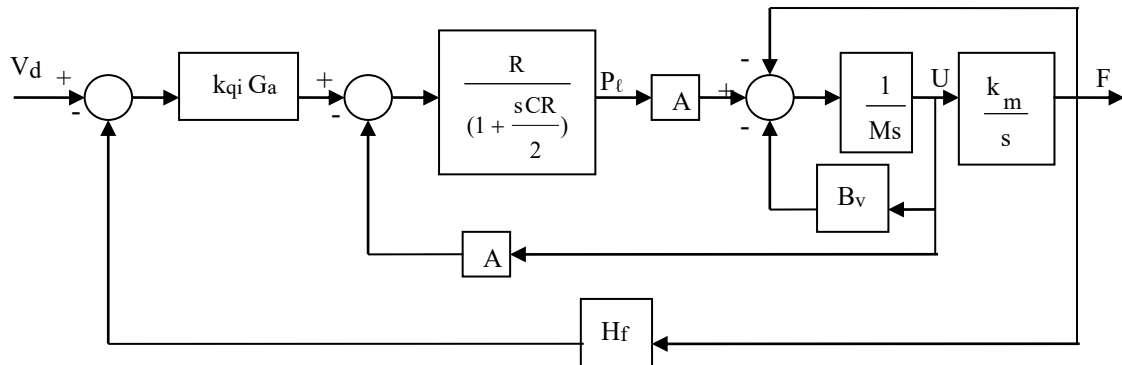


Figure 8.6 Force control for materials testing, P control

When a moving component with mass has a spring-type characteristic it is usual to add 1/3 of the mass of the component to the actuator/load cell mass.

The closed-loop linearised force and velocity transfer functions are as follows:

$$\frac{F(s)}{F_d(s)} = \frac{K}{1 + K + sC_m R(1 + \frac{R_v}{R} + \frac{C}{2C_m}) + s^2 C_m R(\frac{L}{R} + \frac{CR_v}{2}) + s^3 \frac{LCC_m R}{2}} \quad (8.20)$$

$$\frac{U(s)}{F_d(s)} = \frac{s \frac{K}{k_m}}{1 + K + sC_m R(1 + \frac{R_v}{R} + \frac{C}{2C_m}) + s^2 C_m R(\frac{L}{R} + \frac{CR_v}{2}) + s^3 \frac{LCC_m R}{2}} \quad (8.21)$$

$$K = H_f G_a k_{qi} R A \quad R_v = \frac{B_v}{A^2} \quad L = \frac{M}{A^2} \quad C = \frac{V}{\beta} \quad \frac{1}{R} = \frac{1}{R_{act}} + \frac{1}{R_{sv}} \quad (8.22)$$

The mechanical capacitance is defined as $C_m = \frac{A^2}{k_m}$ (8.23)

The closed-loop transfer functions are 3rd order and for the closed-loop system to be stable, given that R_v/R may usually be neglected, then:

$$K < \frac{2C_m}{C} + \frac{RCR_v}{2L} (\frac{2C_m}{C} + 1) \quad (8.24)$$

Applying the Final Value Theorem to each transfer function then gives the following steady-state condition:

$$\frac{F}{F_d} = \frac{K}{1+K} = \frac{H_f G_a k_{qi} RA}{1+H_f G_a k_{qi} RA} \quad U = 0 \quad (8.25)$$

The following observations are made:

- this 3rd order system can become unstable and a suitable gain K must be selected, and different to that given by (8.24) if servovalve dynamics are included
- the steady-state force will not achieve the demanded value unless $K \gg 1$ or flow losses are negligible such that $R = \infty$. However, this is only an input calibration issue in practice since the input signal may be adjusted to give the required steady-state load force
- the steady-state velocity will be zero as required irrespective of the value of leakage resistance R

PID control.

This is considered to ostensibly improve performance but results in a higher-order characteristic equation. This means that explicit PID gain selection requires care and controller tuning information will be supplied by the experienced testing machine manufacturer. Consider therefore the system with **PI control only** as shown in figure 8.7.

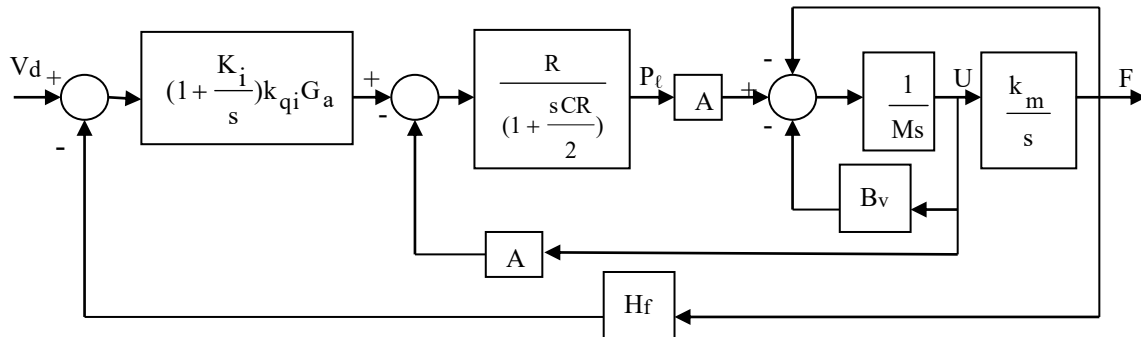


Figure 8.7 Force control for materials testing, PI control

The appropriate transfer functions now become:

$$\frac{F(s)}{F_d(s)} = \frac{K(s + K_i)}{G(s)} \quad \frac{U(s)}{F_d(s)} = \frac{s \frac{K}{k_m} (s + K_i)}{G(s)} \quad (8.26)$$

$$G(s) = KK_i + s(1 + K) + s^2 C_m R \left(1 + \frac{R_v}{R} + \frac{C}{2C_m}\right) + s^3 C_m R \left(\frac{L}{R} + \frac{CR_v}{2}\right) + s^4 \frac{LCC_m R}{2} \quad (8.27)$$

Considering the Final Value Theorem now gives the following steady-state conditions:

$$F = F_d \quad U = 0 \quad (8.28)$$

The following observations are made:

- the closed-loop characteristic equation is now 4th order and the conditions to avoid closed-loop instability are not in a meaningful explicit design form. However, a suitable gain must be selected to avoid closed-loop instability
- the closed-loop response to a step input force demand will now result in no steady-state error in force and velocity and irrespective of any system leakage resistance R

Excellent Economics and Business programmes at:



university of
 groningen



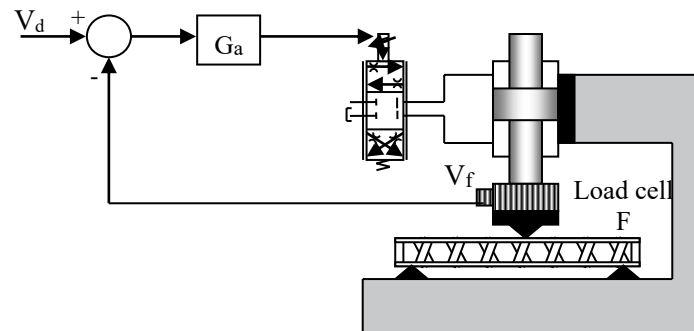

“The perfect start
 of a successful,
 international career.”

CLICK HERE
 to discover why both socially
 and academically the University
 of Groningen is one of the best
 places for a student to be

www.rug.nl/feb/education

Example 8.2

Consider a test system under force control with the test specimen to be deflected by 1mm prior to cyclic fatigue testing. Determine the possible significance of servovalve dynamics on the step response. Data are as follows:



Servoactuator bore 80mm diameter, double-rod 56mm diameter, full stroke 200mm.

The actuator piston is operating about its mid position

Servoactuator leakage resistance $R_{act} = 5 \times 10^{12} \text{ Nm}^{-2}/\text{m}^3\text{s}^{-1}$

Servovalve supply pressure $P_s = 140\text{bar}$

Servovalve flow equation is $Q = 1.05 \times 10^{-8} i \sqrt{\frac{P_s - P_\ell}{2}}$ i mA, pressure N/m^2

Servovalve dynamics damping ratio $\zeta = 1.0$, undamped natural frequency $\omega_n = 110\text{Hz}$

Structure stiffness $k_m = 2 \times 10^7 \text{ N}/\text{m}$ Fluid bulk modulus $\beta = 1.4 \times 10^9 \text{ N}/\text{m}^2$

Viscous damping $B_v = 10^4 \text{ N}/\text{ms}^{-1}$ Moving mass $M = 85\text{kg}$ Load cell gain $H_f = 10^{-4} \text{ V}/\text{N}$

The calculations proceed as follows:

$$\text{Mean load force} \quad F_d = k_m y_{\text{mean}} = (2 \times 10^7)(0.001) = 2 \times 10^4 \text{ N}$$

$$\text{Actuator net cross-sectional-area} \quad A = \frac{\pi}{4} [80^2 - 56^2] \times 10^{-6} = 2.56 \times 10^{-3} \text{ m}^2$$

$$\text{Load pressure differential} \quad P_\ell(o) = (2 \times 10^4)/(2.56 \times 10^{-3}) = 0.78 \times 10^7 \text{ N}/\text{m}^2 = 78\text{bar}$$

To overcome losses and dynamic operation it is usual practice to select a supply pressure using:

$$P_s = 1.5 \times P_\ell(o) = 117\text{bar}$$

So, a supply pressure of 140bar should be adequate to provide the additional force required for fatigue testing, as discussed in the next example.

Now consider the terms needed to evaluate the linearised transfer function *neglecting servovalve dynamics*.

$$\text{OLTF } G(s)H(s) = \frac{K}{1 + sC_m R \left(1 + \frac{R_v}{R} + \frac{C}{2C_m}\right) + s^2 C_m R \left(\frac{L}{R} + \frac{CR_v}{2}\right) + s^3 \frac{LCC_m R}{2}}$$

$$k_{qi} = 1.05 \times 10^{-8} \sqrt{\frac{P_s - P_{\ell(o)}}{2}} = 1.05 \times 10^{-8} \sqrt{\frac{(140 - 78)10^5}{2}} = 1.85 \times 10^{-5} \text{ m}^3 \text{ s}^{-1} / \text{mA}$$

$$L = \frac{M}{A^2} = \frac{85}{2.56^2 \times 10^{-6}} = 13 \times 10^6 \text{ kg/m}^4$$

$$C = \frac{V}{\beta} = \frac{(2.56 \times 10^{-3})(0.1)}{1.4 \times 10^9} = 0.183 \times 10^{-12} \text{ m}^5 / \text{N}$$

$$C_m = \frac{A^2}{k} = \frac{2.56^2 \times 10^{-6}}{2 \times 10^7} = 3.28 \times 10^{-13} \text{ m}^5 / \text{N}$$

$$R_v = \frac{B_v}{A^2} = \frac{10^4}{2.56^2 \times 10^{-6}} = 0.153 \times 10^{10} \text{ Nm}^{-2} / \text{m}^3 \text{ s}^{-1}$$

$$R = R_{act} = 5 \times 10^{12} \text{ Nm}^{-2} / \text{m}^3 \text{ s}^{-1}$$

$$K = H_f G_a k_{qi} R A = (10^{-4})(G_a)(1.85 \times 10^{-5})(5 \times 10^{12})(2.56 \times 10^{-3}) = 23.7 G_a$$

$$\frac{C}{2C_m} = \frac{0.183 \times 10^{-12}}{2(3.28 \times 10^{-13})} = 0.28 \quad \frac{R_v}{R} = \frac{0.153 \times 10^{10}}{5 \times 10^{12}} = 0.00031 \text{ and negligible}$$

The OLTF may now be evaluated:


$$G(s)H(s) = \frac{23.7 G_a}{1 + 2.1s + 2.35 \times 10^{-4} s^2 + 1.95 \times 10^{-6} s^3}$$

It is particularly useful to now use Matlab Control System Toolbox to investigate this OLTF. First consider the roots of the denominator and determined as follows:

```
a = [1.95e-6 2.35e-4 2.1 1];
roots(a);
-60 + j1036
-60 - j1036
-0.5
```

Clearly the denominator of the OLTF is characterised by a 1st order component and a very lightly damped 2nd order high frequency component. Now using the frequency response plotting facility assuming unity gain in the numerator:

```
a = tf([0 0 0 1],[1.95e-6 2.35e-4 2.1 1]);
bodeplot(a);
```



In the past four years we have drilled

89,000 km

That's more than **twice** around the world.

Who are we?
We are the world's largest oilfield services company¹. Working globally—often in remote and challenging locations—we invent, design, engineer, and apply technology to help our customers find and produce oil and gas safely.

Who are we looking for?
Every year, we need thousands of graduates to begin dynamic careers in the following domains:

- Engineering, Research and Operations
- Geoscience and Petrotechnical
- Commercial and Business

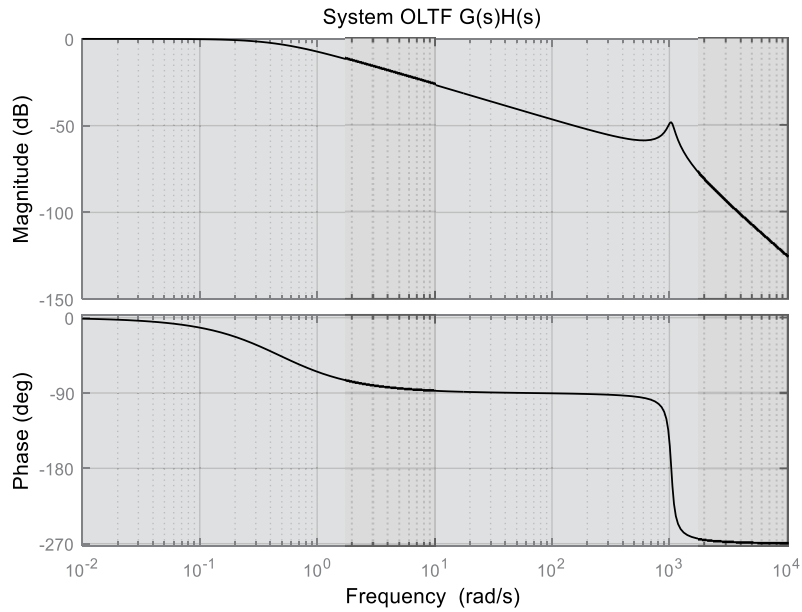
What will you be?

careers.slb.com

Schlumberger

¹Based on Fortune 500 ranking 2011. Copyright © 2015 Schlumberger. All rights reserved.





The components of the OLTF may clearly be seen, and by zooming into a narrower frequency range the -180° phase angle occurs when $\omega = 1038\text{rad/s}$ and with a gain of -48dB . Hence the onset of closed-loop instability occurs when the magnitude is lifted by $+48\text{dB}$. This gives:

$$+48 = 20\log(23.7G_a) \rightarrow G_a = 10.6\text{mA/V}$$

Using the traditional approach the closed-loop characteristic equation is given by:

$$1 + 23.7 G_a + 2.1s + 2.35 \times 10^{-4} s^2 + 1.95 \times 10^{-6} s^3 = 0$$

$$b_0 + b_1 s + b_2 s^2 + b_3 s^3 = 0$$

The onset of closed-loop instability occurs when $b_1 b_2 = b_0 b_3$

$$(2.1)(2.35 \times 10^{-4}) = (1 + 23.7 G_a)(1.95 \times 10^{-6})$$

$$G_a = 10.6 \text{ mA/V}$$

The frequency of oscillation $\omega = \sqrt{b_1 / b_3} = \sqrt{2.1 / 1.95 \times 10^{-6}} = 1038\text{rad/s}$ (165Hz)

Alternatively in the frequency domain the characteristic equation is:

$$(1 + 23.7 G_a - 2.35 \times 10^{-4} \omega^2) + j(2.1 \omega - 1.95 \times 10^{-6} \omega^3) = 0$$

The onset of instability occurs, by equating the Imaginary term to zero, which gives $\omega = 1038\text{rad/s}$ (165Hz) and from the Real term, when equated to zero, then $G_a = 10.6 \text{ mA/V}$.

The important conclusion at this stage is that the servovalve undamped natural frequency is 110Hz so it is clear that ***the linearised OLTF must also include servovalve dynamics.***

The new OLTF is now 5th order and is given by:

$$G(s)H(s) = \frac{23.7 G_a}{(1 + 2.9 \times 10^{-3} s + 2.1 \times 10^{-6} s^2)(1 + 2.1 s + 2.35 \times 10^{-4} s^2 + 1.95 \times 10^{-6} s^3)}$$

$$G(s)H(s) = \frac{23.7 G_a}{(1 + 2.1 s + 6.33 \times 10^{-3} s^2 + 7.04 \times 10^{-6} s^3 + 6.15 \times 10^{-9} s^4 + 4.1 \times 10^{-12} s^5)}$$

`ce = [4.1e-12 6.15e-9 7.04e-6 6.33e-3 2.1 1];`

`roots(ce);`

`-59.6 ± j1036, -0.5, -728, -653`

The first three roots for the system only are clearly identified again and the other two real roots relate to the addition of the servovalve critically-damped dynamics.

`gh = tf([0 0 0 0 1],[4.1e-12 6.15e-9 7.04e-6 6.33e-3 2.1 1]);`

`bodeplot(gh);`

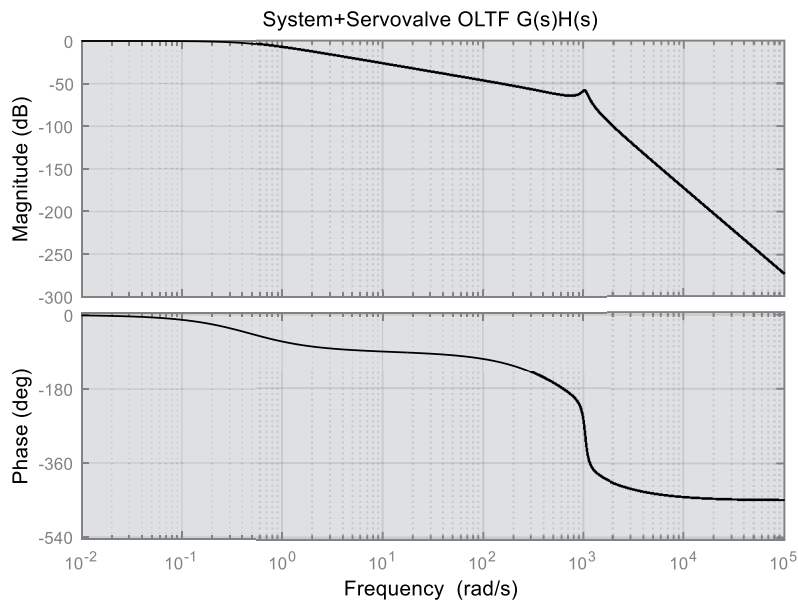
or

`g1=tf([0 0 1],[2.1e-6 2.9e-3 1]);`

`g2=([0 0 0 1],[1.95e-6 2.35e-4 2.1 1]);`

`gh=g1*g2;`

`bodeplot(gh);`



The condition for the onset of closed-loop instability, when the phase angle is -180° , gives:

$$\omega = 620 \text{ rad/s (98.6 Hz)} \quad G_a = 64 \text{ mA/V}$$

American online

LIGS University

is currently enrolling in the
Interactive Online **BBA, MBA, MSc,**
DBA and PhD programs:

- ▶ enroll **by September 30th, 2014** and
- ▶ **save up to 16%** on the tuition!
- ▶ pay in 10 installments / 2 years
- ▶ Interactive **Online** education
- ▶ visit www.ligsuniversity.com to find out more!

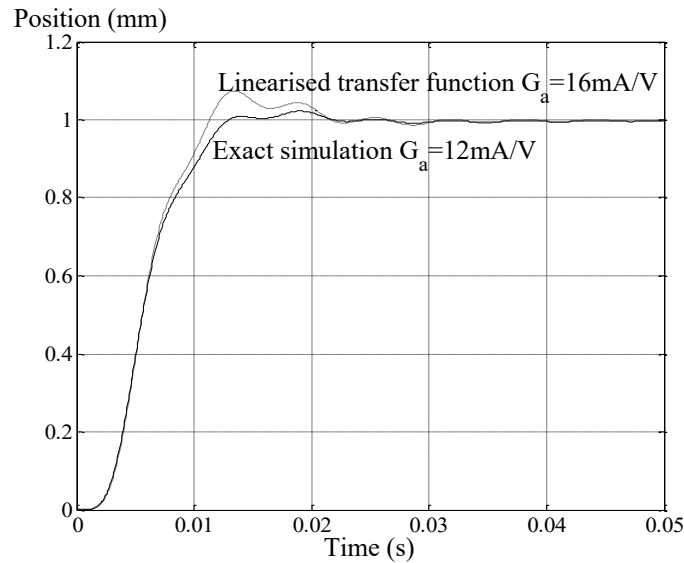
Note: LIGS University is not accredited by any nationally recognized accrediting agency listed by the US Secretary of Education. More info [here](#).



The exact simulation was then investigated and gave:

$$\omega = 597 \text{ rad/s (95Hz)} \quad G_a = 50 \text{ mA/V}$$

Results are now compared with gains set at approximately $\frac{1}{4}$ of the value required to cause closed-loop instability. The linearised transfer function gain was set to $G_a = 16 \text{ mA/V}$ and the gain in the exact simulation was set to $G_a = 12 \text{ mA/V}$.



Other points drawn from this study are as follows:

- the general transient trend between the linearised analysis and the exact solution compare well, highlighting again the value of a preliminary linearised analysis
- it will be recalled that under Proportional control the linearised analysis and the exact simulation predict the same steady-state conditions as follows:

$$\frac{F}{F_d} = \frac{23.7 G_a}{1 + 23.7 G_a}$$

For the gains selected in the previous diagram the steady-state errors are negligible.

- the **addition of either Integral control and/or Derivative control**, not shown here, makes little difference to the dynamic response
- adding Integral control for the gain used was of little value since the steady-state error was negligible under Proportional control. In addition, the transient response took much longer to decay to its steady-state value
- the addition of Derivative control had no effect on the overshoot, the closed-loop being more prone to instability even when the Derivative gain was set to just a small value

Now consider cyclic fatigue testing at low frequencies.

A small amplitude sinusoid is used for fatigue testing and over many cycles that could last from hours to days. The mean force may be large and the servoactuator must be able to provide this value in addition to the cyclic force.

Following the application of the demand sinusoid, at the structure mean deflection, the displacement settles to its sinusoidal motion and actuator higher-order actuator dynamics may be neglected as a first approximation and equivalent to *neglecting fluid compressibility and moving inertia*, $C = 0$ and $L = 0$.

For the PI control case the load force transfer function is as follows, and also assuming that Rv/R is *negligible*:

$$\text{PI control } \frac{F(s)}{F_d(s)} = \frac{KK_i + Ks}{[KK_i + s(1 + K) + s^2 C_m R]} \quad (8.29)$$

The denominator is defined in the usual 2nd order form:

$$\text{undamped natural frequency } \omega_n = \sqrt{\frac{KK_i}{C_m R}} \quad \text{damping ratio } \zeta = \frac{(1 + K)}{2\sqrt{C_m R K K_i}}$$

The important points that arise from this analysis are:

- since $K = H_f G_a k_{qi} R A$ then the undamped natural frequency ω_n is independent of the resistance R as would be expected
- both the undamped natural frequency ω_n and the damping ratio ζ are affected by the values of the integrator gain K_i and the servoamplifier gain G_a assuming the remaining system parameters are fixed
- the actual amplitude of excitation achieved depends upon the appropriate transfer function magnitude ratio at the frequency of interest
- the selection of the appropriate operating resistance R a very important issue. The spool is dynamically open during each half cycle and the spool valve provides resistive damping R_{sv} . This must be added, in parallel, to any actuator leakage resistance R_{act} .

Example 8.3

Consider example 8.2. Fatigue testing is now to be undertaken at a frequency of 2Hz with an amplitude of 0.5mm at a mean deflection of 1mm. Investigate PI control, the application of an additional sinusoidal input for fatigue testing and the generation of a digital control algorithm. The data required are repeated:

Servoactuator bore 80mm diameter, double-rod 56mm diameter, full stroke 200mm.

Servoactuator leakage resistance $R_{act} = 5 \times 10^{12} \text{ Nm}^{-2}/\text{m}^3\text{s}^{-1}$

Servovalve supply pressure $P_s = 140\text{bar}$ mean load pressure $P_l(o) = 78\text{bar}$


Structure stiffness $k_m = 2 \times 10^7 \text{ N/m}$

Load cell gain $H_f = 10^{-4} \text{ V/N}$

$$C_m = 3.28 \times 10^{-13} \text{ m}^5/\text{N} \quad k_{qi} = 1.85 \times 10^{-5} \text{ m}^3\text{s}^{-1}/\text{mA}$$

Consider first the linearised transfer function with actuator dynamics neglected at such a low excitation frequency of 2Hz:

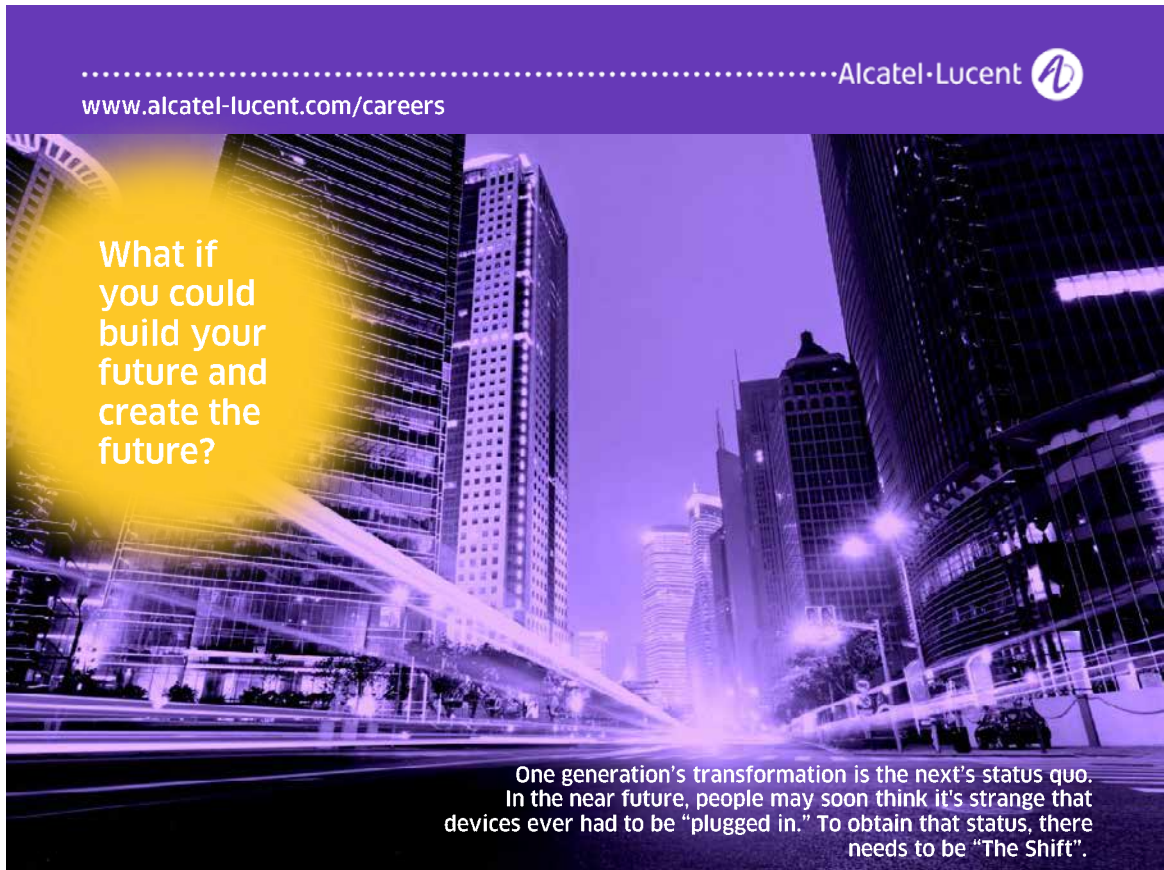
$$\frac{F(s)}{F_d(s)} = \frac{KK_i + Ks}{[KK_i + s(1 + K) + s^2 C_m R]}$$

.....Alcatel-Lucent 

www.alcatel-lucent.com/careers

What if you could build your future and create the future?

One generation's transformation is the next's status quo. In the near future, people may soon think it's strange that devices ever had to be "plugged in." To obtain that status, there needs to be "The Shift".



Recalling that if the spool is dynamically open then flow is being delivered and the spool valve provides resistive damping R_{sv} . This must be added, in parallel, to any actuator resistance R_{act} should it be appropriate. To get a 'feel' for the servovalve damping effect then consider a servovalve average resistance over one half cycle and assume sinusoidal motion at the required amplitude, whatever the value of the Integrator gain K_i .

$$y = y_m \sin(\omega t) \quad U = \omega y_m \cos(\omega t)$$

The maximum flow rate $Q = \omega y_m A = k_{qi} i_{max}$

In this example $(2\pi \times 2)(0.5 \times 10^{-3})(2.56 \times 10^{-3}) = (1.85 \times 10^{-5})(i_{max})$
 $i_{max} = 0.87 \text{mA}$

So, assume an average current $i \approx 0.5 \text{mA}$ during each half cycle.

$$R_{sv} = \frac{2[P_s - P_\ell(o)]}{Q(o)} = \frac{2(140 - 78) \times 10^5}{(1.85 \times 10^{-5})(0.5)}$$

$$R_{sv} = 1.34 \times 10^{12} \text{Nm}^{-2}/\text{m}^3 \text{s}^{-1}$$

$$\frac{1}{R} = \frac{1}{R_{act}} + \frac{1}{R_{sv}} = \frac{1}{5 \times 10^{12}} + \frac{1}{1.34 \times 10^{12}}$$

$$R = 1.06 \times 10^{12} \text{Nm}^{-2}/\text{m}^3 \text{s}^{-1}$$

For the purpose of example assume a servoamplifier gain $G_a = 1 \text{mA/V}$.

Actuator leakage only:

$$K = H_f G_a k_{qi} R A = (10^{-4})(1)(1.85 \times 10^{-5})(5 \times 10^{12})(2.56 \times 10^{-3}) = 23.7$$

$$C_m R = 1.64 \text{s}$$

Actuator leakage and servovalve average leakage:

$$K = H_f G_a k_{qi} R A = (10^{-4})(1)(1.85 \times 10^{-5})(1.06 \times 10^{12})(2.56 \times 10^{-3}) = 5.0$$

$$C_m R = 0.348 \text{s}$$

$$\text{undamped natural frequency } \omega_n = \sqrt{\frac{K K_i}{C_m R}} \quad \text{damping ratio } \zeta = \frac{(1 + K)}{2\sqrt{C_m R K K_i}}$$

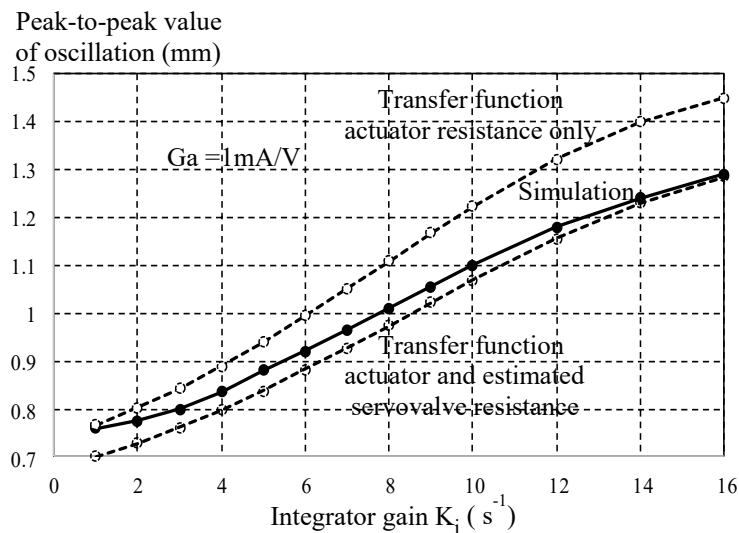
If *servovalve average leakage is included with actuator leakage* then as the integrator gain is increased from $K_i = 1 \rightarrow 16 \text{ s}^{-1}$ the system data are as follows:

$G_a = 1 \text{ mA/V}$	$K = 5.0$	$K_i =$	1	16
		ω_n	0.6Hz	2.4Hz
		ζ	2.27	0.57

Such low undamped natural frequencies justifies the neglect of actuator dynamics.

For completeness, the linearised transfer function is transformed into the frequency domain and the magnitude ratio is evaluated at a frequency of 2Hz.

When this magnitude ratio is multiplied by the demanded peak-to-peak value of oscillation required (1mm) then the actual peak-to-peak value may be determined. This is now shown together with the variation measured from the exact simulation with all system dynamics included.



The following observations are therefore made:

- the mean position/force value was readily achieved for any servoamplifier gain by adjustment of the input mean voltage. This was not required if Integral control is added
- servovalve damping is important during cyclic testing, even with a critically-lapped spool
- the desired cyclic peak-to-peak value of 1mm could only be achieved around an integrator gain setting of $K_i \approx 8 \text{ s}^{-1}$ unless the demand signal amplitude is changed
- for a particular leakage resistance R a unique integrator gain is required to produce the required force variation for testing
- if leakage develops with use then the addition of integral control can help, but gain selection may need continual tuning

- with some simple pre-calculations a linearised transfer function evaluation can give a very good estimate of the closed-loop frequency response to a demanded sinusoid
- force control is more complicated than might initially be expected

Finally consider now a digital control algorithm for PI control.

Recalling that a value of the integrator gain $K_i = 8s^{-1}$ was chosen for the purpose of illustration. Hence $\tau = 1/K_i = 0.125s$. For this example a low sampling frequency of 100Hz is selected giving a sampling interval $T=10ms$. The PI algorithm then becomes:

$$V_{out} = \left(1 + \frac{T}{\tau}\right)[V_{in}] - [z^{-1}V_{in}] + [z^{-1}V_{out}]$$

$$V_{out} = 1.08[V_{in}] - [z^{-1}V_{in}] + [z^{-1}V_{out}]$$

Alternatively, if a filter is selected using the Programmable Servo Controller library then the digital transfer function set up will be as follows:

$$G(s) = 1 + \frac{8}{s} \rightarrow \frac{1.08 - z^{-1}}{(1 - z^{-1})}$$

The following results compare digital control with analogue control.



**Join the best at
the Maastricht University
School of Business and
Economics!**

Top master's programmes

- 33rd place Financial Times worldwide ranking: MSc International Business
- 1st place: MSc International Business
- 1st place: MSc Financial Economics
- 2nd place: MSc Management of Learning
- 2nd place: MSc Economics
- 2nd place: MSc Econometrics and Operations Research
- 2nd place: MSc Global Supply Chain Management and Change

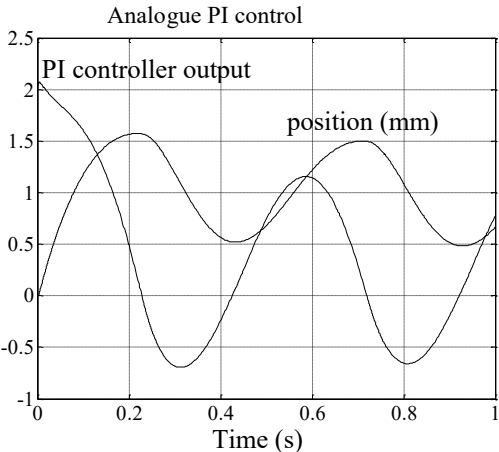
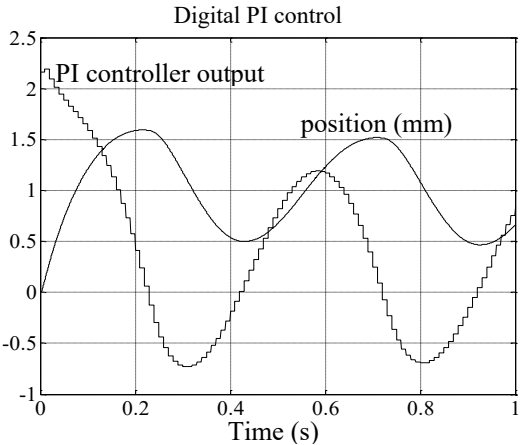
Sources: Keuzegids Master ranking 2013; Elsevier 'Beste Studies' ranking 2012; Financial Times Global Masters in Management ranking 2012

Maastricht University is the best specialist university in the Netherlands
(Elsevier)

Visit us and find out why we are the best!
Master's Open Day: 22 February 2014

www.mastersopenday.nl





No detectable difference in dynamic performance is evident, even for this relatively low sampling frequency, and aided by the low testing frequency. The sampling effect can just be seen at the PI output under digital control.

9 Closing comments and further reading guidance

The direction of this introduction to servovalve-controlled systems design should indicate to the reader that in practice a pragmatic approach will probably have to be adopted, particularly when open-loop models are experimentally obtained, or are a combination of well-established theory combined with experimental data. Another problem is that models change with operating conditions and control strategies must be robust over the entire operating range of the system.

Clearly the vast amount of industrial and commercial applications around the world illustrates that servodrive systems successfully operate and there would not appear to be a problem. However, are the systems operating at an optimum level of control and efficiency and will the control challenges of, for example, using non-mineral oil fluids in the future be overcome, particularly for very high power systems?

Notwithstanding the undisclosed research and development effort by industry, there is a vast amount of fluid power literature in journals and international conferences. This shows that fluid power control is being studied, to an advanced level in some cases. A variety of modern control techniques, including artificial intelligence methods, have been applied to very specific circuits and with perhaps a reluctance by the industry to accept them as sufficiently robust for commercial take-up; this should not deter continuing research and development. Many useful references and more detailed background theory are given in the following author's supporting books together with other industrial, journal and conference information.

www.Moog.com

Mannesmann Rexroth, Lohr am Main, Germany. The hydraulic trainer, volume 2, Proportional and Servovalve technology, 3rd issue 1989

Parker Hannifin Corporation, Motion and Control training Department, Cleveland, Ohio. Design Engineers Handbook, volume 1, 2001

Vickers Inc Training Centre, Rochester Hills, Michigan USA. Closed loop electrohydraulic systems manual, 1992

International Journal of Fluid Power ISSN 1439-9776. Published quarterly by Taylor & Francis. Also see <http://fluidpower.net>

FPMC Fluid Power and Motion Control Symposium series. Originating at Bath University UK this now alternates between Bath University and ASME USA. The 2015 symposium was held in Chicago USA

Proceedings of the Japanese Fluid Power Society International Symposium on Fluid Power. Held every three years in Japan since 1989

Proceedings of the Scandinavian International Conference on Fluid Power. A Biennial event alternating between Tampere University of Technology TUT Finland and Linköping University LIU Sweden. The 14th Scandinavian International Conference on Fluid Power – SICFP15 was held in May 2015, Tampere, Finland

RWTH Aachen Germany, International Fluid Power Conference series. The 9th conference was held in 2014, Aachen University

Hangzhou International Conference on Fluid Power Transmission and Control series, Zhejiang University, Hangzhou, China. The 8th conference was held in 2013

J Watton. Modelling, Monitoring and Diagnostic techniques for Fluid Power Systems. Published by Springer Verlag, 2007



> **Apply now**

REDEFINE YOUR FUTURE
**AXA GLOBAL GRADUATE
PROGRAM 2015**

redefining / standards 

agence.cdg. © Photonistop

J Watton. *Fundamentals of Fluid Power Control*. Published by Cambridge University Press 2009

and also published in Portuguese as follows:

J Watton. *Fundamentos de Controle em Sistemas Fluidomecânicos*. Direitos exclusivos para a língua portuguesa, LTC Rio de Janeiro 2012. ISBN 978-85-216-2025-9

WR Anderson. *Controlling electrohydraulic Systems*. Published by Marcel Dekker Inc, New York and Basel, 1988

ND Manring. *Hydraulic Control Systems*. Published by John Wiley & Sons Inc, 2005

It will probably be self-evident from this chapter that closed-loop control of pressure and force systems presents unique challenges. In addition to the information that may be found in the conference proceedings mentioned previously, the reader may care to look at some specific publications which also include many other relevant references:

AR Plummer. Robust electrohydraulic force control. *Proceedings IMechE*, Volume 221, 2007, 717–731

J Kennedy and R Fales. Experimental modeling and control of a servo-hydraulic force control system. *International Journal of Fluid Power*, Volume 11, Number 1, March 2010

M Liermann. PID tuning rule for pressure control applications. *International Journal of Fluid Power*, Volume 14, Number 1, March 2013, 7–15